Netherlands society for Biomaterials and Tissue Engineering

Program 31st Annual Meeting, 1 & 2 December 2022
at
the Conference center De Werelt

Conference rooms: AIR & FIRE

Thursday, 1st December 2022

9.00-9.45	Registration & coffee
9.45-10.00	Welcome (Room: AIR)

10.00-11.15 (10+2 min)	**Oral Presentation Session 1** (Room: AIR) *Mechanosensing, mechanical stimulation & topographies* Chair: Torben van der Boon	**Oral Presentation Session 2** (Room: FIRE) *Engineering cellular niches & bottom-up tissue engineering* Chair: Niels Willemen
01/02	**Zyg B.M. Bijonowski** **Technical University Eindhoven** *Cell-Cell Membrane Tethering Results in PLD2-Based Coordinated Migration of MDA-MB-231 Cells*	**Simone M.J. de Jong** **Technical University Eindhoven** *Engineering A Synthetic Niche For Pluripotent Stem Cells*
03/04	**Maaike J. Bril** **Technical University Eindhoven** *A Photoresponsive Hydrogel to Investigate Cell Responses to Dynamically Changing Topographies*	**Andrea Schwab** **Erasmus MC** *Effect of biomaterial composition on cell migration and tissue formation for cell-free osteochondral defect repair*
05/06	**Tianqi Feng** **Groningen UMC/University of Groningen** *Topography mediated muscle engineering using ECM-based scaffold*	**Esra Güben Kaçmaz** **Maastricht University** *Collagen Microparticle Building Blocks for Bottom-Up Bone Tissue Engineering*
07/08	**Amal K. Mansoor** **Technical University Eindhoven** *Restoring Disorganised Tendinopathic Tissue using Magnetic Topographical Cues*	**Castro Johnbosco** **University of Twente** *Engineering tissues with multiscale mechanics via modular bio-inks using single cell microniches*

09/10	**Maria M. Lobita** **Groningen UMC/University of Groningen** *Development of Dissolving Microneedles to Stimulate Polarization of M1-type Macrophages and Lead to Cardiac Repair*	**Maritza M. Rovers** **Technical University Eindhoven** *Microgels as Building Blocks to Bioengineer Tissue Constructs*
11/12	**Klaudia M. Jurczak** **Groningen UMC/University of Groningen** *Porous in vitro Model with a Wrinkle Topography to Mimic Tunica Media of a Blood Vessel*	**Marloes van Mourik** **Technical University Eindhoven** *Towards the Engineered Chondron: Pericellular Matrix Synthesis by Articular Cartilage Chondroprogenitors in Agarose and GelMA Microgels*

11.15-11.45	Coffee break

11.45-13.00 (10+2 min)	**Oral Presentation Session 3** (Room: AIR) *Micro- and nano(bio)material technologies* Chair: Maik Schot	**Oral Presentation Session 4** (Room: FIRE) *3D bioprinting & biofabrication (smart materials)* Chair: Martina Viola
13/14	**Marieke Meteling** **University of Twente** *Extracellular Protein Identification Cytometry (EPIC) to quantify single cell matrix* deposition *in high-throughput*	**Greta Di Marco** **Utrecht University** *Shrinking Hydrogels By Thermosensitive Interactions: A New Material-based Approach To Enhance 3D Printing Resolution For Kidney Tissue Engineering*
15/16	**Katrin A. Münzebrock** **UMC Utrecht** *Poly(amido amine) Nanoparticles enable mRNA Delivery into Cells of Cartilaginous Tissues*	**Marta G. Valverde** **Utrecht University** *Fibrous Patterned Melt-Electrowriten Membranes for Proximal Tubule Tissue Engineering*
17/18	**Maryam Parvizifard** **Maastricht University** *Designing the next generation of biomaterials through screening hybrid cell-microparticle spheroidal tissue assemblies*	**Niko E. Putra** **Delft University of Technology** *Extrusion-based 3D printing of Fe-based bone substitution*
19/20	**Lizzy A.B. Cuypers** **Radboudumc Nijmegen** *Zinc-doped Hydroxyapatite Nanoparticles for the Treatment of Bone infection*	**Dmitrii Iudin** **Utrecht University** *Hydrogel Shrinking by Electrostatic Interactions for Resolution Enhancement in 3D Bioprinting*
21/22	**Luanda Lins** **University of Twente**	**Alejandro Reina Mahecha** **Groningen UMC**

	Mechanically and chemically tunable microcarriers using In-air-microfluidics for enzyme-free cell release	*3D Printed Biocompatible Molds for High Production of Homogeneous Embryoid Bodies for Specific Differentiation*
23/24	**Shuang Tian** **Groningen UMC/University of Groningen** *Protection of DNase in the shell of a pH-responsive, antibiotic-loaded micelle for biofilm targeting, dispersal and eradication*	**Anne Metje van Genderen** **Utrecht University** *Well Organized Melt-Electrowritten Tubular Scaffolds to Engineer Vascularized Kidney Proximal Tubules*

13.00-14.00	Lunch
14.00-15.30	**Working in- & outside of academia** (Room: AIR) Panel discussion (moderator: *Patrick van Rijn*) **Panelists:** *Lorenzo Moroni, Maastricht University (academia)* *Lavinia Panella, DSM (company)* *Sieger Henke, TNO (research institute)* *Lise de Jonge, NWO (funding agency)* *Tom Kamperman, IamFluidics (start-up company)*
15.30-15.45	Short coffee break

15.45-17.00 (10+2 min)	**Oral Presentation Session 5** (Room: AIR) *Enhancing tissue survival, regeneration & wound healing* Chair: Zahra Gorgin Karaji	**Oral Presentation Session 6** (Room: FIRE) *3D cell culture, organ and disease models* Chair: Laís Ribovski
25/26	**Melvin Gurian** **University of Twente** *Preventing anoxia induced stem cell death through controlled metabolite release for tissue survival and integration*	**Ceri-Anne E. Suurmond** **Radboudumc Nijmegen** *3D Co-Culture Spheroid Model to Assess the Response of Bone Metastases to Anticancer Drugs*
27/28	**Nancy M. Avila-Martinez** **Radboudumc Nijmegen** *Isolation of type III collagen and preparation of type I/III collagen scaffolds for scarless skin regeneration*	**Hannah F.M. Brouwer** **Technical University Eindhoven** *The Influence of Macrophage Phenotype on Tendon Tissue Remodeling*
29/30	**Gizem Babuccu** **Amsterdamumc/University of Amsterdam**	**Jyoti Kumari** **Radboud University/Radboudumc Nijmegen**

	Development of diagnostic and antimicrobial triggered release systems for wound dressings	*Polyisocyanide hydrogel for 3D Contraction Assay: A Versatile Preclinical Research Platform for Fibrosis*
31/32	**Roman Krymchenko** **Radboudumc Nijmegen** *Preparation of specific elastin hydrolysates and incorporation in biomaterials to enhance skin wound healing*	**Jelle J.F. Sleeboom** **Delft University of Technology/Erasmus MC** *Development of A Perfusable 3D Bioprinted Liver Tissue Model*
33/34	**Lisanne C.M. Morshuis** **University of Twente** *VHHs for sequestering endogenous BMP7 in tissue engineering strategies*	**Annika F. Vrehen** **Technical University Eindhoven** *Towards a Fully Synthetic Corneal Stromal Construct: using a Supramolecular hydrogel*
35/36	**Merel Gansevoort** **Radboudumc Nijmegen** *Harnessing Click-to-Release Chemistry for the Development of Spatiotemporal Signaling Scaffolds*	**Melissa J.J. van Velthoven** **Radboud University/Radboudumc Nijmegen** *Cyclic Straining of In Vitro Tissue-Engineered 3D Models: Investigating the Effects on ADSC differentiation and the Extracellular Matrix*

17.00-17.30	Coffee break
17.30-18.30	**NBTE general assembly & scientific image competition** (Room: AIR)
18.30-20.00	Dinner
20.00-21.00	**Evening lecture**: Debora Angeloni, PhD (Room: AIR) Associate Professor of Molecular Biology at Scuola Universitaria Superiore Sant'Anna (SSSA), Pisa, Italy *Space, the new frontier and a resource for tissue engineering*
21.00-22.00	**Pubquiz** (Room: FIRE)
From 22.00	Get together with drinks (Room: FIRE)

Friday, 2nd December 2022

7.00-9.00	Breakfast & poster mounting
9.00-10.00	**Keynote lecture**: Vanessa LaPointe, PhD (Room: AIR) Associate Professor at MERLN Institute for Technology-Inspired Regenerative Medicine at Maastricht University *Cell therapies for regenerating the corneal endothelium*
10.00-11.00	**Rapid-fire Poster Session** (Room: AIR)
11.00-12.00	**Poster Session** (Rooms: FIRE & AIR)
12.00-13.30	Lunch – Meet the Mentors

13.30-14.45 (10+2 min)	**Oral Presentation Session 7** (Room: AIR) *Tuning the immune response* Chair: Monika Salandova	**Oral Presentation Session 8** (Room: FIRE) *Blood, vessel engineering & cardiac regeneration* Chair: Cansu Karakaya
37/38	**Pardis Keikhosravani** **UMC Utrecht** *Antibacterial CATH-2 Peptide Coating to Prevent Implant-related Infection*	**Dina M. Ibrahim** **Technical University Eindhoven** *The Role of Monocyte-Derived Macrophages as Endothelial Progenitors in Endothelium Injury*
39/40	**Lanhui Li** **Technical University Eindhoven** *Magnetically-actuated dynamic surfaces (MadSurface) for regulating immune response*	**Francisca L. Fernandes Gomes** **University of Twente** *Erythrocyte-Inspired Lipid Coatings for Improved Particle Hemocompatibility*
41/42	**Guang Yang** **Groningen UMC** *In-biofilm Generation of Nitric Oxide using a Magnetically-Targetable Cascade-Reaction Container for Eradication of Infectious Biofilms*	**Dewy C. van der Valk** **Technical University Eindhoven** *Analyzing The Risk Of Calcification In Materials Used For In Situ Heart Valve Tissue Engineering*
43/44	**Lisa E. Tromp** **Groningen UMC/University of Groningen** *High-Throughput Screening to Elucidate Implant-Associated Complications*	**Raquel Bártolo** **Groningen UMC/University of Groningen** *Injectable Nanoparticle-Hydrogel Composite for Cardiac Tissue Regeneration*
45/46	**Patrick P.G. Mulder** **Radboudumc Nijmegen**	**Jordy G.M. van Asten** **Technical University Eindhoven**

	Full Skin Equivalents to Simulate Burn Wound Healing and Inflammation	*Cell-cell signaling to control arterial growth and remodeling: a computational approach*
47/48	**Miranda Jekhmane** **Amsterdamumc** *Towards the Native Skin: ex vivo development of skin appendices*	**Valentine C. Vetter** **Technical University Eindhoven** *A novel method for cell delivery in decellularized heart valves using injectable hydrogels*

14.45-15.00	Short coffee break

15.00-16.15 (10+2 min)	**Oral Presentation Session 9** (Room: AIR) *Towards bone development* Chair: Michelle Vis	**Oral Presentation Session 10** (Room: FIRE) *Translational research* Chair: Zhule Wang
49/50	**Amaia Garmendia Urdalleta** **Delft University of Technology/Erasmus MC** *The differential response of human macrophages to 3D printed titanium antibacterial implants does not affect the osteogenic differentiation of hMSCs*	**Anneli A.A. Duits** **UMC Utrecht** *Rationale and guideline for translational research using the small ruminant lumbar interbody fusion*
51/52	**Paree K. Khokhani** **UMC Utrecht** *Gamma-irradiated S. aureus and combination of synthetic TLR-agonists for MSC osteogenic differentiation*	**Rob Meuwese** **Radboudumc Nijmegen** *Development of an expandable plug and preliminary evaluation in an ex vivo human fetal membrane model*
53/54	**Ebrahim Yarali** **Delft University of Technology** *Poisson's Ratio-Driven Bone Cell Growth in Meta-Biomaterials*	**Anniek M.C. Gielen** **University of Amsterdam/RIVM** *A Safe-by-Design Approach for Medical Implants*
55/56	**Roderick H.J. de Hilster** **Groningen UMC/University of Groningen** *Screening for osteogenic differentiation stimulating surface characteristics on Poly(Lactic Acid) using Double Orthogonal Gradients*	**Janne Spierings** **Technical University Eindhoven** *Can osteoarthritis after ACL reconstruction be explained by altered graft mechanical properties?*
57/58	**Mahya Ganjian** **Delft University of Technology** *From nanopatterned sheets to stiff meta-biomaterial*	**Yuanyuan Sun** **Vrije Universiteit Amsterdam & University of Amsterdam** *Biomimetic Bone Substitute as a Medical Device for Socket Preservation*

59/60	**Liline Fermin** **Maastricht University** *A Biomimetic In Vitro Bone Model Based on Spheroidal Co-Culture of Osteoclasts and Osteoblasts*	**Kest Verstappen** **Radboudumc Nijmegen** *In Vivo Biocompatibility of Xenogeneic Extracellular Matrix and Reduced Graphene Oxide Foams*

16.15-16.30	Short coffee break
16.30-17.00	**Announcements, awards ceremony & closure of the meeting** (Room: AIR)

Sponsors

Miltenyi Biotec

IamFluidics
revolutionize microparticles

Rapid-fire poster session

#	Presenter & Topic
1	**Malin Becker, University of Twente** *Low Viscosity 3D (LoV3D) Bioprinting exploiting aqueous-two phase stabilization*
2	**Leanne de Silva, UMC Utrecht** *Implementing an Arteriovenous (AV) Loop in Endochondral Bone Regeneration*
3	**Magdalena Z. Gladysz, University of Groningen** *Fibrous Melt-Electrowritten Scaffolds to Investigate Cellular Behaviour for in Vitro Blood-Brain Barrier Model Development*
4	**Jing Han, Radboudumc Nijmegen** *Immune Modulation of Zinc via THP-1 Derived Macrophage Polarization*
5	**Celien A.M. Jacobs, Technical University Eindhoven** *Mechanical characterization of a unique biomimetic artificial disc for the cervical spine*
6	**Cansu Karakaya, Technical University Eindhoven** *Uniaxial and equibiaxial strain differently affect the phenotypic switching of vascular smooth muscle cells*
7	**Carlos J. Peniche Silva, Maastricht University** *MiRNAs as Potential Regulators of Enthesis Healing in a Rodent Injury Model*
8	**Claire Polain, Maastricht University** *A Co-Culture Model For Innervation In Bone Regeneration Using NGF cmRNA*
9	**Laura Rijns, Technical University Eindhoven** *Synthetic supramolecular hydrogels to steer the polarity of kidney epithelial cells and intestinal organoids in 3D*
10	**Flurina Staubli, UMC Utrecht** *Extended storage of soft callus mimetics permits endochondral bone regeneration*
11	**Michelle A.M. Vis, Technical University Eindhoven** *A dialysis medium refreshment cell culture set-up for an osteoblast-osteoclast coculture*
12	**Zhule Wang, Radboudumc Nijmegen** *Bifunctional Bone Substitute Granules Loaded with Cisplatin Aiming to Minimize Malignant Bone Tumor Recurrence via Local Treatment*
13	**Niels G.A. Willemen, University of Twente** *Steering Stem Cell Fate within 3D Living Composite Tissues using Stimuli-responsive Cell-adhesive Micromaterials*
14	**Piotr Zielinski, University of Groningen** *Melt Electrowriting of Scaffolds for Soft-to-Hard Tissue Engineering*
15	**Mirko D'Urso, Technical University Eindhoven** *Mechanosensing of tissue environment regulates fibroblast activation*
16	**Leonardo Cecotto, UMC Utrecht** *Immunomodulatory and Antibacterial Properties of Host Defense Peptides Against Staphylococcus aureus*
17	**Martina Viola, UMC Utrecht/University of Utrecht** *Thermosensitive Shrinking Behavior of Biopolymer-based Hydrogels for High Resolution Printing*
18	**Xixi Wu, Groningen UMC/University of Groningen** *Fabrication of visibly degradation-monitored PCL/FNDs (Fluorescent nanodiamonds) bioscaffolds using MEW method*
19	**Gabriele Addario, Maastricht University** *Improving human kidney fibrosis in vitro models: a mechanical, protein, gene study*
20	**Maik R. Schot, University of Twente** *Bioengineering a Modular, Immunoprotective, and Microporous Mini-Pancreas for Type 1 Diabetes*

Thursday

1st December 2022

Oral Session 1

Cell-Cell Membrane Tethering Results in PLD2-Based Coordinated Migration of MDA-MB-231 Cells

B.M. Bijonowski[1,2] and S.V. Wegner[1]
[1] Universitätsklinikum Münster, Albert-Schweitzer-Campus 1, 48149 Münster, Germany
[2] University of Technology Eindhoven, Groene Loper 5, 5612 AE Eindhoven, Netherlands

Introduction: Collective cell migration typically results from cadherin-based cell-cell adhesions, which link to the underlaying cytoskeleton relaying mechanotransductive signals. Similarly, cells can be shown to migrate with respect to cytokine gradients; however, the role of non-cytoskeletal interacting cell-cell adhesions remains largely unexplored due to their quick turnover.

Materials and Methods: Optogenetic proteins were incorporated on the plasma membrane to enable the spatiotemporal control of cell-cell adhesions without cytoskeletal activation. Cph1 derived from *Synechocystis sp.* homodimerizes under red light and reverts to the monomer under far-red light.

Results: Using this system, collective migration was observed when cell-cell adhesions were activated, but cells migrated individually without activation. Further analysis revealed that these connections resulted in a shift in local membrane tension along with an increase in cellular phosphatidic acid. This was determined to result from activation of phospholipase D2, as inhibition resulted in reduced migration coordination.

Summary: Utilizing an optogenetic cell-cell adhesion system it was revealed that adhesions without cytoskeletal interactions result in altered local membrane composition. These changes then result in phospholipase D2 based release of phosphatidic acid and altered actin structure. These effects lead to collective migration in cells that do not normally undergo collective migration.

A Photoresponsive Hydrogel to Investigate Cell Responses to Dynamically Changing Topographies

M.J. Bril[1,2], C.V.C. Bouten[1,2], N.A. Kurniawan[1,2]

[1] Department of Biomedical Engineering, Eindhoven University of Technology, PO Box 513 5600 MB Eindhoven, The Netherlands
[2] Institute for Complex Molecular Systems, Eindhoven University of Technology, PO Box 513 5600 MB Eindhoven, The Netherlands

Introduction: *In vivo*, cells continually engage in a complex and highly dynamic interplay with their extracellular microenvironment[1]. However, the majority of in vitro cell studies are performed under static conditions, i.e., a constant topographical signal is presented to the cells, which is a poor recapitulation of the native cellular microenvironment. Here, we introduce a new approach to create biocompatible cell substrates whose microscale topography can be dynamically changed on demand, allowing a systematic study of cell responses to biophysical events.

Materials & Methods: A light-responsive poly(N-isopropylacrylamide) (pNIPAM) hydrogel is used that changes topography upon masked illumination with blue light[2]. Local illumination converts the light-responsive hydrophilic merocyanine (McH^+) to the hydrophobic spiropyran (Sp) moiety, which results in local hydrogel shrinking. Removal of the light returns the hydrogel towards its original flat state. Subsequently, normal human dermal fibroblasts (nhDF) are seeded on top, and nuclei, actin cytoskeleton, intermediate filament, and microtubule morphology are investigated using fluorescence staining and confocal imaging.

Results & Discussion: UV-vis data confirm that the hydrogel is photoresponsive under cell culture conditions after three rounds of illumination. Profilometry measurements reveal that a variety of topographies (lateral dimensions > 50 µm, z_{max} = 1 µm) can be controllably induced within 15 min, while hydrogel stiffness is not altered (E = ~350 kPa). Testing with cells (human dermal fibroblasts) indicates that the cells can adhere to the hydrogel and their viability is not affected by illumination with blue light. A systematic investigation of all cytoskeleton components reveals that microtubule do not seem to respond to dynamic topographies, whereas the actin cytoskeleton and intermediate filaments show remodeling. Moreover, we find that dynamic anisotropic topographies provoke cells to reorient in distinct ways compared to cell response to static topographies. This unexpected finding not only demonstrates that cells are able to respond to induced topographies, but also highlights the need to better understand mechanisms of cellular sensing of dynamic microenvironmental cues.

Conclusion: We propose a novel promising approach to gain a fundamental insight into the complex cellular sensing of spatiotemporal events at the cell-substrate interface and the ensuing dynamic cell-microenvironment interactions. Ultimately, this knowledge can aid the development of better tissue engineering constructs.

References:

1. Bril, M. et al. Smart Mater. Med. 3, 257–273 (2022).
2. Stumpel, J. E. et al. ACS Appl. Mater. Interfaces 6, 7268–7274 (2014).

Topography mediated muscle engineering using ECM-based scaffold

Tianqi Feng, L.E. Tromp, Roderick H.J. de Hilster, T.A.B. van der Boon, Patrick van Rijn
W.J. Kolff Institute for Biomedical Engineering and Materials Science, University of Groningen/ University of Groningen, University Medical Center Groningen, Deusinglaan 1, 9713 AV Groningen, The Netherlands
t.feng@umcg.nl

Introduction: Facial palsy, the paralysis of facial muscles, is a major social burden for affected patients which profoundly alters an individual self-image and ability to communicate and express emotion.[1-3] One of the efficient treatment approach of facial palsy is muscle engineering which means using biological scaffolds combined with bioactive tissues or cells in order to repair or construct tissue or organ[4]. Skeletal muscle tissue engineering is a promising alternative to traditional volumetric muscle loss surgical treatments that use autogenic tissue grafts, and rather use isolated stem cells with myogenic potential to generate new skeletal muscle tissues to treat volumetric muscle loss[5]. Biological scaffolds used for medical implants, tissue engineering scaffolds, not only provide structural support for the promotion of cellular ingrowth but also impart potent modulatory signaling cues that may be beneficial for tissue regeneration[6].

So the main idea is essentially to combine bio-interfaces to explore the full potential of existing clinical biomaterials currently serving as implants and tissue scaffolds. Using modified-scaffolds would offer control over cellular arrangement, differentiation and functions and yield a construct that closely resembles natural striated muscle. Combining applicable physical surface parameters with Extracellular matrix (ECM)-based hydrogels will drive differentiation and align all three essential constituents of muscle i.e. myofibers, vasculature and neurons[7-8] and bring these into contact with each other.

Method: Imprint technology is used to prepare hydrogel wrinkle topography to form topography surface of hydrogel This approach will function as a screening platform together with altering the stiffness via cross linking to determine the influence on cells of combined parameters and thereby offering a superior choice of biomaterial properties. We aim to explore the full potential of existing clinical ECM sources to greatly enhance the clinical translation.

Results and Discussion: Topography Mediating biomaterial surface character could endow new functions for ECM-based materials to direct cellular behavior to a great extent as excellent biocompatible biomaterials and implant. Transferring topography from PDMS to ECM-based material through Imprint technology worked well. It is expected that the the wrinkled ECM-based hydrogels will provide the optimum bio-interface for offering striking detailed insights for cell behavior towards enabling it to be transferred to clinical applications such as the development of implantable tissue engineered constructs.

Conclusion: The approach will explore full potential of ECM-based material, which could increase new function and diminish implant associated medical complications as a secondary problem and thereby reducing implant impairment as well as lowering patient morbidity and mortality.

References:

1. Langhals NB, Urbanchek MG, Ray A, Brenner MJ. Update i n facial nerve paralysis: tissue engineering and new technologies. Curr Opin Otolaryngol Head Neck Surg. 2014 Aug;22(4):291-9.
2. George E, Richie MB, Glastonbury CM. Facial Nerve Palsy: Clinical Practice and Cognitive Errors. Am J Med. 2020 Sep;133(9):1039-1044.
3. O TM. Medical Management of Acute Facial Paralysis. Otolaryngol Clin North Am. 2018 Dec;51(6):1051-1075.
4. Nakayama KH, Shayan M, Huang NF. Engineering Biomimetic Materials for Skeletal Muscle Repair and Regeneration. Adv Healthc Mater. 2019 Mar;8(5):e1801168.
5. Pantelic MN, Larkin LM. Stem Cells for Skeletal Muscle Tissue Engineering. Tissue Eng Part B Rev. 2018 Oct;24(5):373-391.
6. Lenci E, Menchi G, Saldívar-Gonzalez FI, Medina-Franco JL, Trabocchi A. Bicyclic acetals: biological relevance, scaffold analysis, and applications in diversity-oriented synthesis. Org Biomol Chem. 2019 Jan 31;17(5):1037-1052.
7. Andrew, Dunn, Muhamed, et al. Biomaterial and stem cell-based strategies for skeletal muscle regeneration.[J]. Journal of Orthopaedic Research Official Publication of the Orthopaedic Research Society, 2019.
8. Xie Y, Schneider KJ, Ali SA, Hogikyan ND, Feldman EL, Brenner MJ. Current landscape in motoneuron regeneration and reconstruction for motor cranial nerve injuries.

Restoring Disorganised Tendinopathic Tissue using Magnetic Topographical Cues

A. K. Mansoor [1], A. Omidinia-Anarkoli [2], L. De Laporte [2], L. van IJzendoorn [1], K. Ito [1], J. Foolen [1]

[1] Department of Biomedical Engineering, Eindhoven University of Technology, PO Box 513 5600 MB Eindhoven, The Netherlands
[2] DWI Leibniz Institute for Interactive Materials, RWTH Aachen University, PO Box 52074 Aachen, Germany

Introduction: Tendons, which connect muscle to bone, are comprised of longitudinally-packed collagen type I fibres at length scales that range from the nano to the macroscale [1]. The main cell type in tendons, tenocytes, are arranged in between these collagen structures [2]. The strong anisotropy of the tendon's collagen matrix network results in a high cell aspect ratio, co-aligned with the collagen, ideal for proper tendon functioning [3].
However, in tendinopathy, i.e., tendon disease, cell and matrix anisotropy are lost, affecting tissue function and thus increasing rupture risk. As cells are known to be able to manipulate collagen organization [4], we hypothesise that recovering the lost cell alignment promotes functional remodelling to anisotropic and healthy tendon. Our aim was thus to control cell aspect ratio and orientation, using injectable magnetic rods, in an isotropic collagen matrix, to promote functional tissue remodelling towards strong collagen anisotropy.
Materials & Methods: Super Paramagnetic iron-oxide nanoparticle MicroRods (SPµRs) were used to provide topographical cues to the cells.

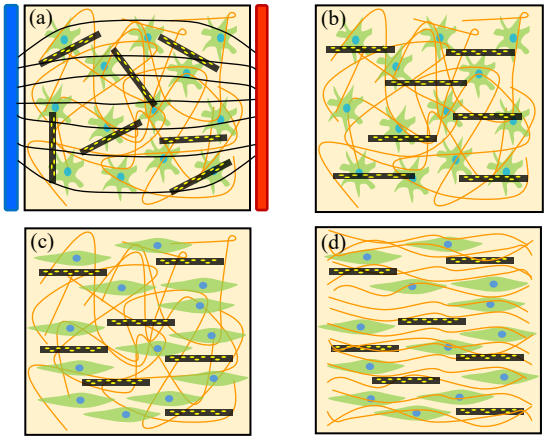

Figure 1: Graphical representation of experimental steps; SPµRS (black), collagen (orange), cells (green)

Miniaturised tendon tissues that mimic a tendinopathic isotropic collagen matrix were created in-vitro by embedding the SPµRs in a gel mixture of collagen type I and tendon derived cells. The SPµRS were aligned using an external magnetic field (fig 1a). Microtissues were kept in culture for 3-6 days, and alignment was assessed using confocal microscopy (fig 1b-d).
Results & Discussion: In the absence of SPµRs, an isotropic distribution of cellular actin stress fibres developed in the microtissues (fig 2a). Whereas in the presence of magnetically aligned SPµRs, microtissues displayed local preferential cellular co-alignment (fig 2b). With these results, it was shown that cells can respond to the topographical cues provided by the SPµRs.

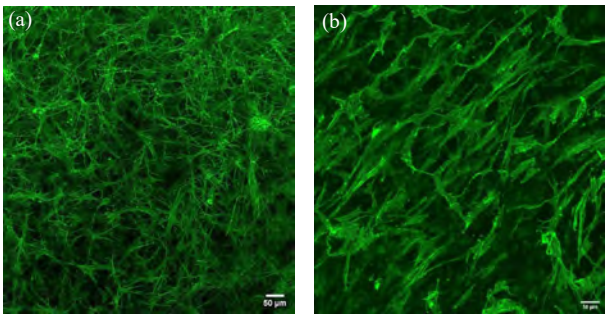

Figure 2: (a) Unaligned cellular actin stress fibres (b) Anisotropic alignment of actin fibres (SPµRs not shown)

However, local densities of cells and SPµRs appeared to be determinant in whether co-alignment was established or not. Currently, the underlying mechanisms that we think are responsible for establishing cell orientation are being explored, e.g., the presence of cell-cell contact, cell-to-SPµRs ratio, cell-to-SPµRs binding affinity, mechanical stimulation.
Conclusion: A tool to promote the functional remodelling of disorganised tissue by promoting cell alignment is being developed. Once the ability to align cells is established, this can ultimately help in reversing disorganised states in tissue to regain structure and function.

References:

1. Gomez-Florit M, Labrador-Rached CJ, Domingues RMA, Gomes ME. The tendon microenvironment: Engineered in vitro models to study cellular crosstalk. *Adv Drug Deliv Rev*. 2022;185.
2. Nichols AEC, Best KT, Loiselle AE. The cellular basis of fibrotic tendon healing: challenges and opportunities. *Translational Research*. 2019;209:156-168.
3. Foolen J, Wunderli SL, Loerakker S, Snedeker JG. Tissue alignment enhances remodeling potential of tendon-derived cells - Lessons from a novel microtissue model of tendon scarring. *Matrix Biology*. 2018;65:14-29.
4. Birk DE, Trelstad RL. Extracellular compartments in tendon morphogenesis: Collagen fibril, bundle, and macroaggregate formation. *Journal of Cell Biology*. 1986;103(1):231-240.

Development of Dissolving Microneedles to Stimulate Polarization of M1-type Macrophages and Lead to Cardiac Repair

M.M. Lobita[1], T. Bauleth-Ramos[1,2], M.-A. Shahbazi[1], P. van der Meer,[1] H.A. Santos[1,2]

[1] Department of Biomedical Engineering and W.J.Kolff Institute of Biomedical Engineering and Materials Science, University Medical Center Groningen/ University Groningen, 9713 AV Groningen, Netherlands

[2] Drug Research Program, Division of Pharmaceutical Chemistry and Technology, Faculty of Pharmacy, University of Helsinki, FI-00014, Helsinki, Finland

Introduction

Myocardial infarction is one of the most common causes of early death in adults worldwide. Two inflammatory phases are present after MI. The M1 macrophages appear in a higher number, in the infarcted area, leading to a dysregulated inflammation interfering with the cardiac repair[1].

Extracellular vesicles are a small heterogeneous population, present in numerous tissues and biological fluids, playing an important role in intercellular communication and immunological responses[2].

Furthermore, microneedles (MNs), a three-dimensional microstructure, are an outstanding transdermal delivery system capable of immunomodulation in a non-invasive and painless manner[3,4].

The hypothesis relies on the development and fabrication of dissolving microneedles, selecting micromolding as the preferred method, to prepare MNs with suitable mechanical properties capable of piercing into skin barrier and deliver the desired cargos, exosomes.

Materials and Methods

The selected method for MNs production was micromolding[5]. Firstly, the polymeric solutions were prepared and, afterwards, the same solution was poured into the top of the molds, followed by centrifugation and vacuum techniques. All the patches were removed from the molds and visualized under bright field microscopy and characterized using texture analyzer. Further characterization will be performed using scanning electron microscopy (SEM).

Results and Discussion

Different concentrations of the selected polymer were tested to form MNs with the proper characteristics. MNs arrays presented an average height of 690±19 µm (Figures 1A and 1B). These microneedles patches showed suitable mechanical properties being able to reach completely the fourth layer of Parafilm M® membrane (Figure 1E) with a depth of approximately 500 µm.

Conclusion

This initial data shows the successful formation of MNs with suitable properties, capable of reaching the desired layer to efficiently deliver the bio cargos.

We look forward to, after collecting all data, effectively delivering exosomes, while stimulating macrophage polarization in order to regulate inflammation and promote cardiac tissue regeneration.

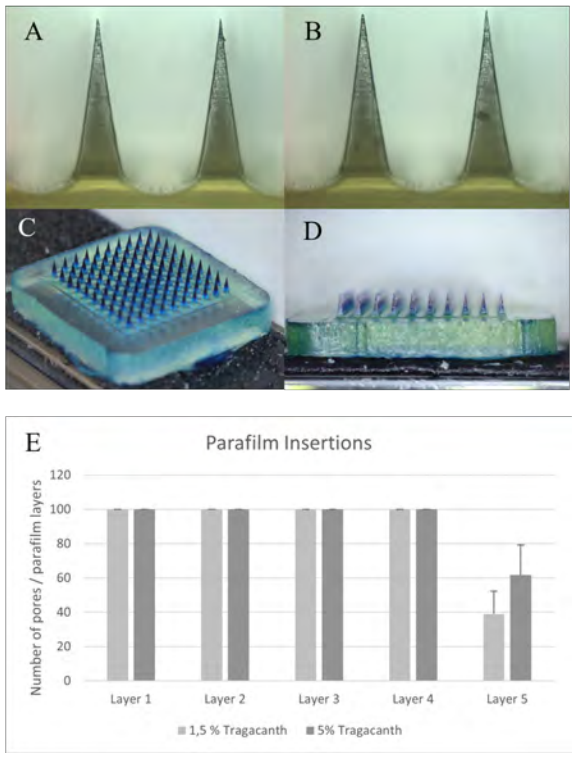

Figure 1: (A) and (B) light microscope images, magnification 10x. (C) and (D) Brightfield microscope images from MN patch, top view, and side view, respectively. (E) The number of pores counted in each layer of Parafilm® after MNs penetration.

References

1. Zhang *et al.* Signaling pathways and targeted therapy for myocardial infarction. *Signal Transduct. Target. Ther.* **7**, 78 (2022).
2. Jung *et al.* miR-106a–363 cluster in extracellular vesicles promotes endogenous myocardial repair via Notch3 pathway in ischemic heart injury. *Basic Res. Cardiol.* **116**, (2021).
3. Ali *et al.* Dissolvable polymer microneedles for drug delivery and diagnostics. *J. Control. Release* **347**, 561–589 (2022).
4. Prausnitz. Engineering microneedle patches for vaccination and drug delivery to skin. *Annu. Rev. Chem. Biomol. Eng.* **8**, 177–200 (2017).
5. Sabbagh and Kim. Recent advances in polymeric transdermal drug delivery systems. *J. Control. Release* **341**, 132–146 (2022).

Porous *in vitro* Model with a Wrinkle Topography to Mimic Tunica Media of a Blood Vessel

K.M. Jurczak[1*], R. Zhang[1], R. Schuurmann[2], H.G.D. Leuvenink[3], J.L. Hillebrands[4], R. Bank[4], J.P.P.M de Vries[2], P. van Rijn[1]

1. W.J. Kolff Institute for Biomedical Engineering and Materials Science, University Medical Center Groningen, Groningen, The Netherlands
2. Department of Surgery, University Medical Center Groningen, Groningen, The Netherlands
3. Department of Cardiology/Thoracic Surgery, University Medical Center Groningen, Groningen, The Netherlands
4. Departement of Pathology and Medical Biology, University Medical Center Groningen, Groningen, The Netherlands

*k.m.jurczak@umcg.nl

Key words: *blood vessel engineering, high throughput screening platform, porous poly (trimethylene carbonate)*

INTRODUCTION:

Although the replacement of live animal models in biomedical research and reduction of animal distress led to the rapid development of blood vessel scaffolds, the ideal vascular model remains a challenge and prevents the standardized studies in cardiovascular diseases (CVD) research. The engineered artery should resemble the 3D geometry of native blood vessel and reconstitute its three layers including tunica intima, tunica media, and tunica adventitia (1). The medial layer consists of circumferentially oriented smooth muscle cells (SMCs), which are responsible for the contractile function of a blood vessel. We hypothesized that the accurate representation of the cellular orientation of SMCs is paramount to the success of a functional blood vessel scaffold. In this study, we translate optimal topography as determined via high-throughput screening (HTS) to the fabrication of a vascular scaffolds from biodegradable and biocompatible polymer - poly(trimethylene carbonate) (PTMC) (2). Our research focuses on directing smooth muscle orientation hence, we are investigating the biophysical factors such as anisotropic topography using in house high throughput screening platform (HTS). The technology enables to identify optimum material parameters in a single cell experiment at the same time evading adverse effects of cell-material interactions (3).

EXPERIMENTAL METHODS:

The PTMC films were prepared by the means of freeze extraction and exhibited interconnected porous structures and gel content around 80%. The film morphology was investigated using scanning electron microscopy (SEM). To promote continuously varying surface parameter, PTMC was directly imprinted from stretched and plasma oxidized PDMS molds as described previously (4). The SMCs derived from porcine origin were further used for an alignment and smooth muscle marker expression screening on a wrinkle topography.

RESULTS AND DISCUSSION:

The SEM data showed that pore size diameter is in range of 0.5 μm to 140 μm on the air side of the PTMC film and from 0.7 μm to 181 μm on the bottom side. A mean pore diameter was 11.3 μm and 22.3 μm on the air and bottom side of the PTMC film, respectively. The PTMC anisotropic topography gradients were characterized via atomic force microscopy (AFM). Measurements of created wrinkles were taken along the surface gradient. AFM data revealed that the wavelength (W) and amplitude (A) of the wrinkles increased from the least exposed side of the prism mask – W: 1.4 μm, A: 121nm; to the most exposed side of the prism mask – W: 5.3 μm, A: 1176 nm.

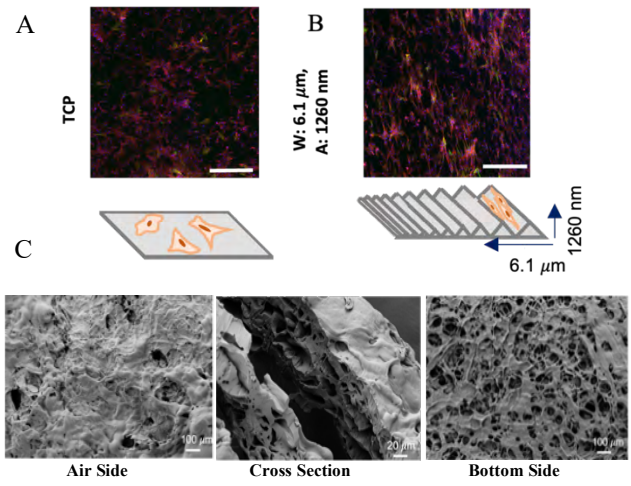

Figure 1 *Smooth muscle cells after 3 days of culture on a tissue culture plate (**A**) and a wrinkle gradient (**B**) (cytoskeleton is presented in red, smooth muscle actin expression is shown in green; cell nuclei is visible in blue) scale bar 500um. SEM images of porous PTMC prepared by freeze extraction method (**C**).*

CONCLUSION:

We performed a topography screening on SMCs to determine the optimum topography for alignment which were successfully transferred to PTMC via imprinting technology. In parallel we identified the optimum method for creating the porosity in PTMC films pivotal for the flow of nutrients in a blood vessel model. In the next steps, the combination of the surface topography and porous structures will be incorporated to the PTMC films. Development of such tissue engineered vascular scaffolds can provide a real benefit in pre-clinical testing of CVD.

REFERENCES:

1. T. Wu, *et al.*, *ACS Appl. Bio Mater.* **1**, 833–844 (2018).
2. Z. Guo, D. W. Grijpma, A. A. Poot, *Polym. Adv. Technol.* **28**, 1239–1244 (2017).
3. L. Yang, K. M. Jurczak, L. Ge, P. van Rijn, *Adv. Healthc. Mater.* **2000117** (2020).
4. Q. Zhou, *et al.*, *Sci. Rep.* **5**, 16240 (2015).

Oral Session 2

Engineering A Synthetic Niche For Pluripotent Stem Cells

S.M.J. de Jong, P.Y.W. Dankers[1,2,3]

[1]Institute for Complex Molecular Systems, [2]Department of Biomedical Engineering, [3]Laboratory for Cell and Tissue Engineering, Eindhoven University of Technology, P.O. Box 513, 5600 MB Eindhoven, The Netherlands

Introduction

Stem cell morphogenesis heavily relies on cell-matrix interactions. For example, epiblast formation by the inner cell mass of an embryo is induced by the binding of the blastocyst to the ECM of the uterus. This phenomenon is initiated by the binding of β1-integrins to the ECM, which consists mostly of laminin.[1] To mimic this mechanism *in vitro*, a biomaterial is required with suitable bioactive and mechanical properties. Matrigel is a material derived from EHS-mouse tumors, representing a matrix with highly bioactive characteristics. Although it has been shown to be a good candidate[2] for many stem cell studies, it has drawbacks due to its immunogenic properties, batch-to-batch differences and inability to alter the mechanical properties. Supramolecular biomaterials can be used to exactly control the bioactivity and mechanical properties of a material, offering an interesting platform for stem cell research.[3] Here, the use of ureido-pyrimidinone (UPy)-based hydrogels for the culture of human induced pluripotent stem cells (hiPSCs) was investigated.

Materials & Methods

Hydrogels were created by dissolving UPy-PEG and UPy-Gly or UPy-Lys in PBS under neutral or basic conditions. UPy-functionalized peptides were incorporated to introduce bioactivity in the matrices. After neutralization, the dissolved polymers were mixed to induce gelation. For 3D gels, single hiPSCs were mixed into the polymer solutions. For 2D gels, the gels were put in an incubator and hiPSCs were seeded the next day. 2.5D matrices were created by dissolving UPy-Lys with UPy-peptides in the culture medium. For this, hiPSCs were seeded on top of 2D gels and the fibers were added to the medium the next day. All cultures took 3 days and the medium was refreshed every day.

Results & Discussion

Surprisingly, the type of UPy-monomer to form the nanofibers in the gel was found to influence the cell adhesion to the gels. Unlike other cell types, hiPSCs cultured on UPy-Gly-based gels were unable to adhere and survive. The replacement by UPy-Lys significantly improved the cell adhesion, probably due to the positively charged NH_2-group, interacting with negatively charged medium proteins. hiPSCs cultured on top of the UPy-gels form clusters and remain positive for Sox2, Nanog and Oct4. Depending on the dynamics of the gel, the cells can form spreading out monolayers, or more round, 3D clusters. When subjected to 3-days of CHIR99021, the cells lose their Oct4 expression and start to express Brachyury (T) and TBX6, indicating the capacity to form the primitive streak.

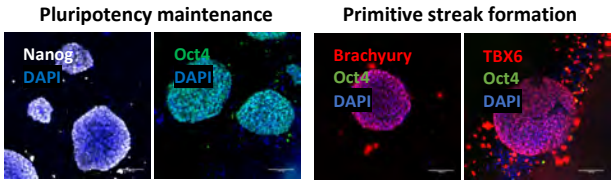

Also in 3D, the chemical nature of the gel influences hiPSC survival and growth. In less dynamic UPy-hydrogels with UPy-cRGD, single hiPSCs are unable to survive. In similar, but more dynamic gels, the cells are able to proliferate and form clusters of cells. To specifically activate β1-integrins, a laminin-derived UPy-IKVAV peptide was incorporated. This improves the proliferation, switches the polarization of the cells, and promotes the formation of epiblasts.

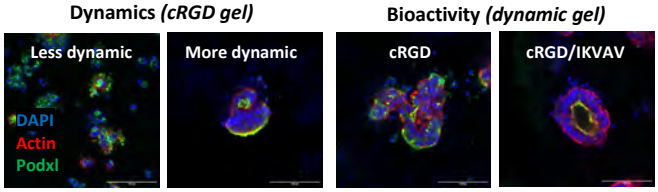

When cultured on top of 2D UPy-hydrogels, hiPSCs form clusters with mostly inside-out polarization. By diluting fibers of UPy-Lys/UPy-cRGD/UPy-IKVAV into the medium (2.5D matrices), we can specifically target β1-integrins on top of these clusters, without any mechanical stimulations. This resulted in a polarization switch and the formation of a (single) lumen, inducing epiblast formation on top of these gels.

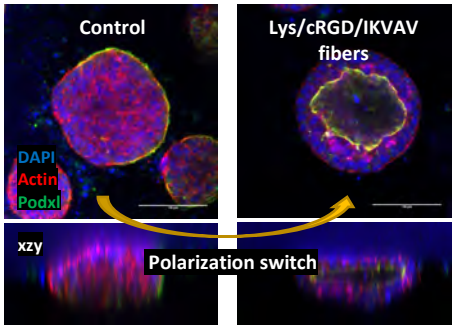

Conclusions

Here, completely synthetic niches were designed for hiPSCs and presented as an exciting alternative for EHS-derived matrices. The supramolecular UPy-system can be used to create 2D and 3D gels for hiPSC cultures, with the ability to vary the bioactivity, dynamics and stiffness of the matrix. The cells remain pluripotent on and in the gels, and retain their differentiation capacity. Interestingly, UPy-fibers in the medium also induce morphogenesis in the cells, creating epiblasts similar to the 3D confinement. These fibers can specifically target integrin receptors to drive morphogenesis, while neglecting mechanical influences. This method could serve as a simple and accessible alternative for 3D cultures. All in all, this supramolecular system proves to be a promising platform for hiPSC cultures.

References

1) Mole, Cell Rep., 2021; 2) Bedzhov, Cell, 2014; 3) Diba, Adv. Mat., 2021

Effect of biomaterial composition on cell migration and tissue formation for cell-free osteochondral defect repair

A.Schwab[1,2], TM.Wesdorp[1,2], J.Xu[2], F.Abinzano[3,4], R.Levato[4,5], C.Loebel[6,7], R.Narcisi[2], J.Burdick[6], J.Malda[4,5], D.Eglin[1,8,9], MJ.Stoddart[1], M.D'Este[1], GJVM. van Osch[2,10]

[1] AO Research Institute Davos, AO Foundation, Davos Platz, CH; [2] Erasmus University Medical Center Rotterdam, NL; [3] Technical University Eindhoven, NL; [4] University Medical Center Utrecht, NL; [5] Faculty of Veterinary Medicine, Utrecht University, NL; [6] Polymeric Biomaterials Laboratory, Department of Bioengineering, University of Pennsylvania, USA; [7] University of Michigan, USA; [8]Mines Saint-Etienne, INSERM, U1059, FR [9] University of Twente, NL; [10] Delft University of Technology, NL

Introduction Despite the improvements in regenerative procedures including autologous chondrocyte implantation, cartilage and osteochondral defects remain a challenge in orthopedic surgery. Cell-free approaches are an alternative to cell-based procedures due to the reduced donor-site morbidity and the possibility of a single-stage procedure. Injectable hydrogels are highly hydrated scaffolds providing a 3-dimensional environment and can be easily filled in the defect. While chondrogenic capacity of gels are commonly investigated, the materials ability to be invaded by cells is often neglected and poorly understood in respect to the hydrogel. The aim of this study was to investigate the effect of the degree of functionalization (DoF), the degradability of the crosslinker and the incorporation of a fibrillar component in 3 biopolymer-based hydrogels on cell migration and related tissue formation *in vitro, ex vivo* and *in vivo*.

Materials and Methods The three hydrogels, gelatin methacryloyl (GelMA, 5% wt), norbornene hyaluronic acid (NorHA, 2% wt) and tyramine functionalized hyaluronic acid (THA, 2.5% wt) hydrogels were modified respectively with DoF 50% and 80%, introduction of a protease degradable crosslinker and addition of collagen fibrils. Mesenchymal stromal cell (MSC) migration was studied *in vitro* using a 3D migration assay (n=5-6 samples per group). Fluorescently labeled MSC were imaged, and migration area was calculated after 48h. Chondrocyte migration was investigated in a bovine cartilage ring model (3 weeks). Safranin O-stained sections were analyzed with a migration score on the presence and location of migrating cells and biomaterial-tissue integration (n=3 samples and 2 locations, 3 blinded observer). Osteochondral defect repair was studied in a semi-orthotopic *in vivo* mouse model (6 weeks, n=5 samples per group) using bovine osteochondral plugs. Hematoxylin and Eosin staining were used and tissue volume (%) within the defect assessed.

Results and Discussion *In vitro* migration assay and *ex vivo* cartilage ring model resulted in similar trends comparing the migration of hMSCs and chondrocytes. A lower DoF in GelMA hydrogels led to a higher MSC migration *in vitro* (p=0.394, Fig. 1A) and a significant increase in migration score (p=0.014, Fig. 1B). The lower crosslinking density showed only a limited improvement in tissue formation *in vivo* (p=0.149). GelMA 50% and 80% DoF had comparable E-modulus (6.8 ± 1.3 kPa vs. 7.3 ± 1.7 kPa). Interestingly, norHA with non-degradable crosslinker (DTT) and higher E-modulus (DTT 36.3 ± 6.8 kPa, MMP 13.4 ± 3.5 kPa) resulted in significant more MSC migration (p=0.002) and migration score *ex vivo* (p<0.001) compared to protease (MMP) cleavable crosslinker. It is possible that the proteases secreted by the MSCs and the cartilage explants in this study are not capable of degrading the peptide of the protease cleavable crosslinker. *In vivo* a significant higher tissue volume was formed in the norHA MMP gels compared to norHA DTT samples (p<0.001, Fig. 1C). The addition of collagen to THA led to an increase in bulk mechanical properties (THA 38.3 ± 8.5 kPa, THA-col: 60.4 ± 24.9 kPa).

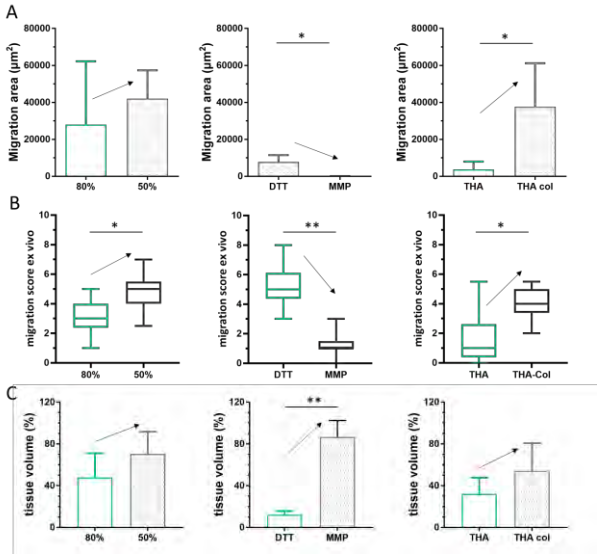

Figure 1: A) MSC migration area B) migration score and C) percentage tissue formation in GelMA DoF 80% and 50%, norHA DTT and norHA MMP and THA and THA-col. Statistical significance * p<0.05, ** p<0.001.

significant increase in MSC migration (p=0.004), a significantly higher migration score (p=0.001) and an increase in tissue volume (p=0.095) compared resulted for THA-col comparted to THA. Collagen forms fibrils within continuous HA matrix that might be sensed by the cells and naturally provides cell adhesion sites that result in increased cell migration.

Conclusion This study showed that hydrogel composition can be used as a tool to control cell migration and tissue formation for cell free osteochondral defect repair. A lower crosslinking density and collagen fibrils positively affect cell migration and tissue formation. The bulk mechanical properties seemed to be not a driving property controlling cell migration. Instead, this study indicates that cell migration is dependent on multiple material characteristics, including physicochemical and bio instructive properties. This study also emphasizes the importance of screening biomaterials with a range of *in vitro/ex vivo* and *in vivo* models to reveal different properties.

Collagen Microparticle Building Blocks for Bottom-Up Bone Tissue Engineering

E. Güben Kaçmaz, P. Habibović, R. Truckenmüller, Z. Tahmasebi Birgani
Department of Instructive Biomaterials Engineering, MERLN Institute for Technology-Inspired Regenerative Medicine, Maastricht University, Universiteitssingel 40, 6229 ER Maastricht, The Netherlands

Introduction: Bone tissue has an intrinsic self-healing capacity, often sufficient to repair small injuries. Yet, it may fall short in case of larger critical-sized injuries, exerting the need for additional treatments such as tissue transplants. Engineered tissues or tissue-mimicking biomaterials are more and more in demand in such cases, as transplants are not always a viable treatment option [1]. Different approaches have been utilized to develop engineered alternatives to transplants with most similarities with the original bone tissue [2]. In this context, the widely used top-down tissue engineering (TE) approach is based on three-dimensional (3D) biocompatible scaffolds that, prior or after implantation in the defect site, can be populated with cells. In this case, upon scaffold degradation over time, de novo bone tissue fills the defect site [3]. Alternatively, in bottom-up TE, cell and (matrix-mimicking) biomaterial building blocks are assembled together to form tissue units. Guided- or self-assembly of building blocks offers a refined control over spatial cell distribution in these engineered tissue units [4]. Here, we opted to use the bottom-up TE approach for generating bone micro tissue units, and to that end, we first created bone matrix-mimicking mineralized collagen microparticle building blocks. These microparticles can later take part in cell-guided assembly to form microtissues with a matrix composition close to that in native bone tissue.

Materials and methods: A 3.7 mg/ml collagen solution in 0.1 M NaOH and 10X phosphate-buffered saline (PBS) was casted onto poly (dimethyl siloxane) (PDMS) templates prepared with a standard soft lithography technique, featuring designed micromolds. In short, the micromolds were degassed to 0.1 atm in a vacuum chamber and while releasing the vacuum, layered with a flat PDMS bearing the collagen solution. Collagen solution consequently filled the micromolds. Followed by fibrillation of collagen at 37 °C, a poly (vinyl alcohol) (PVA) solution was casted onto the PDMS templates and peeled off after drying in order to remove the collagen microparticle from the micromolds. Dissolving the PVA in water resulted in releasing free-standing microparticles. To stabilize the structures of the particles, crosslinking with 50 mM 1-ethyl-3-(3-dimethylaminopropyl) carbodiimide (EDC) and 25 mM N-hydroxysulfosuccinimide sodium (NHS) overnight at room temperature was performed.

Results and discussion: Our preliminary results showed successful application of degassing technique described here for fabrication of collagen microparticles with various shapes and sizes. The particles maintained their shape and structural integrity in the micromolds and also during releasing (Figure 1), and their collagenous composition was confirmed post-fabrication (Figure 2). In the next step, the microparticles will undergo an intrafibrillar mineralization process to mimic the mineralized matrix of bone tissue, and later will be co-aggregated with human mesenchymal stromal cells (hMSCs) to generate bone-like microtissues [5].

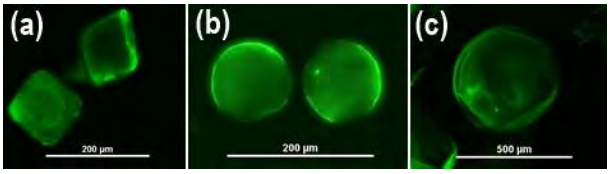

Figure 1. Fluorescent images of collagen microparticles with different shapes and sizes

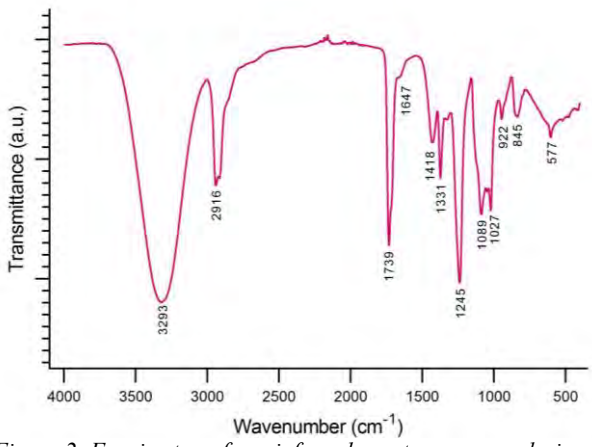

Figure 2. Fourier-transform infrared spectroscopy analysis of collagen microparticles on PVA film

Conclusion and perspective: Here, we have shown the development of collagen microparticles with engineered shapes in a particle replication precision method. These particles will be further characterized and mineralized in order to mimic the composition of the native matrix of bone tissue.

References:

[1] A. Oryan et al., 2014, J. Orthop. Surg. Res. 9(1), 1-27.
[2] L.E. Miller & J.E. Block, 2011, Orthop. Res. Rev. 3, 31-37.
[3] Z. Sheikh et al., 2015, Materials 8(9) 5744-5794.
[4] V.M. Gasper et al., 2020, Adv. Mater.32, 1903975.
[5] D. de Melo Pereira et al., 2020, Front. Bioeng. Biotechnol. 8, 554565.

Acknowledgements: This study is conducted with the support of the Study Abroad Program of the Ministry of National Education of the Republic of Turkey. This research has been in part made possible by the Gravitation Program of the Netherlands Organisation for Scientific Research (NWO) (project "Materials-Driven Regeneration"), the Dutch Province of Limburg (program "Limburg INvesteert in haar Kenniseconomie/LINK"), and the NWO Incentive Grant for Women in STEM (project "Biotetris").

Engineering tissues with multiscale mechanics via modular bio-inks using single cell microniches

Castro Johnbosco[1], Lin Chen[1], Niels Willemen[1], and Jeroen Leijten[1]

[1]Leijten Laboratory, Dept. of Developmental Bioengineering, TechMed Centre, University of Twente, The Netherlands

Introduction

Native tissues are highly complex in composition owing to their inherent hierarchical architecture. These multiscale designs are essential to the multifunctional activities of the tissue. For example, while cartilage is defined by up to several MPa stiffness, the cells within the cartilage matrix experience only kPa stiffness due to the hierarchical and modular design of cartilage. Despite this knowledge, the engineering of tissues, including cartilage, has relied on the use of homogeneous cell-material mixtures. Consequently, engineered cartilage is either initially fully soft (associating with long tissue maturation and patient revalidation) or fully stiff (associating with poor chondrogenesis and fibrocartilage formation). Technological solutions to introduce the spatial hierarchy that defines cartilage structure and function have remained elusive. Here, we propose using modular bio-inks composed of soft single cell microniches within a stiff secondary polymer to introduce the desired hierarchical mechanical properties and functional capabilities within engineered cartilage.

Methodology

Droplet-based microfluidic emulsification was used to position individual single cells inside the center of a droplet made of a polymer solution. Specifically, we emulsified a non-swelling, non-degradable Dextran conjugated with tyramine moieties (Dex-TA) with a 14% degree of substitution containing human mesenchymal stromal cells (MSCs) within a constant oil flow using a focusing microfluidic chip. The emulsion was in-line flown into a distinct microfluidic chip to enable the crosslinking of the microdroplets into microniches via the controlled diffusion of cytocompatible levels of (H_2O_2). The resulting soft single cell microniches were mixed into a polymer solution composed of polyethylene-glycol-dimethacrylate and alginate that upon crosslinking can form a mechanically strong double network hydrogel. The double network hydrogels were obtained via a dual crosslinking strategy, based on initial photocrosslinking to form covalent bonds followed by ionic crosslinking to form dynamic and energy dissipating non-covalent bonds. The stability of modular bio-inks (e.g., absence of diffusion of secondary polymer solution into the microniches) was investigated using fluorescent confocal microscopy. Mechanical properties of single cell-laden micromaterials and macro material were determined using interferometry-based nanoindentation and rheological techniques, respectively. Cytocompatibility of microniches in residing engineered tissue constructs were analyzed and differentiation potential to specific cell type was checked using immunofluorescence imaging and gene expression markers.

Results

Centered single cell microniches and double network hydrogels were successfully produced. When mixed to formulate modular bio-inks, single-cell microniches and secondary polymer remained phase separated as confirmed using fluorescently-labeled polymers and fluorescence confocal microscopy. Rheological and nanoindentation measurements confirmed the decoupled micro and macro environmental mechanical properties, which matched those of natural cartilage. Specifically, the soft single-cell microniches offered pericellular niches with a stiffness of 10 kPa, which was conducive to the chondrogenesis of the microencapsulated MSCs. Notably, we demonstrated that a further increase in microgel stiffness is inversely correlated with the chondrogenic outcome. On the tissue level, engineered constructs were characterized by a 1.3 MPa stiffness owing to the mechanical properties of the double crosslinked hydrogel network. We confirmed that essential molecules such as metabolites could readily diffuse through all areas of the engineered hierarchical cartilage-like constructs. Lastly, MSCs within the engineered hierarchical cartilage-like tissues could effectively undergo chondrogenic differentiation.

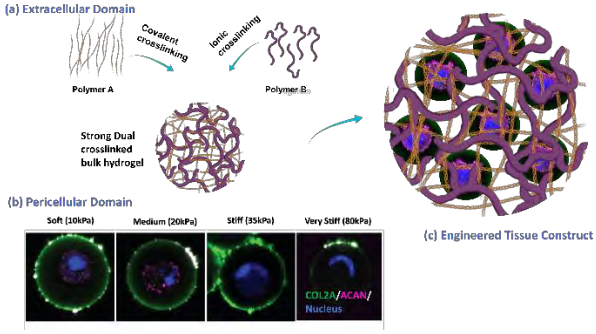

Conclusions

We present a novel approach to endowing engineered tissues with a hierarchical nature that offers highly controlled multiscale mechanical properties, where pericellular and interterritorial matrices can be designed and tuned in an uncoupled manner to resemble native tissue structures.

Acknowledgments

Financial support was received from the Dutch Research Council (NWO, Vidi Grant, #17522).

References

1. de Melo, B et al *Adv. Funct. Mater.* 2019, 29, 1906330.
2. Kamperman.T et al *Adv. Materials*. 2021. 2102660.

Contact

Castro Johnbosco: c.johnbosco@utwente.nl

Microgels as Building Blocks to Bioengineer Tissue Constructs

Maritza M. Rovers*[1-3], Annika F. Vrehen*[1-3], and Patricia Y.W. Dankers[1-3]

[1]*Institute for Complex Molecular Systems,* [2]*Laboratory for Cell and Tissue Engineering and* [3]*Chemical Biology, Department of Biomedical Engineering, Eindhoven University of Technology, The Netherlands*

Introduction

Tissue engineering entails the combination of mechanical, chemical and biological components to process materials that can be engineered towards artificial tissue structures in order to mimic the extracellular matrix (ECM). The ECM provides cells with structural support as well as biochemical, biophysical, and mechanical cues. Biomaterials such as hydrogels have been studied as ECM-mimicking substrates by cell culture to assess the influence of material cues (e.g. stiffness, porosity, and adhesion-ligands) on cellular mechanisms. To study the cell-material interactions, cells could be encapsulated in a micro-hydrogel (microgel). Microgels can assemble into macroscopic aggregates, which are formed due to cell-cell and cell-material interactions by cell migration and proliferation of the cell from the microgel. This principle is attractive in the field of regenerative medicine because microgels are well-defined, injectable, biocompatible, resemble the natural ECM, can entrap cells, and have good regulation over biodegradability, porosity and mechanical properties. For this purpose, synthetic microgels were generated based on supramolecular ureido-pyrimidinone (UPy) molecules according to *Diba et al.* (Fig 1) using droplet microfluidics [2]. Two UPy-molecules can self-assemble by the formation of non-covalent complementary quadruple hydrogen bonds. Bioactivity can easily be introduced to the hydrogel system by a modular approach via the incorporation of UPy-functionalized additives, such as UPy-cRGD. The modularity of the UPy-hydrogel system provides the opportunity to create a variety of different microgel compositions, e.g. bioactivity, mechanics and dynamics.

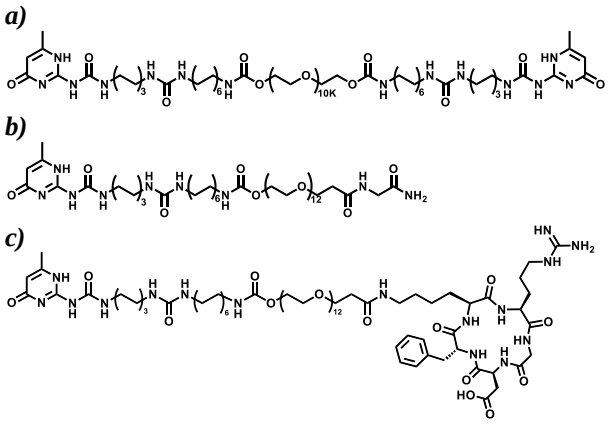

Figure 1. Chemical structures of used polymers: ***a)*** bifunctional UPy$_2$-PEG$_{10K}$, ***b)*** monofunctional UPy-Glycine, and ***c)*** UPy-functionalized additive UPy-cRGDfk to introduce bioactivity.

Results and Discussion

Here we report the encapsulation of primary keratocytes in 2.5 w/v% microgels via droplet microfluidics. At the start, the cell encapsulation rate was 7.8% (Fig 2a). Then, the microgels assembled into macroscopic aggregates via cell interactions by cell migration and proliferation (Fig 2b). At day 10, the cells were fixated and stained for immunofluorescence microscopy (Fig 2 c&d). Cells were positive for α-sma (Fig 2e), YAP was localized in the nuclei (Fig 2f), collagen 6 and tubulin β3 were expressed (Fig 2 g&h, respectively), and cells throughout the whole tissue construct were positive for the proliferation marker ki67 (Fig 2i).

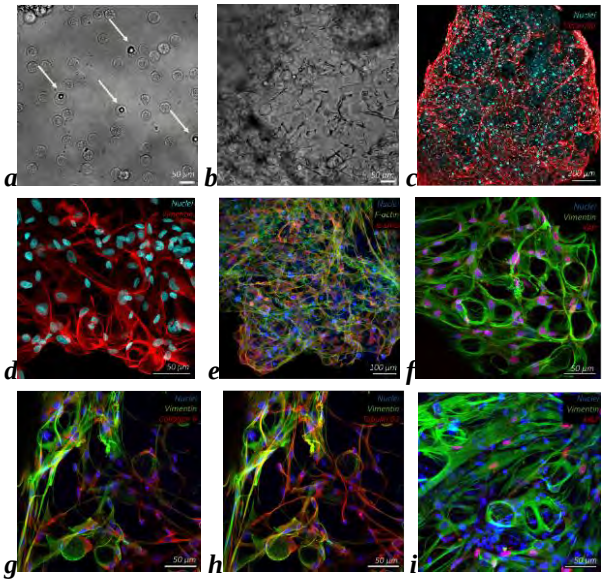

Figure 2. Brightfield images show a ~8% cell encapsulation rate ***a)*** and a cell sheet was formed after 7 days of culture ***b)***. Cells were fixated after 10 days and stained for fluorescence microscopy analysis: ***c-d)*** vimentin and nuclei (red and cyan, respectively), ***e)*** F-actin, α-sma and nuclei (green, red, and blue, respectively), ***f)*** vimentin, YAP and nuclei (green, red and blue, respectively, ***g)*** vimentin, Collagen VI and nuclei (green, red, and blue, respectively), ***h)*** vimentin, Tubulin β3 and nuclei (green, red, and blue, respectively), and ***i)*** vimentin, KI67, and nuclei (green, red and blue, respectively).

Conclusion and Outlook

To summarize, cell encapsulated UPy-based supramolecular microgels were successfully generated by droplet microfluidics and formed aggregates. In general, these microgels are easily tunable due to the modularity of the UPy-building blocks and allow it to be used as building blocks towards bioengineered tissue constructs. In future research, microgel injectability will be further explored.

References

[1] Diba, M. et al., Advanced Materials 33, 2008111 (2021).
[2] Sinha, N., et al., J. Vis. Exp 144, 57848 (2019).

Towards the Engineered Chondron: Pericellular Matrix Synthesis by Articular Cartilage Chondroprogenitors in Agarose and GelMA Microgels

M. van Mourik [1,3], B.M. Tiemeijer [2,3], M. van Zon [1], K. Ito [1,3], J. Tel [2,3], J. Foolen [1,3]

[1] Orthopaedic Biomechanics, Dept. of Biomedical Engineering; [2] Laboratory of Immunoengineering, Dept. of Biomedical Engineering, [3] Institute of Complex Molecular Systems, Eindhoven University of Technology, P.O. Box 513, 5600 MB Eindhoven, The Netherlands

Introduction: In cartilage tissue engineering, chondrocytes are often encapsulated in bulk hydrogels at high densities. However, mass transfer in bulk hydrogels is poor, and chondrocyte expansion while maintaining phenotype is limited.[1,2] To overcome these issues, alternative methods should be explored. Microfluidics produced single cell-laden hydrogel microgels are presented as a system to overcome the heterogenous mass transfer limitations of bulk hydrogels. By exploiting these droplets, this study aims to compare pericellular matrix (PCM) production, a hallmark of chondrogenic characteristic phenotype and the necessary first step in cartilage regeneration, by primary chondrocytes and articular cartilage chondroprogenitors, a potential alternative cell source with increased expansion capabilities.

Methods: Articular chondrocytes were enzymatically isolated from fresh bovine articular cartilage. From the obtained cell population, chondroprogenitors were isolated using the standard protocol involving differential adhesion to fibronectin. A previously described microfluidic device was used for the encapsulation of the cells in microgels (Fig. 1).[3] Cells were suspended in either ultra-low gelling temperature agarose or GelMA. After encapsulation, the hydrogels were polymerized before breaking the oil emulsion with PFO. To determine cell distribution, the microgels were observed with microscopy. Microgels were cultured in 6-wells plates with chondrogenic medium. Cells were provided with one dose of BMP-9 and TGF-β conditioned medium or control medium thereafter, or were stimulated continuously with TGF-β or BMP-9. Cell viability was assessed with trypan blue. Matrix synthesis was assessed with immunostaining for collagen type-II, collagen type-VI and perlecan. Flow cytometry was performed using a FACS Symphony. Cells were imaged using a Zeiss Axio Observer 7 fluorescent microscope.

Results and discussion: Primary chondrocytes and chondroprogenitors were successfully encapsulated in agarose and GelMA microgels. Microscopic observation showed that cell-laden microgels mainly consist of one cell and microgels have an average diameter of 50 µm (Fig 1A). Cells were viable after encapsulation and remained viable for 7 days of culture in control medium. Preliminary results of flow cytometry analysis showed

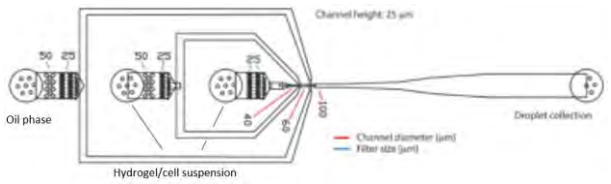

Figure 1: Design of microfluidic device, image edited from Sinha *et al.* [3]

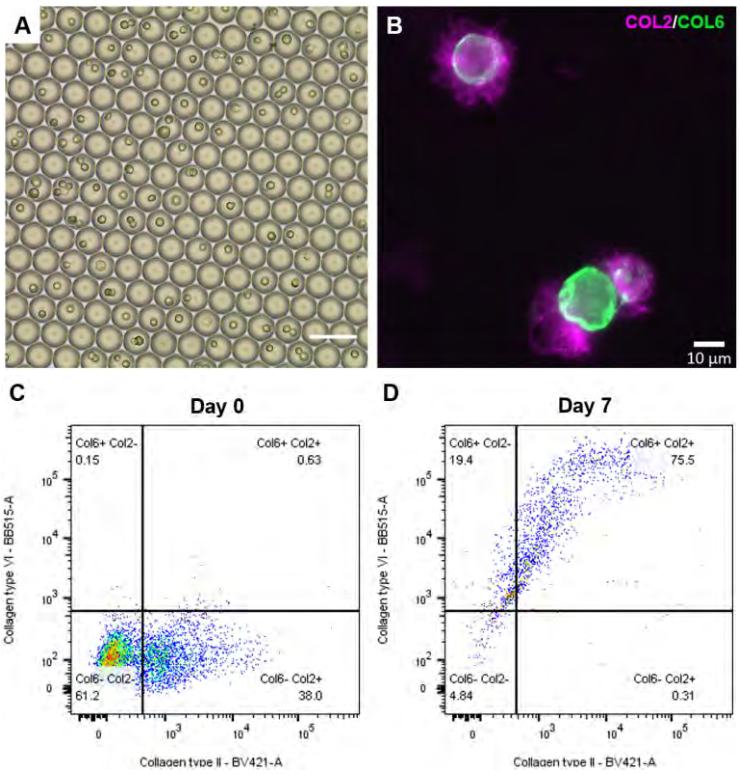

Figure 2: Cell-laden microgels in oil emulsion (A, scale bar = 100 µm). Representative fluorescent microscopy image of chondrocytes in agarose microgels after 7 days of culture (B). Flow cytometry analysis of collagen type-II and collagen type-VI after 0 (C) and 7 (D) days of culture.

that collagen type-II and collagen type-VI were synthesized by chondrocytes in both hydrogel types after 7 days of culture. Interestingly, positive collagen type-II staining always coincided with the presence of collagen type-VI. These results were confirmed by microscopy, showing a compact ring of collagen type-VI and a more diffuse distribution of collagen type-II (Fig. 1B-D). This structural distribution of collagens is similar to the native cell microenvironment. Further analysis and comparison between chondrocytes and chondroprogenitors stimulated with different growth factor regimes are pending.

Conclusion: Chondrogenic matrix production was obtained in cell-laden agarose and GelMA microgels. The presented culture method has great potential for *in vitro* production of articular chondrons.

Acknowledgements: This research was financially supported by the Gravitation Program "Materials Driven Regeneration", funded by the Netherlands Organization for Scientific Research (024.003.013) and the European Research Council (ERC) under the European Union's Horizon 2020 research and innovation program (Grant agreement No. 802791).

References: [1] Liu *et al*, 2015; [2] Parreno *et al*, 2017; [3] Sinha *et al*, 2019

Oral Session 3

Extracellular Protein Identification Cytometry (EPIC) to quantify single cell matrix deposition in high-throughput

Marieke Meteling[1], Castro Johnbosco[1], Tom Kamperman[1], Jeroen Leijten[1]
[1]*Leijten Lab, Department of Developmental BioEngineering, TechMed Centre, University of Twente, Drienerlolaan 5, 7522NB Enschede, The Netherlands,* Contact: m.a.w.meteling@utwente.nl, jeroen.leijten@utwente.nl

Introduction

Analysing the extracellular matrix (ECM) is one of the main methods to investigate cell behaviour, including stem cell differentiation, pathophysiology, and drug responsiveness. Conventional ECM analyses such as western blot, mass spectroscopy, or immunostaining have a destructive nature and/or are incompatible with high-throughput single-cell readouts[1,2]. Consequently, heterogeneity within large cell populations currently cannot be revealed via single-cell ECM analysis. Here, we present Extracellular Protein Identification Cytometry (EPIC) as a novel method that enables the quantification of specific pericellular matrix proteins of individual cells within a 3D microenvironment in a high-throughput manner. A microniche was created around a cell via single cell encapsulation in a hydrogel[3]. Subsequently the cell-laden gels were cultured to allow for matrix deposition. For flow cytometry analysis of the deposited matrix, indirect immunostaining was employed. EPIC enabled quantification of extracellular protein deposition at a single cell level in an ultra-high throughput and non-destructive manner.

Methods

Single cell encapsulation of human chondrocytes was performed with two distinct microfluidic chip designs, one for droplet generation and another for delayed gelation[3]. Chondrocytes were microencapsulated in 5% Dex-TA dissolved in PBS solution and enzymatically crosslinked using HRP and H_2O_2. To obtain the highest purity of single cell microgels, one in ten microgels contained a cell, as dictated by the Poisson distribution[4]. Microencapsulated cells were retrieved and cultured in chondrogenic medium for three weeks. For indirect immunostaining, microgels were fixed with 4% PFA, permeated using Tween-20, and subsequently blocked with 3% BSA solution. DAPI was used as counterstaining. Imaging was performed with a confocal microscope. A FACS Aria II was used for flow cytometry analysis.

Results and Discussion

Individual cells were encapsulated within hydrogel microniches (Fig. 1A) that could be cultured for three weeks with minimal cell escape[1], which allowed for ECM deposition. Live-dead staining confirmed high cell viability after three weeks of culture (Fig. 1B). As a proof of principle, chondrogenic differentiation was assessed via indirect immunostaining of the cell-laden microgels using antibodies against collagen types I and VI. Collagen deposition was visualized with confocal microscopy to verify that the labelled matrix was located extracellularly (Fig. 1C).

Quantitative analysis was performed with flow cytometry at a rate of up to 1000 events per second. DAPI staining allowed to differentiate between empty and cell-laden gels, and an isotype control was taken along to correct for non-specific binding (Fig. 1D-F). Taking the isotype control signal into account, allowed for efficient gaiting of the single cell microgel population, of which ~80% deposited COL I (Fig. 1E) and ~23% deposited COL VI (Fig. 1F) in a detectable manner. Moreover, levels of matrix deposition varied between individual cells thus revealing heterogeneity in collagen deposition.

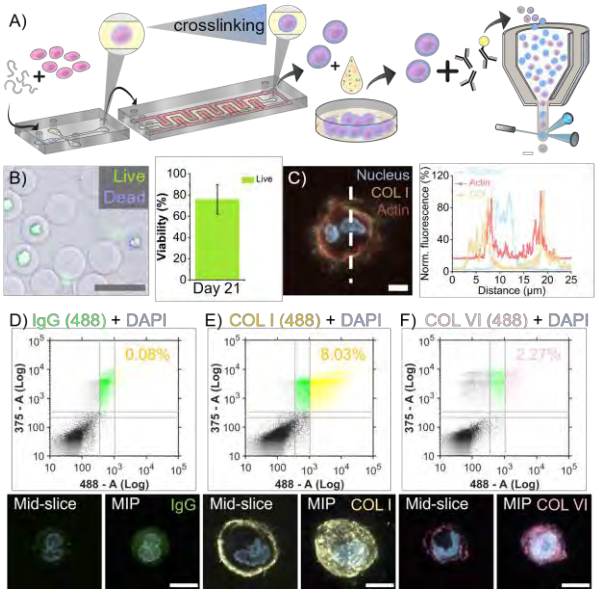

Figure 1: *A) Schematic of EPIC: Cell encapsulation, cell culture, ECM labelling, and flow cytometry analysis. B) High viability following 21 days of culture. C) Cell-laden microgel stained for COL I and actin, confirming extracellular protein labelling, D-F) Flow cytometry results and respective confocal images with isotype control (D), COL I (E) and COL VI (F). MIP: maximum intensity projection, Scale bars: grey 50 µm, white 5 µm*

Conclusion & Outlook

EPIC enabled the detection of extracellular matrix deposition at single cell resolution in high-throughput by immunolabelling microfluidically generated single cell microgels. EPIC is non-destructive and inherently compatible with 3D cell culture. Moreover, we demonstrated that EPIC has the potential to reveal heterogeneity in matrix deposition within cell populations and thus allows for subpopulation analysis.

References

1. Kular JK, et al. J Tissue Eng. 2014; 5
2. Labib M, et al. Nat Rev Chem. 2020; 4 (3)
3. Kamperman T, et al. Small. 2017; 13 (22)
4. Kamperman T, et al. Adv Healthc Mater. 2017; 6 (3)

Acknowledgements

Financial support was received from the European Research Council (ERC, Starting Grant, #759425) and the Dutch Research Council (NWO, Vidi Grant, #17522).

Poly(amido amine) Nanoparticles enable mRNA Delivery into Cells of Cartilaginous Tissues

K.A. Münzebrock[1], A. Pontes[2], F.Y.W. Ho[1], J.P. Garcia[1], J. Rip[2], L.B. Creemers[1]
[1]Dept Orthopaedics, University Medical Centre Utrecht, The Netherlands
[2]20Med Therapeutics BV, Leiden, The Netherlands.

Poly(amido amine) Nanoparticles enable mRNA Delivery into Cells of Cartilaginous Tissues

Authors: K.A. Münzebrock[1], A. Pontes[2], F.Y.W. Ho[1], J.P. Garcia[1], J. Rip[2], L.B. Creemers[1]
[1]Dept Orthopaedics, University Medical Centre Utrecht, Uppsalalaan 8, 3584CT Utrecht The Netherlands
[2]20Med Therapeutics BV, Galileiweg 8, 2333 BD Leiden, The Netherlands.

INTRODUCTION: Osteoarthritis (OA) and inter-vertebral disc degeneration (IVDD) annually affect hundreds of million people worldwide. With pain management and surgical treatment merely alleviating symptoms, currently there are no disease modifying treatment options. Non-viral gene therapy has great potential to address this issue by delivering oligonucleotides that can halt inflammatory and degenerative processes and induce regeneration. In this study we used poly(amido)amine-based polymeric nano-particles (20Medtx) to deliver mRNA to cells of human cartilaginous tissues

METHODS: Human OA chondrocytes, human nucleus pulposus (NP) cells or human annulus fibrosus (AF) cells (3 donors in triplicates each) were seeded into 96 well plates (20,000/cm^2). After 24h they were transfected with nanoparticles (uncoated or PEG-coated) loaded with mRNA coding for EGFP at mRNA concentrations of 0.8 to 3.2 µg/ml (weight ratio mRNA:nanoparticles= 1:25). 24h after transfection, SYTOX™ Orange assay was used to assess toxicity. To assess transfection in 3D, in an IVD model consisting of nucleus pulposus cells within a 2% agarose gel, cells were transfected using concentrations of 1,2 and 4 µg mRNA/ml for up to 96 hours. Gels were cryosectioned and transfection analysed for 2D and 3D culture by confocal imaging and calculating the ratio of EGFP positive cells to total cell count (identified by Hoechst or Dapi stain).

RESULTS: In 2D culture, no significant decrease in cell viability compared to the untreated control cells was observed in most conditions, except for the 2.4 µg/ml concentration in NP cells, in contrast to lipofectamine, which was toxic for both NP and AF cells. The transfection efficiency reached up to 31% in OA chondrocytes treated with PEG-coated or uncoated nanoparticles (fig.1). NP cells reached a maximum of 58% transfection using PEG-coated or uncoated poly(amido amide) nanoparticles ((SD=3.9 and SD=16.3, respectively; fig. 2). In AF cells the transfection efficiency reached a maximum of 39% (SD=4.8) and 44% (SD=13.0) when transfected with PEG-coated nanoparticles and uncoated nanoparticles, respectively (fig. 3). Dose dependency seemed most clear for the coated nanoparticles. In the IVD model transfection efficiency reached up to 23 % (SD=8.9).

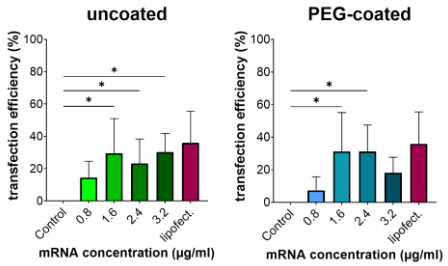

Figure 1:
Transfection efficiency in primary OA chondrocyte

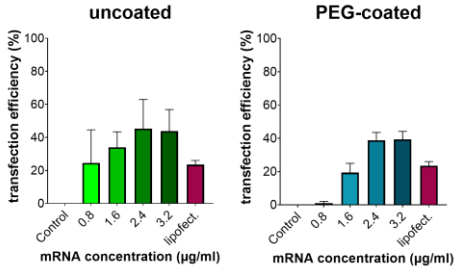

Figure 2:
Transfection efficiency in primary annulus fibrosus cells

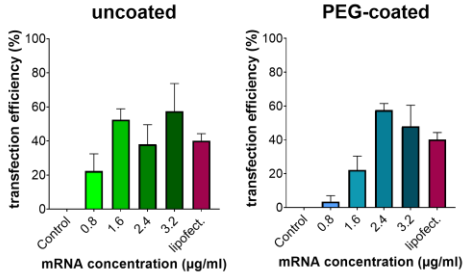

Figure 3:
Transfection efficiency in primary nucleus pulposus cells

DISCUSSION & CONCLUSIONS: We showed a novel way of transfecting primary human cartilaginous cells with mRNA for future therapy in OA and IVDD. The two different nanoparticle formulations showed similar dose dependent transfection efficiency and no impairment in cell viability. Successful transfection of cells within a 3D model indicates the potential of the nanoparticles in more relevant models of OA and IVDD. Next experiments will be focused on the in situ transfection of human cartilaginous cells. Ultimately, the delivery of biologically relevant targets (i.e. mRNA encoding for regenerative factors) will be tested.

ACKNOWLEDGEMENTS: This project has received funding from the European Union's Horizon 2020 research and innovation programme under Marie Sklodowska-Curie grant agreement No. 955335 and grant agreement No. 825925 and the Dutch Arthritis Foundation (LLP12).

Designing the next generation of biomaterials through screening hybrid cell-microparticle spheroidal tissue assemblies

Maryam Parvizifard, Pamela Habibović, Roman Truckenmüller, Zeinab Tahmasebi Birgani
Department of Instructive Biomaterials Engineering, MERLN Institute for Technology-Inspired Regenerative Medicine, Maastricht University, Universiteitssingel 40, 6229 ER Maastricht, The Netherlands

m.parvizifard@maastrichtuniversity.nl

Introduction:
Biomaterials, an integral part of tissue engineering, have a fundamental role in providing housing and (mechanical) support as well as in creating (temporary) extracellular matrix (ECMs) for cells, aiming to instruct and/or maintain cell differentiation and help restoring tissue functions [1].
To date, early-stage assessment of newly developed biomaterials is often based on *in vitro* two-dimensional (2D) cell culture models, which may not fully recapitulate the complexity of cell-cell and cell-matrix interactions provided in three-dimensional (3D) native tissues [2]. Therefore, 3D culture models, for example culturing cells onto a prefabricated scaffold made of new biomaterials, have gained popularity. It is however challenging to achieve desired cell density and homogeneous spatial cell distribution in meso-scale scaffolds. Importantly, tailoring biomaterials' physicochemical and mechanical properties that affect cell fate [3] requires exploring numerous formulations of biomaterials, which may be time-consuming and costly when using meso-scale prefabricated scaffolds.
Therefore, our research group has recently suggested hybrid cell-microparticle spheroidal bottom-up assemblies as an alternative 3D model for the early-stage assessment of biomaterials [4]. As a follow-up, we strive to demonstrate the potential of this model combined with a design-of-experiment (DoE) approach, as a smart screening tool, for designing tailored biomaterials. To that end, we have used three model particle biomaterials, known to be used in bone regeneration, and varied their concentration and particle size to generate biomaterial combinations. The biomaterial combinations will be then screened for their osteogenic properties in a hybrid cell-microparticle spheroid model to identify the most desired biomaterial combinations.

Materials and Methods:
Three model biomaterials, including gelatin (GEL), poly (lactic-co-glycolic acid) (PLGA), and hydroxyapatite (HA), in the form of microparticles with two size ranges were included in this study. GEL microparticles were purchased commercially. PLGA microparticles were fabricated in an oil-in-water single emulsion, with a PLGA in dichloromethane (DCM) and an aqueous Poly (vinyl alcohol) (PVA) solution, respectively as oil and water phases. HA microparticles were fabricated in an oil-in-water single emulsion too, with a slurry made from poly(vinyl butyral) (PVB) in DCM solution mixed with HA nanopowder, and PVA, respectively as oil and water phases, followed by sintering at 1100 °C. A DoE method using Minitab software was used to determine the minimum essential combinations of the three model microparticles needed to explore varying sizes and concentrations. These combinations will be screened for their osteogenic properties in a 3D cell-microparticle hybrid spheroidal model.

Results and discussion:
We could successfully obtain the PLGA and HA microparticles (average diameters for PLGA: 53.6 ± 7.3 and 89.7 ± 10.5 µm, and for HA: 57.33 ± 11.11 and 94.24 ± 11.9 µm) (Figure 1a-b). GEL microparticle showed average diameters of 42.12 ± 6.4 and 81.07 ± 5.0 µm (Figure 1c). Besides their chemical composition, the three model microparticles presented different surface profiles and microstructures. Screening the defined design space by Minitab (i.e., varying microparticles' concentration and diameter) suggested a screening experiment with 38 microparticle combinations as the next step.

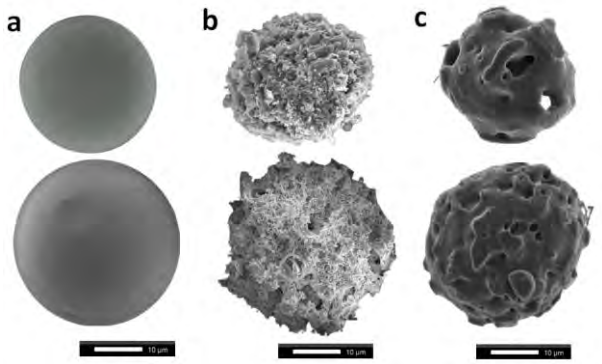

Figure 1. SEM images of a) PLGA, b) HA and c) GEL microparticles.

Conclusion:
Here, we aimed to use hybrid cell-microparticle spheroidal tissue assemblies as a model for high-throughput screening of biomaterials with different properties. We have shown the initial steps including particle preparation and defining the experimental conditions on the screen using a DoE approach. In the next step, we will show the potential of the model for identifying 'hit biomaterial formulations' that, alone or even as hybrid cell-microparticle microtissues, can be used in the next generation of regenerative therapies.

Acknowledgment:
This research was supported by the NWO Gravitation Program (project "Materials-Driven Regeneration") and the Dutch Province of Limburg (program "Limburg INvesteert in haar Kenniseconomie/ LINK").

References:
1. Thakuri, P.S. et al. Advanced Healthcare Materials 7 (2018) 1700980.
2. Kapałczyńska, M. et al. Archives of Medical Science 14.4 (2018) 910-919.
3. Aguado, B.A. et al. Science Translational Medicine 10 (2018) eaam8645.
4. Fois, M.G. et al. Small 18 (2022) 2202112.

Zinc-doped Hydroxyapatite Nanoparticles for the Treatment of Bone infection

L.A.B. Cuypers, P. Bertsch, F. Yang, X. F. Walboomers, S.C.G Leeuwenburgh

Radboud university medical center, Radboud Institute for Molecular Life Sciences, Department of Dentistry-Regenerative Biomaterials, Philips van Leydenlaan 25, 6525 EX Nijmegen, The Netherlands

Contact: lizzy.cuypers@radboudumc.nl

Introduction: Osteomyelitis often occurs after hip or knee replacement surgery. The most prevalent pathogen causing osteomyelitis is *Staphylococcus aureus* (*S. aureus*) [1]. Treatment of osteomyelitis often requires a combination of surgical debridement and prolonged use of antibiotics. However, this treatment is not always effective due to 1) antibiotics poorly penetrating the infected region, 2) multidrug-resistant bacteria leading to untreatable infections [2], and 3) the ability of *S. aureus* to invade mammalian cells like osteoblasts and survive within these cells. The intracellular survival of *S. aureus* could explain the persistence of bone infections [1] since antibiotics display poor intracellular retention [3]. Here, we propose the use of hydroxyapatite nanoparticles (HA NPs) to treat intracellular bone infections, due to their structural resemblance to the mineral phase of bone and ability to cross the cell membrane. Doping HA NPs with ions like zinc (Zn-HA NPs) can endow these nanoparticles with antibacterial properties. The aim of this study was to identify the optimal physicochemical properties and concentrations of such antibacterial Zn-HA NPs for the treatment of osteomyelitis.

Methods: Zn-HA NPs were synthesized through a precipitation reaction using calcium acetate, sodium phosphate, sodium citrate and zinc nitrate with three concentrations to obtain Zn-HA NPs with different zinc contents, namely 10, 15 and 20 mol%. Undoped HA NPs were also prepared as a control group. All NPs were characterized by scanning electron microscopy (SEM), dynamic light scattering (DLS) and zeta potential measurement. The crystal structure of the NPs was characterized by X-ray diffraction (XRD) and Fourier-transform infrared spectroscopy (FTIR). The degradation and release kinetics of zinc from the different Zn-HA NPs were investigated at pH 5.5 and 7.4 representing physiological and inflammatory pH values, respectively. Afterwards, the antibacterial effect of the particles against *S. aureus* was investigated at different concentrations using a 24 h time-kill assay. Also, the cytocompatibility of the particles on pre-osteoblastic MC3T3 cells was tested with CCK8 assay.

Results and discussion: SEM images showed spherical particles in all groups. DLS indicated that the particles were 185 ± 3 nm for undoped HA NPs and 250 ± 2 nm for Zn-HA NPs. Zeta potential measurements revealed a surface charge of around -25 mV for all particles. XRD diffractograms and FTIR spectra showed the presence of characteristic peaks of HA in all samples. Release kinetic data showed that all particles dissolved faster in acidic pH compared to more neutral conditions. Generally, faster NP degradation resulted in a faster release of zinc ions. During the time-kill curve assay, adding Zn-HA and HA NPs delayed the *S.* aureus bacteria from entering the log phase in the growth curves in a dose-dependent manner when compared to the no-treatment control group (Figure 1 and 2). This confirms the antibacterial effect of the particles which increased with increased zinc doping concentration. Cytotoxicity assays showed that Zn-HA NPs in concentrations up to 2 mg/ml did not influence the metabolic activity of pre-osteoblast MC3T3 cells after 24h compared to the control group. However, prolonging the culture to 72h shows decreased metabolic activity of the pre-osteoblast MC3T3 cells exposed to ≥ 1 mg/ml Zn-HA particles compared to the no-treatment control group.

Conclusion: Different Zn-HA NPs were successfully synthesized and all NPs delay the *S. aureus* bacteria from entering the log phase while being cytocompatible for MC3T3 pre-osteoblast cells. The antibacterial effect was enhanced by increasing the zinc doping concentration. Future studies will include co-culture studies of *S. aureus* and pre-osteoblast MC3T3 cells to investigate the ability of the different Zn-HA NP to kill intracellular bacteria.

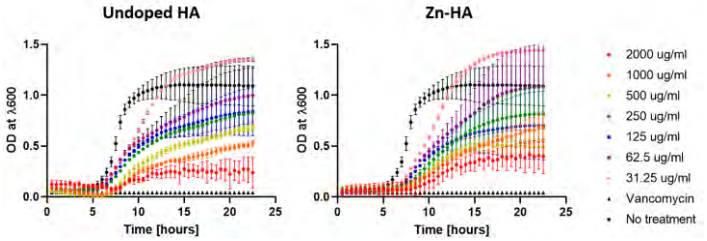

Figure 1: A typical 24 h Time-kill curve assay of Undoped HA and Zn-HA NPs in particle concentrations of 2 mg/ml till 31.25 ug/ml against S. aureus.

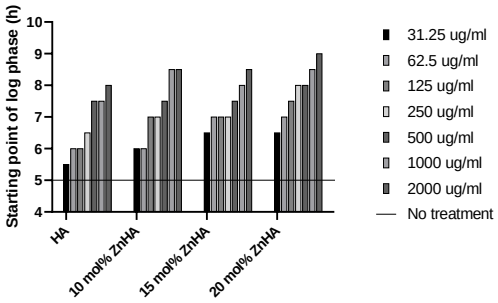

Figure 2 Starting point of the bacterial log phase delays with increasing particle concentration.

Bibliography:

[1] Lew, D.P. and F.A. Waldvogel, *Osteomyelitis.* he Lancet, 2004. **364**(9431): p. 369-379.

[2] Blair, J., et al., *Molecular mechanisms of antibiotic resistance.* Nature reviews microbiology, 2015. **13**(1): p. 42-51.

[3] Barcia-Macay, M., et al., *Pharmacodynamic evaluation of the intracellular activities of antibiotics against Staphylococcus aureus in a model of THP-1 macrophages.* Antimicrobial agents and chemotherapy, 2006. **50**(3): p. 841-851.

Mechanically and chemically tunable microcarriers using In-air-microfluidics for enzyme-free cell release

Luanda Lins[1], Tom Kamperman[1], and Jeroen Leijten[1]
[1]Leijten Lab, Dept. of Developmental BioEngineering, TechMed Centre, University of Twente, Enschede, The Netherlands
Contact presenting author: l.chavesvieiralins@utwente.nl

INTRODUCTION

3D cell culture microcarriers feature a high surface area to volume ratio, which allows more cells to connect per culture volume. Conventional microcarriers are designed to promote effective cell attachment and a high rate of cell proliferation. However, the cell harvest step is still challenging for many microcarriers as it can associate with a complex procedure, which hinders scaling-up of production, causes significant cell loss, reduces viability of harvested cells, and causes cell-product contamination [1]. In order to overcome these problems, we designed an innovative dissolvable microcarrier for bioreactor cell culture with an efficient harvest. The use of dissolvable microcarriers at the end of the cell culture is a strategy that allows to eliminate the respective separation step with benefits in terms of cell yield and cell-product purity [2]. The here presented soft, on-demand dissolvable, cell microcarriers do not require enzymatic degradation or chemical destabilization of the polymeric substrate, but rather depend only on the material used to manufacture the microcarrier. These next-gen, soft, dissolvable, scalable microcarriers were produced in monodisperse and ultra-high throughput manner by combining soft biomaterials with In-air microfluidics (IAMF), which is a scalable microtechnology that was recently invented in our lab [3].

EXPERIMENTAL METHODS

To generate microgels, a piezo-actuated microjet composed of 1% (w/v) alginate (80-120 cP) was collided with a continuous microjet of 0.01 M CaCl2 and 10% (v/v) ethanol (EtOH) allowing for Marangoni flow-driven engulfment of alginate microdroplets. Physical cross-linking occurred immediately after impacting the calcium chloride solution due to outside-in diffusion of calcium ions (Figure 1-a). Microgel size, sphericity, and monodispersity of microgels were characterized using phase contrast microscopy. Surface biofunctionalization was performed using electrostatic interaction between microgels and polyelectrolytes functionalized with RGD-peptide moieties. C2C12 myoblast were used as a model in order to analyze cell attach and proliferation on soft microcarriers in spinner flasks (shear stress: 70 rpm). Viability was assessed using live/dead staining and metabolic activity was assessed using Presto Blue.

RESULTS AND DISCUSSION

IAMF droplet generation proved to be a viable technology for the reliable ultra-high throughout generation of monodisperse soft microcarriers (220 µm, figure 1-a and -b) with excellent surface biomodification capacity. As demonstrated in Figure 1-c, after three days of culture, numerous cells had adhered to the surface of IAMFs microcarriers. Nine days post-seeding, many of the IAMFs microcarriers were linked together by cells, and numerous tridimensional structures were created by interaction between adherent cells. Moreover, a continuous increase in total viable cell number was demonstrated for at least nine days (Figure 1-c, Figure 1-d), with a daily proliferation yield >20%. Microcarriers could be cytocompatibly and rapidly be dissolved by scavenging alginate's calcium ions via exposure to phosphate buffered saline enabling effective harvest of expanded cells.

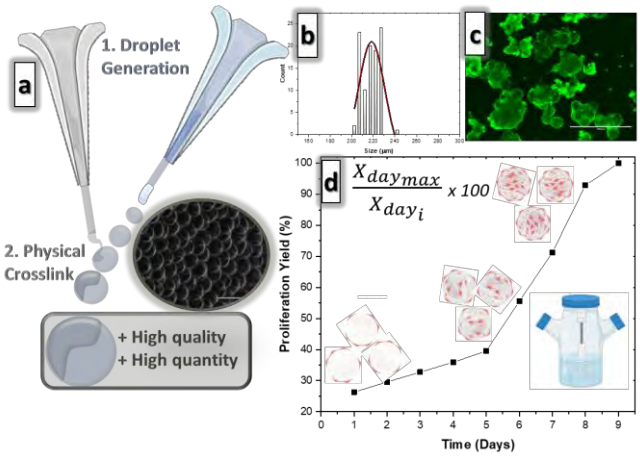

Figure 1. a. Schematic representation of ultra-high throughput production of microgels using in-air microfluidics and physical crosslinking, **b.** Illustrative particle size distribution of alginate microcarriers, **c.** Live/dead image of nine days expanded cell-laden microcarriers, **d.** Fold increase in total cell number was calculated as the ratio $Xday_{max}/Xi$, where X_{max} was the maximum cell density (between day 9 and 1) and Xi is the number of cells microgels were inoculated with.

CONCLUSION

Here, we demonstrate that the use of IAMFs as a promising technology for ultra-high throughput production of microcarriers with adjustable mechanical properties in a manner that allows accurate control over the chemical structure of the surface components of the material.

REFERENCES

1. Rodrigues, A. L.; *et al.*,. *Biotechnology Journal* **2019,** *14* (4), 1800461.
2. Ng, E. X.; *et al.*, *Biotechnology Journal* **2021,** *16* (3), 2000048.
3. Visser, C. W.; *et al.*, *Science Advances* **2018,** *4* (1), eaao1175.

ACKNOWLEDGMENTS

Financial support was received from the European Research Council (ERC Starting Grant, #759425) and European Fund for Regional Development (EFRO #00963).

Protection of DNase in the shell of a pH-responsive, antibiotic-loaded micelle for biofilm targeting, dispersal and eradication

S. Tian[1], Linzhu Su[2], Yingli An[2], Henny C. van der Mei[1], Yijin Ren[3], Henk J. Busscher[1], Linqi Shi[2]

[1] University of Groningen and University Medical Center Groningen, Department of Biomedical Engineering, Antonius Deusinglaan 1, 9713 AV Groningen, The Netherlands
[2] State Key Laboratory of Medicinal Chemical Biology, Nankai University, Tianjin 300071, P.R. China
[3] University of Groningen and University Medical Center Groningen, Department of Orthodontics, Hanzeplein 1, 9700 RB Groningen, The Netherlands
Presenting author's email: s.tian@umcg.nl

Introduction

The role of eDNA in maintaining the structural integrity of infectious biofilms is crucial for the protection of bacterial inhabitants against antimicrobials and the host immune system. Deoxyribonuclease I (DNase) is a specific endonuclease facilitating cleavage of single- and double-stranded DNA. The degradation of eDNA in biofilms suggests the use of DNase as a biofilm dispersant to make a biofilm more penetrable. However, DNase, as an enzyme, was easy to be inactivated after administration *in vivo*, which hinder its application in clinical practice.

The present study aims to develop a novel micellar nanocarrier to protect DNase *in vivo*, self-target to infectious biofilms, disperse biofilms and kill its inhabiting bacteria by including antibiotics in the micelle.

Materials and Methods

The micelles were first self-assembled by poly(ethylene glycol)-*block*-poly(ε-caprolactone) (PEG-*b*-PCL) and poly(ε-caprolactone)-*block*-poly(amino ester) (PCL-*b*-PAE). DNase was then conjugated to poly(amino ester) via 1-ethyl-3-(3-dimethylaminopropyl)carbodiimide/N-hydroxysuccinimide coupling. The hydrophobic micellar core was loaded with antibiotics. In addition, the ability of PEG/PAE-DNase micelles, with ciprofloxacin internally core-loaded, to self-target to infectious staphylococcal biofilms, as well as their ability to disperse biofilms and kill its inhabiting bacteria will be studied.

Results and Discussion

Bovine pancreatic DNase was conjugated to poly(amino ester) inside the shell of a micellar nanocarrier composed of PEG-*b*-PCL and PCL-*b*-PAE. At physiological pH, DNase was hidden in the micellar shell, while in the acidic environment of an infectious biofilm, DNase was exposed and degraded the biofilm. DNase protected in the shell of PEG/PAE-DNase micelles maintained a significantly higher concentration during circulation in blood than when dissolved unprotected in blood (Figure 1A). Terminal half-life times of 2.5 ± 0.2 h and 9.7 ± 0.5 h were calculated for DNase and PEG/PAE-DNase micelles, respectively. The prolonged activity of DNase in PEG/PAE-DNase micelles as compared with DNase free in solution during blood circulation *in vivo* is attributed to the combination of in-shell hiding of DNase and PEG preventing non-specific adsorption of blood-borne proteins during blood circulation at physiological pH. To kill bacteria in their biofilm mode of growth, hydrophobic antibiotics were loaded in the micellar core through hydrophobic interaction. A murine pneumonia model was used for *in vivo* evaluation. Survival was maximal for mice treated with ciprofloxacin-loaded PEG/PAE-DNase micelles (Figure 1B).

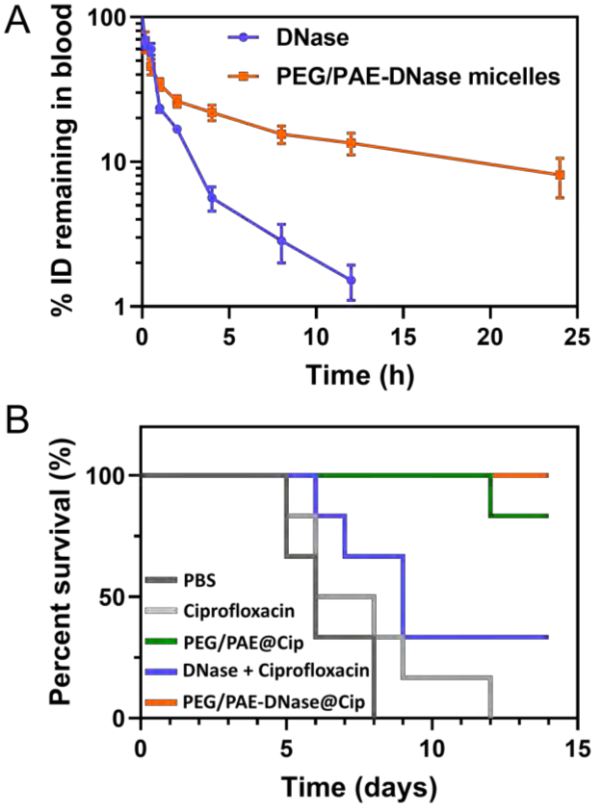

Figure 1. (A) Prolonged blood circulation of DNase in the shell of PEG/PAE-DNase micelles. (B) Kaplan-Meier survival curve of pneumonia infected mice with different treatment groups as a function of time.

Conclusions and Outlook

Dispersing biofilms is more and more accepted for assisting antibiotic killing of bacteria through the degradation of the matrix of infectious biofilms. We successfully synthesized PEG/PAE-DNase micelles with DNase conjugated to PAE-blocks inside the micellar shell and antibiotics loaded in the micellar core. The micellar nanocarriers protected DNase from clearing *in vivo* and enhanced antibiotic killing efficiency.

Development of new antibiotics requires a long time and huge economic costs. The clinical introduction of new antibiotics and the emergence of resistant strains are getting shorter and shorter. Strategies to make better use of existing antibiotics is a more feasible approach in the clinical treatment of biofilm infections to which end PEG/PAE-DNase micelles may contribute.

Oral Session 4

Shrinking Hydrogels By Thermosensitive Interactions: A New Material-based Approach To Enhance 3D Printing Resolution For Kidney Tissue Engineering

G. Di Marco[1], T. Sampon[1], M. Viola[1,2], M. Falandt[3], M. Neumann[1], B. Ilochonwu[1], M.J. van Steenbergen[1], B. G. P. van Ravensteijn[1], R. Levato[2,3], C. F. van Nostrum[1], T. Vermonden[1] (t.vermonden@uu.nl)
[1]Department of Pharmaceutics, Utrecht Institute for Pharmaceutical Sciences (UIPS), Utrecht University, 3584 CG, Utrecht, the Netherlands
[2]Department of Orthopaedics, University Medical Center Utrecht, Utrecht University, 3584 CX, Utrecht, the Netherlands
[3]Department of Clinical Sciences, Faculty of Veterinary Medicine, Utrecht University, 3584 CL, Utrecht, The Netherlands

Introduction

A major challenge in hydrogel 3D bioprinting is fabricating complex tissue-mimicking constructs with physiologically relevant dimensions to ensure their function[1] (Fig.1).

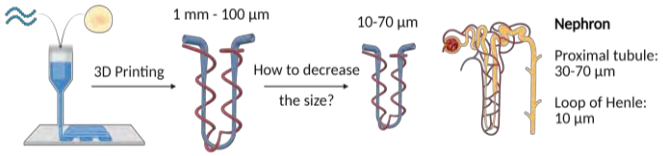

Fig.1 Schematic overview of the main project goal.

Adjusting the printing parameters to enhance the resolution also implies increasing shear strains, which can damage the encapsulated cells. A new strategy to decrease the dimension of the final object while limiting these shear stresses is based on shrinkable hydrogels[2]. This new material-based approach relies on shrinking the hydrogel construct by applying on demand an external trigger after the printing process. The shrinking mechanism is driven by an increase in hydrophobicity of the crosslinked polymers, which leads to partial dehydration/water expulsion and consequently a reduction in size of the printed construct.

Project aim

This project aims at uniformly decreasing the size of a printed hydrogel via a shrinking process driven by a mild, cytocompatible temperature increase. To achieve this, we have developed a new synthetic polymer that has the ability to yield hydrogels via photo-crosslinking and shows thermo-responsive behavior. To imprint thermo-responsiveness, we took advantage of the lower critical solution temperature (LCST) behavior at about 32 °C of incorporated poly(N-isopropylacrylamide) (PNIPAM).

Materials and Methods

The polymer PEG/NIPAM/HEA (PNH) was obtained by polymerizing NIPAM and hydroxyethyl acrylate (HEA) monomers via atom transfer radical polymerization (ATRP) from a bivalent PEG macroinitiator. Subsequently, methacrylate (MA) groups were coupled to the hydroxyl moieties of the incorporated HEA monomers to form PNH-MA. The installed MA groups enables photo-crosslinking. Cylinder-shape hydrogels were prepared by irradiating (@ λ=390-500 nm) PNH-MA solutions in PBS with solid contents of 5, 10, 20 wt% and 0.1 wt% of lithium phenyl- 2,4,6-trimethyl-benzoylphosphinate (LAP) as photoinitiator in silicon molds. For the printability tests, a volumetric printer (@ λ=405 nm) and a 5 wt% PNH-MA solution in PBS with 0.1-0.25 wt% LAP were used.

Results and Discussion

Upon incubation at 37 °C, PNH-MA-based hydrogels with the lowest polymer concentration presented the highest shrinking percentage, as shown in Fig.2. Moreover, the shrinking process was fully reversible when the gels were incubated back to 22 °C. Most importantly, the shrinking/swelling process occurred in a uniform way, so no deformation in the shape of the gels was observed.

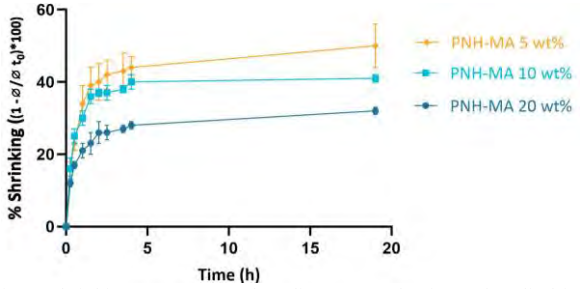

Fig.2 Shrinking percentage by diameter reduction of cylindrical PNH-MA-based hydrogels incubated in PBS at 37°C.

By photorheology characterization, all tested polymer solutions presented nearly instantaneous crosslinking (within 30 sec), and the formed hydrogels became increasingly stiffer as the higher polymer concentrations were used. The same trend was displayed by compressive dynamic mechanical analysis. Since our final target was mimicking the kidney tubular system, objects presenting hollow channels were successfully printed via volumetric printing and uniformly shrunk at 37 °C, as illustrated in Fig. 3. For the printed object in Fig. 3D, the channel average diameter of 608±68 µm was decreased to 397±36 µm via the shrinking process.

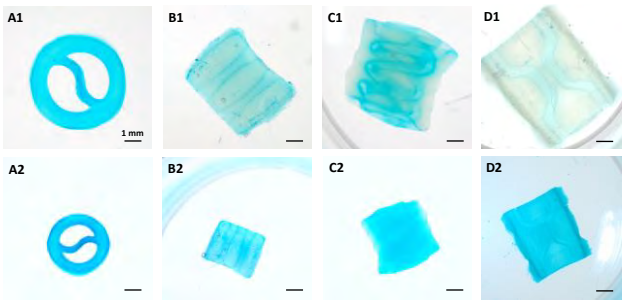

Fig.3 Printed hydrogels: sequence no.1 incubated at 22 °C, no.2 at 37 °C.

Conclusions and outlook

The new polymer PNH-MA was suitable for yielding shrinking hydrogels and showed rapid photo-crosslinking. Gels formed of 5 wt% solutions shrank of about 50% in diameter, displayed adequate mechanical properties for soft tissue applications and excellent printability. Since our final goal is fabricating an advanced *in vitro* model of the nephron with physiologically relevant dimensions, the next steps will be to evaluate cytocompatibility by seeding kidney cells onto the gel surfaces and to further optimize both the printing resolution and the shrinking process.

References

(1) Levato, R. *et al. Advanced Materials* **32**, 1906423 (2020)
(2) Gong, J. *et al. Nature Communications 2020 11:1* **11**, 1–14 (2020)

Fibrous Patterned Melt-Electrowriten Membranes for Proximal Tubule Tissue Engineering

M. G. Valverde[1], L. Benito Zarza[1], A.M. van Genderen[1], T. Vermonden[2], R. Masereeuw[1], M. Castilho[3], S.M. Mihăilă[1]
1 Div. Pharmacology, Utrecht Institute for Pharmaceutical Sciences, Utrecht University, Universiteitsweg 99, 3584 CG Utrecht, The Netherlands
2 Div. Pharmaceutics, Utrecht Institute for Pharmaceutical Sciences, Utrecht University, Universiteitsweg 99, 3584 CG Utrecht, The Netherlands
3 Dept. Biomedical Engineering, Institute for Complex Molecular Systems, Eindhoven University of Technology, De Zaale 7, 5612 AJ Eindhoven, The Netherlands

Introduction

Flat substrates and porous membranes are the gold standard in kidney research, mimicking active and passive transport across the proximal tubule (PT) barrier. While effective, they lack 3D architecture, including curvature and biomimetic extracellular matrix (ECM)-like properties[1,2]. It has been previously shown melt-electrowriten (MEW) porous scaffolds provide topographical guidance enhancing engineered PT performance[1]. However, more insights in how different diameters direct PT function are needed. Thus, we explored the contribution of solid and MEW fibrous substrates in PT cell behavior.

Materials and Methods

CAD designs of grooved patterns were printed with stereolithography (SLA), and the pattern was transferred to aluminium foils via compression moulding. The substrates were placed on top of the collector of a MEW 3D printer, and polycarbonate membranes were deposited on top. The fibrous patterned MEW membranes were characterized with scanning electron microscope (SEM) J. After sterilization, MEW membranes assembled in inserts were biofunctionalized. Conditionally immortalized proximal tubule epithelial cells (ciPTECs) were seeded and cultured at the proliferation permissive temperature of 33ºC and matured at 37ºC. The cell organization and maturation of the cells were characterized via immunostainings for actin filaments, and polarization markers (Na^+/K^+-ATPase, acetylated tubulin).

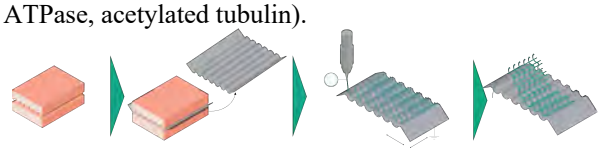

Figure 1. Schematics on patterned MEW membranes preparation.

Results and Discussion

Soft lithography is a versatile tool for creating patterned further used in combination with MEW technologies for creating patterned fibrous membranes (**Fig. 2a**). Cells cultured in the membranes, aligned along the filaments of the membrane, following curvature (**Fig. 2b**).

Conclusions

The combination of silicon soft lithography and melt-electrowriting (MEW) enables the robust fabrication of grooved membranes that support PT phenotypes similar to those seen *in vivo*. Patterned membranes allow transport and barrier studies since apical and basal compartments can be accessed. These engineered PT-membranes allow researchers to investigate the synergistic contributions of curvature and an ECM-like microenvironment that enhance and redefine cell behavior.

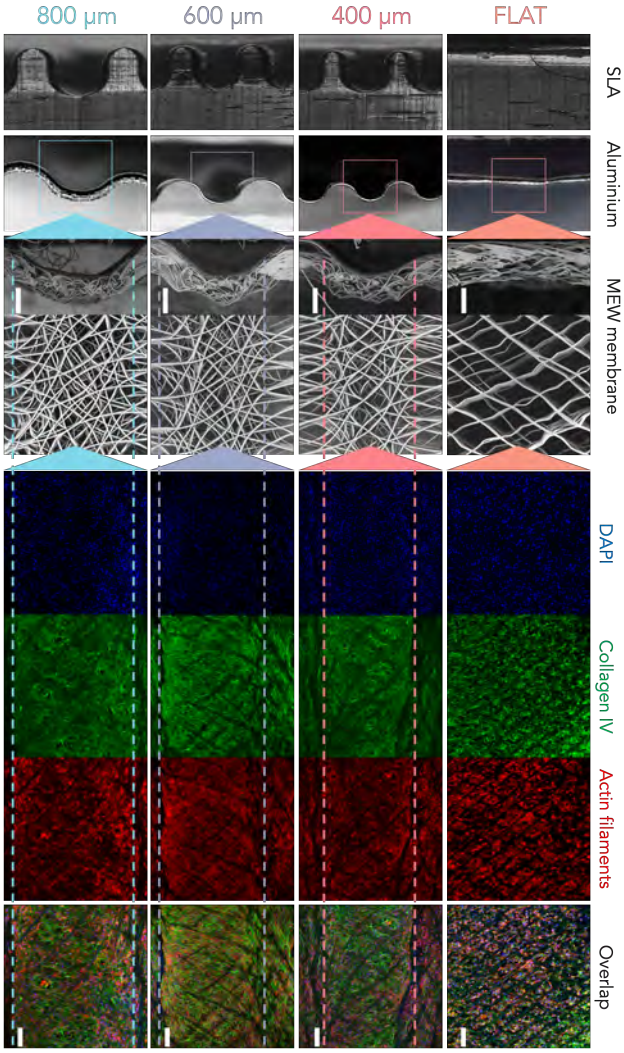

Figure 2. Images of the SLA moulds, aluminium substrates, MEW membranes under the SEM, and immunofluorescent images of the PT cells after maturation for the different groove sizes showing monolater formation and ECM deposition.

References

1. van Genderen et al. Front. Bioeng. Biotech. 8: 617364, 2021
2. Yu et al. A. Biomater. 77: 311-321, 2018

Acknowledgements

Funding for the project provided by Utrecht Institute of Ph armaceutical Sciences, Utrecht University, The Netherlands.

Extrusion-based 3D printing of Fe-based bone substitution

N.E. Putra[a*], L.E. Fratila-Apachitei[a], J. Zhou[a], A.A. Zadpoor[a]

[a]*Department of Biomechanical Engineering, Faculty of Mechanical, Maritime, and Materials Engineering, Delft University of Technology, Mekelweg 2, 2628 CD Delft, The Netherlands*

Abstract

The development of Fe-based materials as biodegradable bone implants has advanced a great deal in the recent years. To guide the bone tissue regeneration, Fe-based bone implants should precisely fit the bone defect structure, have mechanical properties in the range of bone tissue to prevent stress shielding effect, have a high interconnected porosity to allow for bone ingrowth and angiogenesis and be able to biodegrade while providing the temporary mechanical support during the entire process of bone healing process. Today, the slow rate of *in vivo* biodegradation, MRI-incompatibility, and inadequate of osteogenic property have been the main issue preventing Fe-based bone substitutes for use in clinics. Although most of the challenges encountered in developing such implants have been tackled individually or in combination using 3D printing technologies. Yet not all the challenges have been overcome. Here, we propose porous FeMn-akermanite composite scaffolds fabricated by extrusion-based 3D printing to meet all the clinical needs associated with Fe-based biomaterials for bone regeneration.

Extrusion-based 3D printing is a straightforward multi-material additive manufacturing technology, allowing for the addition of alloying elements or reinforcing material components to the primary metallic material (*i.e.*, Fe). We chose Mn as the alloying element to address the ferromagnetic behavior of Fe, and akermanite as the reinforcing element for bioactive property. In addition, Mn and akermanite in the Fe matrix will improve the overall biodegradability of the material. Mn will lower the standard potential of the material, increasing its tendency to corrode, while akermanite bioceramics have a high solubility in bodily fluid.

We developed 3D printable inks (containing Fe, 35 wt% Mn and 20-30 vol% akermanite powder particles) and optimized the 3D printing parameters along with the post-processing steps of debinding and sintering. The FeMn-akermanite composite scaffolds, in a laydown pattern design, possessed a 69% interconnected porosity measured using the oil-impregnation method.

The phases present in the composite scaffolds were the γ-FeMn phase and nesosilicate phases. The γ-FeMn phase made the composite scaffolds weakly paramagnetic, therefore MRI-friendly comparable to Ti6Al4V. The scaffolds possessed a low magnetization value at 2 T magnetic field (*i.e.*, 0.64 Am^2/kg and 0.71 Am^2/kg for Fe35Mn-20Ak and Fe-35Mn-30Ak, respectively), compared to 190 Am^2/kg of pure Fe, fabricated with extrusion-based 3D printing in the same geometrical design.

The *in vitro* biodegradation of the composite scaffolds was assessed with static immersion tests in a revised simulated body fluid under 5% CO_2 atmospheric condition for up to 28 days. The composite scaffolds biodegraded with rates of 0.24 and 0.27 mm/y, respectively for Fe35Mn-20Ak and Fe35Mn-30Ak. These values fall in the range of the ideal biodegradation rate of bone substitutes (*i.e.*, 0.2 – 0.5 mm/year). The biodegradation rates of FeMn-akermanite scaffolds were much higher than those of pure Fe, FeMn alloy scaffolds, Fe-akermanite composite scaffolds, fabricated with extrusion-based 3D printing in the same geometrical design.

The mechanical properties were assessed using a uniaxial compression test. The elastic moduli and yield strengths of the FeMn-akermanite composites were in the range of the values of the trabecular bone, despite *in vitro* biodegradation for 28 days (*i.e.*, E = 0.3–0.5 GPa and σ_y = 3.1–8.3 MPa)

Regarding the biocompatibility and osteogenic potential, the FeMn-akermanite composite scaffolds favored the adhesion and proliferation of preosteoblasts MC3T3-E1, observed *via* live/dead staining assay and SEM imaging. The addition of akermanite into the Fe-based matrix indeed improved the biocompatibility of the material, that otherwise would be cytotoxic. Moreover, the FeMn-akermanite composite scaffolds also allowed the osteogenic differentiation of preosteoblasts, as visualized by Runx2 assay. At day 21 of cell culture, osteopontin matrix can be visualized on composite scaffolds, which highlighted the initiation of *in vitro* biomineralization.

In conclusion, these results show an exceptional potential of the FeMn-akermanite composite scaffolds in fulfilling all the prerequisite of porous biodegradable Fe-based bone substitutes, motivating future research to evaluate their performance *in vivo*.

Keywords: multi-material additive manufacturing; extrusion-based 3D printing; biodegradable; iron; manganese; akermanite; composite; bone substitution

***Email**: n.e.putra@tudelft.nl

Hydrogel Shrinking by Electrostatic Interactions for Resolution Enhancement in 3D Bioprinting

D. Iudin, M. J. van Steenbergen, B. G. P. van Ravensteijn, T. Vermonden
Div. Pharmaceutics, Utrecht Institute of Pharmaceutical Sciences, Utrecht University, 3584 CG, Utrecht, The Netherlands

Introduction:

A major challenge in 3D bioprinting of functional parts of organs using soft hydrogel materials is reaching a sufficient resolution to mimic the complex organization in many tissues. So far, the general strategy to overcome the resolution limitations has been adjusting the printing hardware parameters. Although higher resolutions can be obtained, such a machine-based approach generally results in high shear strains on the printing inks which could be harmful to incorporated cells.

For this reason, we are developing hydrogel materials that can shrink on demand after the printing step. This post-processing leads to resolution enhancement of the (bio)printed structures, allowing us to create realistic in vitro models of complex tissues.

The presented project focusses on a shrinking approach that relies on electrostatic interactions between cationic polymers and hydrogels consisting of crosslinked anionic polymers. This process leads to partial charge neutralization and an increase in hydrophobicity, promoting water expulsion, that, in turn, results in shrunken hydrogels (Figure 1.).[1]

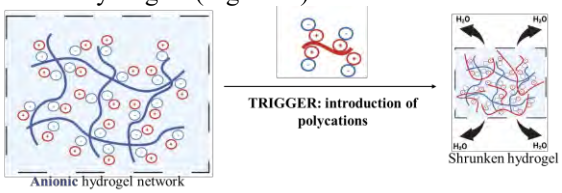

Figure 1. Mechanism of the shrinking process.

Currently, we focus on determining the amount of oppositely charged polymers necessary to reach maximum shrinking. This information will help us to keep the exposure of potentially cytotoxic polycations to cells limited during the shrinking step. Moreover, we investigate the dependence of the shrinking kinetics on different parameters such as molecular weight of the polycation, hydrogel volume, temperature during the shrinking process and hydrogel macromer concentration to make the developed technique tunable and predictable.

Materials and methods:

To address the above mentioned research challenge, a fluorescently labeled polycation was used to quantify the polycation uptake into the hydrogel matrix by analyzing the fluorescent signal reduction of the supernatant.

Specifically, hyaluronic acid (HA) with an average molecular weight of 1.47 MDa was selected to prepare the hydrogel matrix as it is a highly negatively charged polymer under physiological conditions. HA was methacrylated to enable photo-crosslinking of the polymers in the presence of photoinitiator (Irgacure 2595) to obtain mechanically robust hydrogels.

Hydrogels were casted in PDMS molds out of which the final hydrogels with the desired diameter were cut with biopsy punches. Size measurements before and after shrinking were performed using Vernier calipers.

Poly(2-(dimethylamino)ethyl methacrylate) (pDMAEMA) was synthesized by RAFT polymerization and the trithiocarbonate chain end was used to introduce a Cy3-fluorescent label. Additionally, pDMAEMA was quaternized to introduce a higher charge density on the polycation. These polymers were used to investigate hydrogel shrinking, shrinking kinetics and quantify polycation absorption as a function of polymer concentration. All studies were performed in PBS buffer, pH = 7.4 under room temperature.

Results and discussion:

According to HPLC analysis the degree of methacrylation of hyaluronic acid was 28% that was enough to form stable hydrogels at 1 wt% of HAMA and 0.1 wt% of Irgacure in MilliQ water. To obtain a fully crosslinked polymer network we illuminated the samples for 2 minutes (320-500 nm).

pDMAEMA with Mw = 210 kDa and PDI = 1.53 synthesized by RAFT polymerisation was successfully modified with Cy3-maleimide dye. Part of pDMAEMA-Cy3 was quaternized to obtain the fully charged polymer QpDMAEMA-Cy3 as confirmed by ^{1}H NMR.

The comparison of the shrinking extent of HAMA hydrogels for pDMAEMA and QpDMAEMA showed that they present similar efficiency up to 8 times in the hydrogel volume.

The shrinking kinetics for different concentrations of pDMAEMA-Cy3 revealed that the same shrinking efficiency can be reached over time, although, the lower the concentration, the more time it takes. An example of the shrinking process is shown in Figure 2. Moreover, analysis of the absorbed amounts of pDMAEMA-Cy3 showed that the maximum shrinking was achieved close to theoretical point of charge neutralization.

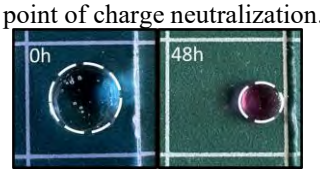

Figure 2. Shrinking of HAMA hydrogel upon exposure to pDMAEMA-Cy3 *(Scale of the square is 100 mm^2)*.

In addition, we determined that the diffusion of pDMAEMA-Cy3 into HAMA hydrogels proceeds via a diffusion front that moves radially inwards, reaching a homogeneous polycation distribution over time.

Conclusions:

1. (Q)pDMAEMA is an effective agent to shrink HAMA hydrogels up to 8 times in their volume. This volumetric shrinkage degree is expected to be sufficient to reach the desired resolution for complex tissue engineering.
2. Relatively low concentrations of polycation can be used to reach maximum shrinking of HAMA hydrogels. This will be beneficial for cell viability and functionality of cell-containing hydrogel objects.

Reference:

1. Gong, J., Schuurmans, C.C.L., et al., Complexation-induced resolution enhancement of 3D-printed hydrogel constructs, Nat. Commun. 11, 1267 (2020).

3D Printed Biocompatible Molds for High Production of Homogeneous Embryoid Bodies for Specific Differentiation

A. Reina Mahecha*, P. Schaafsma, T. van Kooten, I. Zuhoorn, P. Sharma
Department of Biomedical Engineering, University medical centrum Groningen (UMCG), Groningen, The Netherlands

INTRODUCTION

3D printing is a technology that has revolutionized the scientific community due to its versatility for producing prototypes and final products. This technology has significantly reduced outsourcing costs for tissue engineering (TE) and opened doors for new business models. 3D printing Stereolithography (SLA) is a high-resolution technique using resin photopolymerization.

Recently for TE, compared to monolayer cell culture, the incorporation of 3D cell culture techniques, such as spheroid cell aggregates (SCA), is becoming more relevant, as it is possible to understand better intrinsic biological pathways present on target tissues. For this study, SLA was used to create 3D printed molds containing optimal microwells that were cast into polydimethylsiloxane (PDMS) for the formation of SCA. SCA from pluripotent stem cells called embryoid bodies (EB) are widely studied as they emulate early embryogenesis, a fundamental step in cell differentiation[1]. The designed microwells outperformed 2 different commercially available plates and yielded a high production and homogeneous EBs. This system opens the doors for multiple TE applications such as drug testing and cancer research.

KEYWORDS: Tissue engineering, 3D printing, Cell aggregates

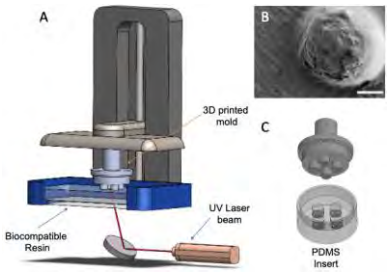

Figure 1. A)schematic overview of SLA printer, B) Printed Microwells SEM Scalebar= 200µm, C) Cast mold on PDMS

EXPERIMENTAL METHODS

The computer-aided design (CAD) to print the molds was developed using SolidWorks software. The molds were printed using the 3B+ printer (FormLabs) with dental biocompatible resin (fig. 1). The printing resolution was analyzed under scanning electron microscopy to determine the minimum microwell size limitation. Conical and semispherical geometries with different radii were tested for the formation of a single SCA per microwell. The molds were cast in PDMS (10:1), degasified by centrifugation, and crosslinked at 70ºC for 3 hours. Casted PDMS was sterilized using a sonicator bath with 70% ethanol. Alternatively, UV-light and autoclaving were also tested to check the hydrophobicity of the material after sterilization.

The pluripotent stem cell guide from Stemcell Technologies™ was followed for culturing Hues9-embryonic stem cells. To test the homogeneity of the EBs on the designed microwells, 2500 and 5000 cells per microwell were seeded and controlled 24, 48, and 72 h after seeding. Then, the microwells were compared to 2 commercially available plates for cell aggregate fabrication. Finally, to analyze the application potential of microwells, a glioblastoma stem cell line (GSC23) was tested for SCA tumor formation.

RESULTS AND DISCUSSION

Due to the printing resolution, microwell radii between 1.5 mm and 500 µm with conical and semispherical geometries were used to test the EB formation. After the assessment, the semispherical 500 µm radius microwells showed the capacity to form a single SCA with homogenous morphology.

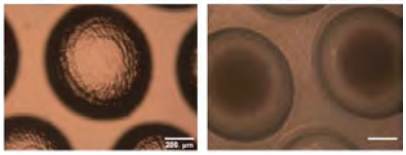

Figure 2. Microwell cast on PDMS and EB after 72h after seeding. (scalebar = 200 µm)

To analyze the size control of the EBs, 2500 and 5000 cells/microwell were used, reporting homogeneous size after 24, 48, and 72 hours of incubation (fig. 2). The possibility of controlling the size of the EBs is a significant advantage of the system as different cell differentiation approaches require EBs of specific sizes ranging between 100 and 300 µm [1]. In comparison with the designed system and the commercial plates. The cast microwells showed outstanding performance and reproducibility.

To extend the application of the system, glyoblastoma stem cells were tested and showed that it is possible to control the size of the SCA, advantageous for oxygen concentration tests, metastasis, and drug treatment assays.

CONCLUSION

The microwells created using 3D printed molds showed the capacity to form numerous homogeneous and size controllable SCA, outperforming commercially available plates. This system will provide better control and flexibility for differentiation applications, and will help to reduce the variance involved in EB-based and cancer research.

REFERENCES

1. Zeevaert. *et al*., cells. 9:10, 2020

ACKNOWLEDGMENTS

The authors would like to thank the Kolff intitute and the UMCG (Project number: 54515) for providing the financial support to this project

Well Organized Melt-Electrowritten Tubular Scaffolds to Engineer Vascularized Kidney Proximal Tubules

Anne Metje (A.M.) van Genderen, E. Al-Jehani[1], M.G. Valverde[1], M.V. Kersten[1], J. Malda[2], J. Jansen[3], T. Vermonden[4], R. Masereeuw[1], S.M. Mihăilă[1], M. Castilho[5]

[1] *Division of Pharmacology, Utrecht Institute for Pharmaceutical Sciences, Utrecht University, The Netherlands*
[2] *Department of Orthopaedics, University Medical Center Utrecht, Utrecht University, Utrecht, Netherlands*
[3] *Department of Pathology and Pediatric Nephrology, Radboud University Medical Center, The Netherlands*
[4] *Division of Pharmaceutics, Utrecht Institute for Pharmaceutical Sciences, Utrecht University, The Netherlands*
[5] *Department of Biomedical Engineering, Eindhoven University of Technology, The Netherlands*

Intro: Kidney tubular engineering requires tubular structures of small sizes (≤ 1 mm) to mimic curvature of native kidney proximal tubule, which is key for cell functionality and maturation. In a proof-of-concept work, we showed that topographic guidance can enhance kidney tubule performance in rhombus shaped melt-electrowritten (MEW) tubular scaffolds [1]. However, endothelial cells did not form monolayers in these scaffolds, and only one winding angle (30°) was studied. Here, we create highly porous rhombus tubules to engineer a vascular and an epithelial tubular scaffold, for the formation of a vascularized proximal tubule.

Materials and methods: A custom-built MEW device was used to fabricate small poly ε-caprolactone (PCL)-tubular scaffolds (inner ∅ ≤ 1 mm) with defined rhombus microarchitectures (winding angles of 30°, 50° and 70°) (Figure 1,2A-C). Printed tubes were functionalized using L-DOPA, whereafter conditionally immortalized proximal tubule epithelial cells (ciPTEC), glomerular endothelial cells (ciGEnC) or a co-culture (Figure 2D) of both cell types was seeded in the tubes. To evaluate the effect of the different winding angles on the cells, various immunofluorescent stainings were performed: F-actin (cell directionality), CD31/ZO-1 (endothelial and epithelial adherent/tight junctions, respectively), and collagen I/IV (extracellular matrix production). Finally, we studied the effect of the winding angles on the mechanical properties before and after *in vitro* culture for 2 weeks.

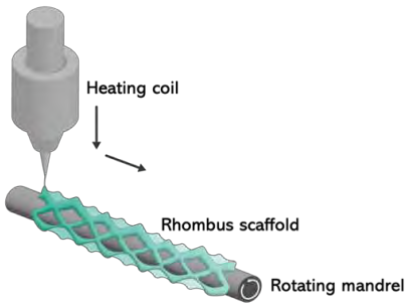

Figure 1. MEW printing set-up

Results and discussion: Engineered tubular scaffolds with different rhombus microarchitectures were successfully manufactured by fine controlling key instrument parameters (i.e. mandrel rotation and translation velocity, accelerating voltage and collection distance). Both cell-lines formed tight, homogenous monolayers within the tubular scaffolds (Figure 2E-F). ciPTEC and ciGEnC indicated the formation of a healthy ECM (low collagen I, high collagen IV expression). CD31 was present in all geometries, while ZO-1 was only expressed in 30° tubes. 30° winding angles caused preferential cell alignment along the scaffold fiber direction for both ciPTEC and ciGEnC. The co-culture system showed that the ECM formed by ciPTEC can function as support for ciGEnC (Figure 2G).

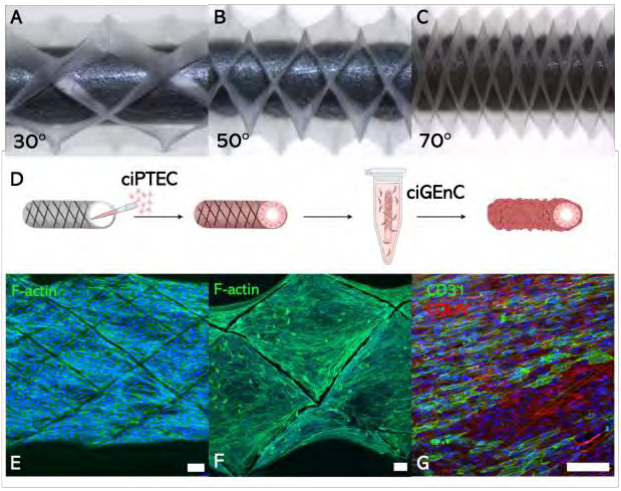

Figure 2. A-C) printed tubular MEW scaffolds D) Graphic of co-culture seeding process E-F) Cytoskeleton organization (F-actin, green, dapi, blue) of ciPTEC.(E) and ciGEnC (F) G) co-culture. scale bar: 100μm

Conclusions: MEW tubes with highly controlled fibrous microarchitectures advance both ciPTEC and ciGEnC cell organization and ECM deposition. Due to the highly porous nature of fabricated tubular scaffolds, cells form the 'only' barrier between the inner and outer lumen. Thus, the MEW scaffolds are not expected to hamper transport from apical to basolateral side and vice versa, which is a limitation of existing tubular scaffolds. In ongoing studies, we are combining both the vascular and proximal units. This will allow us to engineer a vascularized proximal tubule for studying transport between the proximal tubule and its surrounding peritubular capillaries.

References:

1. van Genderen, A.M. et al. Frontiers in Bioengineering and Biotechnology (2021); 1542.

Acknowledgements:
The Dutch Kidney Foundation, the Dutch Research Council, H2020 WIDESPREAD-05-2018-TWINNING Remodel and Health~Holland, Top Sector Life Sciences & Health.

14.00 – 15.30	***Working in- & outside of academia*** ***Panel discussion***

Lorenzo Moroni

Professor at Dept. of Complex Tissue Regeneration
MERLN Institute, Maastricht University

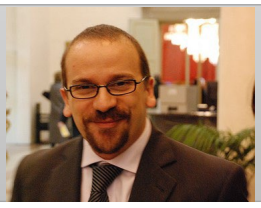

Prof. Dr. Lorenzo Moroni received his Ph.D. cum laude in 2006 at University of Twente on 3D scaffolds for osteochondral regeneration, for which he was awarded the European doctorate award in Biomaterials and Tissue Engineering from the European Society of Biomaterials (ESB). Since 2014 he works at Maastricht University, where he is a founding member of the MERLN Institute for Technology-Inspired Regenerative Medicine. In 2016, he became full professor in biofabrication for regenerative medicine. Since 2019, he is chair of the Complex Tissue Regeneration department. He was vice-director of MERLN from 2019 till 2022. Since 2022, he is director of MERLN.

Lavinia Panella

Application Development Engineer & Sustainability Specialist
DSM Biomedical, Geleen

In 2000, with a master's degree in organic chemistry from the University of Padua, Lavinia Panella moved to the Netherlands to join DSM Corporate Research (Geleen) as scientist with a temporary contract. Afterwards, she received a PhD in organic chemistry from the University of Groningen. She rejoined DSM in 2006 for an industrial post-doc, followed by a permanent position as senior scientist in the same corporate research department. In 2013, Lavinia joined DSM Biomedical as Application Development & Technical Support (ADTS) engineer within the commercial team. In 2020, she transitioned into the current mentioned role within the DSM Biomedical innovation team. At this moment in time, Lavinia is actively working on pursuing a fulltime sustainability-driven career outside DSM Biomedical.

Sieger Henke

Program Manager Microplastics
TNO Energy and Materials Transition, Utrecht

Sieger Henke obtained his BSc and MSc degree in Biomedical Engineering from the University of Twente. He obtained his PhD from the University of Twente on "Microgel technology for improved beta cell transplantation" under supervision of Jeroen Leijten, Aart van Apeldoorn and Marcel Karperien. After finishing his PhD he started in 2017 at TNO as a scientist on particle analysis. Currently he is Program Manager Microplastics at TNO, leading a team of scientists that work on understanding the microplastics problem and developing mitigation strategies. TNO is the Netherlands organization for applied scientific research, an independent research organization with approximately 3500 employees, founded in 1932 to make knowledge applicable for companies and governments.

Lise de Jonge

Head of Dept. MedTech & Health for NWO-domain
Applied and Engineering Sciences

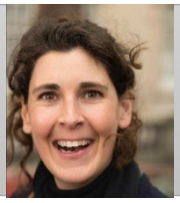

In 2009, Lise de Jonge obtained her PhD in Biomaterials at the Radboud University Nijmegen, after which she was awarded a Rubicon Grant to conduct further research at Imperial College in London. In 2012, she briefly joined Imperial Innovations, a technology commercialisation company, before becoming a policy officer at Technology Foundation STW. Since 2017 STW's activities are incorporated in the Domain Applied and Engineering Sciences (TTW) of the Netherlands Organisation for Scientific Research (NWO), where Lise now heads the Department of MedTech & Health.

Tom Kamperman

CTO and co-founder
IamFluidics, Enschede

Tom is an entrepreneurial biomedical engineer with a strong background in microfluidics, tissue engineering, and enabling (micro)technologies. Before starting IamFluidics, he has been working at various internationally recognized institutes including the Max-Planck Institute in Muenster (DE), the MESA+ Institute for Nanotechnology (NL), the Technical Medical Centre (NL), and the Division of Engineering in Medicine at Harvard Medical School (USA). Tom is co-inventor of the in-air microfluidics technology, co-founder of the company, and responsible for the technical management and product development of IamFluidics. Besides CTO for IamFluidics, he is also affiliated as a Research Fellow in Medicine at Brigham and Women's Hospital (USA).

Oral Session 5

Preventing anoxia induced stem cell death through controlled metabolite release for tissue survival and integration

M. Gurian[1], I.A. Allijn[1], L. Veenendal[1], and J. Leijten[1]

[1]*Leijten Laboratory, Dept. of Developmental BioEngineering, TechMed Centre, University of Twente, The Netherlands*

Introduction: In the last decade, many advancements have been made in the engineering of functional tissue replacements for malfunctioning or damaged tissues and organs[1–3]. However, the current state of the art is mostly limited to the engineering of tissues that are either thin such as skin or bladder[4], or small-sized thus only truly offering solutions to smaller animal models[2]. Scaling up the production towards the engineering of clinically relevant sized tissues currently still faces major unresolved challenges. Specifically, increasing tissue size associates with progressively severe oxygen and nutrient diffusion limitations, which causes cellular necrosis and ultimately implant failure[1–3]. Currently, lack of oxygen is considered the main factor leading to necrotic core formation. As a result, a variety of solutions to oxygenate engineered tissues have been explored, including the development of oxygen-generating biomaterials[5,6]. Despite initial success, the use of oxygen-generating biomaterials associates with the production of highly toxic radicals. Moreover, oxygen sustains cell survival by oxidizing metabolites. However, the availability of nutrients under diffusion limit-induced anoxic conditions has remained largely unstudied, and no metabolite-releasing strategies have been reported. Therefore, we have investigated the effect of various metabolites on cell survival under anoxic conditions.

Methodology: Human mesenchymal stem cells (hMSCs) were seeded at a density of 10^4 cells/cm^2, and cultured without media change for seven days in serum-free and metabolite-free chemically defined media, except for a single type of metabolite that was introduced as the experimental condition. A wide variety of metabolites including various sugars, lipids, amino acids, and vitamins were investigated. Cell viability and functionality were determined using standard cell culture techniques. A glucose release system was engineered by casting polycaprolactone-glucose melt into discs, which were then embedded into gelatin-methacryloyl hydrogels containing 3x10^6 hMSCs/ml. Glucose release was determined using a glucose oxidase-DAB assay.

Results: Sugars consistently allowed for high percentage of hMSC viability, while other metabolites such as lipids and amino acids consistently resulted in massive cell death (figure 1). This indicated that nutrient (e.g., sugar) depravation rather than anoxia induced cell death. Glucose was then chosen as the model sugar that was incorporated in a hydrogel, which acted as a metabolite releasing system. This system was able to maintain viability and metabolic activity in 3D cell laden hydrogel constructs under anoxia for prolonged periods of time. Notably, the glucose concentration not only associated with high cell viability but also with subsequent secretion of high amounts of pro-angiogenic factors such as VEGF (figure 2). This resulted in the vascularization and therefore integration of a subcutaneously implanted tissue. Moreover, unlike commonly explored oxygen generating peroxides, glucose achieved this survival and vascularization in the absence of cytotoxic radical formation.

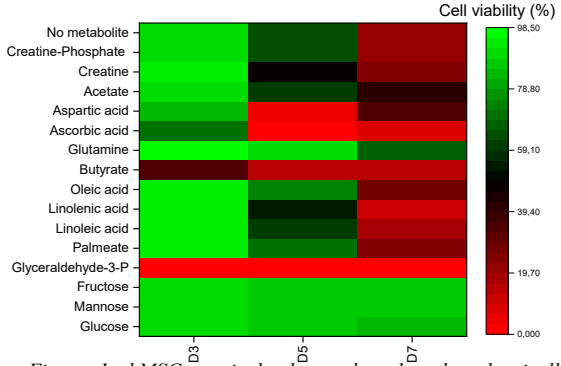

Figure 1: hMSC survival when cultured under chemically-defined media containing a single type of metabolite under anoxic conditions cultured for up to seven days.

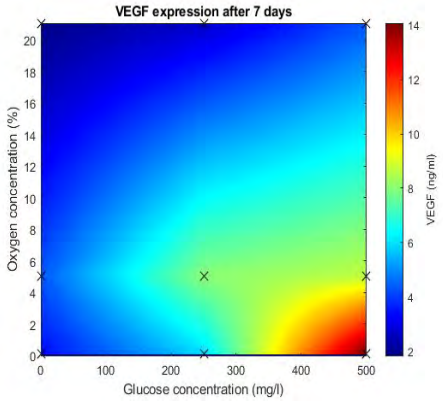

Figure 2: VEGF secreted by hMSCs at different glucose and oxygen concentrations under anoxia after seven days.

Conclusion: Metabolism supporting biomaterials are introduced as a novel method to support implant survival and realize functional integration within a host. Specifically, a glucose is identified as a key metabolite maintain cell survival under anoxic conditions, and controlled release of glucose allows for the survival and vascularization of living implants.

Acknowledgements: Financial support was received from the European Research Council (ERC, Starting Grant, #759425) and the Dutch Research Council (NWO, Vidi Grant, #17522).

References

1. Elkhoury, K. *et al., Polymers (Basel).* **12**, 1–16 (2020).
2. Farzin, A. *et al., Adv. Funct. Mater.* **31**, (2021).
3. Rustad, K. C. *et al., Organogenesis* **6**, 151–157 (2010).
4. Mandrycky, C. *et al., MRS Commun.* **7**, 332–347 (2017).
5. Camci-Unal, G. *et al Polym. Int.* **62**, 843–848 (2013).
6. Ashammakhi, N. *et al. Biomacromolecules* **21**, 56–72 (2020).

Isolation of type III collagen and preparation of type I/III collagen scaffolds for scarless skin regeneration

N.M. Avila-Martinez[1*], R. Krymchenko[1], E.M.M. Versteeg[1], T.H. van Kuppevelt[1], W.F. Daamen[1]
[1]Department of Biochemistry, Radboud Institute for Molecular Life Sciences, Radboud university medical center, Nijmegen, The Netherlands

Introduction: After a full-thickness skin (burn) injury in adults, the end stage of wound healing is characterized by contractures and fibrotic tissue. However, human skin regenerates without a scar in early pregnancy (Lorenz *et al.* 1999). A main difference between fetal and adult wound healing is that type III collagen (Col III) is abundantly present in embryonic skin but not in adult skin. This collagen may promote cell migration and proliferation in wounds. The ratio of type I to III collagen in the human skin differs with age (Cheng *et al.* 2011) (Table 1).

Table 1. Ratio of type I:III collagen in human skin at different life stages.

Col I:III	Life stage
1:2	Fetal
1:1	Newborn
3:1	Adult

In order to test whether type III collagen biomaterials improve wound healing, we isolated soluble type III collagen from human placenta and made scaffolds in combination with insoluble type I collagen.

Materials & Methods: Type III collagen was pre-treated with different combinations of salts and isolated by pepsin digestion, salt precipitations with different NaCl molarities, and filtration to remove molecules smaller than 100 kDa. Protein analysis was performed to determine protein content after isolation. SDS-PAGE and Western blotting were used to detect type III collagen in the sample. Four different scaffolds were prepared: type I collagen only (control) and type I collagen with type III collagen using the ratios in Table 1. In short, collagen was suspended in 0.25 M acetic acid, placed in molds and lyophilized. Scaffolds were chemically crosslinked with EDC and NHS and lyophilized again. Morphology of scaffolds was characterized by scanning electron microscopy (SEM) and localization of type III collagen by immune fluorescence assay.

Results: The procedure for collagen isolation resulted in a high protein content. SDS-PAGE and Western blotting revealed the presence of type III collagen as well as a minor amount of type I collagen in the isolation product and showed that molecules smaller than 100 kDa were successfully removed during the filtration process.
Scaffolds from pepsin-solubilized type III collagen and insoluble type I collagen formed coherent structures after lyophilization. SEM revealed that scaffolds containing type III collagen collapsed somewhat in the top part after crosslinking and this effect increased with increasing type III collagen content. However, pore diameters in the middle of the scaffolds prevailed from 50-100 µm in all scaffolds. Immunostainings showed that type III collagen was evenly distributed throughout the scaffolds, displaying successful incorporation.

Conclusion: Pepsin-solubilized type III collagen was isolated from human placenta using pepsin digestion and salt precipitations. Porous scaffolds made with different ratios of type I/III collagen were prepared and characterized, showing colocalization of type I and III collagen. Further *in vitro* analysis using fibroblasts and macrophages will be performed to evaluate contraction behavior and regenerative capacity of cells in scaffolds.

Acknowledgement: The SkinTERM project has received funding from the European Union's Horizon 2020 research and innovation programme under the Marie Skłodowska-Curie grant agreement No 955722.

References:

Cheng *et al.* African Journal of Biotechnology. 2011;10(13):2524-9.Lorenz *et al.* Plastic and Reconstructive Surgery. 1995;96(6):1251-9.

Development of diagnostic and antimicrobial triggered release systems for wound dressings

Gizem Babuccu[1], Nikitha Vavilthota[1], Jan Wouter Drijfhout[2], Robert A. Cordfunke[2], Colin Bournez[3], Gerard J.P. van Westen[3], Martijn Riool[1], Sebastian A.J. Zaat[1]

[1]Dept. of Medical Microbiology and Infection Prevention, Amsterdam institute for Infection and Immunity, Amsterdam UMC, University of Amsterdam,[2]Dept. of Immunology, Leiden University Medical Center, Leiden, The Netherlands,[3]Division of Medicinal Chemistry, Drug Discovery and Safety, Leiden Academic Centre for Drug Research, Leiden University, Leiden, The Netherlands.

g.babuccu@amsterdamumc.nl

Introduction: Healthcare-associated infections (HAIs) include bloodstream infections, wound infections, urinary tract infections, and pneumonia. These infections can be acquired in any healthcare facility, including hospitals and surgical centers. Specifically, wound infections may be obtained in surgery or trauma and induce systemic infection and sepsis with the contribution of planktonic and biofilm modes of growth of microorganisms. According to the World Health Organization (WHO)'s declaration, increasing morbidity, prolonged hospital stay, and increased treatment costs are the consequence of HAIs. Thus, there is a critical need for novel antimicrobial strategies and products for emerging antibiotic resistance and the search for cutting-edge detection systems. **Goal**: This project aims at assessing the antimicrobial and antibiofilm efficacy of novel cationic antimicrobial peptides (CAMPs[1]) and particularly a group of such CAMPs designated as Synthetic Antimicrobial and Antibiofilm Peptides (SAAPs[2]) against relevant bacterial species for wound infection and urinary tract infection, such as *Pseudomonas aeruginosa, Escherichia coli, Proteus mirabilis*, *Staphylococcus aureus, Acinetobacter baumannii, Staphylococcus epidermidis* and *Streptococcus pyogenes*. **Methods**: A novel set of peptides was synthesized, and their antimicrobial activities under physiological conditions, *i.e.* in RPMI-1640 with and without 50% pooled human plasma, were analyzed by defining lethal concentration effects against planktonic *S. aureus* JAR060131 and the multidrug-resistant *A. baumannii* RUH875. The efficacy of selected lead peptides and their retro-inverso variants (RI), *i.e.* AMP-38, AMP-038-RI, AMP-045, and AMP-045-RI, were compared to promising preclinical and clinical phase peptides. According to the first screening tests, the lead peptides of this set were tested against *S. aureus* biofilms *in vitro*. The possible development of resistance to the lead peptides was assessed against *S. aureus* with a comparison to the clinically relevant antibiotic rifampicin by a repeated minimal inhibitory concentration (MIC) assay for 24 passages. Also, the activity of the peptides against *S. aureus* was investigated in a time-dependent manner. **Results**: We screened a set of peptides for their activity against *S. aureus* and *A. baumannii*, and the lethal concentration killing 99.9% of the inoculum ($LC_{99.9}$) of these peptides in RPMI-1640 ranged from 0.47 to 3.75 µM against *S. aureus* and *A. baumanni.* The activity of the peptides in the presence of 50% human plasma was increased to 0.94-15 µM. Then, we analyzed the degradation potency of pooled human plasma by incubating the peptides for 24 hours in the plasma. 24 hours of pre-incubation resulted in only a 3-fold (AMP-038) or 4-fold (AMP-038-RI, AMP-045, and AMP-045-RI) reduced activity against *S. aureus*. Because resistance development is one of the major concerns, we assessed the ability of *S. aureus* bacteria to develop resistance to the potentially most effective peptide in the set (*i.e.,* AMP-038). No significant change in MIC was observed for *S. aureus* (MIC of 0.94 µM at the first passage and 3.75 µM at the last passage) when cultured in the presence of AMP-038 for 24 passages. On the other hand, the MIC for rifampicin started to increase after five passages and had increased ≥4096-fold after 24 passages (from 0.25 to ≥2048 µg/ml). Moreover, we verified the fast permeabilization of *S. aureus* by AMP-038 and its retro-inverso variant. AMP-038 displayed complete killing within 5 minutes at the concentration of 1.88 µM. Likewise, 1.88 µM of AMP-038-RI showed a 3-log reduction in the number of bacteria within 30 minutes. Lastly, the bactericidal activity of the promising peptides and their retro-inverso variants against established biofilms of *S. aureus* was assessed. Within 2 hours, 60 µM AMP-038 showed more than 3-log reduction against biofilm-encased *S. aureus,* and 30 µM of AMP-038-RI eradicated 99.9% of biofilm-encased *S. aureus* in overnight treatment application. **Conclusion:** Summarizing, we aimed to create rapid screening systems for theranostic antimicrobial devices and to analyze the effectiveness of novel antimicrobial peptides that can be used in wound dressing therapies. In order to achieve this, we showed the antimicrobial and antibiofilm efficacy of the candidate peptides, their lack of resistance development, and fast permeabilization of the bacterial membrane which contribute to the death of the bacteria within minutes.

1. Thapa, R. K., Diep, D. B., & Tønnesen, H. H. (2020). Topical antimicrobial peptide formulations for wound healing: Current developments and prospects. *Acta Biomaterialia*, *103, 52-67*.

2. de Breij, A., Riool, M., Cordfunke, R. A., Malanovic, N., de Boer, L., Koning, R. I., ... & Nibbering, P. H. (2analyzee antimicrobial peptide SAAP-148 combats drug-resistant bacteria and biofilms. *Science Translational Medicine*, *10(423).*

This project received funding from the Dutch Scientific Council (NWO) LIFT program (729.001.024) and has been supported by European Union's Horizon 2020 research and innovation program under the Marie Skłodowska-Curie grant agreement No. 955664.

Preparation of specific elastin hydrolysates and incorporation in biomaterials to enhance skin wound healing

R. Krymchenko, N.M. Avila-Martinez, E.M.M. Versteeg, T.H. van Kuppevelt, W.F. Daamen
Radboud university medical center, Radboud Institute for Molecular Life Sciences, Nijmegen, The Netherlands
Contact: Roman.Krymchenko@radboudumc.nl

Introduction

Elastin is a fibrous extracellular matrix protein involved in tissue elasticity and resilience. Although elastin synthesis is promoted during wound healing, its insufficient and disorganized deposition does not lead to functional tissue generation.[1] Degradation products of elastin direct wound healing by affecting cell growth, migration, proliferation and cellular signalling.[2-3] Importantly, the presence of elastin and elastin degradation products suppresses the differentiation of fibroblasts into myofibroblasts, modulates elastin expression, fibroblast and keratinocyte migration and angiogenesis.[2-3] Elastin-based biomaterials may provide a platform for the development of biomimetic wound management therapies that are clinically and economically effective.[4]

In this study, insoluble elastin was purified from pulverized equine *ligamentum nuchae*. Solubilization of elastin fibres was performed in three ways: by oxalic acid (OxA-ELN), potassium hydroxide (KOH-ELN) or the enzyme elastase (Enz-ELN).

Materials and methods

Purified insoluble elastin was obtained from pulverized equine ligamentum nuchae[5] and purified with various solvents extractions: aqueous sodium chloride, chloroform/methanol, acetone, diethyl ether, cyanogen bromide in formic acid, demineralized water, aqueous urea and β-mercaptoethanol, and a trypsin digestion.

Acidic hydrolysis was performed in aqueous oxalic acid solution at 95°C with collection of the supernatant after each incubation hour. Alkaline hydrolysis was done with KOH in 80% EtOH. For enzymatic digestion elastase from porcine pancreas was used.

Solubilized elastin preparations were neutralized, concentrated, and analyzed with sodium dodecyl sulfate polyacrylamide gel electrophoresis, biochemical methods and size exclusion chromatography. Porous scaffolds were obtained with lyophilization of type I collagen together with 3% or 5% elastin hydrolysates.

Results

SDS-PAGE showed that all preparations formed smears from the beginning of the stacking gel and possessed the proteins with different molecular weights in the particular range. While patterns for OxA-ELN and KOH-ELN were similar, Enz-ELN differed and indicated the presence of lower molecular weights.

Lowry protein assay showed correlation with the yellow colour of the solubilized elastins. For oxalic acid hydrolysis, 14 consecutive incubations were needed, where the total yield of fractions 3-12 was approximately 81% of the starting material.

Size exclusion performed on fast protein liquid chromatography showed that the largest molecular weight of soluble elastin was obtained via fractionated oxalic acid hydrolysis, while enzymatic digestion resulted in the peptides with the smallest molecular weights. Analysis of the number of primary amine groups showed highest values for the enzymatic digest, corresponding to the smallest fragments. Fractions showed homogeneity on basis of molecular mass and concentration both theoretically assessed and practically checked.

Scaffolds made with type I collagen with 3 and 5 % (w/v) of solubilized elastin, by lyophilizing a suspension of type I collagen and OxA-ELN or KOH-ELN followed by chemical crosslinking, resulted in stable, porous, coherent scaffolds with even distribution of elastin proteins. Addition of different elastin hydrolysates did not affect overall crosslinking of the scaffolds as was assessed via TNBS assay. However, crosslinking enhanced thermal stability by approximately 20°C as was determined by differential scanning calorimetry.

Conclusions

Insoluble elastin fibres were solubilized using acidic, alkaline and enzymatic methods. Soluble elastin preparations were incorporated in porous collagen scaffolds. Future studies for scarless skin regeneration will include *in vitro* evaluation of the scaffolds for reduction of myofibroblasts formation.

Acknowledgements

The SkinTERM project received funding from the European Union's Horizon 2020 research and innovation programme under the Marie Skłodowska-Curie grant agreement No 955722.

References

1. Almine *et al. Birth Defects Res C Embryo Today* **2012**. *96;*3:248-257
2. de Vries *et al. Wound Repair Regen* **1994**. *2:*1:37-47.
3. Daamen *et al. Tissue Eng Part A* **2008**. *14*;3: 349-360.
4. Sarangthem *et al. Adv Wound Care (New Rochelle)* **2021**. *10*:5:257-269.
5. Daamen *et al. Tissue Eng* **2005**. *11*;7-8:1168-1176.

VHHs for sequestering endogenous BMP7 in tissue engineering strategies

L.C.M. Morshuis[1], M. Koerselman[2], P. Feng[1], B. Zoetebier[1], L. Zhong[1], I. Voogt[1], H.B.J. Karperien[1]

[1]*Department of Developmental BioEngineering, TechMed Centre, University of Twente, The Netherlands*
[2]*Orthros Medical, Raalte, The Netherlands*

Introduction

Bone morphogenetic protein 7 (BMPs) plays an important role in bone and cartilage tissue engineering and has been shown to induce osteogenesis and chondrogenesis.[1] Attracting endogenous BMP7 to an implanted construct in vivo has the potential to improve tissue reconstruction. Antibodies are capable of capturing and releasing growth factors and thus could be used to decorate a scaffold for tissue engineering. However it is imperative to find the right balance between the affinity of the antibody and the affinity of the receptor for BMP7, see Fig 1a. The affinity of the antibody should be sufficiently high to capture the BMP7, but not too high such that it prevents binding to the receptor. By theoretically describing this dynamic balance one could determine the ideal affinity of the antibody for BMP7. However, for conventional antibodies this is difficult to control. Furthermore they are large in size, expansive and relatively unstable limiting their use for chemical coupling to scaffolds. The variable domain of the heavy chain of heavy chain only antibodies (VHH) presents a better alternative for capturing and releasing growth factors compared to conventional antibodies. They have a high affinity and specificity for their target, are small in size (only 15 kDa) and are easy to produce and modify. By genetic engineering the required affinity can be well controlled. In this research we genetically engineered a BMP7 targeting VHH to obtain a range of binding affinities for the interaction with BMP7. These VHHs were tested in vitro to test whether this dynamic balance ensures an enrichment of BMP7 and therefore increases stimulation of the BMP7 pathway.

Method

Llamas were immunized with recombinant human BMP7 and phage display and bio panning were used to select the best clone. This clone was genetically modified by introducing point mutations to create four variants with different affinities and these affinities were determined via Surface Plasmon Resonance imaging (SPRi). Next to that, SPRi was used to test whether the BMP7 could bind to the VHH and the receptor simultaneously and if the VHH would compete with the BMP type 1 receptor (BMPR1) for binding to BMP7. Furthermore, in vitro tests were performed with C2C12 cells stably transfected with a BMP responsive element (Bre)-Luc reporter for measuring luminescence upon BMP7 stimulation. C2C12 cells were starved for 7 hours and then stimulated with 30 ng/ml BMP7 in the presence or absence of 1 or 100 times molar excess of VHH for 16 hours. Cells were lysed and luminescence was measured using Luciferase Assay Reagent. Luminescence values were corrected via a DNA content measurement.

Results en discussion

The resulting VHHs were denoted as wildtype (WT) and modification 1, 2 and 3 (M1, M2, M3 respectively). SPRi results gave kD values of 1.48 nM, 192 nM, 88.5 nM and 641 nM for WT, M1, M2 and M3 respectively, where a lower kD value represents a higher affinity. This means that the WT VHH has the highest affinity for BMP7 and the M3 VHH has the lowest affinity for BMP7. Next to that, it was shown that BMP7 was able to bind simultaneously to the VHH and its receptor.

In vitro is was shown that the C2C12 cells highly respond to BMP7 stimulation and that an equimolar concentration of the WT VHH and M1 VHH almost completely blocked the induction of luciferase activity by BMP7, see Fig 1b. This suggested that in this situation the binding equilibrium shifted to the VHH/BMP7 complex instead of the BMPR1/BMP7 complex. In contrast, a equimolar concentration of M2 and M3 only slightly inhibited luciferase activity. The 100 times molar excess of VHH over BMP7 showed complete inhibition of BMP7 stimulation for all the VHHs.

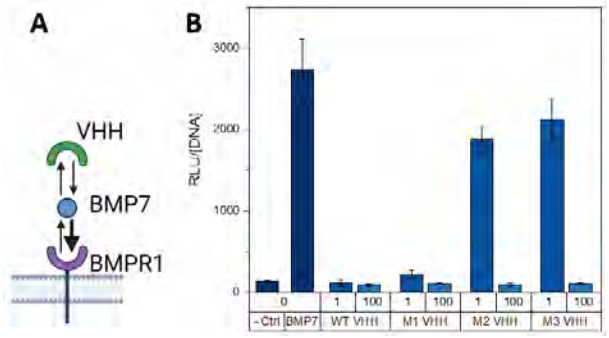

Fig 1. A) Dynamic balance between BMP7, the BMP receptor and a VHH. B) Relative luminescence of C2C12 cells upon stimulation with 30 ng/ml BMP7 in the presence of 1 or 100 times molar excess of VHH.

Conclusion and outlook

Four variants of BMP7-targeting VHHs have been developed which could be used for capturing endogenous BMP7 in a tissue engineered construct. The affinity of the VHH and its abundance relative to the presence of the BMPR1 are critical factors to consider in the engineering strategy. Preliminary data suggests that VHHs with a low affinity for BMP7 compared to BMPR1 may have potential for increasing local binding places for BMP7 without negatively impacting receptor activation. Presently we are testing this concept by coupling these VHHs at various concentrations to hydrogel scaffolds for bone and cartilage tissue engineering.

Acknowledgements

The authors would like to thank Orthros Medical and QVQ Holding for producing the VHHs and Hy2Care for providing the polymers for the hydrogel scaffolds.

References

1. Shen et al, *J. Cell. Biochem.*, 109: 406-416

Contact

Lisanne Morshuis, l.c.m.morshuis@utwente.nl

Harnessing Click-to-Release Chemistry for the Development of Spatiotemporal Signaling Scaffolds

M. Gansevoort[1], J. Merx[2], E.M.M. Versteeg[1], I. Vuckovic[1], T.J. Boltje[2], T.H. van Kuppevelt[1] and W.F. Daamen[1]

[1] Department of Biochemistry, Radboud Institute for Molecular Life Sciences (RIMLS), Radboud university medical center, Geert Grooteplein 28, 6525 GA Nijmegen, The Netherlands
[2] Institute for Molecules and Materials, Synthetic Organic Chemistry, Radboud University, 6500 GL, Nijmegen, The Netherlands

Introduction

The process of wound healing is a tightly controlled cascade of events, where severe skin wounds are resolved with scar tissue. This fibrotic response may be diminished by applying anti-fibrotic factors to the wound, thereby stimulating regeneration over scarring. The development of tunable biomaterials that allow spatiotemporal control over the release of anti-fibrotics would greatly benefit wound healing. Harnessing the power of click-to-release chemistry for regenerative medicine, we here demonstrate the feasibility of such an approach.

Materials and Methods

One side of a bis-N-hydroxysuccinimide-trans-cyclooctene (TCO) linker was functionalized with human epidermal growth factor (hEGF), an important regulator during wound healing. On the other side a carrier protein was conjugated; either type I collagen scaffolds or bovine serum albumin (BSA). Dimethyl-tetrazine (tetrazine) was used to induce 'click-to-release' of hEGF.

Mass spectra were obtained of hEGF, hEGF conjugated to TCO (hEGF-TCO), and hEGF-TCO with tetrazine to investigate ligation and release. Type I collagen scaffolds were combined with hEGF, hEGF-TCO or hEGF-TCO with tetrazine. hEGF was localized on cryo sections of collagen scaffolds using immunofluorescent assays and detected on soluble collagen through Western blotting. Conjugation of BSA to TCO-hEGF and subsequent release of hEGF following tetrazine exposure was investigated using Western blotting with antibodies targeting hEGF and BSA.

Results and Discussion

The mass of hEGF was measured at 6248 to 6253 m/z and in the spectrum of hEGF-TCO various smaller peaks at increasing m/z values were observed. These peaks corresponded to the addition of TCO ligation products to hEGF. Following exposure of hEGF-TCO to tetrazine these smaller peaks were absent, indicating release of hEGF from TCO. Cryo sections of collagen-hEGF stained positive due to non-specific binding of hEGF to TCO. The signal intensity of hEGF on sections of collagen-TCO-hEGF was increased, a sign of successful ligation. These results were confirmed through Western blotting, where collagen-hEGF-TCO stained positive for hEGF. After collagen-TCO-hEGF had been exposed to tetrazine a decrease in the hEGF signal on the Western blot was observed. The ability of hEGF-TCO to couple to BSA was demonstrated through Western blotting. On the blot hEGF (6.2 kDa) was located above BSA (66.5 kDa). When BSA-TCO-hEGF had been exposed to tetrazine the signal of hEGF above BSA diminished.

The results demonstrate TCO can be used to functionalize two carrier proteins with hEGF. Following exposure to tetrazine a 'click-to-release' reaction occurs where hEGF is released.

Conclusions

This work offers proof-of-concept that click-to-release chemistry may be employed to functionalize biomaterials with bioactive factors. Further research will focus on optimizing the reaction parameters.

Acknowledgement

This research was funded by the Radboud Institute for Molecular Life Sciences: PhD round 2020.

Oral Session 6

3D Co-Culture Spheroid Model to Assess the Response of Bone Metastases to Anticancer Drugs

C.E. Suurmond[1*], Rong Wang[1], Sander Leeuwenburgh[1], Jeroen van den Beucken[1]
[1]Department of Dentistry – Regenerative Biomaterials, Radboud Institute for Molecular Life Sciences, Radboud University Medical Center, Nijmegen, The Netherlands.

INTRODUCTION

Malignant prostate and breast cancer are the types of primary cancers that metastasize most frequently to bones. Similar to primary bone cancers, bone metastases are often treated using tumor curettage, which creates a bone defect that requires filling with a suitable graft material. Moreover, cancer cells may still retain in these defects since tumor margins are typically difficult to determine.[1] To prevent recurrence of bone cancer metastases, chemotherapeutics can either be systemically administered or locally delivered from biomaterial carriers that are used to fill bone defects. To date, several bone-regenerative materials with anticancer properties have been developed, but in vitro testing of therapeutic efficacy is still performed in relatively simple 2D cell cultures that are far from mimicking physiological bone tumor conditions.[2,3] Early 3D methods composed of cancer cells showed responses more similar to in vivo efficacy[4], and efforts now have started to explore 3D co-cultures.[5] Here, we aim to develop an easy to use, but clinically highly relevant 3D co-culture spheroid model for application as a tool to investigate anti-cancer efficacy of chemotherapeutic drugs and materials.

EXPERIMENTAL METHODS

All cells were cultured in alphaMEM (Gibco) supplemented with 10% fetal bovine serum (Gibco) and 1% penicillin/streptomycin (Gibco). Primary human bone marrow stromal cells (hBMSC) with either 10% prostate (PC3) or 10% breast cancer cells (MDA-MB-231) were cultured in ultra-low attachment plates (PHCBI) with 30 ug/mL collagen type 1A from rat tail (Corning) as media additive to create 3D spheroids (2000 cells/spheroid). Spheroids were characterized with brightfield microscopy, image analysis protocols were developed to measure the projected area, diameter and circularity of the spheroids during spheroid formation and at days 1, 3, and 7 in culture. Further characterization was performed with laser scanning confocal microscopy (Carl Zeiss LSM880). hBMSCs were stained with CellTrace CFSE green (Invitrogen) before mixing, and cancer cells with CellTrace Far Red (Invitrogen). Hemispheres of 3D spheroids were then further characterized with z-stack confocal imaging. Quantitative image analysis was performed to determine the numbers of hBMSCs and cancer cells and the spatial distribution of the cells throughout the 3D spheroids at days 1, 3, and 7. Various concentrations of cisplatin were added to the spheroid model and the response was assessed by monitoring spheroid characterics.

RESULTS AND DISCUSSION

Spheroids were formed in 24h of cell culture. During this period the projected area and diameter of both the spheroids with 10% PC3 and 10% MDA-MB-231 decreased. Additionally, the circularity increased, showing the formation of stable spheroids. Spheroids were also characterized on days 1, 3, and 7 in culture. Spheroids comprising MDA-MB-231 cells compacted even further showing a decrease in projected area and diameter and a stable high circularity. Alternatively, spheroids comprising PC3 cells increased in projected area and diameter, and decreased in circularity. To further detail hBMSC and cancer cell ratios and distribution in the spheroids, confocal z-stacks imaging was used (Figure 1). This imaging enabled quantitative analyses, showing a relative and gradual increase of cancer cells in the spheroids over time (Figure 2). Furthermore, 3D spheroids showed to decrease in size and form a tight core of predominantly hBMSCs and cancer cells growing peripherally.

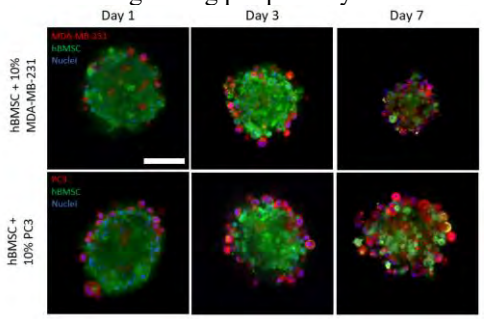

Figure 1 Laser scanning confocal images at 20x magnification of 3D spheroids (2,000 cells per spheroid) of 90% hBMSC (green) with 10% MDA-MB-231(red) or PC3 (red) cells, with stained nuclei (blue) at days 1, 3, and 7 in culture. Scale bar of 50 um.

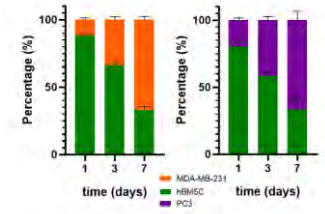

Figure 2 Graphs percentual volumes of the cancer cells and hBMSCs found with quantitative image analysis of confocal z-stacks of 3D spheroids.

To further evaluate chemotherapeutic effects on the 3D co-culture spheroids, their response to the anti-cancer drug cisplatin was assessed. With confocal imaging and quantitative image analysis a robust decrease in cancer cell numbers was observed.

CONCLUSION

A 3D spheroid co-culture model comprising hBMSCs and cancer cells was established, showing generation of stable spheroids for a culture period of up to 7 days. The combination of multiple microscopy techniques demonstrated distinct cell type dependent proliferation and spatial re-organization s within the 3D spheroids and susceptibility to the anticancer drug cisplatin. This model paves the way for testing new drugs and biomaterials.

REFERENCES

1. Buenrostro D, *et al.*, Curr Osteoporos Rep. 2016;14(4):151-8.
2. Li F, *et al.*, Regenerative Biomaterials. 2021;8(6).
3. Hu M, *et al.*, Journal of Colloid and Interface Science. 2020;579:654-66.
4. Huang Z, *et al.*, Onco Targets Ther. 2020;13:5395-405.
5. Saraiva DP, *et al.*, Front Oncol. 2020;10:1543.

E-mail address: ceri-anne.suurmond@radbouducm.nl

The Influence of Macrophage Phenotype on Tendon Tissue Remodeling

H.F.M. Brouwer[1,2 *], A.K. Mansoor[1,2 *], L. Verberne[1,2], C.V.C. Bouten[1,2], A.I.P.M. Smits[1,2], J. Foolen[1,2]
1. Department of Biomedical Engineering, Eindhoven University of Technology, 5600 MB Eindhoven, The Netherlands
2. ICMS, Eindhoven University of Technology, 5600 MB Eindhoven, The Netherlands. *HB & AM contributed equally.

Introduction: Tendinopathy is characterized by tissue degeneration and the transformation of strong extracellular matrix (ECM) anisotropy to isotropy. Simultaneously, highly polarized tenocytes change into stellate-shaped tenocytes.[1] The process of remodeling during tissue healing aims to restore the functional tissue organization, which fails in chronic tendinopathy. Macrophages are thought to be one of the key regulators during tissue healing and remodeling. Their polarization into a spectrum of phenotypes is hypothesized to play an important role in both functional tissue remodeling and fibrosis[2], being influenced by various environmental cues such as cytokines and topographies[3]. The interplay between macrophages and tenocytes, and how this influences tendon healing, in particular restoring tissue organization, remains elusive. We thus aim to investigate the effect of paracrine signaling of distinct macrophage phenotypes on tendon-like tissue remodeling.

Methods: 3D constrained microtissue platforms were used *in vitro* to create aligned tendon-like tissues consisting of tenocytes in a collagen type I gel (Figure 1). The microtissues were cultured in three different macrophage conditioned media, based on the M1, M2a and M2c phenotype. Microtissue contraction, tenocyte gene expression, and cell and ECM orientation were analyzed to assess tissue remodeling behavior.

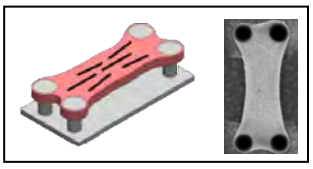

Figure 1. in vitro 3D microtissue model using post-induced constraints[1]

Results: Macrophage-secreted cytokines showed to influence tissue remodeling by differences in actin orientation (Figure 2A), microtissue contraction (Figure 2B), and gene expression (Figure 2C). Culturing in M1-conditioned medium resulted in less contractility, decreased anisotropy of actin and collagen, and decreased expression of remodeling genes compared to M2a- and M2c-conditioned media. Culturing in M2a- and M2c-conditioned media resulted in a similar orientation of actin and collagen, with the highest expression of the remodeling gene CTGF in M2c-conditioned samples, and the highest expression of collagen I and III and tenogenic markers in M2a-conditioned samples.

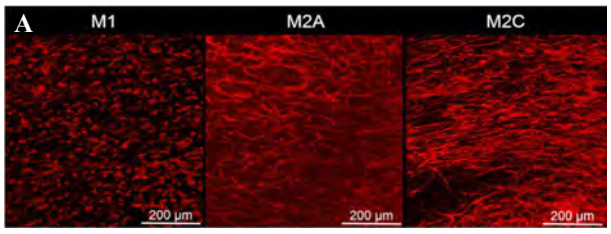

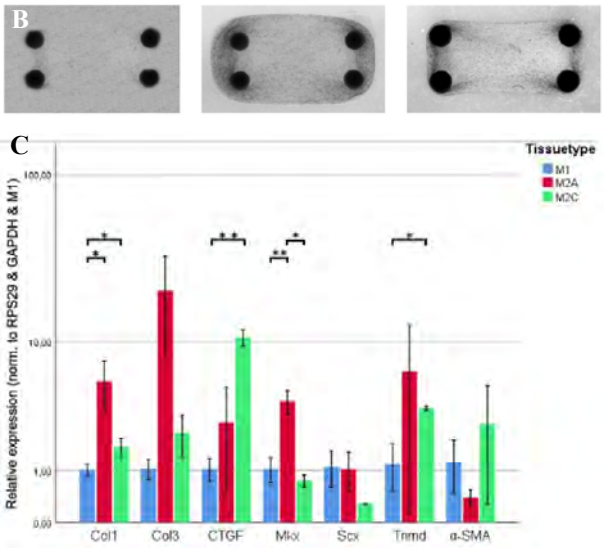

Figure 2. Analysis of tissue remodeling based on (A) Phalloidin staining of actin stress fibers, (B) brightfield images, and (C) qPCR of Col1 (collagen type 1), Col3 (collagen type 3), CTGF (connective tissue growth factor), Mkx (mohawk), Scx (scleraxis), Tnmd (tenomodulin), and α-SMA (alpha smoot muscle actin).

Conclusion & Discussion: Macrophage-secreted cytokines influence tenocyte tissue remodeling by altering cell and ECM organization and tenocyte gene expression levels. M1-conditioned medium resulted in the weakest cell and tissue anisotropy with the lowest expression of tissue remodeling genes, compared to M2a- and M2c-conditioned medium samples. No clear differences in cell and ECM organization between M2a- and M2c-conditioned medium samples was observed. Next, a direct co-culture will be performed to further examine the interplay between distinct macrophage phenotypes and tenocytes during remodeling. This will aim to address the relevant questions that can help us to steer functional tissue remodeling during tendon healing.

References:

[1] Foolen, J., Wunderli, S. L., Loerakker, S. & Snedeker, J. G. Tissue alignment enhances remodeling potential of tendon-derived cells - Lessons from a novel microtissue model of tendon scarring. Matrix Biology 65, 14–29 (2018).
[2] Wissing, T. B., Bonito, V., Bouten, C. V. C. & Smits, A. I. P. M. Biomaterial-driven in situ cardiovascular tissue engineering-a multi-disciplinary perspective. NPJ Regen Med 2, (2017).
[3] Luu, T. U., Gott, S. C., Woo, B. W. K., Rao, M. P. & Liu, W. F. Micro- and Nanopatterned Topographical Cues for Regulating Macrophage Cell Shape and Phenotype. ACS Appl Mater Interfaces 7, 28665–28672 (2015).

Contact details presenting author: h.f.m.brouwer@tue.nl

Polyisocyanide hydrogel for 3D Contraction Assay: A Versatile Preclinical Research Platform for Fibrosis

J. Kumari[1,2], *F.A.D.T.G. Wagener*[2] *and P.H.J. Kouwer*[1]

[1] *Institute for Molecules and Materials, Radboud University, Heyendaalseweg 135, 6525 AJ, Nijmegen, The Netherlands,* [2] *Department of Dentistry, Section of Orthodontics and Craniofacial Biology, Radboud University Medical Centre, Nijmegen, The Netherlands*

INTRODUCTION: Fibrosis contributes to 35-40 percent of deaths worldwide[1]. The key factors involved in fibrosis at the cellular level are increased differentiation of fibroblasts into myofibroblasts and hampered myofibroblast apoptosis, leading to persistent collagen deposition and tissue contraction[2]. Currently only very few drugs are clinically available for fibrosis treatment therefore there is an urgent demand for developing novel therapeutic drugs and *in vitro* fibrosis models to check the efficacy of these putative drugs. In this study, we developed a novel fibrosis model based on synthetic polyisocyanides (PIC-RGD) hydrogels. The model not only measures contraction but, additionally, allows for molecular and cellular analysis.

METHODS: Polyisocyanides (PIC) containing azide groups were reacted with DBCO-functionalized arginine-glycine-aspartic acid (RGD) based peptides to form PIC-RGD hydrogel. The mechanical properties of the hydrogel were characterized by rheology. Fibroblasts were seeded inside PIC-RGD gels in the absence or the presence of 10 ng/mL TGFβ1 to facilitate differentiation into myofibroblasts up to day 6. The immunostaining was performed to confirm the differentiation. Antifibrotic drugs were added at day 6 and inhibitory effects of drug were checked at day 7.

RESULTS: 2 mg/mL of PIC-RGD hydrogel showed an optimal level of contraction in the hydrogel. The fibroblasts seeded hydrogel in presence of TGFβ1 contracted more than its absence. The presence of myofibroblasts in the hydrogel was confirmed by gene expression and immunostaining of both alpha smooth muscle actin (αSMA) and collagen 1α1 (Col1α1) at the gene and protein level. As proof of principle, nintedanib and pirfenidone (both are FDA-approved drugs for pulmonary fibrosis) were probed on our developed fibrosis model. The inhibiting effect of nintedanib and pirfenidone is clearly observed in reduced myofibroblast contraction. The results were confirmed by bright field imaging, immunostaining and PCR of αSMA and live-dead staining processes.

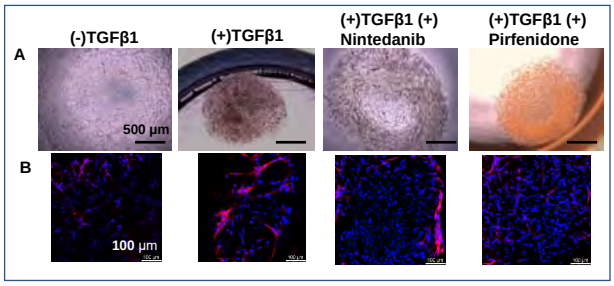

Figure 1; A) Bright field image and (B) Immunostaining of α-SMA (red) and counterstained with DAPI for nucleus (blue) of 2 mg/ml PIC-RGD hydrogels after drug treatment. Scale bar in panel (A): 500 µm; (B): 100 µm. Magnification (A): 50X, (B): 200X.

DISCUSSION & CONCLUSIONS: In summary, the PIC-RGD hydrogel is highly suitable as an *in vitro* contraction and fibrosis platform to monitor the efficacy of various drugs and chemicals on fibrosis, scarring and molecular and cellular analyses. Our newly developed contraction and fibrosis platform offers several advantages: 1) it is synthetic and easy to modify with any desirable peptide and growth factor, 2) it has no batch to batch variations, 3) it is temperature sensitive, which allows easy isolation of cells for downstream assays and analysis such as PCR 4) no excess proteins interfere during the assays 5) the platform has virtually no autofluorescence but can easily be equipped with any fluorophore. The combination of these properties makes our model an attractive candidate for high throughput screening of putative drugs against fibrosis and scarring.

REFERENCES:

1. *Sahai, E. et al., Nat Rev Cancer. 20, 174-186(2020).*
2. *Nanchahal, J., Proc Natl Acad Sci U S A. 113, 7291-7293 (2016).*
3. *Gurtner GC., Nature. 453,314-321 (2008)*

Based on research published in J. Kumari, F. Wagener, P. H. J. Kouwer, *ACS Appl Mater Interfaces* **2022**, 14, 19212.

Development of A Perfusable 3D Bioprinted Liver Tissue Model

J.J.F. Sleeboom[1,2], F.C. Guarnotta[1], M.M.A. Verstegen[2], L.E. Fratila-Apachitei[1], L.J.W. van der Laan[2], A.A. Zadpoor[1]
[1]Department of Biomechanical Engineering, Delft University of Technology, Mekelweg 2, 2628 CD Delft, the Netherlands
[2]Department of Surgery, Erasmus MC Transplant Institute, Erasmus MC University Medical Center Rotterdam, Postbus 2040, 3000CA Rotterdam, The Netherlands

Introduction

Currently, the only viable way to treat patients with end-stage liver disease is to transplant a suitable donor liver. Unfortunately, there is a major donor shortage and the progress in tackling this issue, for example via selection procedures[1], or pre-implantation perfusion[2] is very slow. Therefore, researchers are exploring alternative, tissue engineering approaches to both model and fabricate livers using 3D bioprinting[3]. One of the main challenges in liver bioprinting is that most of the printed models are static. They grow in static culture conditions in well plates or dishes, which is very different from the dynamics of liver *in vivo*. Here, there is constant blood flow and temporal variation of solutes, hormones, and other signaling molecules. Additionally, the liver consists of a multitude of different cell types, such as endothelial cells, hepatocytes, cholangiocytes, stellate cells, and Kupffer cells, which all are essential for liver function[4].

Recently, the dynamic nature of the liver has been replicated in a bioprinted model for the first time. Small perfusable liver modules were made by volumetric bioprinting and embedded in a sterile perfusion chamber[5]. In this model, printed hepatic liver organoids were demonstrated to show dynamic liver specific functions, such as albumin production and active ammonia removal. However, this great leap forward also comes with several challenges: due to limitations of the printing method, it is not possible to directly combine multiple cell types, while keeping control over their positions. Additionally, the volumetric printing method relies on a certain refractory index, which limits the selection of materials.

In this work, we address several of these challenges. We present an approach to create a perfusable liver model, by combining extrusion based bioprinting (EBB) and a microfluidic system, which can facilitate multi-cellular tissue perfusion.

Approach

A microfluidic perfusion device is fabricated using an in-house fabrication method, based on stereolithography (SLA) 3D printing. Briefly, inverse molds are printed, sanded, and replicated in polyurethane. PDMS is then cast, cured, cut, and bonded to glass to complete the device (Fig. 1A). The open top design facilitates direct bioprinting into a chamber, which can later be sealed by clamping a polymer coverslip on top.

The liver bioink consists of a tyramine modified hyaluronic acid hydrogel (HAT), pre-crosslinked with horseradish peroxidase and H_2O_2, and photo-crosslinked with Eosin-Y, mixed with decellularized liver extracellular matrix (dECM) and intrahepatic cholangiocyte organoids (ICOs) (Fig. 1B). Blood-vessel mimicking channels are patterned using a sacrificial Pluronic F-127 based ink, that can be lined with endothelial cells (Fig. 1C, D).

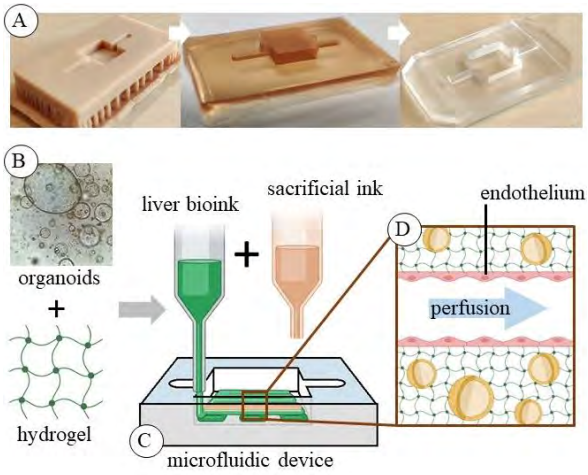

Figure 1. Dynamic liver model fabrication: A) Chip fabrication via SLA printing and double replica molding. B) Bioink with HAT-dECM. C) Direct in-chip printing with bioink and sacrificial ink to form channels that can D) be lined with endothelial cells.

Conclusions

By combining material and cells derived from human liver (dECM and ICOs) with modern materials and fabrication approaches, a more realistic and perfusable multi-cellular model can be established. This approach has the potential to unlock new discoveries in liver (patho-)physiology, by facilitating long term dynamic culture of more complex liver models. In the long run, this can lead to new solutions to the current problems with liver donor shortages.

References

1. Moghe, A., Ganesh, S., Humar, A., Molinari, M., & Jonassaint, N. (2021). Clinics in Liver Disease, 25(1), 121–135.
2. van Leeuwen, O. B., de Vries, Y., Fujiyoshi, M., Nijsten, et al. (2019). Annals of Surgery, 270(5), 906–914.
3. Hosseini, V., Maroufi, N. F., Saghati, S., Asadi, N., Darabi, M., Ahmad, S. N. S., Hosseinkhani, H., & Rahbarghazi, R. (2019). Journal of Translational Medicine, 17(1), 383.
4. Ma, L., Khatib, S., Craig, A. J., & Wang, X. W. (2021). Seminars in Liver Disease, 41(03), 321–330.
5. Bernal, P. N., et al. (2022). Advanced Materials, 2110054.

E-mail: j.j.f.sleeboom@tudelft.nl
Funded by a Medical Delta program grant (Regenerative Medicine 4D)

Towards a Fully Synthetic Corneal Stromal Construct: using a Supramolecular hydrogel.

A.F. Vrehen, M.G.T.A Rutten, P.Y.W. Dankers
Department of Biomedical Engineering, Laboratory for Cell and Tissue Engineering, Institute for Complex Molecular Systems, Department of Biomedical Engineering, Laboratory of Chemical Biology,
Eindhoven University of Technology, PO box 513, 5600 MB Eindhoven, The Netherlands

Introduction | The cornea is located at the outermost of the eye fulfilling two main functions; protecting the inner parts of the eye and allowing for vision by refracting light from the external world towards the retina. An acellular layer, called "Bowman's layer" separates the protective corneal epithelial cell layer from the corneal stroma. The corneal stroma is backed by the acellular Descemet's membrane, separating the stroma from the corneal endothelium layer. About 90% of the cornea is composed of the corneal stroma and therefore it predominantly affects the corneal function. The corneal stromal is a highly organized tissue, existing of condensed collagen type I lamellae in heterodimeric complex with collagen type V and VI, surrounded by specific proteoglycans, like keratocan, lumican and decorin. Causing the stroma to be a highly hydrated tissue. Collagen fibrils within sequential lamellae are oriented in an orthogonal fashion. The high level of organization together with the hydration results in a specific mechanical strength and the ability to refract light. [1] Only 5-10% of the stromal volume comprises of keratocytes, which are characterised by long dendritic protrusions. Corneal keratocytes slowly regenerate the collagen in the stroma and as well produce extra cellular matrix (ECM) components, such as collagen type I and proteoglycans. In case of trauma or disease, keratocytes can undergo metabolic activation and change into a fibroblastic phenotype which results in cell migration, proliferation and upscaled collagen production. A damaged or diseased cornea results in visual impairment or blindness, for which corneal transplantation is the only suitable treatment option, however, the demand substantially exceeds the availability. The last few decades various bioengineered constructs have been studied as mimics of the corneal stroma. [1] Synthetic hydrogels based on supramolecular moieties allow for material tunability by the incorporation of bioactive additives into the material which encourage the mimicking of the natural ECM. In this study, ureido-pyrimidinone (UPy) moieties are modified with a bioactive UPy-cRGD additive to design a fully synthetic in-vitro hydrogel based 3D stromal construct for encapsulation of corneal keratocytes. The characteristics of this synthetic hydrogel are compared with a hybrid hydrogel consisting of UPy moieties and a mixed-in full length collagen type I protein.

Materials and Methods | Supramolecular hydrogels are formed using bivalent and monovalent molecules presenting fourfold hydrogen bonding designs (Fig. 1A). [2] Upon mixing of the bivalent and monovalent molecules, these molecules self-assemble into supramolecular fibers and form a dynamic hydrogel network with an overall stiffness of ~2 kPa. An integrin binding peptide (cRGDfk) is functionalized with a UPy-moiety (Fig. 1B) and used as a bioactive additive, resulting in a synthetic hydrogel with an overall stiffness of 2-2.5 kPa. Full length bovine collagen type I is used together with the UPy molecules to design a hybrid hydrogel with an overall stiffness of 2.5-3 kPa. Prior to cell encapsulation, UV-light is used to sterilize the gels. Primary keratocytes (PKs) are encapsulated within the hydrogel and substantially treated as activated stromal fibroblasts (SFs) using serum enriched culture medium, and treated as corneal stromal keratocytes (CSKs) using culture medium with low serum and high glucose.

Results and Discussion | The culture of encapsulated PKs is successfully abided for 21 days. Subsequently, immunofluorescent staining revealed a phenotypical difference between the PKs treated as SFs or CSKs. For both gels, the PKs treated as CSKs show more individual cells suggesting a lower proliferation rate (Fig. 1E,F). Especially for the synthetic hydrogel, long dendritic protrusions are observed (Fig. 1E). A more fibroblastic phenotype is observed for the SFs treated cells in both hydrogels (Fig. 1C,D). An enzyme-linked immunosorbent assay (ELISA) indicates for both hydrogel systems a substantial decrease in secreted interleukin 8 (IL-8) for the PKs treated as CSKs compared with the PKs treated as SFs.

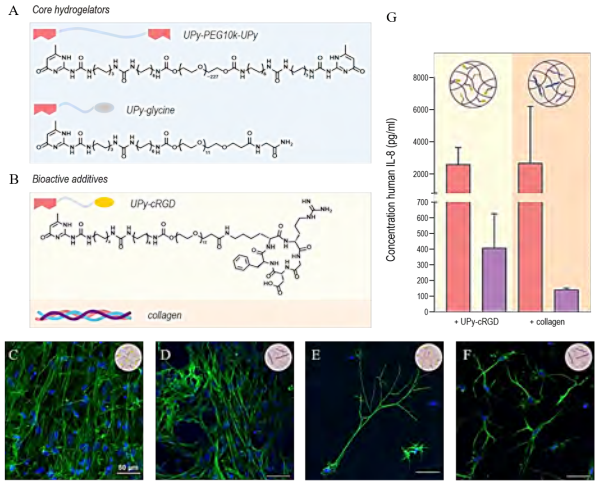

Figure 1. A. Bivalent and monovalent hydrogelators. **B.** UPy-cRGD as a bioactive additive to create a synthetic hydrogel. **C.** PKs treated as SFs in the synthetic hydrogel. **D.** PKs treated as SFs in the hybrid hydrogel. **E.** PKs treated as CSKs in the synthetic hydrogel. **F.** PKs treated as CSKs in the hybrid hydrogel. **G.** Quantification of cellular IL-8 secretion.

Conclusion | Within this study it is successfully achieved to encapsulate, culture and differentiate PKs into SFs or CSKs by using a fully synthetic hydrogel. Due to the tunability and dynamicity of this supramolecular hydrogel lots of opportunities to use this in-vitro stromal construct arise.

This work was performed under the framework of Chemelot InSciTe.
[1] N. Formisano et al., 'Mechanical Properties of Bioengineered Corneal Stroma', advanced healthcare materials, 2021. [2] M. Diba *et al.*, "Engineering the Dynamics of Cell Adhesion Cues in Supramolecular Hydrogels for Facile Control over Cell Encapsulation and Behavior, "Advanced Materials, 2021.

Cyclic Straining of *In Vitro* Tissue-Engineered 3D Models: Investigating the Effects on ADSC differentiation and the Extracellular Matrix

M.J.J. van Velthoven[1,2], M. van Loon[1,2], L. Rasing[1,2], A.N. Gudde[3], F. A. D. T. G. Wagener[4], J.P. Roovers[3], Z. Guler[3], P.H.J. Kouwer[1]

[1] Institute of Molecules and Materials, Radboud University, Nijmegen, The Netherlands [2] Department of Urology, Radboud University Medical Center, Radboud Institute for Molecular Life Sciences, Nijmegen, The Netherlands [3] Department of Obstetrics and Gynecology, Amsterdam University Medical Center, Amsterdam, The Netherlands [4] Department of Dentistry - Orthodontics and Craniofacial Biology, Radboud University Medical Center, Nijmegen, The Netherlands

INTRODUCTION: As cells and tissues in our body are continuously exposed to mechanical forces, mechanical loading should be incorporated in *in vitro* models. Mechanical loading of 3D models better recapitulates the *in vivo* conditions; however, this is more challenging than applying loading on 2D models. Polyisocyanide (PIC) hydrogels are synthetic, thermosensitive and highly biomimetic, displaying stress-stiffening behavior similar to other biomacromolecules [1]. Therefore, the PIC hydrogel has great potential to mimic the 3D native extracellular matrix (ECM) and is an ideal substrate for investigating the effect of mechanical loading of tissue-engineered constructs. In this study, we investigated the effect of cyclic straining on 3D-cultured human adipose-derived stem cells (ADSCs) focusing on ADSC differentiation, gene and protein expression of ECM proteins and collagen alignment.

METHODS: PIC polymers were synthesized and conjugated with a cell-adhesive peptide GRGDS as previously reported [2]. ADSCs (passage 5) were encapsulated in the PIC hydrogel. Eight days post-encapsulation, cyclic straining (2%, 0.2 Hz) was applied for 7 days using the Flexcell® FX-5000™ Tension System. The Flexcell® Bioflex plate was adjusted using similar modifications described in Wissing *et al.* (Fig. 1A) [3]. The static controls did not receive any mechanical loading. The effect of cyclic straining, versus static controls, was evaluated for differentiation into α-SMA-positive myofibroblasts, gene expression of ECM production and remodeling related genes, collagen protein visualization (CNA-OG488), collagen alignment and deposition, and elastin deposition (Fastin™ Elastin assay).

RESULTS: The 3D cultured ADSCs can be successfully cultured up to 7 days of cyclic straining (Fig. 1B). The plate modifications did not interfere with the percentage of applied strain (data not shown). Cyclic straining highly promotes collagen production (Fig. 1C-D). The dynamic samples show an anisotropic fiber alignment, parallel to the strain direction, which is absent in the static control samples. Cyclic straining significantly upregulates α-SMA (ACTA2), collagen type III (COL3A1) and elastin (ELN) expression.

DISCUSSION & CONCLUSIONS: Cyclic straining results in increased myofibroblast differentiation, collagen production and alignment of tissue-engineered constructs, confirming that the PIC hydrogel transfers the mechanical loading to which the cells respond. In the future, we would like to apply our setup to examine the effect of mechanical loading in the context of pelvic organ prolapse (POP). Hereby, we would like to assess whether POP fibroblasts respond differently in terms of collagen metabolism compared to non-POP fibroblasts. Moreover, incorporating mechanical loading in complex 3D *in vitro* models can result in more translatable disease models in the future.

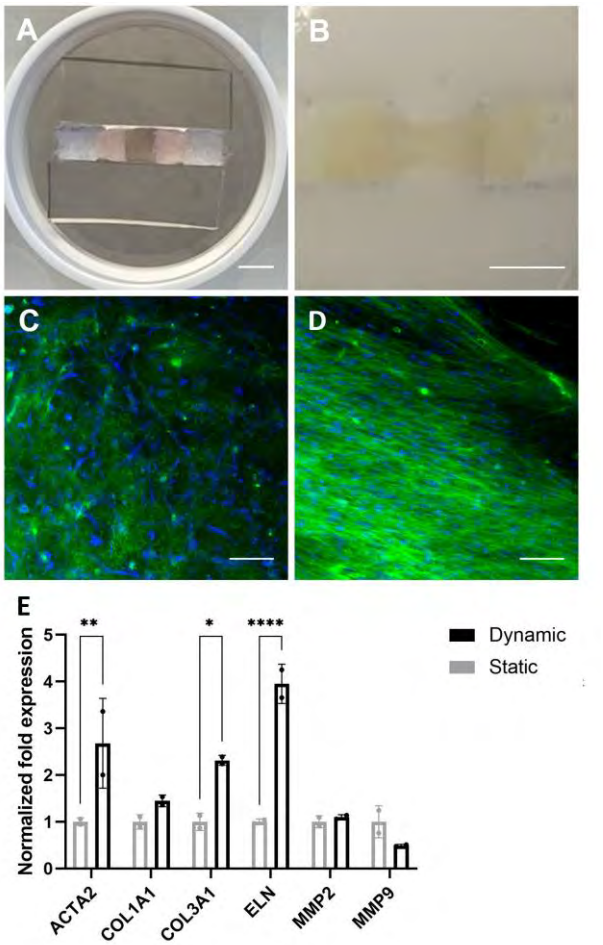

Fig. 1: Setup for dynamic culturing of ADSCs in the PIC hydrogel using the Flexcell® FX-5000™ Tension System (A). ADSCs can be successfully cultured for 7 days in the presence of cyclic strain (2%, 0.2 Hz) (B). Collagen deposition (collagen (green) and nuclei (blue)) is highly promoted in the presence of cyclic strain (horizontal direction), resulting in aligned mature collagen fibers (D) which are absent in the static control (C). Cyclic strain significantly promotes ACTA2, COL3A1 and ELN expression normalized to the static controls ($p < 0.05$, ** $p < 0.01$ and **** $p < 0.0001$) (E). Scale bar = 5 mm (A-B) and 100 µm (C-D).*

REFERENCES:

[1]Das R, Nat. Mater. 2016; 15: 318-325. [2]Liu K, ACS. Appl. Mater. Interfaces 2020; 212: 56723-56730. [3]Wissing T.B., Sci. Rep. 2022; 12: 5434

Evening lecture

Space, the new frontier and a resource for tissue engineering

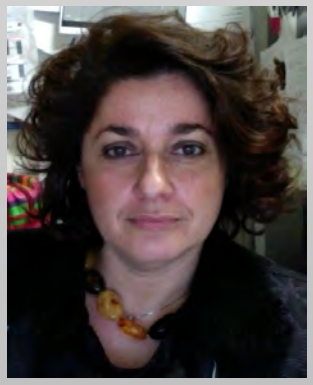

Dr. Debora Angeloni

The Institute of Biorobotics
Sant'Anna School of Advanced Studies, Pisa, Italy

Space flight has a deep effect on living beings due to a combination of physical stimulations among which radiations and changes of gravitational load (microgravity and hypergravity) are the most distinctive.
Space biology is a branch of experimental biology that deals with the effects of space flight on living beings, aiming at understanding what molecular events of the cell are modified by space and what adaptive/maladaptive responses the cell enacts, and how we can exploit the extraordinary Space environment to improve life and biomedical research on Earth.
Currently, experimental cell research on three-dimensional tissues in Space and on Earth using real or simulated microgravity is a hot topic in Space biology and Biomedicine, because microgravity strongly affects cell proliferation, differentiation and aggregation, which in turn may affect therapeutic cell properties in biotechnological applications. Several in-flight as well as ground-based platforms are now available to scientists for tissue engineering and regenerative medicine applications.
Considering the commercialization of spaceflight, future space exploration, and long-term manned flights, Space biology may gain more and more space in cancer research and regenerative medicine.
The lecture will provide an overview of Space biology with specific reference to cell biology and tissue engineering.

Biography:

Debora Angeloni, Ph.D., is Associate Professor of Molecular biology, and group leader of the Unit of Cancer Molecular Genetics, at The Institute of Biorobotics, Sant'Anna School of Advanced Studies, Pisa, Italy. Her education includes Laurea cum Laude in Biological Sciences (University of Pisa), PhD in Chemotherapy (University of Milan, Italy), and post-doctoral training in Molecular genetics of cancer, at the National Cancer Institute - NIH, USA. Her research focuses mainly on cancer biology and genetics. Recently she developed an interest in Space biology because Space offers a new, unprecedented way to study life. Prof. Angeloni contributed to the ESA 'Science Road Maps In Life And Physical Sciences In Space'. Early in her career, Debora developed an interest in science communication, as a part of the Third Mission of University. Her research activity is strongly connected to her academic teaching.

Friday

2nd December 2022

Keynote lecture

Cell therapies for regenerating the corneal endothelium

Dr. Vanessa LaPointe

MERLN Institute for Technology-Inspired Regenerative Medicine, Maastricht University

The cornea is a highly specialized tissue that acts as a window for light to enter the eye. There are many diseases and injuries that can render it opaque, leading to pain and loss of vision with a substantial reduction of quality of life. For tissue engineers, the cornea is an interesting and underappreciated target tissue. Its characteristics are well-defined, it is accessible for intervention and easily monitored with imaging techniques, and parts of it are immunoprivileged. Furthermore, a proof-of-concept stem cell–based therapy already exists clinically. However, for patients with corneal endothelial cell disorders, the treatment options are more limited. While the cornea is the most transplanted tissue worldwide, there are still approximately 70 patients demanding every donor tissue available. I will present our efforts to address this shortage with cell therapies and will discuss the possibilities for tissue engineers to contribute their expertise to address this challenge.

Biography:

Vanessa LaPointe is an Associate Professor in the MERLN Institute for Technology-Inspired Regenerative Medicine at Maastricht University. She first trained as a biomedical engineer at The Johns Hopkins University (USA) and moved into the field of tissue engineering and regenerative medicine during her PhD with Prof. Molly Stevens at Imperial College London (UK) where she studied stem cell–material interactions. She received a CIHR Fellowship for her postdoctoral research at the University of Twente (the Netherlands) with Prof. Jan de Boer. Since 2016, she leads a group aiming to develop cell therapies for a variety of tissues and organs. The lab is proud to work on the whole spectrum of fundamental research to translational activities necessary to both discover and develop cell therapies. From 2016–2020, Dr LaPointe was the Scientific Coordinator and Deputy Programme Director of RegMed XB, an international public–private partnership to cure chronic diseases by bringing regenerative medicine solutions to patients.

Oral Session 7

Antibacterial CATH-2 Peptide Coating to Prevent Implant-related Infection

Pardis (P.) Keikhosravani[1,*], Fatemeh Jahanmard[1], Leonardo Cecotto[1], Azin Khodaei[1], Floris J. Bikker[2], Kamran Nazmi[2], Bart Van der Wal[1], Charls Vogely[1], Harrie Weinans[1], Saber Amin Yavari[1]

[1] Department of Orthopedics, University Medical Center Utrecht, Utrecht, The Netherlands
[2] Department of Oral Biochemistry, Academic Center for Dentistry Amsterdam (ACTA), the Netherlands
*email address: p.keikhosravani-2@umcutrecht.nl

Introduction

Total joint replacement and reconstructive bone surgery are the most frequently performed orthopedic procedures. Their success rate is, however, limited mainly due to aseptic loosening and infection [1]. Implant-related infection results from bacteria that initially colonize on the surface of the implants and then form a biofilm. Host defence peptides (HDPs) are considered interesting broad-spectrum alternatives to antibiotics in preventing implant-related infection (IRI) [2]. In particular, CATH-2 peptide (as one of the HDPs) causes a direct disruption of the microbial membrane thanks to its strong cationic charge [3]. Here, we aim to apply CATH-2 on porous titanium (Ti) surfaces using a base layer of electrosprayed Poly (D, Llactide-co-glycolide) copolymers (PDLG) and a coating layer of electrosprayed Gelatin methacryloyl (GelMA) to form Layer-by-layer assembly (LbL) and prolonged release profile of the peptide.

Materials and Methods

PDLG (50 mg/ml) was dissolved in trifluoroethanol (TFE) solvent at room temperature after stirring for 2h to have a complete dissolution. The PCL solution was applied by electrospraying method under 8 kV voltage, flow rate of 0.5 mL/h and sample distance from nozzle of 100 mm. Subsequently, 40, 80, 120 µg of CATH-2 was added on PDLG-coated samples to prepare different group of samples. As per the second coating, GelMA (3% wt.) was dissolved in MQ water and electrosprayed on peptide-loaded samples under same electrospray condition. *In vitro* antibacterial activity behaviour was investigated by colony-forming unit (CFU) of Methicillin resistant Staphylococcus aureus strain (SH100). Samples were immersed in PBS at 37° C for different time-points (1, 2, 3 and 4 days) and the released solution was collected for the CFU counting. On the other hand, cytotoxicity of the coated implants was tested by Alamar blue activity of human mesenchymal stem cells (hMSCs) and macrophage cell line and compared with the control groups.

Results and Discussion

The antibacterial properties of all the CATH-2 coated groups were 100% successful in killing the planktonic bacteria after 1 day. Nonetheless, LBL coating with 80 and 120 µg peptide yielded the best antibacterial properties after 2 days and 4 days, respectively (Fig 1).
In terms of the cytotoxicity, Alamar blue activity of hMSCs verified no significant difference among the groups. However, after 5 days the number of macrophage cells was reduced in PDLG-coated samples with 80 and 120 µg and LBL-coated samples with 120 µg peptide. In fact, use of GelMA prohibited the immediate release of peptide in the media. Further experiments to optimize the kinetic of peptide release and characterization of the coating is ongoing.

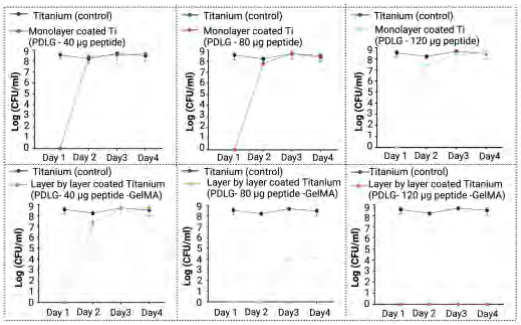

Figure 1. CFU analysis of collected release media of coated

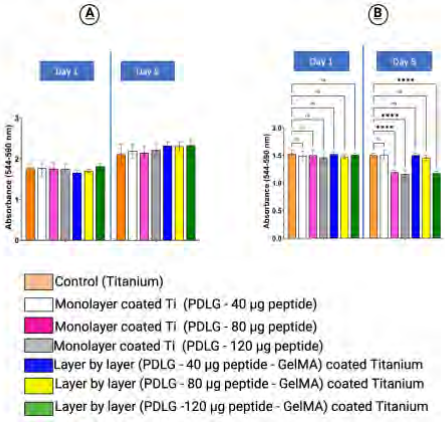

Figure 2. Alamar blue activity of A) hMSCs B) macrophage cell line.

Conclusion

This study used LBL assembly technology to make three layers of electrosprayed PDLG, CATH-2 peptide, and electrosprayed GelMA. The coated PDLG on the surface of Ti worked as a protective layer for peptide, and the GelMA layer plays a critical role in controlling CATH-2 release. The result showed that 80 ug/ml CATH-2 is the optimum concentration to fully eradicate bacteria without cytotoxicity effect on macrophage and human mesenchymal stem cells (hMSCs). Taken together, the developed peptide coating can be potentially used as a new generation of bactericidal coating to prevent early IRI and tackle current antibiotic resistance.

References

[1] A. Trampuz, et al., J. Current opinion in infectious diseases 19(4) (2006) 349-356.
[2] S. Amin Yavari, et al., Advanced Materials 32(43) (2020) 2002962.
[3] M.R. Scheenstra, et al., J. Scientific reports 9(1) (2019) 1-12.

Magnetically-actuated dynamic surfaces ($_{Mad}$Surface) for regulating immune response

L. Li[1,2] and B. Gumuscu Sefunc[1,2]
1 Biointerface Science Group, Eindhoven University of Technology, Eindhoven, The Netherlands
2 Biosensors and Devices Group, Eindhoven University of Technology, Eindhoven, The Netherlands

Introduction

Immune responses play a crucial role in tissue repair after medical device implantation. However, immune response can also lead to abnormal tissue reconstruction and scar formation.[1] Implant mechanical properties, e.g. stiffness and roughness is known to largely influence the immune response in implant/medical device rejection.[2] Current implantable biomaterials with fixed mechanical properties are not flexible in regulating immune response. Designing and developing biomaterials with dynamic mechanical properties, to modulate infection, has become a critical target of recent studies.[3] Here, we report on a magnetically-actuated dynamic hydrogel surfaces ($_{Mad}$Surface) with a pulsatile and tunable stiffness change for modulating macrophage polarization to better understand immune response as a road-mapping strategy for producing next-generation implants.

Experimental

The $_{Mad}$Surfaces were fabricated from polyacrylamide (PAAm) and magnetic microbeads on glass-bottom ibidi chips using APS/TEMED polymerization method. The pulsatile gel stiffness was actuated by a magnetic field of ~50 mT at a frequency of 0.1 Hz (*Figure 1a*). For the cell response study, Phorbol 12-myristate 13-acetate (PMA) differentiated-THP-1 cells (M0 macrophages) were seeded on the gel surfaces for 48 h, then differentiated in LPS+IFN-γ and IL4 to M1 and M2 types, respectively. During the cell differentiation process, a pulsatile magnetic field was applied to the $_{Mad}$Surfaces to induce macrophage polarization. After differentiation for 48 h, cells were stained with CD80 and CD206 macrophage markers, and analyzed by multicolor flow cytometry on a FACS Canto II (*Figure 1b*).

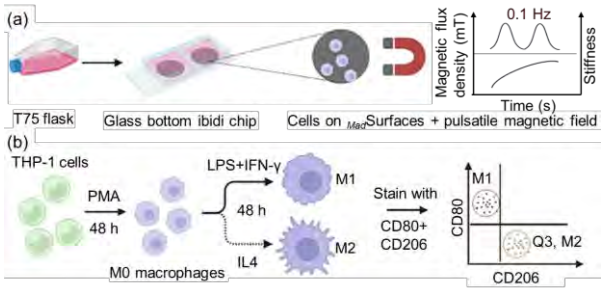

Figure 1 Schematic drawing of experimental setup (a) and design (b).

Results and discussion

Two types of $_{Mad}$Surfaces, including PAAm+30% v/v beads gel and PAAm+60% v/v beads gel were fabricated by adding different amount of magnetic beads into PAAm gel. PAAm gel without beads was used as a control. *Figure 2(a-c)* shows the scanning electron microscope (SEM) image of different gel surfaces. The gel stiffness increase with the increasing of beads concentration and the existence of magnetic field, and a reversible gel stiffness change between 130 - 450 kPa was obtained with (Magnetic (+)) and without (Magnetic (-)) magnetic field (*Figure 2d*).

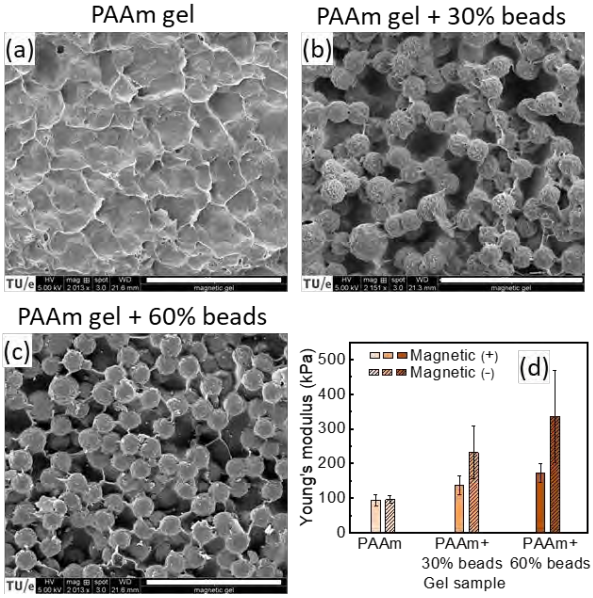

Figure 2 SEM (a-c) and stiffness (d) characterization of hydrogel samples.

The flow cytometry analysis on cell population after macrophages differentiation with LPS+IFN-γ and IL4 in Magnetic (+) and Magnetic (-) condition is shown in *Figure 3*. CD80-CD206+ (Q3, M2 macrophage) gates were drawn and the amount of cells in Q3 gate on each surfaces were plotted in the histogram graph. In LPS+IFN-γ differentiated cells, a higher population of M2 macrophages was observed on Magnetic (+) $_{Mad}$Surface compare to the M2 macrophage population on Magnetic (-) $_{Mad}$Surface (*Figure 3a*), while in IL4 differenciated cells, no big difference between M2 macrophage population on Magnetic (+) and Magnetic (-) $_{Mad}$Surfaces were observed (Figure 3b), indicating a polarization of M0 macrophage to M2 macrophage facilitated by pulsatile magnetic field in .

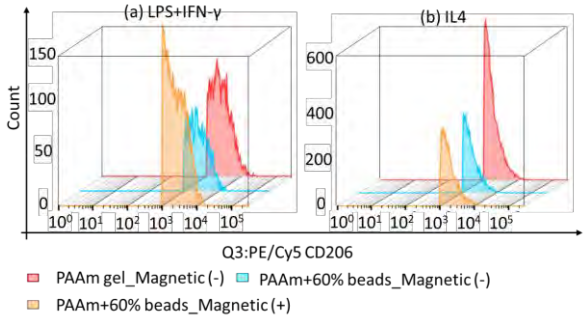

Conclusion

We have developed an $_{Mad}$Surface with pulsatile stiffness change and investigated its modulatory role on macrophage polarization. We observed a facilitating of macrophage polarization from M0 to M2 type induced by a pulsatile stiffness change instead of stiffness increasing only. Such a platform can be a useful in vitro model for study cell-biomatrix interactions and even lead to novel fabrication strategies for smart medical devices.

References

1. Zhang, Ben, et al. Advanced Science 8.16 (2021): 2100446.
2. Sridharan, R. et.al. (2019). Acta biomaterialia, 89, 47-59.
3. Tanaka, M. et.al. (2020). Polymer journal, 52(8), 861-870.

In-biofilm Generation of Nitric Oxide using a Magnetically-Targetable Cascade-Reaction Container for Eradication of Infectious Biofilms

Guang Yang, Linqi Shi, Yijin Ren, Henny C. van der Mei, Henk J. Busscher
Department of Biomedical Engineering, University Medical Center Groningen,
Antonius Deusinglaan 1, 9713 AV Groningen, The Netherlands

Abstract:
Development of new antibiotics to face the increasing threat of antimicrobial-resistant bacterial infections seems futile, considering the ever-shorter time between market-introduction and the appearance of the first signs of bacterial resistance against a new antibiotic. Non-antibiotic-based infection-control strategies are therefore considered preferable and more likely to yield return of investment upon market introduction and associated clinical benefits than the development of new antibiotics.

Therefore, we developed a magnetic cascade-reaction container composed of mesoporous Fe_3O_4@SiO_2 nanoparticles containing glucose-oxidase and L-arginine for generation of reactive-oxygen-species. Glucose-oxidase was conjugated to Fe_3O_4@SiO_2 nanoparticles for generation of H_2O_2 from glucose. L-arginine was loaded into the nanoparticles to generate NO from the H_2O_2 generated. Using an externally-applied magnetic field, cascade-reaction containers could be homogeneously distributed across the depth of an infectious biofilm. Cascade-reaction containers with coupled glucose-oxidase were effective in killing planktonic, Gram-positive and Gram-negative bacteria. Additional efficacy of the L-arginine based second cascade-reaction was only observed when H_2O_2 as well as NO were generated in-biofilm. *In vivo* cascade-reaction containers could target inside abdominal *Staphylococcus aureus* biofilms upon magnetic targeting. Moreover, *S. aureus* biofilms could be eradicated consuming solely endogenous glucose, without any glucose addition.

Magnetic targeting over a biofilm *in vitro*

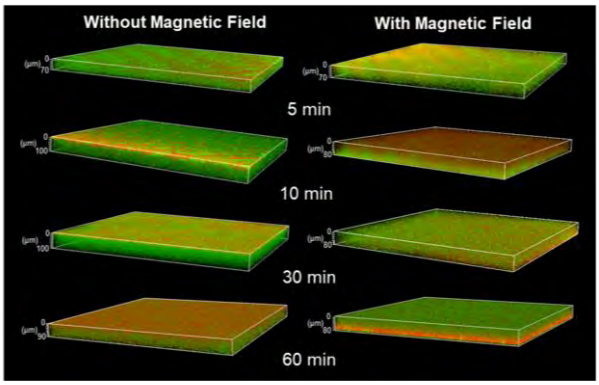

***In vitro*,** magnetic cascade-reaction containers could be homogeneously distributed across the depth of an infectious biofilm under the application of a magnetic field.

Killing against bacteria in biofilm *in vitro*

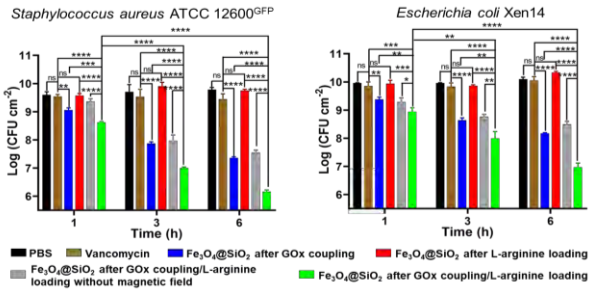

***In vitro*,** magnetic cascade-reaction containers yielded significantly better killing upon magnetic targeting at all time points. Thus, in-biofilm generation of NO is a *condition sine qua non* for eradicating infectious biofilms.

Magnetic targeting in an abdominal biofilm *in vivo*

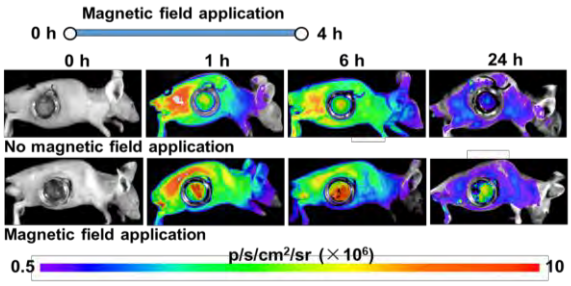

***In vivo*,** magnetic cascade-reaction containers could be accumulated inside an abdominal biofilm under the application of a magnetic field.

Eradication abdominal biofilm *in vivo*

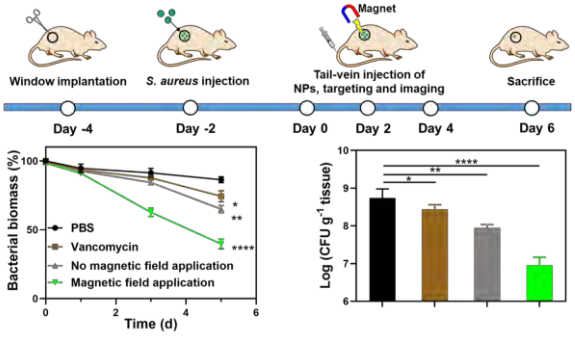

***In vivo*,** superior eradication of the intra-abdominal biofilm was observed, when magnetic cascade-reaction containers were targeted into the biofilm by an applied magnetic field.

Conclusion

A magnetic cascade-reaction container composed of mesoporous Fe_3O_4@SiO_2 nanoparticles containing glucose-oxidase and L-arginine for generation of reactive-oxygen-species to accomplish non-antibiotic-based infection-control was successfully designed.

High-Throughput Screening to Elucidate Implant-Associated Complications

L.E. Tromp*, T.A.B. van der Boon, L. Yang, L. Ge, Q. Zhou, R.A. Bank, P. van Rijn
W.J. Kolff Institute for Biomedical Engineering and Materials Science, University of Groningen/ University Medical Center Groningen (UMCG), Ant. Deusinglaan 1, Groningen, The Netherlands
*l.e.tromp@umcg.nl

INTRODUCTION

Despite the successes of biomedical implants, which are able to solve many biomedical problems, major drawbacks remain. Implant-associated complications frequently arise, such as biomaterial-associated infection, fibrosis, and implant rejection.[1, 2] Therefore, there is a need for innovative approaches that enhance biomedical device function. To achieve control over cellular behavior, it is crucial to understand the interplay between the biomaterial, microbes, and host cells. It is well-known that all cells respond to their microenvironment and that their behavior can be modulated by, for example, altering physicochemical material properties.[3] Although cell-material interactions are studied widely, conventional approaches do not reach the level of complexity as seen in vivo, where cells respond to multiple biophysical and biochemical cues simultaneously. Studies often focus on the effect of individual parameters and only assess specific values, leaving out a significant number of variables and data points. Closing this knowledge gap is essential to fully understand how the body responds to biomaterials and will aid us in further developing medical implant technology. We have developed a double orthogonal gradient (DOG) platform that enables us to effectively screen the cell response to an extremely broad range of combined physicochemical material properties in a high-throughput screening (HTS) manner. The platform offers a long-awaited change in approach, as it offers the ability to screen thousands of combined parameters in a single experiment. Currently, the platform is being used to screen cell-material interactions of fibroblasts with different material properties of silicone rubber to prevent fibrosis.

EXPERIMENTAL METHODS

Polydimethylsiloxane DOGs are formed that consist of two linear parameter gradients under a 90º angle on the same surface. The DOGs are prepared by a specific set of plasma oxidation treatments following protocols of previously published single linear gradients.[4–6]

RESULTS AND DISCUSSION

The developed platform is based on double orthogonal gradients, on which every position on the surface has a unique combination of the parameters topography, stiffness, and wettability (Figure 1). The wrinkled topography gradients range from wavelength (λ) = ~1–12 µm and amplitude (A) = ~100–1500 nm, with wavelength and amplitude increasing in a coupled fashion. The stiffness gradients range from Young's Modulus (E) = 20-500 MPa and the wettability gradients range from water contact angle (WCA) = 10-90º. Our current work focuses on the effect of combined material properties on the behavior of fibroblasts, which play a major role in the development of implant-associated complications. We will identify regions of interest (ROIs) with specific combinations of material properties that show the most pronounced effect in enhancing or reducing fibroblast adhesion, spreading, proliferation, and differentiation towards myofibroblasts. In the future, this screening approach will also be used to investigate the behavior of bacteria and macrophages to provide an extensive overview of how material properties can contribute to the development of an infection.

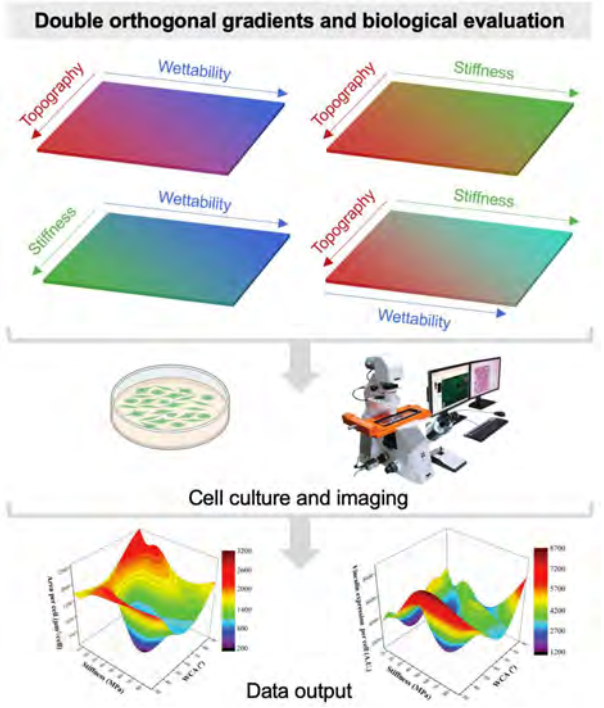

Figure 1 HTS approach. The screening platforms (top) provide all parameter combinations between topography, stiffness, and wettability. The influence on cell behavior is analyzed through immunofluorescence staining and automated imaging.

CONCLUSION

To achieve enhanced implant design, it is crucial to understand the interplay between the biomaterial, microbes, and host cells. The DOG platform developed enables us to effectively screen thousands of cell-material responses in a high-throughput fashion. This will generate knowledge that can be used to enhance biomaterials for medical implant technology.

REFERENCES

1. C. R. Arciola *et al.*, *Nat. Rev. Microbiol.* 16, 397–409 (2018).
2. E. Mariani *et al.*, *Int. J. Mol. Sci.* 20 (2019).
3. M. Rahmati *et al., Chem. Soc. Rev.* 49, 5178–5224 (2020).
4. P. T. Kühn *et al.*, *ChemNanoMat*. 2, 407–413 (2016).
5. Q. Zhou *et al.*, *Sci. Rep.* 5, 1–12 (2015).
6. Q. Zhou *et al.*, *Adv. Mater. Interfaces*. 5, 4–11 (2018).

Full Skin Equivalents to Simulate Burn Wound Healing and Inflammation

Patrick P.G. Mulder[1,2], Rajiv S. Raktoe[1], Leonore S. Mastenbroek[1], Marcel Vlig[1], Anouk Elgersma[1], Esther Middelkoop[1,3,4], Irma Joosten[2], Hans J.P.M. Koenen[2], Bouke K.H.L. Boekema[1]

[1]Preclinical Research, Association of Dutch Burn Centres (ADBC), Zeestraat 29, 1941 AJ Beverwijk, The Netherlands
[2]Laboratory of Medical Immunology, Department of Laboratory Medicine, Radboud University Medical Center, Geert Grooteplein Zuid 10, 6525 GA Nijmegen, The Netherlands
[3]Amsterdam UMC location Vrije Universiteit Amsterdam, Plastic, Reconstructive and Hand Surgery, De Boelelaan 1117, 1081 HV Amsterdam, The Netherlands
[4]Amsterdam Movement Sciences, Tissue Function and Regeneration, De Boelelaan 1117, 1081 HV Amsterdam, The Netherlands

Background
Healing of (deep) burn injury is a complex process that often leads to functional as well as aesthetic complications. Split-thickness skin autograft surgery is a successful treatment option to cover deep wounds, but can introduce unwanted side-effects such as severe, irregular scars, reduced elasticity and impaired joint function. Clinically approved dermal substitutes are available but their performance needs improvement. Full skin equivalents (FSEs) generated from dermal substitutes can be used to pre-clinically test the potential of these substitutes for skin morphogenesis. Furthermore, these FSEs can be used as a platform to study other aspects of burn injury, such as wound healing and inflammatory response.

Materials and Methods
Here, we generated full skin equivalents (FSEs) by culturing human keratinocytes and dermal fibroblasts on different dermal substitutes, namely de-epidermalized dermis and collagen-based matrices from Mucomaix and Matriderm. Control models were produced from human *ex vivo* skin. FSEs were cultured at air-liquid interface up to 5 weeks to study skin development, wound repair and cytokine response. Immunohistochemical analysis of skin morphogenesis and wound healing was performed on tissue sections. Cytokine levels were determined in the culture medium using immunoassays.

Results
In these FSEs, proper dermal and epidermal morphogenesis was established as the expression of markers for early and late differentiation (cytokeratins) and basement membrane (laminin-α5 and collagen-4) were similar to models produced from de-epidermalized dermis and human *ex vivo* skin. Re-epithelization and cell proliferation in FSEs with standardized burn injury was determined at 1 week and 2 weeks post burn. Mucomaix rapidly degraded in this system and was therefore less suitable as a matrix for FSEs for extended culture times. Cytokines IL-6, IL-8 and MCP-1 were actively produced by the FSEs and highest levels were detected early after burn injury.

Discussion and Conclusions
We propose a novel *in vitro* platform that facilitates the investigation of skin development, wound repair and inflammation. This model can be used to evaluate medicinal intervention for improvement of wound healing. For the development of a more sophisticated model, we are currently testing the effect of different immune cell types on wound repair and inflammation.

Towards the Native Skin: ex vivo development of skin appendices

S. Jekhmane[1,2], K.S. Schilders[1], M. Vlig[1], A. Elgersma[1], S. van den Berg[1], C. Gho[3], B.K.H.L. Boekema[1], E. Middelkoop[1,2]

[1]Preclinical Research, Association of Dutch Burn Centres (ADBC), Zeestraat 29, 2518AA Beverwijk, the Netherlands
[2]Department of Plastic, Reconstructive & Hand Surgery, Amsterdam University Medical Centre, De Boelelaan 1117-1118, 1081HV Amsterdam, the Netherlands
[3]Hair Science Institute (HASCI), Claude Debussylaan 263, 1082MC Amsterdam, the Netherlands

Introduction. Skin defects resulting from burns, trauma or chronic wounds are a major burden. Split-thickness skin autograft surgery represents the current clinical gold-standard, but is limited by donor-site shortage and morbidity and scarring at the transplantation site thereby causing an urgent call for alternatives. Commercially available dermal substitutes have advanced over the years, yet have failed to fully recapitulate form and function of skin. This is largely due to the absence of aesthetic skin features such as colour, hair and sebaceous and sweat glands. Hair follicles (HF), in particular dermal papilla (DP) cells residing in HF, bear interesting wound healing and hair-inductive characteristics. Given their properties, DP cells provide an accessible option to engineer a full skin equivalent (FSE) that extends far beyond wound healing by introducing skin appendices. Indeed, DP cells are able to generate hair growth when implemented *in vivo* in animal models[1]. The successful translation of such strategy to humans in combination with dermal substitutes may pave a way for a broad clinical application of skin tissue engineering. **Materials and Methods.** This study exploits the possibility to incorporate DP cells to bioengineer FSE's with skin appendices. As a first step, DP cells were isolated from human HF kindly provided by HASCI using the enzymatic digestion or microdissection procedure adapted from [1] and [2],respectively. Cultured DP cells between passage 2 and 8 were quantified and characterized by flow cytometry. **Results and Discussion.** Both isolation procedures led to a successful culture of DP cells in a 2D format with the majority of cells expressing proliferation marker CD71. In contrast to microdissection, DP cells isolated by enzymatic digestion exhibited slower growth rates, presumably an effect caused by exposure to collagenase. Hence, microdissection is favoured for the isolation of DP cells. Characterization of DP cells revealed consistent high expression of the cellular markers CD90 (fibroblasts), CD49f (keratinocytes), CD200 (mesenchymal stem cells) and CD31 (endothelial cells) throughout passage 2 to 8. These data support the suggested stem cell activities of DP cells in wound healing. **Conclusion.** We have successfully isolated, cultured and characterized DP cells from HF, yet it is unlikely that these cells will generate hair as they lose their hair-inductive properties when cultured in 2D for extended time[3]. Hence, a next step will be to restore the 3D microenvironment by generating spheroids using DP cells.

References

1 Nilforoushzadeh, M. *et al.* Hair follicle generation by injections of adult human follicular epithelial and dermal papilla cells into nude mice. *Cell Journal (Yakhteh)* **19**, 259 (2017).

2 Topouzi, H., Logan, N. J., Williams, G. & Higgins, C. A. Methods for the isolation and 3D culture of dermal papilla cells from human hair follicles. *Experimental dermatology* **26**, 491-496 (2017).

3 Kishimoto, J., Burgeson, R. E. & Morgan, B. A. Wnt signaling maintains the hair-inducing activity of the dermal papilla. *Genes & development* **14**, 1181-1185 (2000).

Oral Session 8

The Role of Monocyte-Derived Macrophages as Endothelial Progenitors in Endothelium Injury

Dina M. Ibrahim[1,2], Hiuching Cheung[1], Carlijn V.C. Bouten[1,2], Anthal I.P.M. Smits [1,2]
[1]Department of Biomedical Engineering, Eindhoven University of Technology, Eindhoven, The Netherlands
[2]Institute for Complex Molecular Systems, Eindhoven University of Technology, Eindhoven, The Netherlands

Introduction

Endothelialization of implanted cardiovascular devices is the golden standard for obtaining a hemocompatible surface, yet it has not shown a complete success. Typically, the pool of cells contributing to endothelialization is thought to be limited to mature ECs, EPCs, and small population of other stem cells. Recently, monocytes have been reported as an additional source of endothelial-like cells in implanted vascular grafts. However, to what extent these cells can exert endothelial functions and the exact mechanism of how they integrate within a newly formed/injured endothelium is yet to be explored.

Aim

In this work we investigate to what extent monocyte-derived macrophages can functionally integrate in an injured endothelium and whether this is dependent on biochemical priming.

Materials and Methods

To achieve this, a wound healing model was established in which an endothelial monolayer is co-cultured in direct contact with human monocyte-derived macrophages that are primed into various polarization states (i.e., M1, M2a & M2c). The extent of monocyte-to-endothelial differentiation and functional integration into the endothelium was characterized by live-cell imaging, immunofluorescence, and flow cytometry.

Results

Our results showed that the scratch closure was faster in the co-cultures containing M2a and M2c macrophages. Interestingly, looking closer into all co-culture conditions, physical contact via VE-cadherin was noticed in the co-culture of endothelial cells and M2a in addition to endothelial cells and M2c after 48 hours.

Further quantification of the transitions in cell phenotypes via flow cytometry showed an increased expression of CD144 in M2a macrophages in the co-culture with endothelial cells. This was accompanied with and increased expression of CD163 and CD206 in in the co-culture containing M2c and M2a, respectively.

Conclusion and Outlook

The current results showed the tendency of M2a and M2c to shift towards endothelial phenotype with them forming physical contact with the injured endothelial monolayer. We are currently exploring the long-term co-culture condition to elaborate more on phenotype transition of macrophages and determine whether specific monocyte subsets have an increased potential to give rise to macrophage-EC transdifferentiation, to steer biomaterial design choices (e.g., surface bioactivation) for implanted cardiovascular devices. Additionally,

The results of this study reveal a new aspect of endothelial regeneration, namely through macrophage differentiation.

Funding

This project has received funding from the European Union's Horizon 2020 programme under grant agreement No 767195.

Erythrocyte-Inspired Lipid Coatings for Improved Particle Hemocompatibility

F.L. Fernandes Gomes[1], R. Edelbroek[2], J. van Weerd[3], P. Jonkheijm[2*], and J. Leijten[1*]
[1]Leijten Lab, Dept. of Developmental BioEngineering, Faculty of Science and Technology, Technical Medical Centre, University of Twente; [2]Dept. of Molecules and Materials, Laboratory of Biointerface Chemistry, Faculty of Science and Technology, MESA+ Institute for Nanotechnology, University of Twente; [3]LipoCoat BV; Enschede, The Netherlands.
[*]*authors contributed equally*. Contact: f.l.fernandesgomes@utwente.nl

Introduction

Blood-contacting biomaterials, such as vascular stents, grafts, catheters, or drug delivery systems require a particularly thorough hemocompatibility study prior to application *in vivo*. A wide range of polymeric and inorganic sources are used; however, not all of them elicit a safe blood-contacting response without a surface modification or coating.

Natural circulating living structures are inherently hemocompatible due to their lipid membranes. Lipids have an innate biocompatibility that has been consistently proven in marketed products, such as the SARS-CoV-2 vaccines[1], and their added versatility renders them one of the most promising building blocks for bioinert coatings. However, the hemocompatibility of different lipid coatings has remained largely unexplored for injectables.

In this work, we assessed whether erythrocyte membrane-inspired lipid coatings improved the hemocompatibility of micro- and nanoparticles. A simple bottom-up coating method based on a solvent gradient was first adapted to particle suspensions using fluorescent silica microparticles (SiO_2 MPs). Four biomimicking lipid coatings of increasing complexity were then applied to other small spherical substrates, and their hemocompatibility profiles were compared.

Our results showed that SiO_2 MPs were successfully coated through a bottom-up method using different lipid compositions. All coatings reduced silica nanoparticle-induced hemolysis rates and delayed plasma coagulation. Ongoing work focuses on protein adsorption assays on different substrates, and future work will include a screening of inflammatory response, platelet activation, and complement activation of lipid-coated materials.

Methodology

DiagNano™ Green Fluorescent Silica Particles of 5 µm (SiO_2 MPs, CD Bioparticles) were coated through a solvent gradient method. In short, solvent-based fluorescent lipid solutions of different compositions (Avanti Polar Lipids, Inc.; Sigma-Aldrich; Invitrogen™) were added to SiO_2 MPs in the respective solvent, and a solvent-buffer gradient was induced through a gradual addition of DPBS. Heating and osmotic shock steps were added to facilitate coating formation. Finally, particles were washed and resuspended in DPBS. The coating was studied using a Zeiss LSM 880 (Zeiss). For hemocompatibility studies, SiO_2 MPs and SiO_2 nanoparticles (0.1 µm, SiO_2 NPs; Polysciences Inc.,) were used. Hemolysis assays were conducted by incubating 0.2 mg of particles with human red blood cells at 37°C (4 h) and assessing hemoglobin release. Coagulation time assays were conducted by analyzing fibrin clot formation kinetics after plasma-material incubation (0.5 h) and recalcification with 20 mM $CaCl_2$.

Results and Discussion

A solvent gradient-assisted lipid coating method was first optimized with a simple lipid formulation through the screening of a number of gradient conditions. Four biomimicking lipid coatings were then applied to SiO_2 MPs using the solvent-based method, which confirmed satisfactory surface coverage (Fig.1a). Next, the coatings were applied to SiO_2 NPs, and both types of substrates were used in hemolysis and coagulation kinetics assays. Coatings showed a ten-fold reduction in SiO_2 NP-induced hemolysis (Fig.1b) and a delay in coagulation onset by SiO_2 NPs (Fig.1c). Minimal differences in hemolysis rate and coagulation time were observed in SiO_2 MPs due to their larger size and lower surface area-to-volume ratio. Other biological studies are currently being performed to assess potential bio-responsive differences between the tested lipid formulations.

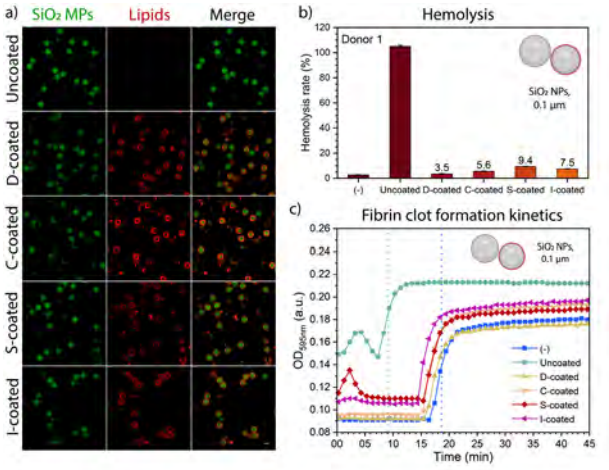

Figure 1. a) *Confocal microscopy images of four lipid coatings (referred in image as D,C,S,I) applied on SiO_2 MPs. Scale bar equals 5 µm.* ***b)****. Hemolysis rates and* ***c)*** *fibrin clot formation kinetics of uncoated and coated SiO_2 NPs.*

Conclusions

We report on an innovative way of lipid-coating microparticles and nanoparticles with complex formulations using a bottom-up approach. Blood assays indicated lipid coatings substantially reduced nanoparticle-induced hemolysis and delayed coagulation. Upcoming efforts will focus on hemocompatibility based on immunological responses.

References

1.Schoenmaker et al., *Int J Pharm*, 2021. **601**: p. 120586.

Acknowledgements

F.L.F.G. acknowledges the TechMed Donor Service of the University of Twente and all its collaborators and donors. Authors acknowledge financial support from Health~Holland (Project LSHM19074).

Analyzing The Risk Of Calcification In Materials Used For In Situ Heart Valve Tissue Engineering

D.C. van der Valk[1,2], C.M.H. Hoes[1], Y.M.H.R Rasenberg[1], W. Szymczyk[1], A. Akiva[3], A.I.P.M. Smits[1,2], C.V.C. Bouten[1,2].

1 Department of Biomedical Engineering, Eindhoven University of Technology, Eindhoven, The Netherlands
2 Institute for Complex Molecular Systems, Eindhoven University of Technology, Eindhoven, The Netherlands
3 Department of Cell Biology, Radboud UMC, Nijmegen, The Netherlands

INTRODUCTION

Material-driven *in situ* tissue engineering (TE) of valvular grafts prospects a great alternative to current autologous, xenografted, and non-biological valve replacements. In this *in situ* approach, a synthetic degradable valve replacement is implanted at the site of a diseased valve, where it gradually remodels into viable tissue.[1] However promising, some risks need assessment to ensure safe clinical translation. Among these is calcific nodule formation during *in vivo* assessment of the grafts, reported in 35% of current TE grafts in preclinical animal studies.[2-4] This study established an *in vitro* model to assess calcification potential of materials for *in situ* TE.

EXPERIMENTAL METHODS

Three candidate materials for *in situ* TE were electrospun into fibrous scaffolds with a fiber diameter ranging from 4-6 um; widely used Polycaprolactone (PCL), as well as two supramolecular polymers Bis-Urea extended PCL (PCL-BU), and Bis-Urea extended Polycarbonate (PC-BU). A glutaraldehyde-treated bovine pericardial patch was used as control for current clinical practice. Circular scaffolds of 8 mm Ø were clamped in membrane-free transwell inserts and seeded with porcine Valvular Interstitial Cells (pVICs) or used unseeded. Scaffolds were then cultured for three weeks in phosphate-enhanced calcification medium (CM). PCL scaffolds were furthermore cultured in CM enhanced with Macrophage conditioned inflammation medium (IM). Calcification and collagen formation were assessed with live hydroxyapatite and collagen staining. Cell differentiation was analyzed using real time polymerase chain reaction (PCR)

RESULTS AND DISCUSSION

After three weeks of culture, PC-BU scaffolds showed little calcification, were calcification in PCL as well as PCL-BU scaffolds increased (Figure). Collagen formation was similar between PCL and PC-BU, but more compared to PCL-BU scaffolds. pVIC osteogenic gene expression was increased in scaffolds cultured in CM compared to NM, but not differentially expressed in different scaffold-types. Expectedly, scaffolds cultured without pVICs stained negative for collagen and hydroxyapatite. Seeded PCL scaffolds cultured in IM showed increased calcification compared to CM. Cell expression of osteogenic genes was increased in these scaffolds cultured in IM compared to CM. Pericardial patch scaffolds showed more calcification than all other scaffold types. Overall, materials for *in situ* TE of valvular grafts showed a differential potential for calcification.

CONCLUSION

This study established a model to find differential calcification potential of scaffolds for *in situ* TE. PC-BU scaffolds, which show good results with little calcification in *in vivo* animal studies, showed little calcification potential in our model, unrelated to the amount of collagen formation. Scaffold calcification was mediated by cellular activity and increased with inflammation. The established *in vitro* model can be used to assess if materials for in situ TE calcify and can help discover the reasons why. Moving forward, this model will be extended with hemodynamic loads and patient specific culture conditions to assess risk of calcification under in vivo clinically relevant conditions. This data may support optimization of biomaterials for *in situ* valvular TE, aiding safe clinical translation.

REFERENCES

1. Wissing TB *et al*., Npj Regen Med. 2(1):18, 2017.
2. Bennink G *et al*., J Thorac Cardiovasc Surg. 55(6):2591-2601, 2018.
3. Kluin J, *et al.*, Biomaterials. 125:101–17, 2017.
4. Valk DC van der *et al.* Under review in JACC: BTS, 2022.

ACKNOWLEDGEMENT

We gratefully acknowledge the Gravitation Program “Materials Driven Regeneration”, funded by the Netherlands Organization for Scientific Research (024.003.013)

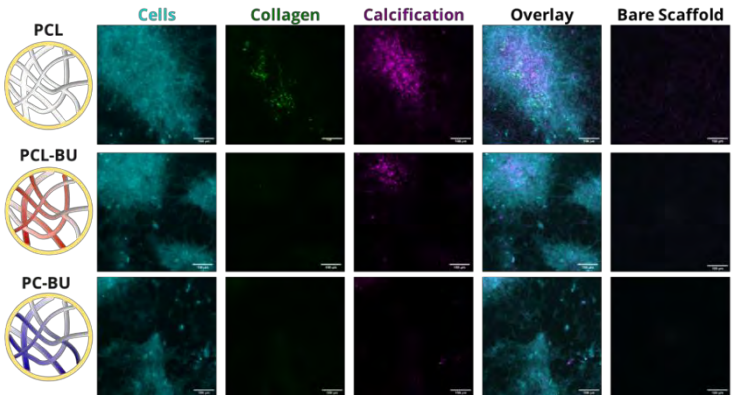

Figure 1 Collagen formation (green) and calcification (pink) in PCL (top), PCL-BU (middle), and PC-BU (bottom) scaffold materials.

Injectable Nanoparticle-Hydrogel Composite for Cardiac Tissue Regeneration

R. Bártolo[1], T. Bauleth-Ramos[1,2], G. Torrieri[2], A. Esquivel[3], K. Gomez[3], M. Shahbazi[1], P. v. d. Meer[3], H. A. Santos[1,2]

1 Department of Biomedical Engineering and W.J. Kolff Institute for Biomedical Engineering and Materials Science, University Medical Center Groningen/University of Groningen, 9713 Gz Groningen, the Netherlands
2 Drug Research program, Division of Pharmaceutical Chemistry and Technology, Faculty of Pharmacy, University of Helsinki, 00100 Helsinki, Finland
3 Department of Cardiology, University Medical Center Groningen, 9713 Gz Groningen, the Netherlands

Myocardial infarction (MI) is a life-threatening condition characterized by irreversible cell death. During the past decades, several therapeutic strategies have held the promise of restoring the full functionality of a damaged heart. However, MI approved therapies, to date, only ameliorate the state of care of these patients. Therefore, new therapeutic approaches need to be explored. Herein, we have developed a nanoparticle (NP) composite injectable hydrogel for MI treatment. This system consists of a tragacanth-based injectable hydrogel, containing cytokines and spermine-acetalated dextran-based (AcDXSp) functional NPs loaded with miRNA. We hypothesized that this system can modulate the immunoenvironment present in the heart after MI and induce cardiac fibroblasts differentiation to myofibroblasts.

AcDXSp NPs were prepared by double emulsion technique and functionalized with PEG and Atrial natriuretic peptide. These NPs were characterized by dynamic light scattering and Fourier transform infrared spectroscopy (FTIR). Cytocompatibility and cell–nanoparticle interactions were performed using STEM cell derived cardiomyocytes and fibroblasts.

Tragacanth (Tr) and hyaluronic acid (HA) solution were crosslinked with iron chloride hexahydrate to create an injectable hydrogel, which was further analyzed by cryogenic transmission electron microscopy and FTIR. Rheometer properties were measured using TA Instruments AR2000 stress-controlled rheometer. Cytokine release was measured using ELISA.

To achieve the final system, Tr/HA polymer solution was loaded with miRNA/AcDXSp-PEG-ANP NPs and cytokines prior to cross-linkage. The final system was characterized using confocal microscopy. The cytocompatibility and cell–system interactions were demonstrated *in vitro*.

The successful functionalization of AcDXSp NPs with PEG and ANP was demonstrated by shift of ζ-potential and FTIR band. Further, the functionalization led to an increased uptake of the NPs. pH-dependent degradation was accessed at pH 7.4 and 5.5.

The final system was injectable using a 27G needle and demonstrated self-healing properties. Moreover, it showed no toxicity *in vitro* up to 48h in cardiomyocytes and macrophages.

The preliminary data show that the final system was biocompatible, and it is expected to successfully deliver miRNA, highlighting the potential of this system toward improved gene delivery, and thus, potential cardiac regeneration therapy.

Cell-cell signaling to control arterial growth and remodeling: a computational approach

JGM van Asten[1], M Latorre[2], C Karakaya[1], FPT Baaijens[1], C Sahlgren[1,3], T Ristori[1], JD Humphrey[2], S Loerakker[1]
1: Department of Biomedical Engineering, Eindhoven University of Technology, the Netherlands
2: Department of Biomedical Engineering, Yale University, New Haven, CT, USA
3: Faculty of Science and Engineering, Biosciences, Åbo Akademi, Turku, Finland

Introduction

Vascular Tissue Engineering (TE) has not yet reached widespread clinical application. We hypothesize that establishing a native-like tissue organization is crucial to overcome current limitations[1]. To achieve such an organization, a better understanding of vascular growth and remodeling (G&R) is vital. This G&R is known to be regulated by vascular smooth muscle cells (VSMCs) populating the vessel wall. In addition, mechanical stimuli strongly affect this regulation[2]. Notch signaling, a cell-cell signaling pathway that plays a key role in vascular development[3], influences VSMC behavior and is sensitive to mechanical stimuli[4]. Notch signaling may therefore be a crucial factor in mechano-regulated G&R in vascular TE. A more detailed understanding of this process may inspire ways to control G&R by targeting Notch. To explore this, we developed a computational model to predict the role of Notch in vascular G&R.

Materials and Methods

A multiscale computational model was developed. At the cell-scale, an agent-based model[4] was adopted describing stretch-sensitive Notch signaling kinetics in VSMCs using a system of ordinary differential equations. At the tissue-scale, a constrained mixture model[5] was chosen that simulates vascular tissue as a mixture of collagen, smooth muscle, and elastin whose mechanics, production and removal are captured over time. The coupling between these models was informed by in vitro data obtained from human VSMCs.

Results and Discussion

The computational model was used to investigate a vessel's response to an increase in blood pressure, as an illustrative example of vascular G&R. Our predictions suggest that an increase in pressure, resulting in an increase in stretch experienced by the VSMCs (Fig.1a), leads to lower Notch activity (Fig.1b). In turn, this was predicted to increase the mass density of smooth muscle and decrease that of collagen (Fig.1c), based on the collected in vitro data. Finally, these changes in density result in an increase in vessel thickness (Fig.1d). The altered geometry and composition of the vessel restore the stretch to their original value (Fig.1a), thereby maintaining a mechanical homeostasis in the vessel. This predicted thickening response corresponds well with experimental findings[6]. However, the response usually occurs faster in vivo and an increase in both smooth muscle and collagen content is commonly observed[6]. This indicates that Notch signaling likely contributes to vascular G&R, but that other factors also play a role. Future models should therefore incorporate these factors to describe vascular G&R more completely.

Next, the model was adopted to explore the effects of targeted Notch manipulations on vascular G&R. In particular, the introduction of external Jagged ligands, either soluble or immobilized to a scaffold, was investigated. Simulations predicted that introducing immobilized Jagged ligands leads to a higher smooth muscle density and a lower collagen density (Fig.1c), resulting in a slightly thicker vessel (Fig.1d). Soluble Jagged ligands were predicted to have the opposite effect (Fig.1c), causing a slightly thinner vessel (Fig.1d). These results suggest that vascular growth can be both induced and inhibited by introducing external Jagged ligands, affecting the final composition and geometry of the vessel. This provides a potential avenue for controlling vascular regeneration by targeting Notch signaling.

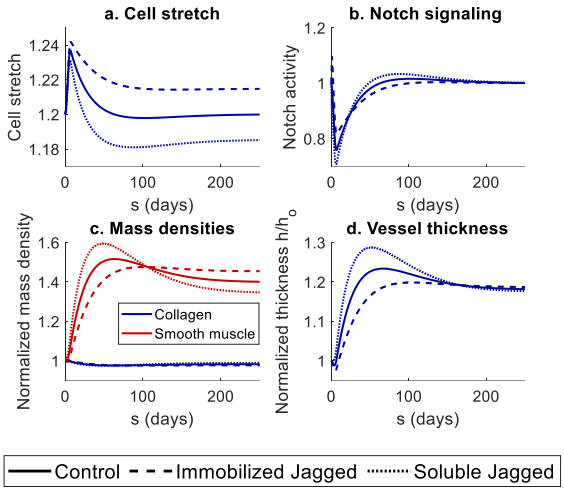

Figure 1: predicted time course of vascular G&R in response to a 20% increase in blood pressure

Conclusions

We developed a computational model to simulate the role of Notch signaling on vascular G&R. Our simulations predict that Notch signaling can restore mechanical homeostasis in hypertension by inducing thickening of the vessel wall. In addition, Notch signaling may be targeted to control vascular G&R, for example by introducing external Jagged ligands, which can inspire new strategies to improve the outcome of vascular TE.

References

1. Karakaya & Van Asten et al. BMMB, 21(1):5-54, 2022. **2.** Humphrey et al. Hypertension, 52:195-200, 2008. **3.** Iso et al., Arterioscler Thromb Vasc Biol, 23:543-553, 2003. **4.** Loerakker et al. PNAS, 115(16): E3682-E3691, 2018. **5.** Humphrey et al., Math Models Methods Appl Sci, 12(3):407-430, 2002. **6.** Bersi et al. J. R. Soc. Interface 14: 20170327, 2017.

Acknowledgements

This work has received funding from the European Research Council (ERC) (Grant No. [802967]).

A novel method for cell delivery in decellularized heart valves using injectable hydrogels

V.C. Vetter[123], N. Masoumi[12], Z. Machaidze[1], M. Gansevoort[1], J.L. Andresen[2], O.S. Fenton[2], A.I.P.M. Smits[3], C.V.C. Bouten[3], R. Langer[2], J.E. Mayer[1]

[1]Department of Cardiovascular Surgery, Boston Children's Hospital, Harvard Medical School, Boston, The United States of America
[2]Department of Chemical, Biological and Mechanical Engineering, Koch Institute for Integrative Cancer Research, Massachusetts Institute of Technology, Cambridge, The United States of America
[3]Department of Biomedical Engineering, Eindhoven University of Technology, Eindhoven, The Netherlands

Introduction

Tissue engineered heart valves (TEHVs) offer a promising alternative strategy for heart valve disease, combining engineered materials as scaffolds and stem cells to create living valve replacements. One strategy involves the use of decellularized donor heart valves as scaffolds, removing native cells and other bioactive components while preserving the structural proteins, known as the extracellular matrix (ECM). In recent years, progress has been made in decellularization strategies and decellularized xenograft or homograft valve tissues are attractive scaffold materials for TEHVs. However, the subsequent repopulation of the tissues by host-cells *in vivo* has challenges including limited cell ingrowth and non-homogeneous cell distribution. The long-term success of TEHVs depends on the scaffold transformation after implantation into living tissue through the interactions between scaffold properties and the regenerative capacity of the host. In this proof-of-concept study we developed a novel method to introduce cells inside the spongiosa (middle) layer of decellularized heterograft valve scaffolds prior to implantation.

Material and Methods

In this xenograft model semilunar porcine heart valves were decellularized and combined with isolated Dorset sheep cells.

To investigate the feasibility of this method, sheep valvular interstitial cells (VICs) were isolated and cultured *in-vitro*. The VICs were encapsulated in an in-house developed β-aminoacrylate synthetic polyethylene glycol (PEG) based hydrogel with a click-like polymerization and combined with decellularized valves. These TEHVs were cultured for 0,5,7 days and fixed for histology processing.

To investigate the translation of this method, three sheep underwent a single pulmonary valve leaflet replacement via left-thoracotomy. Sheep mesenchymal stem cells (MSCs) and endothelial colony forming cells (ECFCs) were isolated and cultured *in-vitro*. The decellularized valve scaffolds were combined with the MSCs encapsulated in a widely used GelMA-HAMA hydrogel and the outside of the leaflets were seeded with ECFCs. The TEHVs were cultured *in-vitro* and implanted in the donor matched sheep for up to six weeks.

Results

We show that we can achieve a homogeneous cell distribution throughout the entire decellularized scaffold. *In vivo,* the leaflets showed good function without stenosis, regurgitation, or valve thickening. Post-explant histology showed persistence of the seeded cells inside the scaffold. In addition, cellular infiltration by both M1 as M2 macrophages was observed.

Conclusions

In this study we show that we can successfully deliver cells into the spongiosa layer of a valve leaflet with a good spatial cell distribution using hydrogels. In addition, single leaflet implantations show that our leaflet functions well for up to six weeks *in vivo* with persistence of seeded cells inside the leaflet.

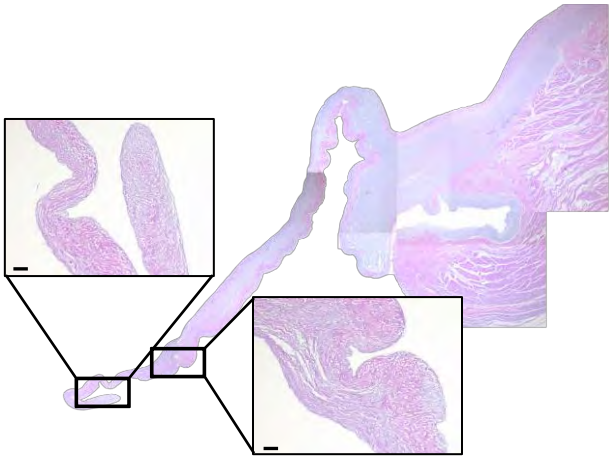

H&E staining of VIC-injected decellularized pulmonary valve leaflet using a β-aminoacrylate synthetic hydrogel after 7 days in-vitro.

Acknowledgement

We gratefully acknowledge the Gravitation Program "Materials Driven Regeneration", funded by the Netherlands Organization for Scientific Research (024.003.013)

v.c.vetter@tue.nl

Oral Session 9

The differential response of human macrophages to 3D printed titanium antibacterial implants does not affect the osteogenic differentiation of hMSCs

A. Garmendia Urdalleta (1) (2), M. Van Poll (1) (2), N. Fahy (2) (3), J. Witte-Bouma (2), W. Van Wamel (4), I. Apachitei (1), A. A. Zadpoor (1), L. E. Fratila-Apachitei (1), E. Farrell (2)

(1) Department of Biomechanical Engineering, Faculty of Mechanical, Maritime and Materials Engineering, TU Delft, Mekelweg 2, 2628 CN Delft, The Netherlands
(2) Department of Oral and Maxillofacial Surgery, Erasmus MC, Doctor Molewaterplein 40, 3015 GD Rotterdam, The Netherlands
(3) Department of Orthopaedics, Erasmus MC
(4) Department of Medical Microbiology and Infectious Diseases, Erasmus MC

Introduction. Despite considerable developments in the field of orthopaedic implants, complications including poor bone ingrowth and implant-associated infections (IAI) persist. Macrophages have recently been acknowledged to be essential for the implant success in the body, partly through intimate crosstalk with human marrow stromal cells (hMSCs) in the process of new bone formation [1]. However, the behavior of these immune cells is known to be affected by environmental cues, including the implant surface properties. Additive manufacturing (AM), surface biofunctionalization, and silver nanoparticles incorporation are promising techniques to achieve orthopaedic implants with osteogenic, immunomodulatory, and antibacterial biofunctionalities [2–4]. The osteoimmunomodulatory properties of such implants are, however, not yet well understood. We, therefore, investigated the effects of human macrophages on the hMSCs when co-cultured *in vitro* with AM titanium implants biofunctionalised via plasma electrolytic oxidation (PEO) and incorporated with silver nanoparticles (AgNPs).

Methodology. AM generated Ti-6Al-4V implants were biofunctionalised via PEO with/without AgNPs. Surface characterisation was performed with a scanning electron microscope (SEM) and silver ion release was measured. The effects of the incorporation of AgNPs at different concentrations on human macrophages and bacterial cells were assessed by evaluating the viability of human macrophages and performing an isothermal microcalorimetry assay where bacterial metabolic activity was measured. The response of human macrophages and hMSCs monocultures to the PEO-treated Ti-6Al-4V implants were subsequently evaluated by measuring mineralisation, protein, and gene expression. Finally, an indirect co-culture of macrophage-hMSCs was performed to study the effects of the macrophage response induced by the implants on the hMSCs osteogenic differentiation.

Results. The PEO modification of the AM implants created TiO_2 surfaces with micro- and nano-porosities. AgNPs were successfully incorporated into the TiO_2 layer. A concentration of 0.3 g/L AgNPs was found to be optimal to maintain the viability of human macrophages while imparting sufficient antibacterial properties to prevent bacterial growth on their surfaces. The expression of tissue repair related factors decreased in the specimens containing 0.3 g/L AgNPs as compared to the PEO-treated specimens not incorporating AgNPs. The same trend was observed for the macrophages co-cultured with hMSCs. However, this did not affect the osteogenic differentiation of hMSCs. Both co- and single-cultured hMSCs could osteogenically differentiate without any adverse effects caused by the presence of macrophages that were exposed to the either surface.

Conclusions. Based on the findings of this study, the incorporation of AgNPs into the PEO layers does not compromise the osteogenic differentiation and mineralization of hMSCs when co-cultured with human macrophages, while adding antibacterial functionalities to AM surfaces. Further evaluation of these promising implants in a bony *in vivo* environment with and without infection is, thus, recommended, and may prove them worthy of further development for potential clinical use.

References:

[1] Chen, Z. et al., Mater. Today 19, 304–321 (2016)
[2] Taniguchi, N. et al., Mater. Sci. Eng. 59, 690–701 (2016)
[3] Van Hengel, I. A. J. et al., Mater. Today Bio. 7, 1–12 (2020)
[4] F. Razzi et al., Biomed Mater. 15, 035017 (2020)

Gamma-irradiated *S. aureus* and combination of synthetic TLR-agonists for MSC osteogenic differentiation

P.K. Khokhani[1,3], M.C. Kruyt[1] , H. Weinans[1,3], D. Gawlitta[2,3]

[1]Department of Orthopaedics, University Medical Center Utrecht, Utrecht, The Netherlands
[2] Department Oral and Maxillofacial Surgery & Special Dental Care, University Medical Center Utrecht, Utrecht, The Netherlands
[3]Regenerative Medicine Center, Utrecht, The Netherlands

Introduction:

Strategies to enhance local bone formation, especially those synergizing with osteoinductive signals, are of great interest. Multiple studies indicate that pro-inflammatory mediators can act to stimulate bone formation.[1] Therefore we addressed the question of whether pathogen-derived factors leading to a broad activation of the innate and adaptive immune system, could enhance the efficacy of bone substitutes.

Bacterial infections generally lead to osteolysis and impaired bone healing, however, it was observed in a previous study that gamma-irradiated (γi) *Staphylococcus aureus* led to excessive subperiosteal bone formation in a rabbit tibia model. This underscored that sterile inflammation from γi *S. aureus* could be harnessed for osteo-immunomodulation[1].

Upon infection, *S. aureus* and its components are detected and processed predominantly by the host immune system via the toll-like receptors (TLRs) namely TLR2, TLR8, TLR9, and NOD-2[2]. Activation of TLRs results in the release of pro-inflammatory cytokines that affect MSC differentiation[3]. Recent evidence from *in vitro* studies shows that synthetic TLR-agonists possess immune-modulatory properties that may promote osteogenesis[4]. In this study, we aim at recreating the immune-modulatory response exhibited by γi *S. aureus* by using a combination of various synthetic TLR-agonists (mixtures). Furthermore, we aim to understand the underlying mechanisms and signaling pathways that may be beneficial for bone formation.

Methods:

The direct pro-osteogenic potential of γi *S. aureus* and mixtures was investigated by adding these components to a standard assay for MSC differentiation (medium including dexamethasone) (direct stimulation). The indirect, immune-mediated effect was investigated by deriving conditioned medium from human immune cells that were stimulated with γi *S. aureus* and mixtures, to the MSC differentiation media.

Peripheral blood mononuclear cells (PBMCs) were isolated from the blood of healthy human donors (n = 6) using the density gradient centrifugation method. After isolation, PBMCs were stimulated with γi *S. aureus* or individual synthetic TLR agonists or different mixtures prepared by combining agonists for TLR2, TLR9, TLR8, and NOD-2 (Table 1). After 24 hours, the conditioned medium (CM) from all donors was pooled, and stored.

MSCs were obtained from bone marrow aspirates obtained from healthy patients (n = 3). MSCs were cultured in expansion medium until passage 5. For direct stimulation experiments, MSCs were cultured in osteogenic medium supplemented with γi *S. aureus* or various mixtures of the TLR agonists. MSCs cultured in osteogenic medium were used as control. For indirect stimulation experiments, MSCs were cultured in 75% medium supplemented with/without dexamethasone and 25% conditioned medium obtained from the unstimulated and/or stimulated PBMCs. Alkaline phosphatase activity was measured on days 3,7,10, and 14, and mineralization (Alizarin red) on day 21. Bone-specific osteocalcin and osteonectin were measured by immunohistochemistry on day 14. Bulk RNA sequencing experiments were performed on PBMCs (n = 3) stimulated with γi *S. aureus* and compared with unstimulated PBMCs to identify the underlying mechanism that may be responsible for enhancing osteogenic differentiation.

Results and Discussion:

The direct stimulation of MSCs with γi *S. aureus* and the mixtures (see table) did not increase or inhibit their ALP activity. However, indirect stimulation with conditioned medium from both γi *S. aureus* and the TLR agonists mixtures MIX 1, MIX 4 and MIX 5 showed a 5-fold increase in ALP activity. Experiments for mineralization assays, bone-specific marker expression, and bulk RNA sequencing are ongoing.

In this study, we demonstrate that γi *S. aureus* enhances the osteogenic differentiation of MSCs via indirect immune-mediated stimulation. Furthermore, we show that the cellular responses of immune cells and MSCs to γi *S. aureus* exposure can be recreated by substituting it with a combination of synthetic TLR-agonists (mixtures). In terms of safety and clinical translation, TLR-agonists are advantageous as immune modulators since they are already being used in clinical trials[5]. Thus, formulations with TLR-agonists used in this study can serve as clinically relevant immune-modulatory bone enhancing agents.

References:

1. Croes, M. *et al. Eur. Cell. Mater.* **37**, 402–419 (2019).
2. Askarian, F., Wagner, T., Johannessen, M. & Nizet, V. *FEMS Microbiol. Rev.* **42**, 656–671 (2018).
3. Khokhani, P. *et al. Tissue Eng. Part C Methods* (2022) doi:10.1089/ten.TEC.2022.0086.
4. Khokhani, P. *et al. Materials* **14**, 1119 (2021).
5. Luchner, M., Reinke, S. & Milicic, A. *et al. Pharmaceutics* **13**, 142 (2021).

Funding/acknowledgments

This work is funded by PPS allowance from Health~Holland LSH-TKI (grant number: LSHM18011) and EU's H2020 research and innovation programme under Marie S. Curie Cofund RESCUE (grant agreement No 801540).

Synthetic TLR agonists mixtures	Synthetic TLR agonists used in this study			
	TLR 2/1	**NOD-2**	**TLR 9**	**TLR 8**
MIX 1	Pam3CSK4	Murabutide	CpG ODN C	X
MIX 2	CL429	PGN + Murabutide	CpG ODN C	X
MIX 3	X	Murabutide	CpG ODN C	X
MIX 4	CL429	Murabutide	CpG ODN C	Resiquimod
MIX 5	LTA	Murabutide	CpG ODN C	Resiquimod
MIX 6	X	PGN + Murabutide	CpG ODN C	X
MIX 7	CL429	Murabutide	CpG ODN C	X

Table 1. Overview of the mixtures (MIX)1 -7 prepared using the synthetic TLR agonists and the involved TLR.

Poisson's Ratio-Driven Bone Cell Growth in Meta-Biomaterials

E. Yarali[1,2], M. Klimopoulou[1], U. Staufer[2], A.A. Zadpoor[1], L.E. Fratila-Apachitei[1], A. Accardo[2], M.J. Mirzaali[1]

[1]Department of Biomechanical Engineering & [2]Department of Precision and Microsystems Engineering (PME), Faculty of Mechanical Maritime and Materials Engineering, Delft University of Technology (TU Delft), Mekelweg 2, 2628 CD, Delft, the Netherlands

Introduction

Aging, infection, and tumor compromise the osseointegration of bone implants. To address this challenge, biophysical and biochemical cues such as geometry (*e.g.,* surface curvature, pore shape), stiffness, surface topography and chemistry can be used to enhance implant osseointegration. Meta-biomaterials represent successful candidates in terms of mimicking the geometry and stiffness of bone [1]. In meta-biomaterials, however, it is still not clear how Poisson's ratio (PR), as a representation of pore's shape, can promote bone formation [2]. To do so, other mechanical and geometrical parameters such as stiffness, pore size and porosity should be decoupled. For this purpose, we rationally designed different meta-biomaterials with different stiffness, PR values and porosities at the microscale. The 3D meta-biomaterials were additively manufactured by the two-photon polymerization (2PP) method and were mechanically tested to obtain stiffness. To study the response of bone cells, mouse preosteoblasts (MC3T3-E1) were used.

Materials and Methods

Design and fabrication

Based on the size of the preosteoblast cells and the minimum pore size in bone scaffolds, the strut-based meta-structures were designed at microscale (36 µm to 2 mm) with extremely different PR values. To make such a complex structure at microscale, a Photonic Professional GT (Nanoscribe, Germany) 3D printer with high throughput was used. A commercially available photoresist named IP-Q (Nanoscribe) with a 10x objective in dip-in laser lithography (DiLL) and Piezo writing strategy was employed. Before printing the samples, silicon substrates were cleaned with acetone and isopropyl alcohol (IPA; both Sigma-Aldrich, Germany) followed by a 15 min oxygen plasma machine. To promote the adhesion between the samples and Si substrates, we silanized the substrates with 3-(Trimethoxysilyl) propyl methacrylate (Sigma-Aldrich, Germany) for an hour. To develop the samples after 3D printing, the meta-materials were immersed in propylene glycol monomethyl ether acetate (PGMEA, Sigma-Aldrich, Germany) for an hour followed by 5 min washing in IPA. At the end, to decrease the surface tension aiming for stronger bonding between the meta-biomaterials and Si substrates, Novec 7100 (Sigma-Aldrich, Germany) was used for 30 s.

Cell culture

The response of mouse preosteoblast cells (MC3T3-E1, Sigma-Aldrich, Germany) to the different scaffolds was determined by live/dead assay (Thermo Fisher Scientific, US), Presto blue assay (Thermo Fisher Scientific, US) and SEM imaging.

Results and Discussion

Schematic drawings of the rationally designed meta-biomaterials with different PR values and SEM images of the 2PP 3D-printed meta-biomaterials are shown in Figure 1. The porosity, stiffness and pore size of the designed meta-biomaterials is about 93%, 35-110 MPa and 184 microns, respectively. The PR values for the auxetic, conventional, hybrid and control are -0.91, 2.45, 0, and 0, respectively.

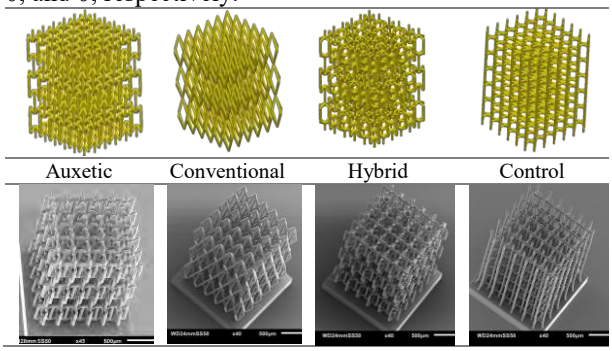

Figure 1. A schematic drawing of the rational design of the meta-biomaterials and SEM images of their 2PP 2D printing.

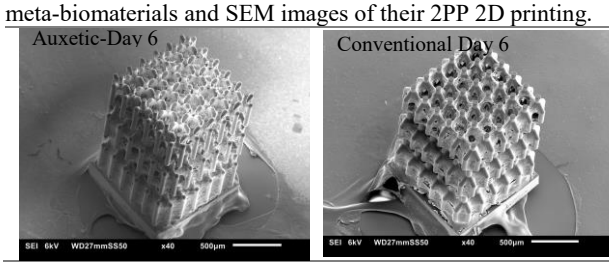

Figure 2. SEM images of the meta-biomaterials cultured preosteoblasts after 6 days of culture. Scale bar is 500 microns.

The preliminary cell experiments showed that all the designed meta-biomaterials supported attachment and proliferation of preosteoblast cells. Nevertheless, the cells in the scaffolds with positive PR (conventional) seemed to have a higher proliferation rate than those cultured on the scaffolds with a negative PR (auxetic) (Figure 2). This may be associated with the different geometry of the unit cell that may have favored migration and proliferation of cells in the case of the conventional scaffolds.

Conclusions

Meta-biomaterials represent a promising tool to make engineered cell micro-environments aiming to improve bone remodeling by controlling stiffness, configuration, mass transport, porosity, and auxeticity. This study showed that PR in meta-biomaterial can effectively tune bone formation.

References

1.Zadpoor, A.A.J.B.s., *Meta-biomaterials.* 2020. **8**(1): p. 18-38.
2.Flamourakis, G., et al., *Laser‐made 3D Auxetic Metamaterial Scaffolds for Tissue Engineering Applications.* 2020. **305**(7): p. 2000238.

Screening for osteogenic differentiation stimulating surface characteristics on Poly(Lactic Acid) using Double Orthogonal Gradients

Roderick H.J. de Hilster[1], Torben A.B. van der Boon[1], Nikita Samochwalow[1] and Patrick van Rijn[1].

[1]W.J. Kolff Institute for Biomedical Engineering and Materials Science, University of Groningen/ University Medical Center Groningen (UMCG), Ant. Deusinglaan 1, Groningen, The Netherlands

INTRODUCTION

Poly (lactic acid) (PLA) has been used as a biomaterial in numerous medical applications such as tissue engineering, drug carriers, medical equipment and orthopaedic implants. PLA is used often used because of its versatility in fabrication, biodegradability, and biocompatibility. The combination of biocompatibility and biodegradability makes PLA an ideal candidate for temporary implantation devices, an application for which it is already readily used in areas such as facial surgery. Our interest lies at the cell-material interface, a crucial point for the successful integration of a medical implant/device. In our research we want to expand on the functionality of PLA by modifying the surface topography in order to promote osteogenic differentiation which in turn will improve the implant integration with the native tissue.

We aim to study the effects of surface roughness and aligned topography on osteogenic differentiation of mesenchymal stem cells (MSCs) on PLA. For this purpose, we used a double orthogonal gradient (DOG) screening platform [1]. This novel platform enables fast screening for a vast amount of combinations of different topographies and surface characteristics such as wettability on their osteogenic differentiation stimulating effects in single cell experiments. We then locate and determine hot-spots, which either promote or inhibit osteogenic differentiation. Transferring the hot spot specific topography enables us to direct the desired cell response on the substrate of interest as well as which to avoid.

EXPERIMENTAL METHODS

The topography gradients were first made on silicone material (PDMS). To generate the roughness gradient, an aluminium template was sandblasted and subsequently gradually chemically etched, creating a gradient. The roughness from that template was transferred to PDMS via liquid curing. The aligned wrinkle topography was created by plasma treating stretched PDMS covered by an angled metal shield that is released after plasma treatment [2,3]. The roughness and wrinkle topographies were transferred to PLA in a heated press. Atomic Force Microscopy (AFM) and Scanning Electron Microscopy (SEM) were used to characterize the surface features qualitatively and quantitatively. A wettability gradient was applied orthogonally to the imprinted roughness and wrinkle gradients via shielded plasma treatment. The effects of the PLA DOG topographies and wettability on osteogenic differentiation will be investigated by culturing of bone marrow derives mesenchymal stromal cells for 1,7 and 21 days. Initially characterizing osteogenic differentiation by staining for alkaline phosphatase (ALP) and osteopontin (OPN) markers and further quantification by immune-fluorescence staining. The staining's are imaged (TissueFAXS) and analysed (TissueQuest) using TissueGnostics equipment. The high-throughput analysis is complemented by confocal laser scanning microscopy (CLSM) to obtain more detailed information on specific regions of interest (ROI) on the gradient substrates. Every ROI is translated to homogeneous, non-gradient surfaces, to verify the screening outcome.

RESULTS AND DISCUSSION

On top of the DOG modified PLA surface, every position represents a unique combination of either roughness/wettability or wrinkles/wettability, within their respective gradient ranges. Transferring topography from PDMS to PLA trough heat press imprinting resulted in little to no loss topography. Wrinkle wavelength ranged from λ = 1,6 µm – 12 µm and amplitude from A = 160 nm – 1650 nm, the smallest wavelengths corresponding with the smallest amplitudes propagating in a coupled fashion along the gradient. Roughness, expressed in sRa values, ranged from ~90 – 450 nm. Cell studies on top of the PLA DOG surfaces are underway and results are expected in the near future. We hypothesize that different combinations of PLA surface modifications either promote or inhibit osteogenic differentiation in MSC's.

CONCLUSION

Using the novel DOG screening platform to characterize and identify optimal osteogenic differentiation stimulating topographies will allow us to expand the possibilities for the use of PLA in medical applications. Furthermore, by changing the topographies applied in the DOG screening we can determine other desired cellular behavior to be had on the PLA cellular interface.

REFERENCES

[1] Zhou Q. *et.al.,* Adv. Mater. Interfaces. 5(18), 2018
[2] Zhou Q. *et.al.*, Sci. Rep. 5:16240, 2015
[3] van der Boon T.A.B. *et.al.*, Adv. Biosyst. 4:1900218, 2020

From nanopatterned sheets to stiff meta-biomaterial

M. Ganjian[1], T. van Manen[1], S. Janbaz[1,2], N. Tümer[1], K. Modaresifar[1], L.E. Fratila-Apachitei[1], A.A. Zadpoor[1]

[1]Department of Biomechanical Engineering, Faculty of Mechanical, Maritime, and Materials Engineering, Delft University of Technology, Mekelweg 2, 2628CD, Delft, The Netherlands.
[2]Institute of Physics, University of Amsterdam, Science Park 904, 1098 XH, Amsterdam, The Netherlands

Introduction

The quest for ideal bone substitutes that mimic the properties of the bone is ongoing. Affording synthetic bone substitutes with functionalities that allow them to regulate cell behavior could greatly increase their chance of successful osseointegration. The introduction of nanotopographies to the surface of bone substitutes is particularly appealing, because well-designed surface ornaments may be able to (simultaneously) kill bacteria and induce osteogenesis. Given the fact that most of the nanopatterning techniques are planar in nature, they cannot be easily applied to porous meta-biomaterials whose surface areas are primarily non-planar. In this work, for the first time ever, we developed and applied two different techniques, namely crumpling and folding, on the nanopatterned flat Ti sheets, to make complex 3D structures which enable the fabrication of meta-biomaterials that combine a rationally designed 3D architecture (*e.g.,* to tune mechanical and mass transport properties) with nanoscale surface features (*e.g.,* to guide the differentiation of stem cells). The proposed approaches are highly scalable given that the pores of the flat sheet can be arbitrarily large in number and small in dimensions. The *in vitro* cell culture (MC3T3-E1 preosteoblasts) on both crumpled and folded surfaces demonstrated the cytocompatibility of the nanopatterned scaffolds.

Materials and Methods

Polished Ti sheets were used for this study. The specimens were cut using laser micromachining (Optec Laser Micromachining Systems, Belgium).

The nanopatterns were fabricated on the polished Ti specimens using an ICP RIE machine (PlasmaLab System 100, Oxford Instruments, UK). Cl_2 and Ar were the etching gasses. The specimens were cleaned in acetone, ethanol, and isopropyl alcohol afterwards.

Crumpling: The size of the 2D flat sheet (22.5×22.5 mm^2), the number of the pores per specimen (12×12), and the center-to-center interspacing (1.87 mm) of the pores were kept constant while the diameter of the pores was varied (1.46, 1.53, and 1.59 mm) using CAD software (Solidworks, Dassault Systèmes) to fabricate scaffolds with different porosities.

The crumpling process (Figure 1) was carried out using a universal mechanical testing bench (Plus/Lloyd Instruments, England) equipped with a 5 kN load cell.

Folding: A biocompatible cyanoacrylate-based adhesive (ethyl cyanoacrylate, MB297Med-2, MasterBond, US) was used to assemble the folded storeys. After the application of the adhesive, the specimens were compressed for at least 2 min to guarantee the sufficient fixation of the components. The mechanical tests were performed after at least 48 h to ensure the adhesive was fully cured (Figure 2).

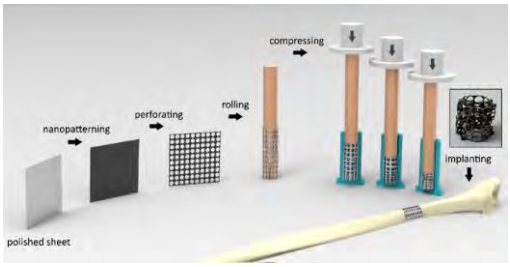

Figure 1. A schematic illustration of the steps involved in the crumpling of nanopatterned porous Ti sheets.

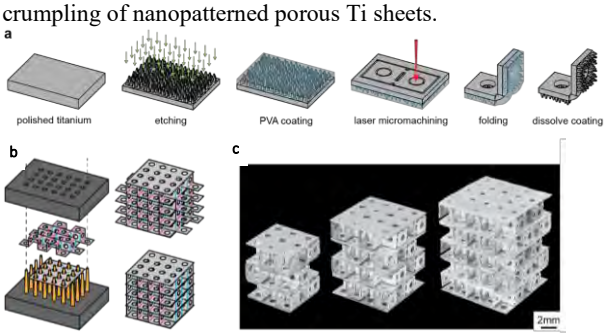

Figure 2. (a) A schematic illustration of the nanopatterning and surface protection steps. (b) The assembly of the folded storeys into a cubic lattice structure. (c) The photographs of the folded cubic lattices with different numbers of unit cells.

MC3T3-E1 preosteoblasts (Sigma-Aldrich, Germany) were seeded on the non-patterned and nanopatterned 3D specimens. The PrestoBlue assay (Thermo Fisher Scientific, US), live/dead, and Alizarin Red staining assay (Thermo Fisher Scientific, US) were used to determine the metabolic activity, viability of the cultured cells, and the mineralized area, respectively.

Results and Discussion

Automated folding and controlled crumpling are interesting alternatives to origami approach, as they greatly simplify the process of going from a flat construct to a 3D porous structure. Given the stochastic nature of the crease patterns and folding sequences, the resulting structure is highly resistant to minor imperfections, while highly regular origami lattices are sensitive to the slightest deviations from the perfect geometry. Moreover, these techniques offer a high degree of tunability in terms of the mechanical properties and morphological features (*i.e.,* pore size, strut size, porosity, etc.) as the crucial factors which determine oxygenation, migration, spreading, settling, and feeding of the cells. The live/dead and cell metabolic activity assays showed that the preosteoblasts can survive and proliferate after adhesion to the crumpled scaffolds. After 7 days, we observed a significant increase in the elongation of the cells residing on the nanopatterned crumpled scaffolds, which is considered beneficial for osteogenic commitment. Moreover, the nanopatterned folded specimens exhibit significantly increased mineralization as compared to their non-patterned counterparts.

A Biomimetic *In Vitro Bone Model Based* on Spheroidal Co-Culture of Osteoclasts and Osteoblasts

L. Fermin[1], N. Davison[1], E. R. Balmayor[2], P. Habibovic[1], Z. Tahmasebi Birgani[1]
[1] Department of Instructive Biomaterials Engineering, MERLN Institute for Technology-Inspired Regenerative Medicine, Maastricht University, Universiteitssingel 40, 6229 ER Maastricht, The Netherlands
[2] Experimental Orthopaedics and Trauma Surgery, Department of Orthopaedic, Trauma, and Reconstructive Surgery, RWTH Aachen University Hospital, 52074 Aachen, Germany

Introduction: Bone is a complex tissue with a specialized extracellular matrix (ECM) providing unique biochemical cues and biomechanical functions. In addition, bone tissue is characterized by a multicellular nature. Bone forming osteoblasts, bone lining cells, bone resorbing osteoclasts, and mature osteocytes compose the main cellular component of the bone tissue. In addition, the presence and pivotal role of immune cells such as macrophage during bone healing and remodeling is known.[1] The *in vitro* bone-mimicking models, developed for studying physiological or pathological states of the tissue, and for screening new drugs or bone graft substitutes, often do not represent the multicellularity of bone. These models often use either osteoblasts/osteocytes alone or simplified co-cultures of osteoblasts and osteoclasts in two-dimensional (2D) set-ups with direct or indirect cell-cell interactions.[2] In this context, three-dimensional (3D) co-cultures, can provide alternative *in vitro* models with more physiological relevance, as they can more closely mimic the structure and cellular content of bone.[3] Therefore, this research aims to develop a 3D co-culture of osteoclasts and osteoblasts, co-aggregated with bone ECM-mimicking calcium phosphate microparticles in a hybrid cell-biomaterials spheroid model.

Materials and Methods: Tricalcium phosphate microparticles (TCP) with different sizes were obtained by grinding larger TCP blocks (microparticle size: 50-250 µm). Particles size and shape was investigated using scanning electron microscopy (SEM). TCP microparticles were placed in non-treated tissue culture plates and sterilized with 70% ethanol. Human peripheral blood mononuclear cells (PBMCs) were isolated from buffy coat and seeded onto TCP microparticles at a density of $3x10^6$ cells/cm^2 in a culture medium composed of Minimum Essential medium (α-mem) supplemented with 10% Hyclone fetal calf serum (FCS), 1% penicillin/streptomycin, and 20 ng/mL macrophage colony-stimulating factor (M-CSF). After 3 days, the medium was supplemented with 25 ng/mL receptor activator of nuclear factor-κB-ligand (RANKL) to induce osteoclastogenesis. PBMCs attachment and osteoclastogenesis on the microparticles were investigated using immunofluorescent staining. In the next step, human mesenchymal stromal cells (hMSCs) will be added to osteoclast-carrying TCP microparticles to form a spheroidal co-culture, which will be analyzed with immunofluorescent staining and qPCR of the relevant osteoblast and osteoclast markers.

Results and Discussion: Preliminary results showed the attachment of the PBMCs on the TCP microparticles. After 7 days of stimulation with RANKL, TRAP-positive (data not shown) fusing cells were observed (Figure 1). Expected is that cells will fuse further and form large resorbing osteoclasts. At this stage, spread cell morphology is also seen, indicating the presence of macrophages.

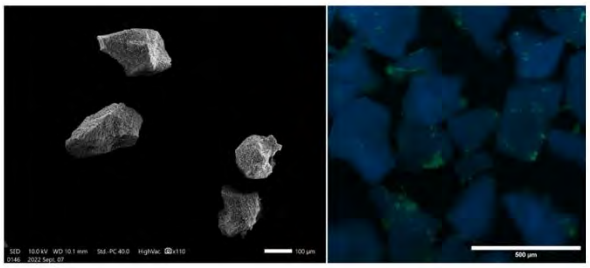

Figure 1. Left: SEM of microparticles Right: Immunofluorescent image of differentiating PBMCs on TCP microparticles; Cell nuclei in blue, cytoskeletal F-actin in green.

In the next step, the osteoclast-loaded particles will be co-aggregated with hMSCs, which in the presence of TCP microparticles can be differentiate into osteoblasts and even osteocytes in the later stages.[4] TCP microparticles, provide a bone mimicking matrix for the osteoclast adherence and resorption. In addition, they act as a source of calcium and phosphate ions, which can be used by the osteoblasts to produce new mineralized matrix.[5]

Conclusion and perspective: Here, we have shown the first steps towards establishing a spheroidal co-culture model of osteoclasts and osteoblasts, aiming to mimic the 3D structure and multicellularity of bone. Next step include optimization of the model and characterization of the cell types and ECM formation in the spheroids.

References:

1. N. Yang et al., 2021, International Journal of Medical Sciences 18(16), 3697-3707
2. G. Jones et al., 2009, Biomaterials 30(29), 5376-5384
3. A. Bernhardt et al., 2021, International Journal of Molecular Sciences 22(14), 7316
4. N. Davison et al., 2014, European Cells and Materials 27, 281-297
5. L. Cheng et al. 2019, Bio-Medical Materials and Engineering 30(3), 287-296

Acknowledgement: We thank Dr. Huipin Yuan for kindly providing the TCP particles. This research has been made possible by the Gravitation Program of the Netherlands Organisation for Scientific Research (NWO) (project "Materials-Driven Regeneration"

Oral Session 10

Rationale and guideline for translational research using the small ruminant lumbar interbody fusion.

A.A.A. Duits[a], D. Salvatori[b], J. Schouten[b], P. van Urk[ac], S v Gaalen[c], K. Ottink[a], FC Oner[a], M Kruyt[ad]

a University Medical Center Utrecht, Department of Orthopedic Surgery, Postbox 85500 3508 GA, Utrecht, The Netherlands
b Utrecht University, Faculty of Veterinary Medicine, Anatomy & Physiology, Yalelaan 1 3584 CL, Utrecht, The Netherlands
c Acibadem Internal Medical Center, Department of Orthopedic Surgery, Aralandaweg 100 1043 HP, Amsterdam, The Netherlands
d University of Twente, Department of Developmental BioEngineering, Enschede the Netherlands

Introduction Lumbar interbody fusion (IBF) is a common surgical procedure to obtain bony fusion of the anterior spinal column by replacement of the intervertebral disc (IVD) with a cage. Optimization of the cage design and bonegraft substitutes are of ongoing interest to obtain bony fusion more consistently and earlier after surgery. In vivo large IBF animal models remain an important preclinical model in which relevant qualities of spinal implants and bonegraft substitutes are tested as toxicity, biological response and biomechanical characteristics. However, the translationability of the model is highly dependent on animal selection and appropriate surgical decisions. Therefore, the research team needs extensive knowledge of spinal anatomy, bone characteristics and spinal function for human, primate, dog(canine), pig (porcine), goat (caprine) and sheep (ovine).
Purpose This study provides a rationale for animal selection and a guide for surgical decision making in small ruminant IBF models.
Methods & Materials The study was divided in two parts. The first one consisted of a narrative review regarding animal selection. The second part consisted of a combination of narrative and systematic review, anatomical preparation and our own experience to describe relevant anatomy and a guide on the selection of surgical levels, surgical approach, endplate preparation and supplemental spinal fixation.
Results Pig, baboon, dog, sheep and goat were sufficiently sized for IBF models. Only moderate differences in cortical bone, trabecular bone and endplate characteristics were described between skeletally mature animals and humans. Moreover, spinal kinematics of both quadrupeds and primates resembled the human spinal kinematics relatively well. But ethical considerations and animal weight shift animal selection towards farm animals, especially sheep and goat.
Figure 1 shows anatomical differences between small ruminants and humans. Compared to humans the small ruminant vertebral bodies were located more dorsal in the trunk, due to the small vertebral depth and kyphosis of the lumbar spine. The transverse processes were taller and start from the base of the vertebrae. The quadratus lumborum (QL) and psoas major muscles (PM) were lateral to the vertebral bodies. The spinal cord reached to the L6 vertebra and filled most of the canal. The lumbar plexus arose below the L4 vertebra and was located medial to the PM.
Fifty-seven papers described the IBF model in small ruminants. Mostly a 1 or 2 level retroperitoneal approach was used. Opposed to human surgery often the endplate was sacrificed to fit the implant and no supplemental fixation was used.

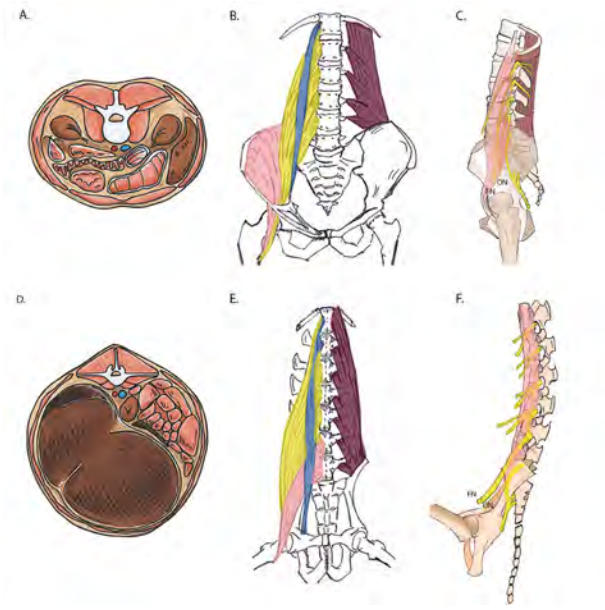

Figure 1: A) Illustration axial view human lumbar spine; B) Illustration coronal view human lumbar spine, QL(purple),PM (yellow), psoas minor(bleu);C)Illustration sagittal view human lumbar spine, position of the lumbar plexus; D) Illustration axial view goat lumbar spine; E) Illustration coronal view goat lumbar spine, QL(purple),PM (yellow), psoas minor(bleu);F)Illustration sagittal view goat lumbar spine, position of the lumbar plexus

Although we performed the model with experienced spinal surgeons there was a steep learning curve. In our study 2/20 goats experienced complete spinal cord injury (SCI). No peripheral nerve damage or wound infection was observed.
Conclusions The small ruminant (sheep and goats) IBF models are feasible models that provide good translationability. A lateral retroperitoneal retropsoas approach at the L1-2 and L3-4 levels is safe and gives adequate access to the spine. Even performed with trained surgeons the surgical procedure has a learning curve. Special attention should be paid to prevent spinal cord injury as the spinal cord is very vulnerable and fills most of the spinal canal. Lumbar plexus damage however is relatively uncommon.

Development of an expandable plug and preliminary evaluation in an *ex vivo* human fetal membrane model

R. Meuwese[1*], E. Versteeg[1], J. van Drongelen[2], A. Ramchandran[1], T. van Kuppevelt[1], W. Daamen[1]
[1] Radboud university medical center, Dept of Biochemistry, Nijmegen, the Netherlands
[2] Radboud university medical center, Dept of Obstetrics & Gynecology, Nijmegen, the Netherlands
*Corresponding author: Rob.Meuwese@radboudumc.nl

Background. Iatrogenic preterm prelabor rupture of fetal membranes (iPPROM) after fetal surgery is a strong trigger for premature birth. As fetal membrane defects do not heal spontaneously and amniotic fluid leakage and chorioamniotic membrane separation may occur, we developed a biocompatible, fetoscopically-applicable collagen plug with shape memory to prevent leakage, while enabling cellular influx to facilitate regeneration. This plug expands directly upon employment and seals fetal membranes, hence preventing amniotic fluid leakage and potentially iPPROM.

Materials & Methods. Lyophilized type I collagen plugs were given shape memory and crimped to fit through a fetoscopic cannula (Ø 3 mm). Expansion of the plug was examined in phosphate buffered saline (PBS). Its sealing capacity was studied *ex vivo* using human fetal membranes. As a pilot, cellular influx into the plug was studied *ex vivo* by placing a plug in fresh human fetal membranes mounted in metal inserts. The plugs were cultured in the membranes for one and three weeks.

Results. The crimped plug with shape memory expanded and tripled in diameter within one minute when placed into PBS, whereas a crimped plug without shape memory did not. In human fetal membranes, the plug expanded in the defect, secured itself and sealed the defect without membrane rupture. Microscopical examination with hematoxylin and eosin staining showed that the plug sealed the defect by forming an hourglass shape around the membranes. Although cellular influx from the human fetal membranes into the plug was not clearly visible after one week, after three weeks, cells did grow on and into the collagen plug.

Discussion and Future Outlook. Collagen plugs with shape memory comprise a promising medical device to rapidly seal defects in fetal membranes and enable cellular influx after fetoscopic surgery. Culture periods, conditions and stains will be optimized to further study cellular migration, proliferation and matrix deposition.

Acknowledgments. This study is funded by ZonMw & Health Holland, project number 40-44600-98-624.

A Safe-by-Design Approach for Medical Implants

Anniek M.C. Gielen[1,2], N.R.M. Beijer[1], A.G. Oomen[1,2], H.M. Braakhuis[1]
[1]Centre for Health Protection, National Institute for Public Health and the Environment (RIVM), Bilthoven, The Netherlands.
[2]Institute for Biodiversity and Ecosystem Dynamics (IBED), University of Amsterdam, Amsterdam, The Netherlands.

Introduction

Biomaterial science has progressed over the last few decades, where the design and development has shifted to more bioactive materials with properties (e.g.) aiming to direct the cell response [1]. The biological response evaluation standards of biomaterials continues to evolve, with revisions to existing standards [2], however has not developed at the same pace as the progression of biomaterials [1]. Current ISO 10993 standards are mainly focused on the effect of leachables. Physical material properties are characterized during material characterization, however not yet related to biological effects. Several studies have demonstrated that cell-biomaterial interactions are modulated by physicochemical properties of the biomaterial. Therefore, it is essential to understand how these properties influence cell response to achieve the desired effect in the host tissue during product development [3]. Additionally, it contributes to early safety assessment, where an approach such as Safe-by-Design (SbD) can be useful. Safe-by-design is an approach that compromises an overview of information needs and accompanying assays to gather information on the safety of innovative technologies at early stages in the development process. The concept is about eliminating or minimizing risks or failure when the technology is introduced to an *in vivo* model by integrating hazard identification and risk assessment methods early in the research and development process. Various inexpensive *in vitro* studies, prior to animal testing, can provide more insight into the initial screening of biomaterial properties and safety, saving a lot of time and resources.

Aim and Approach

The aim of this project is to show the importance of evaluating the influence of physical, chemical and mechanical properties onto biological systems during safety assessment. For a proper SbD strategy a better understanding of cell-biomaterial interaction is needed. Therefore, biomaterial properties that could be valuable for safety assessment will be identified in this project, incorporated in human relevant *in vitro* methods for biomaterial evaluation. Eventually, a SbD strategy will be established for early safety and risk assessment for biomaterials.

Results

Based on evaluation of current biological evaluation standards, we propose a SbD framework (Figure 1). The framework emphasises the importance of the cell-biomaterial interaction that can be evaluated in the design space. Where the optimization of the biomaterial and the safety assessment are carried out parallel using application driven *in vitro* tests.

Outlook

Future experiments will focus on identifying prioritized biomaterial properties to feed in our SbD framework. Additionally, *in vitro* assays will be developed for the evaluation of the prioritized biomaterial properties.

References
[1] Anderson, J. M. (2016). Regen. Biomater, 3(2), 73-77 https://doi.org/10.1093/RB/RBW001
[2] Reeve, L., & Baldrick, P. (2017). Expert Rev. Med. Devices, 14(2), 161-167. https://doi.org/10.1080/17434440.2017.1280392
[3] Zhu, Y., Goh, C., & Shrestha, A. (2021). Marcromol. Biosci., 21(4), 2000365. https://doi.org/10.1002/MABI.202000365
[4] Bernard, M., Jubeli, E., Pungente, M. D., & Yagoubi, N. (2018). Biomater. Sci., 6(8), 2025-2053. https://doi.org/10.1039/C8BM00518D

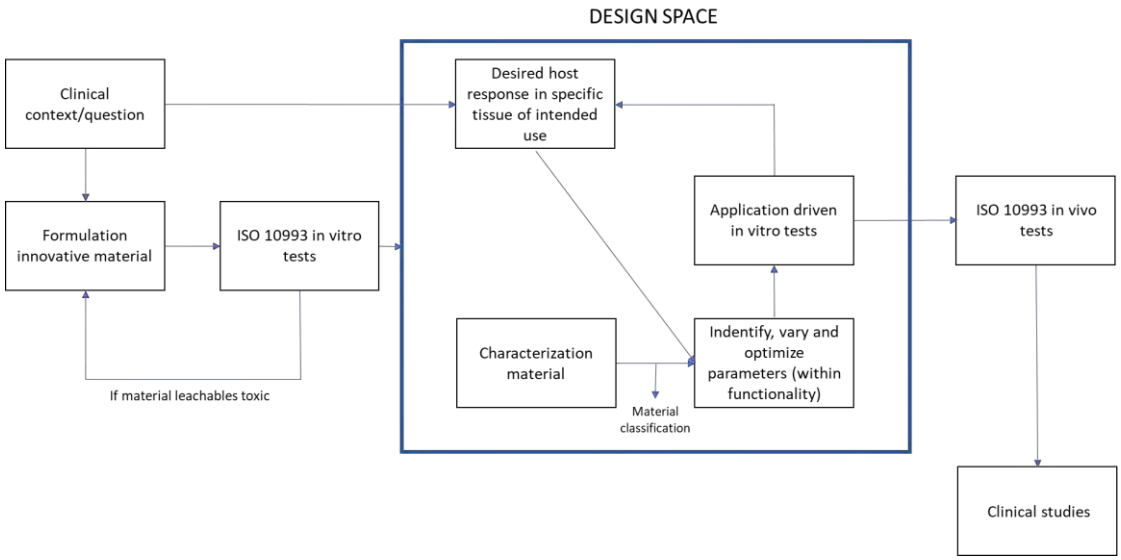

Figure 1: Safe-by-Design strategy flow chart. Prior to animal testing, more extensive in vitro analysis are performed related to biomaterial properties and the influence on the biological properties.

Can osteoarthritis after ACL reconstruction be explained by altered graft mechanical properties?

Janne Spierings[1,2], Marloes van den Hengel[1], Jasper Foolen[1,2]
[1]Orthopaedic Biomechanics, Department of Biomedical Engineering, Eindhoven University of Technology, Eindhoven, The Netherlands. [2]Institute of Complex Molecular Systems, Eindhoven University of Technology, Eindhoven, The Netherlands.

Introduction: Each year, 1% of active individuals rupture their Anterior Cruciate Ligament (ACL) [1]. Torn ACLs are often reconstructed using tendon autografts. However, in approximately half of the patients, ACL reconstruction (ACLR) leads to osteoarthritis (OA) within 5 to 15 years [2]. It is hypothesized that OA results from a mismatch in mechanical properties between the native ACL and the used tendon grafts. Moreover, due to *in vivo* graft remodeling and ligamentization, graft stiffness decreases and graft laxity increases. It remains unknown whether these changes contribute to the development of OA. Therefore, this study aims to assess the influence of these changes in graft mechanical properties on knee translations and the tibial cartilage contact pressure, as a measure for the risk of developing OA.

Methods: The stance phase of the gait cycle was simulated in 4 subject-specific open-source available finite element models in the FEBio software [3,4]. The material properties of the ACL were adjusted to match currently used grafts, e.g. patellar (PT) and hamstring tendons (HT), at surgery. In addition, hypothetical, but clinically relevant, grafts with a range in decreasing stiffness, increasing transition strain (graft laxity), and a combination of both were implemented to mimic grafts during and after *in vivo* graft remodeling and ligamentization. The effect of these grafts on knee translations (anterior tibial translation and internal tibial rotation) and tibial cartilage contact pressure were determined at the point of maximum posterior force on the femur.

Results: Reconstructing the ACL with a PT or HT graft resulted in a decrease in anterior tibial translation and internal tibial rotation, and a minor relocation of tibial cartilage contact pressure. Moreover, both anterior tibial translation and interior tibial rotation increased with a decreasing graft stiffness and/or an increasing graft laxity in 3 out of the 4 patients (Figure 1A, B). Moreover, a clear relocation in tibial cartilage contact pressure was found with a decreasing graft stiffness and/or an increasing graft laxity in those 3 patients (Figure 1C).

Discussion: Currently, ruptured ACLs are mainly reconstructed using PT or HT grafts. Although initially those grafts do not majorly influence knee translations and tibial cartilage pressure patterns, a decreasing graft stiffness and increasing graft laxity, as clinically observed during graft remodeling and ligamentization, do. The increase in anterior tibial translation and internal rotation, both movements the native ACL restricts, indicates changed knee joint mechanics. Together with a relocation of the tibial cartilage contact pressure, this might be a cause for the development of OA. Interestingly, one of the patients did not show altered knee translations or tibial cartilage pressure patterns, indicating not every patient might be at risk for the development of OA, which is in line with clinical outcomes. Altogether, this model paves the way towards the development of a patient-specific prediction model for ACL-reconstruction-induced OA. Besides, these results suggest the need for novel grafts with mechanical properties that match the native ACL and/or grafts that circumvent *in vivo* graft remodeling and ligamentization.

References: [1] Ruano JS, et al. J Athl Train. 2017, [2] Cheung CC, et al. Curr Rev Musculoskelet Med. 2020, [3] Erdemir A, J Knee Surg. 2016, [4] Maas SA, et al. J Biomech Eng. 2012

Funding: The authors acknowledge the financial support of the European Union's Horizon 2020 research and innovation programme [grant number 952981].

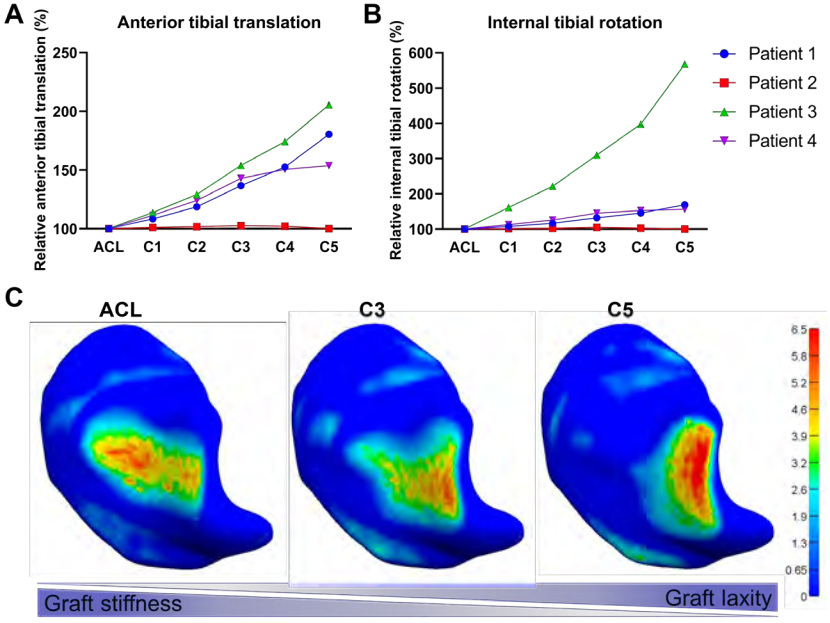

Figure 1. A) The anterior tibial translation is increased in grafts with a combination of decreased stiffness and increased graft laxity. B) The internal tibial rotation is increased in grafts with a combined decreased stiffness and increased graft laxity. C) A relocation in tibial cartilage pressure is found with decreasing graft stiffness and increasing graft laxity. With respect to the native ACL, C1 has 59% stiffness and 132% laxity; C2 has 30% stiffness and 152% laxity; C3 has 19% stiffness and 163% laxity; C4 has 11% stiffness and 198% laxity; C5 has 7% stiffness and 290% laxity.

Biomimetic Bone Substitute as a Medical Device for Socket Preservation

Y. Sun[1, 2], L. Wei[1, 2, 3], D. Yu[2], C. Xu[1], Y. Wu[2], Y. Liu[1*]
1. Academic Centre for Dentistry Amsterdam (ACTA),
Vrije Universiteit Amsterdam and University of Amsterdam, The Netherlands
2.Shanghai Jiao Tong University, School of Medicine, 9th People's Hospital, Shanghai, China
3. Yantai Stomatological Hospital, Yantai, China

Introduction:
Calcium phosphate-based bone substitutes have been widely used for bone regeneration. However, these materials lack osteoinduction, which weakens their potency in bone formation. To address this issue, our group has developed a biomimetic calcium phosphate bone substitute containing micro-gram BMP-2 (BioReBone®). This product has been proven to be effective and safe *in vitro* and in pre-clinical studies. In this project, we aimed to test the efficiency of this product in a clinical trial of socket preservation, a well-known technique for alveolar bone preservation after tooth extraction. For this purpose, the manufacturing and technical development of BioReBone® were executed in compliance with ISO 13485. This study has been approved by the ethics committee of Shanghai Jiao Tong University.

Material and Methods:
Production of BioReBone® was done according to the GMP manufacture specifications. Validated and implemented analysis methods for quality control, biological activity, and stability testing of clinical-grade BioReBone® bone graft was in place. Sufficient clinical-grade products engaged in the clinical trial were manufactured and tested. The clinical trial was designed, accordingly.
A total of 40 patients were included in this trial and were randomly assigned in three groups: control group (natural healing), negative control group (beta-TCP) and experimental with BioReBone®. Preoperative CBCT examinations were carried out to record the initial volume of alveolar bone of each patient in these three groups. Subsequently, after informed consent, with local anesthesia, a tooth from each patient was removed with minimally invasive surgery. Then, beta-TCP and BioReBone® were immediately implanted into the extraction socket, and control group has no bone filling material. All sockets were finally covered by the collagen membrane, and the wounds were sutured. Six weeks after the socket preservation, postoperative, CBCT was performed to analyze the changes of the tooth extraction site; soft tissue healing score was recorded clinically. A bone trephine (with an outer diameter of 3 mm and an inner diameter of 2 mm) was used to collect the bone tissue samples. The final sample of 6 mm length from the preservation area was obtained. Afterwards, early-stage implant surgery was performed.
The samples were histologically prepared and then analyzed morphologically. The safety of BioReBone® was tested by blood examinations (blood routine, blood biochemistry, coagulation function, serum immunoglobulin, and serum bone morphogenic protein 2) before and after the operation.

Results:
The study was carried out strictly accord with the designed technology roadmap (Figure. 1).

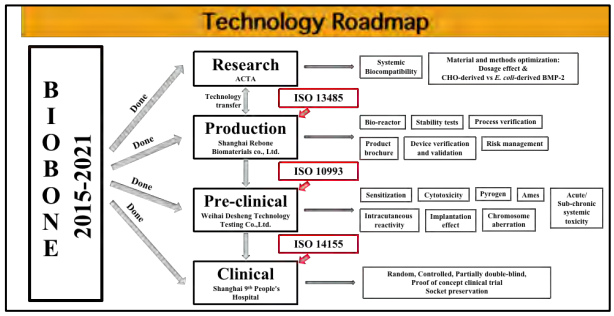

Fig. 1 The designed technology roadmap of this project.

The final clinical trial product, BioReBone®, was manufactured following the GMP regulation. The testing results demonstrated the products meet the standard of clinical medical device. All patients have been included in the trial according to the study design. Serious adverse events or unanticipated reactions were not reported. CBCT results show the absorption of alveolar bone in BioReBone® group is the least than other two groups.
Results from lab examinations (blood routine, blood biochemistry, coagulation function, serum immunoglobulin, and serum bone morphogenic protein 2) manifest there is no significant difference among these three groups and before and after operation for each patient.
The histopathological reports of collected bone tissues are still ongoing.

Conclusion:
Based on the current results, BioReBone® bone graft could be a biocompatible bone graft without systematic adverse reactions and serious adverse events after surgery. Moreover, these results have demonstrated its potential for socket preservation.

Acknowledgement:
This project was supported by the ZonMW grant (No. 436001004).

In Vivo Biocompatibility of Xenogeneic Extracellular Matrix and Reduced Graphene Oxide Foams

K. Verstappen,[1] A. Klymov,[1] M.M.A. School,[2] N.W.M. van Dijk,[1] S.C.G. Leeuwenburgh,[1] and X.F. Walboomers.[1]
[1]Department of Dentistry-Regenerative Biomaterials, Radboud Institute for Molecular Life Sciences, Radboudumc
[2]Central Animal Facility, Radboudumc
Philips van Leydenlaan 25, 6525EX Nijmegen, The Netherlands
kest.verstappen@radboudumc.nl

Introduction

Graphene-based biomaterials have rapidly emerged as a promising novel class of tissue engineering scaffolds to repair the injured spinal cord. Graphene and its derivatives, with reduced graphene oxide (rGO) in particular, have been shown to enhance *in vitro* stem cell growth and differentiation and are generally believed to be cytocompatible.[1] However, these experimental settings do not resemble the complex physiological environment *in vivo* and thus cannot predict the materials' biocompatibility with full reliability. To construct physical scaffolds for *in vivo* implantation, porcine adipose tissue-derived extracellular matrix (adECM) was used as a linking matrix for the GO sheets. The present study aimed to evaluate the biocompatibility of both adECM and adECM-rGO scaffolds, when 1) applied in an experimental setting relevant for neural tissue engineering applications, and 2) for a time period suitable to assess the foreign body response.

Materials and Methods

Adult female Sprague-Dawley rats (n = 29) underwent a laminectomy at T10 and were randomly distributed over the following treatment groups: control (n = 6), adECM (n = 12), and adECM-rGO (n = 11). Depending on the experimental group, adECM or adECM-rGO scaffolds were implanted on the exposed area of the spinal cord. For the control group, the laminectomy defect site was left empty. Adverse effects on animal welfare were monitored using an exhaustive post-operative care protocol to detect any signs of pain or distress. Following 6 weeks of implantation, the foreign body response was histologically assessed by haematoxylin and eosin (H&E), and Masson-Goldner trichrome stainings. Polarization of macrophages infiltrating the implantation area was determined by immunohistochemistry. Relevant organs (including lungs, liver, spleen, kidneys and brain) were harvested and histologically evaluated for any potential accumulation of rGO leachables or degradation products.

Results and Discussion

Scoring of animal welfare did not show any differences between the experimental groups. Following 6 weeks of implantation, histological analysis revealed that porcine-derived adECM scaffolds were largely replaced by collagenous host tissue. In contrast, adECM-rGO scaffolds could still be identified in the implantation area. Preliminary analysis revealed infiltration of cells, primarily macrophages, and substantial tissue ingrowth, along with a very limited fibrous encapsulation (±4-5 layers of collagenous tissue). A fraction of these macrophages fused into foreign body giant cells (FBGCs). Histological assessment did not show any accumulation of leachables or degradation products in lungs, liver, spleen, kidney or brain.

Conclusion

Implantation of both adECM and adECM-rGO scaffolds elicited a moderate foreign body response, including cell infiltration, tissue ingrowth and limited fibrous encapsulation. These constructs are safe for further development into tissue engineering applications.

Acknowledgements

All experimental procedures involving animals adhered to the regulations of the Dutch Government (CCD; AVD10300 2021 14868) and European Union (directives 2010/63/EU and 86/809/EEC). The authors would like to thank the biotechnicians of the Central Animal Facility at the Radboudumc as well as René van Rheden for his help during histological analysis. This project has received funding from the European Union's Horizon 2020 research and innovation program under grant agreement No829060.

References

1. Akhavan, O. Graphene scaffolds in progressive nanotechnology/stem cell-based tissue engineering of the nervous system. *J. Mater. Chem*. B, 2016,4, 3169-3190.

Poster abstracts

#	Presenter & Topic
P1	**Gabriele Addario, Maastricht University** *Improving human kidney fibrosis in vitro models: a mechanical, protein, gene study*
P2	**Lea Andrée, Radboudumc Nijmegen** *Developing Gelatin-Based Hydrogels with Tunable Viscoelasticity for Cell Culture*
P3	**Nuno Araújo-Gomes, University of Twente** *Bioluminescence imaging in organs-on-chips towards non-invasive multi-readouts in real-time*
P4	**Malin Becker, University of Twente** *Low Viscosity 3D (LoV3D) Bioprinting exploiting aqueous-two phase stabilization*
P5	**Torben A.B. van der Boon, Groningen UMC/University of Groningen** *Double Orthogonal Topography Gradients; synergistic effects of isotropic and anisotropic surface features on osteogenic differentiation of mesenchymal stem cells*
P6	**Leonardo Cecotto, UMC Utrecht** *Immunomodulatory and Antibacterial Properties of Host Defense Peptides Against Staphylococcus aureus*
P7	**Leanne de Silva, UMC Utrecht** *Implementing an Arteriovenous (AV) Loop in Endochondral Bone Regeneration*
P8	**Mirko D'Urso, Technical University Eindhoven** *Mechanosensing of tissue environment regulates fibroblast activation*
P9	**Mira El Akkawi, University of Twente** *3D printed Magnetically Deformable Hydrogels as a Granular Medium for Tissue Engineering Applications*
P10	**Magdalena Z. Gladysz, University of Groningen** *Fibrous Melt-Electrowritten Scaffolds to Investigate Cellular Behaviour for in Vitro Blood-Brain Barrier Model Development*
P11	**Zahra Gorgin Karaji, Kermanshah University of Technology** *Fabrication of polyvinyl alcohol/chitosan/silk electrospun mat to improve the wound healing process*
P12	**Rald V.M. Groven, Maastricht University/Maastricht UMC** *Citrulline supplementation enhances in vitro osteogenic capacities of hBMSCs from non-union patients*
P13	**Jing Han, Radboudumc Nijmegen** *Immune Modulation of Zinc via THP-1 Derived Macrophage Polarization*
P14	**Carolin Hermanns, Maastricht University** *Towards a cell based islet delivery*
P15	**Laure S. van Hofewegen, Amsterdam UMC** *Investigating the gene expression profiles underlying biomaterial-associated infection*
P16	**Celien A.M. Jacobs, Technical University Eindhoven** *Mechanical characterization of a unique biomimetic artificial disc for the cervical spine*
P17	**Hamidreza Jafarinia, Maastricht University** *Spatial Modeling of YAP Phosphorylation through Direct Interaction with Integrin Adhesions*
P18	**Encheng Ji, Erasmus MC** *A developmental tissue engineering approach to study breast cancer metastasis to the bone*
P19	**Yangjing Ji, Groningen UMC/University of Groningen** *Development of Novel Cyclodextrin-based Nanogels*
P20	**Cansu Karakaya, Technical University Eindhoven**

	Uniaxial and equibiaxial strain differently affect the phenotypic switching of vascular smooth muscle cells
P21	**Azin Khodaei, University of Erlangen-Nuremberg/UMC Utrecht** *Osteogenic and osteoimmunogenic performance of Cu-doped bioactive glass nanoparticles loaded with flavonoid*
P22	**Jaehyeon Kim, Maastricht University** *OviChip: 3D in vitro human oviduct model*
P23	**Nikita Konshin, Technical University Eindhoven** *Discovery of the Relationship between Biomaterials Properties and Cell Physiology in Implant Related Encapsulation*
P24	**Madalena Lopes Natário Pinto Gomes, Amsterdam UMC/Association of Dutch Burn Centers** *In vitro optimization of extracellular matrix production by primary human mesenchymal cells from fetal and adult dermal skin and eschar tissue*
P25	**Kirill Mikhailov, Groningen UMC/University of Groningen** *Self-synthesizing materials for tissue culture applications*
P26	**Khashayar Modaresifar, Delft University of Technology** *Cell-instructive and Bactericidal Nanopatterned Meta-biomaterials*
P27	**Myriam Neumann, Utrecht University** *Functional materials for high resolution 3D bioprinting in kidney engineering*
P28	**Helda Pahlavani, Delft University of Technology** *AI-Based 3D-Printed Multi-Material Mechanical Metamaterials*
P29	**Carlos J. Peniche Silva, Maastricht University** *MiRNAs as Potential Regulators of Enthesis Healing in a Rodent Injury Model*
P30	**Brandon W. Peterson, Groningen UMC/University of Groningen** *In vitro and in silico Analysis of Staphylococcus epidermidis Extracellular Polymeric Tethers: Viscoelastic Failure and Adaptability to Increasing Shear Stress During Adhesion*
P31	**Claire Polain, Maastricht University** *A Co-Culture Model For Innervation In Bone Regeneration Using NGF cmRNA*
P32	**Deeksha Rajkumar, Amsterdam UMC** *Novel antimicrobial release coating using SAAP-148 to combat biomaterial-associated infection*
P33	**Laís Ribovski, Groningen UMC** *Development of nanogels for crossing of the blood-brain barrier and penetration into glioblastoma spheroids*
P34	**Laura Rijns, Technical University Eindhoven** *Synthetic supramolecular hydrogels to steer the polarity of kidney epithelial cells and intestinal organoids in 3D*
P35	**Monika Salandova, Delft University of Technology** *Assessment of cytotoxicity of antimicrobial peptides LL-37 and SAAP-148 for orthopaedic applications*
P36	**Maik R. Schot, University of Twente** *Bioengineering a Modular, Immunoprotective, and Microporous Mini-Pancreas for Type 1 Diabetes*
P37	**Flurina Staubli, UMC Utrecht** *Extended storage of soft callus mimetics permits endochondral bone regeneration*
P38	**Phanikrishna Sudarsanam, Technical University Eindhoven** *High throughput screening of topographies to mitigate fibrosis in glaucoma filtration surgery devices*
P39	**Nikitha Vavilthota, Amsterdam UMC** *Rationally Designed Antimicrobial Peptides Show Antimicrobial Activity Against Gram-Negative Bacteria in a 3D Human Skin Equivalent Model*
P40	**Victor A. Veenbrink, Technical University of Eindhoven**

	Screening Peptide-Functionalized Supramolecular Assemblies Using Cell Morphological Profiles
P41	**Juul Verbakel, Technical University Eindhoven** *On the Interplay between Cell Metabolism and Biomaterial Properties*
P42	**Martina Viola, UMC Utrecht/University of Utrecht** *Thermosensitive Shrinking Behavior of Biopolymer-based Hydrogels for High Resolution Printing*
P43	**Michelle A.M. Vis, Technical University Eindhoven** *A dialysis medium refreshment cell culture set-up for an osteoblast-osteoclast coculture*
P44	**Zhule Wang, Radboudumc Nijmegen** *Bifunctional Bone Substitute Granules Loaded with Cisplatin Aiming to Minimize Malignant Bone Tumor Recurrence via Local Treatment*
P45	**Niels G.A. Willemen, University of Twente** *Steering Stem Cell Fate within 3D Living Composite Tissues using Stimuli-responsive Cell-adhesive Micromaterials*
P46	**Xixi Wu, Groningen UMC/University of Groningen** *Fabrication of visibly degradation-monitored PCL/FNDs (Fluorescent nanodiamonds) bioscaffolds using MEW method*
P47	**Chungfeng Xu, Vrije Universiteit Amsterdam & University of Amsterdam** *Osteoinductive Biomimetic Calcium Phosphate in Repair of Cancer-related Bone Defect*
P48	**Piotr Zielinski, University of Groningen** *Melt Electrowriting of Scaffolds for Soft-to-Hard Tissue Engineering*

Improving human kidney fibrosis *in vitro* models: a mechanical, protein, gene study

G.Addario[1], L.Moroni[1], C.Mota[1]

[1] Department of Complex Tissue Regeneration, MERLN Institute for Technology-Inspired Regenerative Medicine, Maastricht University, 6229 ER, Maastricht, the Netherlands

Introduction

Chronic kidney diseases (CKD) has been recently classified as the twelfth leading cause of death worldwide, where patients present a gradual loss kidney function, leading to end-stage renal disease (ESD) [1]. Patients with ESRD have limited treatment options, with fibrosis being the pathological endpoint, characterized by a remodeling of the ECM, affecting tissue stiffness [2-4]. Currently, murine *in vivo* models are used to study kidney fibrosis, however unable to completely recapitulate human diseases, hence physiologically relevant *in vitro* models are needed [5]. The limited number of *in vitro* models developed so far are used to study the induction of fibrosis biochemically using profibrotic cytokines, such as TGF-β1, often missing proper follow up assays to assess the progression of the pathology. Here, in our approach we combine the TGF-β1 stimulation with a thorough study of the mechanical properties, protein secretion and gene expression, showing all these aspects are closely interconnected to each other, and essential to build better *in vitro* models for studying the tubulointerstitium fibrosis.

Materials and Methods

We optimised a protocol for the decellularization of fresh kidney pig tissue (dECM), bio-histochemically compared to the native tissue and its cross-linked formed, i.e. gel. The produced dECM was then used to cast gels containing primary human epithelial and fibroblasts renal cells, described as the main ECM producing cells [5]. To study the induction and progression of fibrosis *in vitro,* the cells in the dECM were then treated with TGF-β1, vitamin B2, or the combination of the two, to further stiff the matrix. These multiple conditions were then compared by investigating multiple fibrotic genes, by means of qPCR, together with histology and immunostaining to evaluate the secretion of proteins over time. Finally, the mechanical properties were measured using a nanoindenter and compared with the Young's Moduli obtained from fresh kidney tissues of animal (multiple species), and human.

Results and Discussion

The produced dECM presented a reduced DNA concentration (<50 ng/mg dry tissue), but capable to retain the native protein composition, as proven by histology and immunostaining, together with collagen and GAG quantification. The added cells in the dECM were then treated with TGF-β1 and/or vitamin B2 to study the release of proteins and increase of stiffness. These multiple conditions did not only show an increased Young's Modulus over time, but also an increased released of proteins, both hallmark of fibrosis *in vivo* [4]. Interestingly, the dECM containing cells crosslinked with vitamin B2 and the dECM containing cells treated with TGF-β1 reached similar stiffness values after two weeks in culture, whereas the highest values were measured for the combination of vitamin B2 and TGF-β1. Furthermore, histology and immunostaining, for studying the secretion of proteins, confirmed these results. The qPCR study showed higher fold change for genes Fibronectin, which expression normally increases after injury in fibrosis [4], and Vimentin for the dECM with the vitamin B2 condition. Whereas, the dECM with TGF-β1 showed higher gene expression for ACTA2, Col1a1, Col3a1 and Col4a1, which upregulation is described as an early event in renal fibrosis [4-5]. Finally, the combination of vitamin B2 and TGF-β1 showed the highest gene expressions.

Conclusions

In our approach, we proposed a dECM based gel which is described as a relevant hydrogel for studying fibrosis, due to the functional and structural environment suitable for cells [4]. We showed that a physiologically relevant *in vitro* model for studying kidney fibrosis depends on multiple factors and researchers cannot simply rely only on the treatment of cells with TGF-β1, but also modulate the mechanical properties. We believe these two aspects have to be investigated together, and correlated to protein secretion and gene expression. These models can provide viable humanized *in vitro* models that can overcome the limits of murine *in vivo* models, where fibrosis is only currently evaluated through histological characterization of biopsy tissue.

Acknowledgments

This project has received funding from the European Union's Horizon 2020 research and innovation programme under the Marie Skłodowska-Curie grant agreement No 860715.

References

[1] Bikbov B et al. The Lancet. 2020;395(10225):709-33;
[2] E.M. Buhl et al. EMBO Mol. Med. 12 (3) (2020), e11021;
[3] J. Mjo et al. Curr. Opin. Pharmacol. 49 (2019) 82–89;
[4] R.D. Bulow, P. Boor, Extracellular Matrix in Kidney Fibrosis: More Than Just a Scaffold. J Histochem Cytochem, 2019. 67(9);
[5] S. Djudjaj, P. Boor, Cellular and molecular mechanisms of kidney fibrosis. Mol Aspects Med, 2019. 65.

Developing Gelatin-Based Hydrogels with Tunable Viscoelasticity for Cell Culture

L. Andrée[1]*, P. Bertsch[1]*, R. Wang[1], F. Yang[1], P. Fischer[2], S.C.G. Leeuwenburgh[1]

1 Department of Dentistry – Regenerative Biomaterials, Radboud Institute for Molecular Life Sciences, Radboudumc, Nijmegen, The Netherlands
2 Institute of Food, Nutrition and Health, ETH Zürich, Switzerland

Introduction: Hydrogels are widely used mimics of extracellular matrix (ECM) in cell culture and tissue engineering [1]. In recent years, it has become obvious that not only ECM stiffness but also its time-, stress- and strain-dependent viscoelasticity impacts cell behavior. Particularly fast stress dissipation (stress relaxation) within the hydrogel has been recognized as a key parameter affecting cell activity [2][3]. Conventional gelatin hydrogels are elastic and show limited stress relaxation, whereas we have previously shown that colloidal gelatin hydrogels assembled from nanoparticles exhibit fast stress relaxation [4]. Here we aimed to establish a toolbox of gelatin-based hydrogels with tunable viscoelasticity and study their effect on cell behavior.
Therefore, we investigated photo-crosslinkable gelatin methacryloyl (GelMA), a purely colloidal system of gelatin nanoparticles (GNPs) and a mixed system combining GelMA with GNPs, potentially harnessing the benefits of stiff GelMA and stress-relaxing particles. The gelatin hydrogels were investigated rheologically in terms of stress relaxation and in 2D cell culture.

Methods: Monolithic gelatin hydrogels were prepared from photo-crosslinkable GelMA. The purely colloidal hydrogel was assembled from GNPs of which one third was modified with methacryloyl groups after synthesis (GNPs-MA) to help stabilizing the hydrogel. Furthermore, a mixed system of GelMA filled with unmodified GNPs (w/w ratio 1:1) was prepared. All gelatin hydrogels had a solid content of 6 w/v%.
Photo-crosslinking was monitored in-situ using rheological time sweep measurements at 37°C and stress relaxation was assessed under increasing strain of 10-100% (Fig. 1).
Cytocompatibility was assessed in 2D cell culture using murine pre-osteoblastic cells by cell counting kit 8 (CCK-8) assay, and cell morphology was observed after fluorescent staining of the cytoskeleton by confocal laser scanning microscopy.

Results: For all gelatin hydrogels, photo-crosslinking led to rapid gelation within 1-2 min at 37°C, and comparable storage moduli (G') of ≈1000 Pa were measured. GelMA showed limited stress relaxation of <20% within 10 min at any of the tested strains (Fig. 2A), indicating elastic behavior. The mixed system exhibited some stress relaxation of 50% at strains > 80% (Fig. 2B), suggesting that the material's mechanics at the macroscale are mostly dictated by GelMA. In contrast, colloidal hydrogels showed stress relaxation of 20% and 70% at low strains of 10% and 20%, respectively (Fig. 2C). The hydrogels exhibited no cytotoxic effects in 2D cell culture and induced significantly more pronounced cell spreading compared to conventional tissue culture plastic.

Conclusion: Three gelatin-based hydrogels with different stress relaxation profiles but comparable storage moduli were developed that qualify for cell culture. In the future, these hydrogels will serve us as a platform to study the effect of stress relaxation on cell behaviour in 3D.

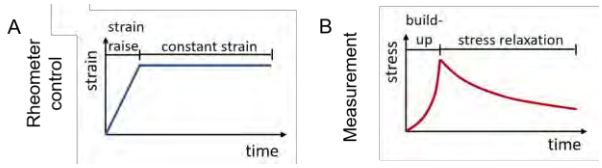

Fig. 1 – Overview of rheometer control and rheological response of a viscoelastic hydrogel in stress relaxation experiments.

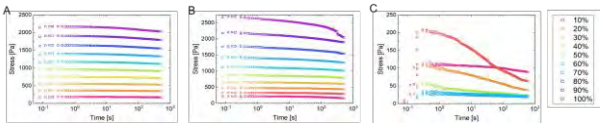

Fig. 2 - Step-strain experiment of (A) gelatin methacryloyl (GelMA) and (B) mixture of GelMA and gelatin nanoparticles (GNPs) showing limited stress relaxation, while (C) colloidal system of GNPs and methacryloylated GNPs-MA shows fast stress relaxation at low strains.

Acknowledgements: The authors would like to thank the Electron Microscopy Center of the Radboudumc for providing access to their imaging facility, and the Netherlands Organization for Scientific Research (NWO, project 17615) for funding.

Contact: lea.andree@radboudumc.nl

Bibliography:

[1] M. W. Tibbitt and K. S. Anseth, "Hydrogels as extracellular matrix mimics for 3D cell culture," *Biotechnol. Bioeng.*, vol. 103, no. 4, pp. 655–663, Jul. 2009, doi: 10.1002/BIT.22361.
[2] O. Chaudhuri, J. Cooper-White, P. A. Janmey, D. J. Mooney, and V. B. Shenoy, "Effects of extracellular matrix viscoelasticity on cellular behaviour," *Nature*, vol. 584, no. 7822. pp. 535–546, 2020. doi: 10.1038/s41586-020-2612-2.
[3] O. Chaudhuri, "Viscoelastic hydrogels for 3D cell culture," *Biomaterials Science*, vol. 5, no. 8. The Royal Society of Chemistry, pp. 1480–1490, Jul. 26, 2017. doi: 10.1039/c7bm00261k.
[4] P. Bertsch, L. Andrée, N. Hassani Besheli, and S. C. G. Leeuwenburgh, "Colloidal hydrogels made of gelatin nanoparticles exhibit fast stress relaxation at strains relevant for cell activity," *Acta Biomater.*, 2021, doi: 10.3390/pharmaceutics13111944.

Bioluminescence imaging in organs-on-chips towards non-invasive multi-readouts in real-time

N. Araújo-Gomes *[1], G. Zambito*[2,3], C. Löwik [2,3], M. Karperien[1], L. Mezzanotte[#2,3]& L. Moreira-Teixeira[#,4]

[1]*Department of Developmental Bioengineering, Technical Medical Centre, University of Twente, Enschede, The Netherlands.*
[2]*Department of Radiology and Nuclear Medicine, Erasmus MC, University Medical Center Rotterdam, Rotterdam, The Netherlands.*
[3] *Department of Molecular Genetics, Erasmus MC, University Medical Center Rotterdam, Rotterdam, The Netherlands*
[4] *Department of Advanced Organ bioengineering and Therapeutics, University of Twente, Enschede, The Netherlands*

Introduction:

Organs-on-chips (OoC) are becoming an established effective alternative to conventional *in vitro* and *in vivo* models, with accurate mimicry of key functions of human native tissues and/or organs. These microfluidic platforms enable a high control over a wide range of biochemical and biomechanical cues, emulating dynamic cellular micro-environments and potentially steering cell behavior on a 3D setting[1]. This demands for the incorporation of biosensing features that allow continuous, non-invasive, and *on-situ* screening of cells, tissues, or miniaturized organs. In this context, optical biosensors offer versatile integration with on-chip approaches. Although fluorescence detection is typically the standard optical biosensing method used in OoC, it is often associated with inherent drawbacks, including the need of invasive analysis and cell bleaching, due to laser exposure, apart from not enabling continuous monitoring of cell behavior[2]. Bioluminescent imaging (BLi) has risen as a promising alternative to conventional fluorescence analysis, allowing real-time, high-content analysis of molecular and cellular processes with high-sensitivity, without the drawbacks of fluorescence [3]. Here, we report the integration and optimization of BLi in OoC, for non-invasive multiple biological readouts, on-site and in real-time.

Materials and Methods:

A poly(dimethylsiloxane) (PDMS)-based microfluidic chip (1,7 x 1,2 x 0,4 cm) with an optical detection central chamber (7,5 x 2 x 0,25 mm) was used in this study. HEK293T-GFP cells were engineered to express NanoLuc® luciferase and encapsulated on-chip, in the central chamber, embedded in extracellular matrix-like hydrogels (e.g., Fibrin gel, GelMA and Agarose) with distinct mechanical properties. Rheological analysis and diffusion studies on the gel properties were performed prior to seeding. In parallel, cell density was optimized to obtain single cell resolution. BLi was induced by dynamic injection of the substrate Fumirazine through the perfusion channels using an infusion pump followed by detection on Zeiss Elyra PS1 SIM microscope installed with a sensitive EMCCD camera.

Results and Discussion:

The diffusion study using FITC-IgG (40kDa) revealed different diffusion rates on the tested ECM-like gels, as expected, showing that the fibrin gel allowed the fastest diffusion of molecules, within 5 minutes of incubation. In contrast, the agarose gel showed the slowest diffusion (20 minutes). Rheological analysis revealed that the matrix of the gels displayed a stiffness range between 0,1 kPa (Fibrin gel) and 10 kPa (Agarose). Cell seeding was optimized for on-chip single cell resolution to a density of to 4 x 10^5 cells/ml and once encapsulated, cells displayed a viability of >90% after 1 day of culture on all tested gels. Photon flux has been measured at IVIS imager spectrum, where Nanoluc® expressing cells were seeded, in the optical detection chamber (≈ 8,5x10^6 photons/sec). Using an adapted BL microscope, it was possible, in real-time and *in vitro,* the dual-color BLi and fluorescence imaging. Sequential bioluminescent detections at a single cell level on-chip (≈ 2,4x10^6 counts/sec) were measured and quantified for 13 minutes post-addition of substrate.

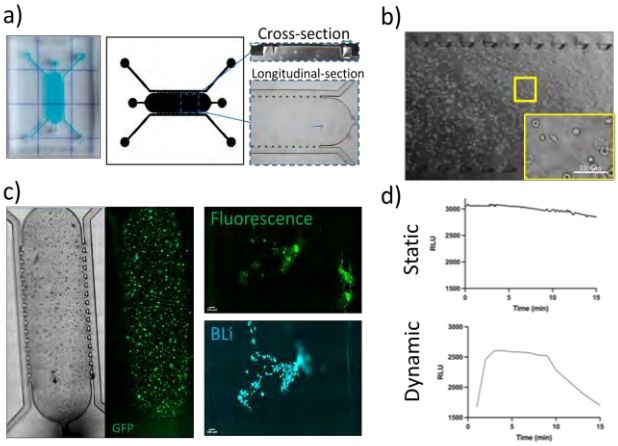

Figure 1: *a) Brightfield microscopy of the microfluidic platform, OoC, with a central optical detection chamber that enables single cell observation within a biomimetic 3D micro-environment. b) HEK293-GFP cell seeding was optimized to obtain single cell resolution, with which both c) Fluorescence and Bioluminescence are detectable and d) quantifiable immediately after injection of the substrate fumirazine, both in static and dynamic conditions within the first 15 minutes.*

Conclusion:

We have successfully combined OoC platforms with real-time BLi for multiple biosensor read-outs, via dynamic infusion of bioluminescence substrates. Our approach allows for simultaneous *in situ* detection, with continuous monitoring of multicolor cell reporters, in a non-invasive manner. The incorporation of BLi on OoC and co-integration with automated perfusion systems uniquely allows real-time and on-site sequential monitoring of biological events, with single-cell resolution.

References:

[1]Chen, X., et al., 2021. **6**(4): p. 1012-1027.
[2]Mezzanotte, L., et al. . PLoS One, 2014. **9**(1): p. e85550.
[3]Moreira Teixeira, L. and L. Mezzanotte, View, 2021. **2**(6).

Low Viscosity 3D (LoV3D) Bioprinting exploiting aqueous-two phase stabilization

Malin Becker[1], Melvin Gurian[1], Maik Schot[1], and Jeroen Leijten[1]
[1] Leijten Lab, Dept. of Developmental BioEngineering, TechMed Centre, University of Twente, Enschede, The Netherlands
Contact of presenting author: m.l.becker@utwente.nl

INTRODUCTION

Embedded bioprinting is a promising additive manufacturing technique that permits the fabrication of large-scale, freeform, complex 3D tissue constructs. During the development of new (bio)inks, the shape-stability of extruded strands plays a major role. To stabilize the strand after extrusion, while allowing for smooth extrusion with limited pressures, shear thinning inks are commonly employed. For these inks, the printing resolution is dictated by nozzle diameter[1], while shear stresses within the nozzle during extrusion determine cell viability[2], which thus limits bioprinting resolution and speed. Here, we report on a low viscosity 3D (LoV3D) liquid printing approach, which is enabled by the innovative use of an aqueous-two phase system (ATPS). LoV3D allows for the highly rapid bioprinting with high cell viability, while allowing for continuous on-the-fly tuning of filament diameter, which ranges from millimetric down to single cell resolution using a single nozzle in a nozzle-diameter independent manner.

EXPERIMENTAL METHODS

Alginate was functionalized with tyramine (TA) groups via DMTMM coupling to form a photo crosslinkable embedding bath. For 3D printing of several inks, a Cellink Inkredible+ printer was combined with a syringe pump to allow for printing at set speeds and extrusion rates. Various mammalian cell types including 3T3 mouse fibroblasts were used to investigate LoV3D's cytocompatibility.

RESULTS AND DISCUSSION

The suitability of a variety of established (bio)polymer solutions for LoV3D printing was confirmed and Dex-TA/PEG as well as Alginate-TA/PEG were chosen as model systems. The formation of a stable ATPS interface was substantiated by establishing the binodal curves of these systems. The use of low viscous solutions allowed for strand elongation (thinning) with increased printing speeds (Figure 1a). Comparing reported print diameters in literature for various nozzle sizes, we determined that LoV3D printing offers a substantially higher resolution printing regime, which can be equally accessed with all tested nozzle diameters (Figure 1b). Printing of low viscous inks compared to conventionally used bioinks (Figure 1c) enables the unique thinning of printed strands and was utilized to create prints with diameters ranging over two orders of magnitude down to single-cell resolution without the need for a nozzle exchange (Figure 2a). The influence of viscosity dependent shear stresses within the printing nozzle on cell viability, was investigated by combining simulation based data with extrusion experiments. Here, we were able to establish, that for a wide range of flow rates, low viscosity inks do not show any significant reduction of cell viability, while higher viscosity inks reduced the viability with increasing flow rates down to 70% (Figure 2b). Conventional complex shapes such as spirals, tubes, and grids could readily be created (Figure 2c). Incorporating cells within a sacrificial ink allowed for a one-step print and seed approach (Figure 2 d). Here, the liquid/liquid interface during printing facilitated additional surface modification, where covalent bonds between coating and channel wall could be formed more-effectively for ATPS liquid/liquid as compared to conventional solid/liquid interfaces.

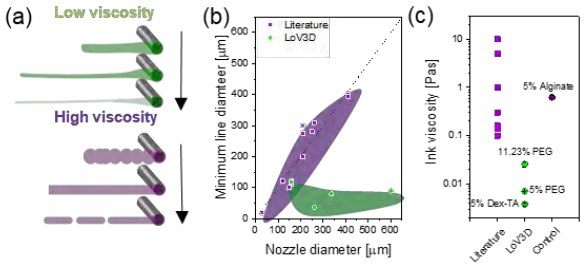

Figure 1: Filament thinning opens up a new high resolution printing regime. (a) Schematic filament shape of low and high viscosity aqueous solutions at different printing speeds and set extrusion rate. (b) Line diameters reported in literature with different nozzle sizes as compared to experimental data with low viscosity inks. (c) Comparison of inks used in LoV3D and conventional embedded printing.

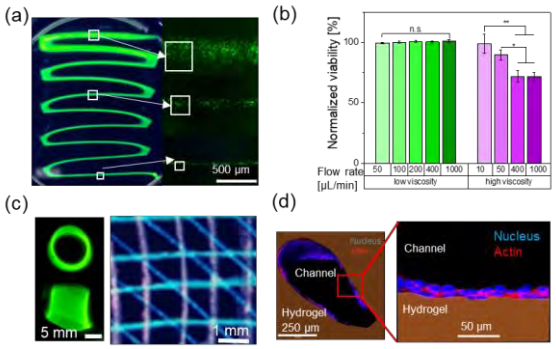

Figure 2: Low viscosity bio-inks allow for high cell viability while enabling high resolution. (a) Printing with increased speed thins filaments and decreases filament diameter down to single-cell resolution. (b) Cell viability after extrusion through a 25G nozzle at various flowrates. (c) 3D printed hollow tube and multi-material grid validating the printability of the low viscous solutions. (d) 3D printed and cell lined channel created in a 1-step print and seed approach.

CONCLUSION

In this study, we introduce LoV3D bioprinting as a highly versatile and rapid bioprinting technique, which is inherently compatible with a wide range of biomaterials and crosslinking strategies, while offering on-the-fly tunable high resolution prints without compromising printing speed or cell viability. Future studies will focus on the cell incorporation within the channels, aiming for the creation of perfusable multiscale vascular networks.

REFERENCES

1. Jin Y. *et al.*, Mater. Sci. Eng., C. 80:313-325, 2017
2. Murphy, S.V. *et al.*, Nat. Biotechnol., 8:773-785, 2014

ACKNOWLEDGMENTS

Financial support was received from the European Research Council (ERC, Starting Grant, #759425) and the Dutch Research Council (NWO, Vidi Grant, #17522).

Double Orthogonal Topography Gradients; synergistic effects of isotropic and anisotropic surface features on osteogenic differentiation of mesenchymal stem cells.

Torben A.B. van der Boon[1], Roderick H.J. de Hilster[1], Hidde Vink[2], dr. Diego R. Gomes[2], dr. Yutao Pei[2], and dr. Patrick van Rijn[1].

[1]W.J. Kolff Institute for Biomedical Engineering and Materials Science, University of Groningen/ University Medical Center Groningen (UMCG), Ant. Deusinglaan 1, Groningen, The Netherlands

[2]Department of Advanced Production Engineering, Engineering and Technology Institute Groningen, Faculty of Science and Engineering, University of Groningen, Nijenborgh 4, 9747 AG Groningen, The Netherlands

t.a.b.van.der.boon@umcg.nl

INTRODUCTION

Until now, the research field of studying the influence of surface topography on cell behaviour has been naturally divided into two branches; 1) surface roughness, and 2) aligned surface features.[1,2] The research presented here is bridging both worlds by studying the synergistic effects of surface nano/micro roughness and aligned nano/micro topography on osteogenic differentiation of mesenchymal stem cells (MSCs), by utilizing a revolutionary, in-house developed, double orthogonal gradient (DOG)[3] screening platform. Conventional research techniques have not lived up to this level of complexity, since they mostly tackle a few distinct situations of a single parameter. By combining the two topography parameters in an orthogonal fashion, we have created a cell screening platform which enables us to screen for vast amounts of data in single cell studies. The power and broader potential of this platform lies in the quick visual assessment of hot-spots, which either promote or inhibit certain cell behaviour, enabling us to direct the cell response into a desired direction and herewith identifying which surface parameters to incorporate into medical implant designs and which to avoid. We foresee that our platform will aid in drastically improving implant effectiveness and quality of life of patients.

EXPERIMENTAL METHODS

The DOG platform is based on silicone material (PDMS). Firstly, an aluminium template is sandblasted and chemically etched to generate a roughness gradient, which is imprinted into PDMS by means of liquid curing. Oriented orthogonally to the imprinted roughness gradient, a gradient of aligned wrinkle topography features is created, using our previously described 'stretch-and-release' approach.[4,5] Atomic Force Microscopy (AFM) and Scanning Electron Microscopy (SEM) were used to characterize the surface features qualitatively and quantitatively (FIGURE1). The effects on osteogenic differentiation of MSCs is investigated by culturing for 14 days and staining for alkaline phosphatase (ALP) and osteopontin (OPN) markers. Read-out and quantification is done using fluorescence immune-staining, imaged (TissueFAXS) and analysed (TissueQuest) using TissueGnostics equipment. The high-throughput analaysis is complemented by confocal laser scanning microscopy (CLSM) to obtain more detailed information on specific regions of interest (ROI) on the gradient substrates. Every ROI is translated to homogeneous, non-gradient surfaces, to verify the screening outcome.

RESULTS AND DISCUSSION

Every imaginable position on the DOG surfaces represents a unique combination of both topography types, within their respective gradient range. Wrinkle features range from λ = 1,6 µm – 12 µm and A = 160 nm – 1650 nm, the smallest wavelengths corresponding with the smallest amplitudes going from small to big, in a coupled fashion. Roughness features, expressed in sRa values, range from ~90 – 450 nm. Further results on cell studies are expected in the near future. We hypothesize that different combinations of both surface parameters influence osteogenic differentiation of MSCs differently, either promoting or impeding it.

CONCLUSION

This novel cell screening platform bridges the two branches in the field of topography feature – cell interactions. The identification of synergistic effects of both topography types on stem cell differentiation will accelerate our understanding of surface topography influence on cell behavior and ultimately enhance biomaterial development.

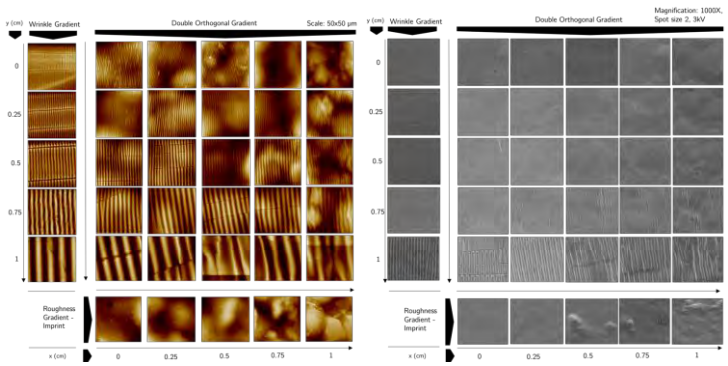

Figure 1. Quantitative (left) and qualitative (right) AFM and SEM images reveal successful gradient preparation and DOG formation.

REFERENCES

[1] Faia-Torres A.B. *et.al.*, Acta Biomaterialia. 28:64-75, 2015
[2] Yang L. *et.al.,* Biomater. Sci. 8:2638-2652, 2020
[3] Zhou Q. *et.al.,* Adv. Mater. Interfaces. 5(18), 2018
[4] Zhou Q. *et.al.*, Sci. Rep. 5:16240, 2015
[5] van der Boon T.A.B. *et.al.*, Adv. Biosyst. 4:1900218, 2020

Immunomodulatory and Antibacterial Properties of Host Defense Peptides Against *Staphylococcus aureus*

L. Cecotto[1,2], K.P.M van Kessel[2], M.A. Wolfert[3], H.C. Vogely[1], B.C.H. van der Wal[1], H.H. Weinans[1], J.A.G. van Strijp[2], S. Amin Yavari[1]

1. Department of Orthopedics, University Medical Center Utrecht, Utrecht, The Netherlands
2. Department of Medical Microbiology, University Medical Center Utrecht, Utrecht, The Netherlands
3. Department of Chemical Biology and Drug Discovery, Utrecht University, Utrecht, The Netherlands

Introduction. In the current study we aim to characterize the use of cationic host defense peptides (HDPs) as alternative antibacterial agents to include into novel antibacterial coatings for orthopaedic implants. *Staphyloccous aureus* represent one the most challenging cause of infections to treat by traditional antibacterial therapies. Thanks to their lack of microbial resistance described so far, HDPs represent an attractive therapeutic alternative to antibiotics. Furthermore, HDPs have been showed to control infections via a dual function: direct antimicrobial activity and regulation of immune response. However, HDPs functions characterization and comparison is controversial, as changing test conditions or cell type used might yield different effects from the same peptide. Therefore, before moving towards the development of HDP-based coatings, we need to characterize and compare the immunomodulatory and antibacterial functions under the same conditions *in vitro* of 3 well-known cathelicidins: bovine-derived IDR-1018, chicken CATH-2, and human LL-37.

Materials and Methods. *S. aureus*, strain SH1000, was incubated with different concentrations of each HDP and bacterial growth was monitored overnight. Primary human monocytes were isolated from buffy coats using Ficoll-Paque density and CD14 microbeads, and differentiated with M-CSF for 7 days to macrophages. After 24h incubation in presence of LPS and HDPs, macrophages cytokines production was measured by ELISA. To assess the peptides influence on macrophages antibacterial properties, two infection models studying *S. aureus* intracellular survival were adopted. The first step concerned the "peptides during infection" model, where cells were incubated with the peptides for 24h and subsequently bacteria were directly added to the culture (Figure 1A). In a subsequent step, we assessed the "peptides during differentiation", where peptides were added to the differentiation media only for the first 3 days, then mature macrophages were infected by bacteria (Figure 1B). 30 min and 24h after infection, bacterial phagocytosis and intracellular killing by macrophages were measured by flow cytometry and colony forming units (CFU) count respectively.

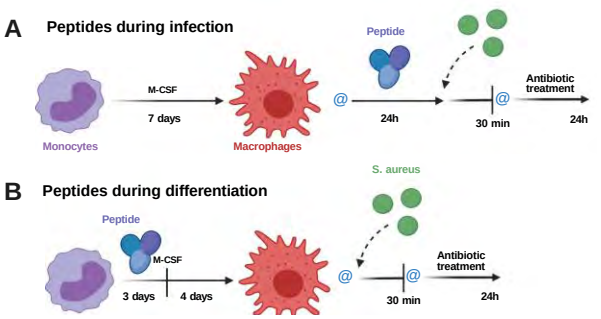

Figure 1. Schematic representation of infection models adopted. (A) Macrophages were first stimulated with the peptides and the infected with S. aureus. (B) Macrophages were differentiated in the presence of each peptide. @ represents 2 washing steps.

Results and Discussion. Among the HDPs tested, only CATH-2 showed direct antibacterial properties against *S. aureus* at concentrations higher than 1 μM. All the HDPs showed a similar inhibitory action against LPS-mediated activation of macrophages, as observed by a reduced production of TNF-α and IL-10.

As direct targeting of intracellular bacteria still remains a challenge, we used HDPs to improve macrophage intrinsic ability to kill intracellular bacteria. In fact, *S. aureus* finds protection against most antibiotics and host defenses by hiding inside the host cells. When immune cells were stimulated with the peptides right before and during infection, only IDR-1018 reduced the proportion of cells that phagocytosed bacteria. Nevertheless, this did not correlate to a lower number of pathogens surviving within macrophages after 24h. In the "peptides during differentiation" model we assessed if monocyte differentiation to macrophage in the presence of HDPs influenced the mature cell functions. In this context, IDR-1018 immunomodulatory function was preserved by mature macrophages, which led to a reduced proportion of infected cells. However, even in this case, IDR-1018 had no impact on immune cells killing efficiency. Similarly, monocytes differentiation in presence of CATH-2 and LL-37 had no impact on mature cells functions, neither on phagocytosis or intracellular killing.

Conclusions. The immunomodulatory and antibacterial properties of IDR-1018, CATH-2, and LL-37 were studied on the same *in vitro* conditions. Despite the strong anti-inflammatory properties of all peptides were verified, they did not improve macrophages antibacterial functions. Only CATH-2 showed promising direct antibacterial properties against *S. aureus*, while IDR-1018 influenced macrophages phagocytosis ability by reducing the number of engulfed bacteria. However, none of the tested peptides enhanced macrophage's ability to kill intracellular *S. aureus*. Future studies should either focus on combining different HDPs or using them synergistically with other antibacterial agents to improve immune cells efficacy against *S. aureus* pathogenesis. Next, loading HDPs into antibacterial coatings should be considered as new local drug delivery strategy to prevent implant-associated infections.

Implementing an Arteriovenous (AV) Loop in Endochondral Bone Regeneration

L. de Silva[1,2], C. Kuijpers[1,2], E. Van Cann[1], R.J.J. van Es[1], A. J. W. P. Rosenberg[1], D. Gawlitta[1,2]
[1]Dept. of Oral and Maxillofacial Surgery & Special Dental Care, [2]Regenerative Medicine Center Utrecht, University Medical Center Utrecht, Utrecht, the Netherlands.

Introduction

The current bottleneck in upscaling tissue engineering is the lack of a functional vascular network. While many *in vitro* approaches have successfully mimicked certain components of the vascular network, none have yet succeeded in fully recapitulating the intricate hierarchical vascular structures. An interesting approach to introduce the vascular tree in engineered tissues such as bone, is the introduction of an arteriovenous (AV) loop [1]. The AV loop model is a microsurgical approach to create a vascular axis that over time undergoes sprouting to vascularize the surrounding tissue. In this approach, an artery is anastomosed to a vein to create a loop that is placed within a chamber, filled with a bone-inductive scaffold, cells and/or growth factors. This chamber is implanted within the body and can be a closed or perforated chamber. Closed chambers are used to grow a tissue ectopically, which is completely isolated from other tissues. It can be retrieved and transplanted together with its vascular axis into a defect site. Perforated chambers are used directly at the site of the defect, allowing vascular ingrowth not only from the AV loop but also from surrounding tissues.

We have previously shown accelerated endochondral bone regeneration (EBR) upon implantation of allogeneic devitalized cartilage constructs [1]. The main aim of the present study is to use the AV loop model to create an upscaled vascularized construct for EBR. It is our hypothesis that an AV loop is necessary for upscaling the size of an endochondral bone tissue engineered construct and that it can accelerate bone formation.

Materials and Methods

Mesenchymal stem cells (MSCs) were harvested from Dark Agouti rats. At passage 4, the cells were encapsulated a collagen carrier ($1x10^6$ MSCs/spheroid) and chondrogenically differentiated. After 28 days, the engineered cartilage spheroids were harvested and devitalized by a mild procedure [2]. A total of 25 spheroids were implanted into a chamber with or without an AV loop. After 3 weeks, vascularization and mineralization of the two groups were assessed by MICROFIL® perfusion and micro-CT analysis. The degree of vessel formation was assessed via ImageJ. Bone formation was assessed via histological (Hematoxylin and Eosin, Safranin-O) and immunohistochemical (Collagen type I and II) staining.

Results and Discussion

After 3 weeks, we found sprouting of microvascular structures originating from the AVloop (Figure 1).Cork-screw tortuous-like vessels sprouting in the direction of the cartilage spheroids were observed, suggesting that chemotactic and angiogenic factors within the spheroids may contribute towards accelerated vascularization.

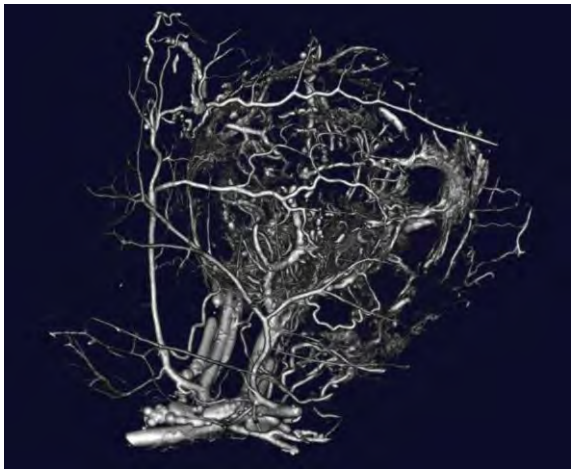

Figure 1. 3D MicroCT renderings of MICROFIL® showing sprouting of microvascular structures from the AV loop after 3 weeks.

Mineralization of the cartilage tissues was observed after 3 weeks, with or without the presence of an AV loop. Increased mineralization was observed when an AV loop was present compared to when an AV loop was no present, indicating that the presence of an AV loop indeed increases mineralization of the implanted cartilage spheroids and/or bone formation (Figure 2). The latter is currently investigated histologically.

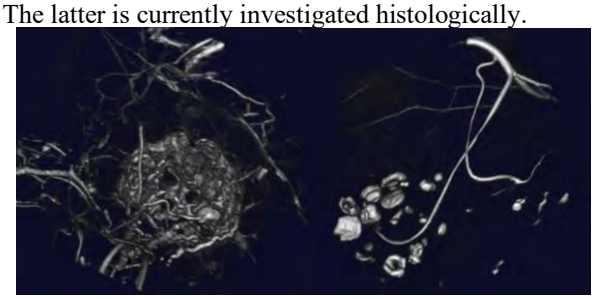

Figure 2. MicroCT images of mineralized cartilage spheroids and MICROFIL® contrasting perfusable vessels. Mineralized spheroids and vessels in a chamber with a (left) patent AV loop and (right) non patent loop.

Conclusion

The development of tortuous-like vessels suggests that the cartilage spheroids may have a migratory and angiogenic effect. This contributes towards enhanced mineralization of the implanted tissues. Initial results indicate that the presence of an AV loop benefits upscaling of bone tissue engineered constructs.

References

[1] Weigand et al.,The Arteriovenous Loop: Engineering of Axially Vascularized Tissue. Eur Surg Res. 2018;59(3-4):286-299.
[2] Longoni et al., Acceleration of Bone Regeneration Induced by a Soft-Callus Mimetic Material. Adv Sci (Weinh). 2022;9(6):e2103284.

Mechanosensing of tissue environment regulates fibroblast activation

M. D'Urso[1,2], N. A. Kurniawan[1,2], C.V.C. Bouten[1,2]
[1] Department of Biomedical Engineering, Eindhoven University of Technology, Eindhoven, The Netherlands
[2] Institute for Complex Molecular Systems, Eindhoven University of Technology, Eindhoven, The Netherlands

A critical biological process in the maintenance of tissue homeostasis is fibroblast to myofibroblast transition (FMT)[1]. This process is triggered by the activation of fibroblasts upon the presence of stresses within the tissue. Fibroblasts produce and release ECM components in order to regulate the environment properties such as stiffness. Upon stress, fibroblasts shift their phenotype, accompanied by cytoskeleton rearrangements and incorporation of alpha smooth muscle actin (αSMA) within the actin stress fibers, resulting in contractile myofibroblasts. The αSMA incorporation into stress fibers is used as marker to discriminate between the two phenotypes. Besides a wide range of chemical factors that are involved in this phenotypical change, such as TGF-β, it is hypothesized that the mechanical and physical properties of the environment are also dynamically involved in regulating the process[2]. The mechanotransductive machinery is used to sense the environment by the cells, where the first step is the formation of contact events with the substrate. The properties of those events can lead to mature focal adhesions with differential morphometric properties. The FAs properties are responsible for the cytoskeletal rearrangements leading a variety of actomyosin behaviors affecting FMT timing. To investigate this, we used a maskless protein micropatterning to tune the first contact events between fibroblasts and the substrate[3,4]. Importantly, this approach enables direct interrogation of the role of mechanosensing in FMT, by independently controlling cell probing and substrate stiffness, mimicking healthy and disease situations. The data are analyzed with an automatized workflow including image preprocessing, morphometric analysis using Cell Profiler, and batch data management to extract key mechanosensing parameters influencing the FMT.

References:

1. Kanekar, S., Hirozanne, T., Terracio, L. & Borg, T. K. Cardiac fibroblasts: Form and function. in *Cardiovascular Pathology* vol. 7 127–133 (1998).
2. D'Urso, M. & Kurniawan, N. A. Mechanical and Physical Regulation of Fibroblast–Myofibroblast Transition: From Cellular Mechanoresponse to Tissue Pathology. *Front Bioeng Biotechnol* **8**, 1459 (2020).
3. van der Putten, C. *et al.* Protein Micropatterning in 2.5D: An Approach to Investigate Cellular Responses in Multi-Cue Environments. *ACS Appl Mater Interfaces* **13**, 25589–25598 (2021).
4. van der Putten, C. *et al.* Generation of Multicue Cellular Microenvironments by UV-photopatterning of Three-dimensional Cell Culture Substrates. *JoVE (Journal of Visualized Experiments)* e63988 (2022) doi:10.3791/63988.

3D printed Magnetically Deformable Hydrogels as a Granular Medium for Tissue Engineering Applications

M. El Akkawi, V Trikalitis, I Gibson, C Goulas, J Rouwkema
Department of Design, Production & Management, Department of Biomechanical Engineering, University of Twente, Enschede, Netherlands.

Extrusion bio printing of hydrogels in a granular gel medium counterbalances the effects of gravity and increases the printing precision in comparison with the conventional 3D printing process where supports need to be placed to maintain the structure's integrity. With the purpose of adding functionality to the printed constructs, by applying a physical or chemical external stimuli to a heterogeneous ink and/or supporting medium, the constructs are capable to respond via shape transformation in a pre-programed manner over time. With this new dimension (i.e. 4D printing), higher structural complexity of constructs can be achieved without compromising their precision. Within this project, the types of direct or indirect external magnetic stimulation on bio-inks during their printing process inside a granular gel supporting medium, made by an "in-air microfluidics" process, will be explored. The potential effect of the stimulation on the shape transformation of the printed construct over time will further be evaluated. Finally, the effect of these controlled perturbations on tissue development within the printed constructs will be evaluated. Initial experiments focus on the selection and optimization of the magnetic particles, their integration within the in-air microfluidics process, and on the controlling of the dynamic response of the constructs by modulating the printing parameters, the intensity of the magnetic field, as well as the composition of the granular bath and bio-ink.

Fibrous Melt-Electrowritten Scaffolds to Investigate Cellular Behaviour for in Vitro Blood-Brain Barrier Model Development

M. Z. Gladysz[1,2], M. Koch[3], M. Kamperman[2], A. Nagelkerke[1], M. K. Wlodarczyk-Biegun[2,4]
[1]Pharmaceutical Analysis, Groningen Research Institute of Pharmacy, University of Groningen, Antonius Deusinglaan 1, 9713 AV Groningen, The Netherlands
[2] Polymer Science, University of Groningen, Nijenborgh 4, 9747 AG Groningen, The Netherlands
[3]Leibniz Institute for New Materials, Campus D2 2, 66123 Saarbrücken, Germany
[4]Biotechnology Centre, Silesian University of Technology, Krzywoustego 8, 44-100 Gliwice, Poland
Contact: m.z.gladysz@rug.nl

Introduction: The blood-brain barrier (BBB) is a selective interface in the brain between blood vessels, composed of a monolayer of endothelial cells, and the central nervous system, mostly made up of astrocytes and pericytes[1]. On the interface of the blood and brain part of the BBB lies a basement membrane. The BBB protects the brain from substances and organisms such as pathogens, but it also inhibits the uptake of therapeutics, including anti-cancer drugs[2]. To make advances in drug therapies tackling brain cancer, the BBB microenvironment should be recapitulated in an in vitro model system.
The goal of the study is to understand cell behaviour on the fibrous scaffolds in order to manufacture an in vitro BBB model facilitating cell-cell interactions.

Materials and Methods: To recapitulate the basement membrane melt electrowriting (MEW) was used (printer: Spraybase, Ireland) – a 3D printing method based on extruding well-organised polymeric fibers with a micrometric print resolution. The polymer used for scaffold fabrication was poly(ε-caprolactone) (PURASORB PC 12, Corbion). Scaffold surface modifications included coating with 2 µg/cm^2 poly-L-lysine (PLL, Innoprot) or 50 µg/mL poly-D-lysine (PDL) (A3890401, Gibco), incubation with fetal bovine serum (FBS) (BSA) (9048-46-8, Sigma-Aldrich) , etching with 1M NaOH and oxygen plasma activation (Harrick Plasma). The Young's modulus of the fibers was determined using atomic force microscopy (AFM). Cell culture studies were performed with the use of the murine brain endothelial cell line bEnd.3 and primary astrocytes derived from rodent brain tissue. The results were assessed via fluorescence microscopy, live cell imaging, and scanning electron microscopy (SEM).

Results and Discussion: The scaffolds obtained via MEW varied in inter-fiber distance between 50 and 100 µm, with the fiber diameter ranging from 6.65±0.75 to 9.73±1.02 µm, depending on the design. The most optimal cell attachment to the scaffolds was observed in samples treated with NaOH etching followed by FBS incubation, and for oxygen plasma treatment followed by PLL coating. Live cell imaging showed differences in cellular behaviour on the scaffold, dependent on the cell type. Astrocytes, upon seeding, were agglomerated which enabled them to attach to the fibers and not fall through the pores. bEnd.3 cells did not form such agglomerates, lowering the probabilities of cells catching onto the fibers. The cells' possibilities of reaching neighbouring fibers also differed (Fig. 1 A, B). The Young's modulus value for a single fiber ranged from 12±4 to 24±4 MPa. However, the staining for YAP, which is a cellular mechanosensor, performed on bEnd.3 cells grown on fibers showed translocation to the cytoplasm associated with softer substrates (Fig. 1 C, D).

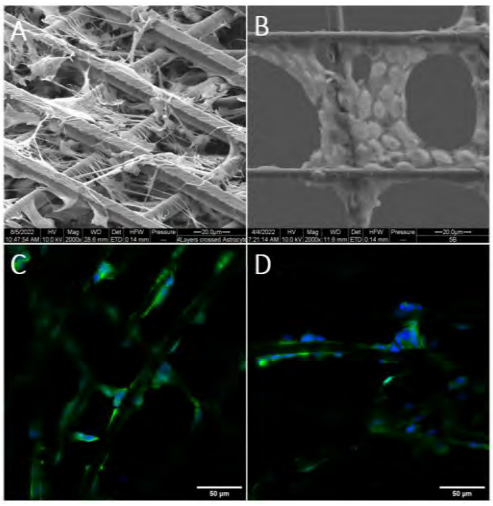

Fig. 1 A) SEM image of bEnd.3 cells on 2-layered PCL scaffold after 41 days of culture. B) SEM image of astrocytes cultured for 21 days on a 4-layered scaffold. C), D) Confocal microscopy images of endothelial cells stained for YAP (green) and Hoechst (blue).

Summary: The obtained inter-fiber distance of 50 µm in a homogenously printed scaffold is among the lower values reported for MEW applications. Endothelial cells' behaviour on the fibrous meshes differs from the behaviour of faster-proliferating and further-reaching astrocytes. The YAP translocation to the cells' cytoplasm is a response to the scaffold's stiffness and its architecture. The investigation of cellular behaviour on the scaffolds not only provides insights helpful for developing a relevant BBB in vitro model, but also sheds light on physical ques used by cells to migrate and proliferate in a specific, cell-dependent way.
The next steps will include enclosing the scaffolds inside of a custom-made microfluidic device and utilizing proteomics for protein identification after cell culture on various PCL scaffolds.

References:

1. Gładysz, M. Z., Stevanoska, M., Włodarczyk-Biegun, M. K. & Nagelkerke, A. Breaking through the barrier: Modelling and exploiting the physical microenvironment to enhance drug transport and efficacy. *Adv. Drug Deliv. Rev.* **184**, 114183 (2022).
2. Arvanitis, C. D., Ferraro, G. B. & Jain, R. K. The blood–brain barrier and blood–tumour barrier in brain tumours and metastases. *Nature Reviews Cancer* vol. 20 26–41 (2020).

Fabrication of polyvinyl alcohol/chitosan/silk electrospun mat to improve the wound healing process

M.H. Kazemi [1], S. Sajadimajd [2], Z. Gorgin Karaji [1]

[1] Department of Mechanical Engineering, Kermanshah University of Technology, Kermanshah 67156-85420, Iran
[2] Department of Biology, Faculty of Science, Razi University, Kermanshah, Iran.

Introduction: The wound healing process is influenced by various factors that depend on each other. Therefore, improving this complex process requires providing the right environment. The wound healing process includes three basic stages, including inflammation, proliferation and maturation. In recent years, with the advancement of medical knowledge, various wound dressings have been produced to help accelerate the healing of wounds, especially chronic wounds. Electrospinning technology has introduced an advanced technology to develop wound dressings with specific characteristics. Biopolymer-made fibrous mats have been extensively studied for tissue engineering due to their similar structure to the extracellular matrix [1, 2]. The purpose of this research work is the effect of micro-nanofibers loaded with effective drugs in wound healing to increase cell adhesion and proliferation along with control of drug release in the wound environment.

Methods: Silk fibroin (SF) was prepared according to the procedure that was performed in our previous research [3]. In the next step, polyvinyl alcohol solution (PVA-12% w/v) was added to chitosan solution (CS-3% w/v) and mixed for one hour. Then silk fibroin solution (SF-8% w/v) was mixed with PVA/CS solution (PCS). In the following, the electrospinning process was carried out by considering the 0.4 ml/h infusion pump the flow rate. Then a high voltage of 10 kV, considering a distance of 10 cm from the collector, was applied. After 8 hours of electrospinning, the nanofiber was dried, followed by 6 hours of cross-linking by applying 5% Glutaraldehyde. To coat the Deferoxamine (DFO) on the scaffold, the polydopamine solution with a specific concentration was prepared in Tris-HCl buffer (10.0 mM, pH=8.5). Following the surface modification, the scaffold was immersed in DFO solution for 24 hours (PCS-DFO). Eventually, the scaffold was dried for 1 hour at room temperature.

Results and discussion: Following the preparation of the electrospun scaffold, it was observed that with the addition of SF to CS and PVA, the tensile strength of the composite scaffold improved from about 6.5 to 10.5 MPa, and subsequently, the strain showed a growth of about 25 % (Fig. 1). Indeed, with the presence of numerous OH and NH_2 groups in CS and SF molecules, the hydrogen bond between the two materials is strengthened, and the mechanical properties are improved. Furthermore, the results of the other analyses, such as thermal degradation, contact angle, and swelling, showed that the PCS scaffold provides more favorable conditions for cell viability compared to PVA and PVA/CS. Also, the high number of viable cells (Fig. 2) showed the potential of this new scaffold to be used for wound healing. Additionally, the scratch assay, which is known as a method to simulate wound healing, clearly showed that in addition to the acceptable performance of the PCS scaffold (82% wound closure in 72 hours - Fig. 3), the coating of DFO on the scaffold improved scaffold function about 8% (Fig. 4).

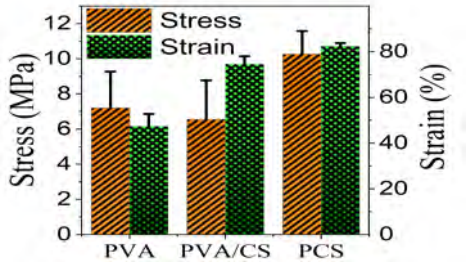

Fig. 1. Tensile properties.

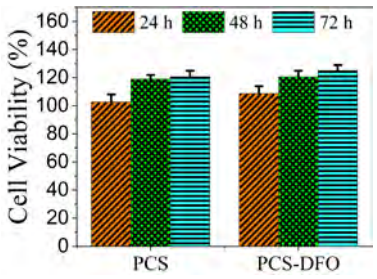

Fig. 2. Cell viability test.

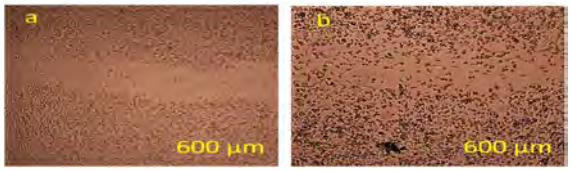

Fig. 3. Scratch assay, PCS, (a) 24 h, (b) 72 h.

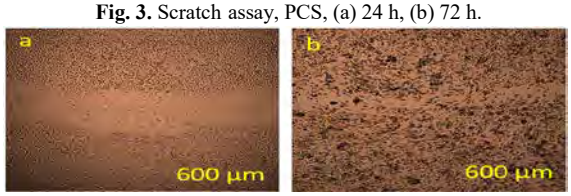

Fig. 4. Scratch assay, PCS-DFO, (a) 24 h, (b) 72 h.

Conclusions: In this research, PCS polymer nanofibers were produced using the electrospinning method. It was found that the addition of SF has a significant effect on increasing the mechanical properties of the scaffold. Moreover, the cell viability test showed that PCS and PCS-DFO scaffolds provide a suitable environment for the growth of human dermal fibroblast cells. Also, based on the scratch test, it was found that DFO can increase the potential of the PCS scaffold to accelerate the wound healing process. Consequently, As a result, these types of scaffolds can be suitable candidates for wound healing, particularly chronic wounds.

References

[1] H. Alipour, A. Saudi, O. Alavi, Z. Zeraatpisheh, S. Abolhassani, M. Rafienia, The Effect of Vitamin C-Loaded Electrospun Polycaprolactone/Poly (Glycerol Sebacate) Fibers for Peripheral Nerve tissue engineering, (2022).
[2] E. Rezvani Ghomi, S. Khalili, S. Nouri Khorasani, R. Esmaeely Neisiany, S. Ramakrishna, Wound dressings: Current advances and future directions, Journal of Applied Polymer Science, 136 (2019) 47738.
[3] Z.G. Karaji, F. Jahanmard, A. Mirzaei, B. Van der Wal, S.A. Yavari, A multifunctional silk coating on additively manufactured porous titanium to prevent implant-associated infection and stimulate bone regeneration, Biomedical Materials, 15 (2020) 065016.

Citrulline supplementation enhances *in vitro* osteogenic capacities of hBMSCs from non-union patients

R.V.M. Groven[1,2], M. Sangen[1,2], T.J. Blokhuis[2], M. van Griensven[1], M. Poeze[2]
Corresponding author: r.groven@maastrichtuniversity.nl

[1] *Department of Cell Biology-Inspired Tissue Engineering, MERLN Institute for Technology-Inspired Regenerative Medicine, Maastricht University, Maastricht, The Netherlands*
[2] *Division of Trauma Surgery, Department of Surgery, Maastricht University Medical Center+, Maastricht, The Netherlands*

Introduction Long bone fractures are common injuries upon trauma. Around 10% of long bone fractures show inadequate fracture healing, leading to delayed- or non-unions. Amino acids have shown to regulate bone regenerative processes. In particular, citrulline has shown to enhance bone regeneration in murine bone defect healing models. Oral citrulline supplementation stimulated callus formation and led to a balanced regulation of inflammation, resulting in a shorter inflammatory phase after fracture, thereby contributing to enhanced bone regeneration. However, exact cellular mechanisms behind these enhanced bone regenerative capacities are unknown. The aim of this study was therefore to determine whether citrulline can enhance the osteogenic capacities of human Bone-marrow Mesenchymal Stem Cells (hBMSCs), derived from non-union patients.

Methods For this study, hBMSCs were isolated from three donors undergoing a bone marrow aspiration for non-union treatment. The hBMSCs were cultured in osteogenic medium, supplemented with citrulline in the following concentrations: 0, 5, 7.5, and 10 mM. Alanine was chosen as an isocaloric control and applied in identical concentrations. Cellular viability was assessed through presto blue assay, proliferation by DNA quantification, and cytotoxicity through lactate-dehydrogenase assay. For the determination of the osteogenic capacity, ALP activity and alizarin red staining were performed, combined with qPCR for osteogenic marker genes. All measurements were performed at days 1, 3, 7, 14, and 21 (Figure 1).

Results Citrulline supplementation increased cellular viability and proliferation while decreasing cytotoxicity in a dose dependent manner. Furthermore, citrulline supplemented hBMSCs showed increased expression of osteogenic marker genes collagen I, RUNX2, osteocalcin, and osteopontin, as well as enhanced mineralization (Figure 2).

Discussion This study revealed potential cellular mechanisms behind enhanced bone regeneration upon supplementation of specific amino acids. Citrulline supplementation resulted in more advanced osteoblastogenesis, extracellular matrix formation and maturation, as well as increased cellular proliferation, and decreased cytotoxicity. In conclusion, the supplementation of citrulline has shown to possess potential beneficial effects on the osteogenic capacity of hBMSCs and is therefore of interest in the field of bone regeneration.

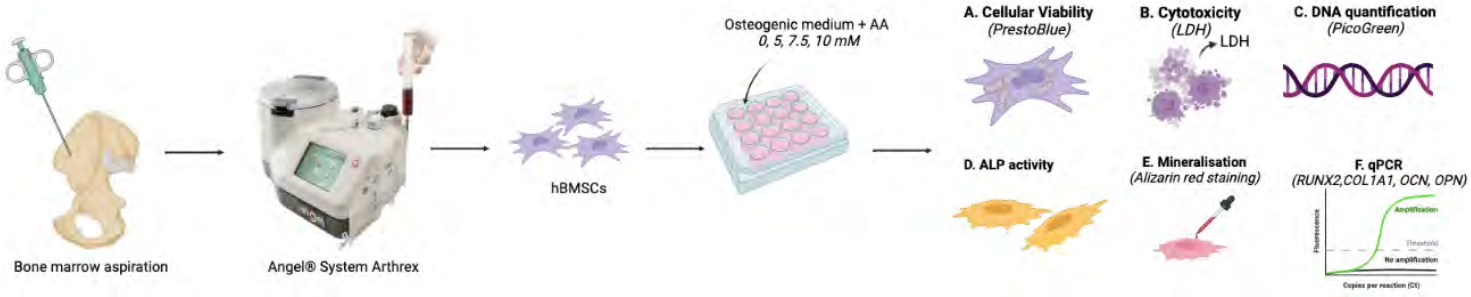

Figure 1: schematic experimental workflow. Cells were harvested and cultured with citrulline or alanine in varying concentrations for maximal 21 days, after which osteogenic capacities were determined.

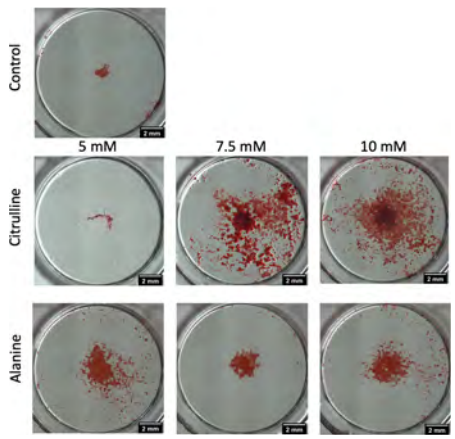

Figure 2: Alizarin Red staining at day 21. All samples, including the control, were cultured in standard osteogenic medium, supplemented with the respective amino acids.

Immune Modulation of Zinc via THP-1 Derived Macrophage Polarization

J. Han, J. Sanders, B.A.J.A van Oirschot, S.C.G. Leeuwenburgh, J.J.J.P. van den Beucken, F. Yang
Radboud University Medical Center, Radboud Institute for Molecular Life Sciences, Department of Dentistry - Regenerative Biomaterials, Radboudumc, Nijmegen, The Netherlands

Introduction: Tissue integration is a prerequisite for successful dental implantation. However, the microenvironment around implants tends to be inflammatory due to foreign body reactions to implants, which compromise tissue integration [1]. Therefore, it is crucial to maintain a pro-reparative microenvironment to improve tissue integration to dental implants. One of the strategies is to modulate macrophage behavior as macrophages are one of the first cell types to be recruited to the peri-implant microenvironment after surgery. Once stimulated, inactive M0 macrophage can polarize to either a pro-inflammatory phenotype, M1 macrophage, or a pro-reparative phenotype, M2 macrophage. Specifically, M2 macrophages support tissue regeneration by secreting pro-regenerative cytokines such as transforming growth factor beta (TGF-β) and interleukin 10 (IL-10) [2]. Many agents have been reported to modulate macrophage polarization towards M2 phenotype such as growth factors and biocompatible ions. Among them, zinc seems promising due to its high biosafety and the supportive role in the immune system. Besides, zinc also showed to improve cell proliferation and extracellular matrix secretion as well as combat bacteria [3]. In this study, we aimed to investigate the effect of zinc on macrophage polarization by using zinc ions, i.e. Zn(II) to treat macrophages derived from human monocytic THP-1 cells.

Materials and methods: First, to determine a safety concentration range of Zn(II), human THP-1 derived macrophages were treated with Zn(II) from 0 to 3 mM. Then, to determine Zn(II) effect on macrophage polarization, Zn(II) treated M0 macrophages were compared with those stimulated by interferon gamma (IFN-γ)/lipopolysaccharide (LPS) (M1 macrophages) and IL-4/IL-13 (M2 macrophages). M1 and M2 macrophage phenotype markers CCR7 and CD36, respectively, were used for immunofluorescent staining. Pro-inflammatory (TNF-α) and anti-inflammatory (TGF-β) cytokines in macrophage-derived conditioned medium were measured by multiplex assay and enzyme-linked immunosorbent assay (ELISA).

Results and discussion: Images of live/dead cell staining showed a significant increase of dead cells when Zn(II) concentration was higher than 300 μM (Fig. 1). Based on this result, we scaled down Zn(II) concentration range to 0-300 μM in the later study. Immunofluorescent images showed that more CD36 positive cells were observed in M2 group compared to M0 and M1 macrophages. M0 treated with high concentration of Zn(II) i.e. 37.5 and 300 μM, resembled the M2 macrophages (Fig. 2). Moreover, cytokine measurement results showed a high ratio of TGF-β/TNF-α in the Zn(II) treated macrophage groups, which was significantly higher than that of M1 macrophages. This ratio was also simulate to that of M2 macrophages. However, we also could not find any significant difference of TGF-β/TNF-α ratios between M2 and M0 macrophages. Therefore, no strong conclusion can be drawn that Zn(II) treatment is in favor of M2 polarization. Nevertheless, the difference between Zn(II) treated groups and M1 suggests its inhibition effect of M1 polarization.

Conclusion: Zn(II) is cytocompatible when the concentration is lower than 300 μM. Zn(II) treatment inhibited macrophage polarization towards M1 phenotype, which is in favor of wound healing. The promising results encourage us to develop zinc-incorporated coatings on dental implant to limit inflammation for improved wound healing.

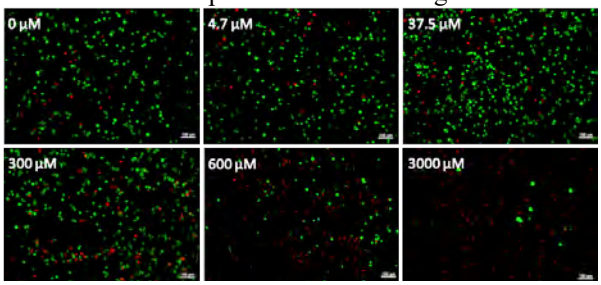

Fig. 1 Live/dead cell staining of M0 macrophages cultured in varying concentrations of Zn(II) containing medium. Living cells were showed in green color while dead cells were showed in red color. When Zn(II) concentration was higher than 300 μM, dead cells increased significantly.

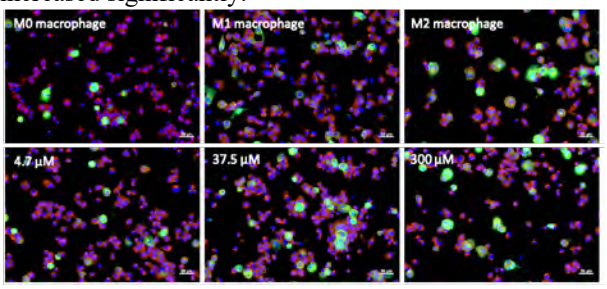

Fig. 2 Immunofluorescent staining of macrophages cultured with varying concentrations of Zn(II) with M1 (CCR7, red) and M2 (CD36, green) markers. More CD36 positive cells were observed as Zn(II) increased from 0 to 37.5 μM.

References: [1] Atsuta I, et al. Soft tissue sealing around dental implants based on histological interpretation. J Prosthodont Res. 2016;60(1):3-11.
[2] Zhang Y, et al. Titanium surfaces characteristics modulate macrophage polarization. Mater Sci Eng C Mater Biol Appl. 2019;95:143-51.
[3] Chen L, et al. Synergistic effects of immunoregulation and osteoinduction of ds-block elements on titanium surface. Bioactive Materials. 2021;6(1):191-207.

Towards a cell based islet delivery

C. Hermanns, A. Seedorf, A.A. van Apeldoorn
MERLN Institute for Technology-Inspired Regenerative Medicine - Cell Biology-Inspired Tissue Engineering (cBITE), Universiteitsingel 40 6229ER Maastricht, The Netherlands

Introduction:

Type 1 diabetes is an autoimmune disorder where the insulin producing cells are destroyed. Under normal circumstance, daily insulin injections are enough to control blood glucose in these patients, but for some patients it isn't. In clinical islet transplantation (CIT) donor islets are delivered into the protal vein of the patient. Although CIT is a promising treatment, limitations remain. During the isolation process the extracellular matrix (ECM) and microvasculature of islets are destroyed leading to poor engraftment and significant loss of transplanted cells. Over the last years, multiple alternative methods have been proposed to create a better environment for islets and improve survivability and function. Most of these strategies are based on synthethic biomaterials, which, eventhough biocompatible, will cause a foreign body response and scar tissue around the implant. Here we are showing two cell based apporaches that are aiming to create a more natural environment for islets.

Material and Methods:

Cell sheets of immortalized mesenchymal stem cells (iMSCs) were created on thermoresponsive NUNC UpCell dishes. Multiple cell sheets were placed on top of each other to encapsulate human donor islets. The function of human islets was measured with a glucose stimulated insulin secretion assay. iMSCs and HUVECs were cocultured in cell sheets to create vascular like structures. CD31 staining was used to visualize possible vascular like structures.

Cell cube cultures

iMSCs were cultured into 150 micrometer cell aggregates and seeded into a stainless steel mold to create tissue cubes of varying sizes. PreSens Oxy 10 system was used to measure the oxygen concentration inside the cube using dedicated oxygen microprobes.

Figure 1: 1x1x1 mm iMSC cube.

Results and Discussion:

Cell sheets

After optimizing cell culture, it was possible to stack four cell sheets and still handle them without rupturing. Primary human islets seeded between two bottom and two top cells sheets were glucose responsive, indicating proper endocrine beta cell function. By coculturing HUVECs with iMSCs, we observed a vascular mimicking network in cell sheets (figure 1), which could help with future *in vivo* vascularization .

Cell cubes

Oxygen measurements at ambient air showed ~5% tissue oxygen conditions in the centre of $1mm^3$ and $36mm^3$ cell cubes. Prevascularization might help to boost vascularization and maintain these conditions once cubes are implanted, which is crucial for proper beta cell function.

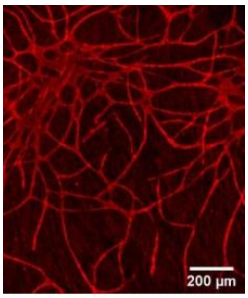

Figure 2 vascular like network in cell sheets

Conclusions:

Here we introduce two cell based strategies to create a synthetis biomaterial free delivery system for beta cells. Primary human islets inbetween cell sheets show good functionality and respond to increasing glucose levels. By addition of HUVECs we were able to generate a vascular like network within these cell sheets. We also showed that by using a stainless-steel mold it is possible to grow small tissue cubes of different sizes. At ambient air oxygen levels inside these cubes was maintained at ~5% tissue oxygen level. Both approaches can be tailored to accommodate beta cells and primary islets for future transplantation and treatment of type 1 diabetes .

Acknowledgement:

This work is financially supported by Stichting DON.

Investigating the gene expression profiles underlying biomaterial-associated infection

L.S. van Hofwegen, P.P.S. Balraadjsing, M. Riool, L. de Boer, S.A.J. Zaat
Dept. of Medical Microbiology and Infection Prevention, Amsterdam UMC, Meibergdreef 9 1105 AZ Amsterdam, The Netherlands

l.s.vanhofwegen@amsterdamumc.nl

Introduction: The most common complication related to implantation of a biomaterial is biomaterial-associated infection (BAI). BAI is predominantly caused by *Staphylococcus aureus* and *Staphylococcus epidermidis*, which are commensal bacteria that cause pathology in the presence of a biomaterial. These infections may lead to chronic inflammation, revision surgeries and in severe cases, loss of function. The molecular details underlying the pathology in BAI and the foreign body response (FBR) to a biomaterial are not well understood. **Goal:** In this study, we aim to elucidate the molecular details of the FBR and the host response in BAI by studying gene expression. **Methods:** We used a mouse model for subcutaneous titanium implant infection. The study groups included mice with only *S. epidermidis* infection to study the role of infection, only titanium implant to study the FBR and the combination of *S. epidermidis* infection with a titanium implant to study BAI. We analyzed gene expression of the tissue surrounding the surgical site at 1h, 6h, 2 days, 6 days, 9 days, 14 days and 21 days after surgery using the microarray technique. Comparing differentially expressed genes between the study groups will give insights into the course of the FBR and BAI over time. Based on these data, we will identify genes that characterize the host response against titanium biomaterials. This information can be used to design follow-up experiments for more detailed studying of key molecules involved in the FBR and/or BAI. **Future directions:** Ultimately, we aim to identify biomarkers that can predict infection susceptibility to biomaterial implantation.

Mechanical characterization of a unique biomimetic artificial disc for the cervical spine

C.A.M. Jacobs[1], Abdelrahman M. Abdelgawad, S. Ghazanfari[2], S. Jockenhoevel[2], K. Ito[1]
[1]Orthopaedic Biomechanics, Dept. of Biomedical Engineering, Eindhoven University of Technology, the Netherlands
[2]Aachen-Maastricht Institute for Biobased Materials, Dept. of Science and Engineering, Maastricht University, the Netherlands

Introduction

Cervical artificial intervertebral discs (AIDs) have been developed as a mobility preserving alternative treatment for disc degeneration. First generation CDRs were based on traditional synovial joint arthroplasty designs, leading to a mismatch in kinematic behavior compared to a natural disc. It is hypothesized that mimicking the native structure of the intervertebral disc (IVD) by using novel biomaterials would lead to appropriate biomechanical properties and less complications Hence, a unique biomimetic AID (bioAID) was developed as shown in Fig. 1 [1]. The design contains a swelling pHEMA-NaMA hydrogel core, mimicking the nucleus pulposus, and an ultra-high-molecular-weight-polyethylene (UHMWPE) fiber jacket mimicking the ligamentous annulus fibrosis. The goal of this study was to evaluate the design of the bioAID based on its compressive strength, its primary fixation as well as its diurnal creep behaviour.

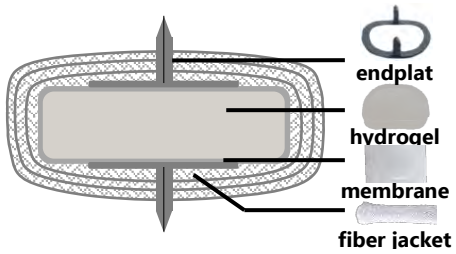

Figure 1: *schematic representation of the design of the*

Materials & Methods

First the bioAIDs were swollen under a 50N load in normal saline until swelling equilibrium, representing the physiological weight of the head. Next, the compressive strength was determined in a quasi-static axial compression test (n=5, 0.001 mm/sec) until failure, where failure was defined as force drop of > 5% or when < 50% of the initial height of the implant was reached. The primary fixation was tested through a subsidence and device expulsion test. Subsidence was examined by a dynamic compression loading protocol (n=5, 0.5 million cycles, sinusoidal waveform 50-225 N at 2 Hz) between two polyurethane foam blocks that mimic the mechanical properties of the vertebrae. The risk of device expulsion was tested by applying an axial preload of 100 N after which the implant was pushed in an anterior-posterior direction until displacement occurred (n=3). To determine the creep characteristics, a diurnal loading regime of 8 hours 60 N (night-loading) followed by 16 hours at a load magnitude alternating every 30 minutes between 60 and 180 N (day-loading) was applied. Disc height changes and rate of creep and recovery were determined.

Results

The compressive failure load at 50% of the initial height of the implant was 973 ± 55 N (Fig 2, around 2.5 mm displacement), being well above the physiological load of the cervical spine ranging between 50 – 100 N [2]. Interestingly, none of the samples showed functional failure up to 4 kN (Fig. 2, limit of the load cell). The

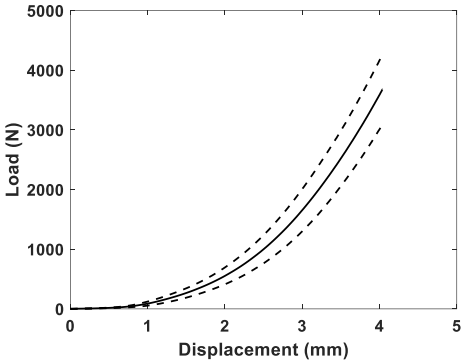

Figure 2: *Interpolated average (solid line) of the load-displacement data of quasi-static axial compression test and its corresponding standard deviation (dashed lines).*

average stiffness was 584 ± 73 N/mm, similar to the values found for a native disc (500 N/mm, [2]). No subsidence was detected and the device expulsion load was higher than the physiological shear load of 28 N [2] (394 ± 9.9 N with corresponding 1.7 ± 0.3 mm displacement). Preliminary data of the diurnal creep behaviour of the bioAID is shown in Fig. 3. Results show that the bioAID can replicate the time-dependent and visco-elastic behaviour of a native disc.

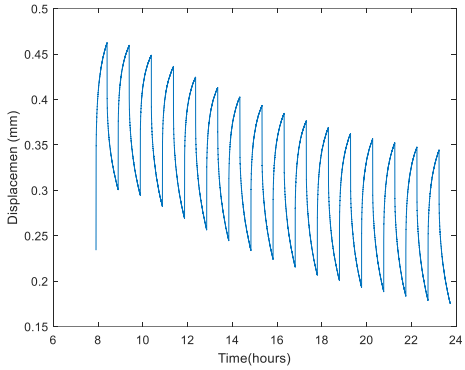

Figure 3: *Displacement vs Time during the day-loading*

Discussion

The overall results indicate that the current design is mechanically safe in compression and able to remain fixed between the vertebral bodies under physiological loads. Moreover, it can replicate the time-dependent and viscoelastic behaviour of a natural disc. The results reported here indicate that this design could be a feasible and promising total disc replacement for treating severely degenerated discs.

References

[1] P. R. Van Den Broek, Eindhoven University of Technology, 2012.
[2] A. White and M. Panjabi, *Clinical Biomechanics of the Spine*, 2nd ed. London: Lip pincott Company, 1990.

Spatial Modeling of YAP Phosphorylation through Direct Interaction with Integrin Adhesions

H. Jafarinia*, L. Shi, H. Wolfenson, A. Carlier
MERLN Institute for Technology-Inspired Regenerative Medicine, Department of Cell Biology-Inspired Tissue Engineering, Maastricht University, Maastricht, The Netherlands.

Introduction

Integrin-based mechanotransduction enables cells to sense and respond to changes in their environment. YAP is a crucial downstream player of integrin-based signaling whose function depends on translocation from the cytoplasm to the nucleus. The phosphorylation of YAP regulates its ability to enter the nucleus. Recent findings show that YAP can be recruited to adhesions to be directly phosphorylated (Elbediwy et al. 2018). It is however not clear how properties of integrin adhesions, such as changes in cluster size and distribution due to stiffness or extracellular matrix composition, can affect this process.

Methods

To investigate adhesion-mediated phosphorylation of YAP, we developed a spatial particle-based model, similar to a previous model for FAK phosphorylation (Cheng et al. 2020), to study how YAP phosphorylation through direct binding to integrin adhesions is regulated by the adhesion properties. In our model, integrin adhesions are randomly fixed on a membrane at the bottom of the simulation box, and inactive YAP molecules are initialized randomly in the simulation box; see figure 1 top panel. Periodic boundary conditions in X and Y directions and closed boundary conditions for the top and bottom surfaces are used. Each particle diffuses or engages in a reaction based on specific probabilities at each time step. Our model takes into account the association and dissociation of YAP with the adhesions and phosphorylation (in the adhesion) and dephosphorylation (in the cytoplasm) of YAP.

Results and Discussions

The simulation results show proof-of-concept of the proposed model for YAP binding to adhesions, phosphorylation, and release. With a fixed adhesion size and adhesion number, our simulation predicts a certain level of YAP phosphorylation at equilibrium that does not depend on the random positions of the adhesions. Figure 1, bottom panel, shows the results from five simulations with different positions of the adhesions. The preliminary results also show that the adhesion cluster size distribution influences the YAP phosphorylation (data not shown); however, the model requires refinement and needs to be validated with experimental data. In summary, this work contributes towards gaining more knowledge on the mechanisms by which cells sense and adapt to their environments, which can aid in developing improved cancer and regenerative medicine treatments.

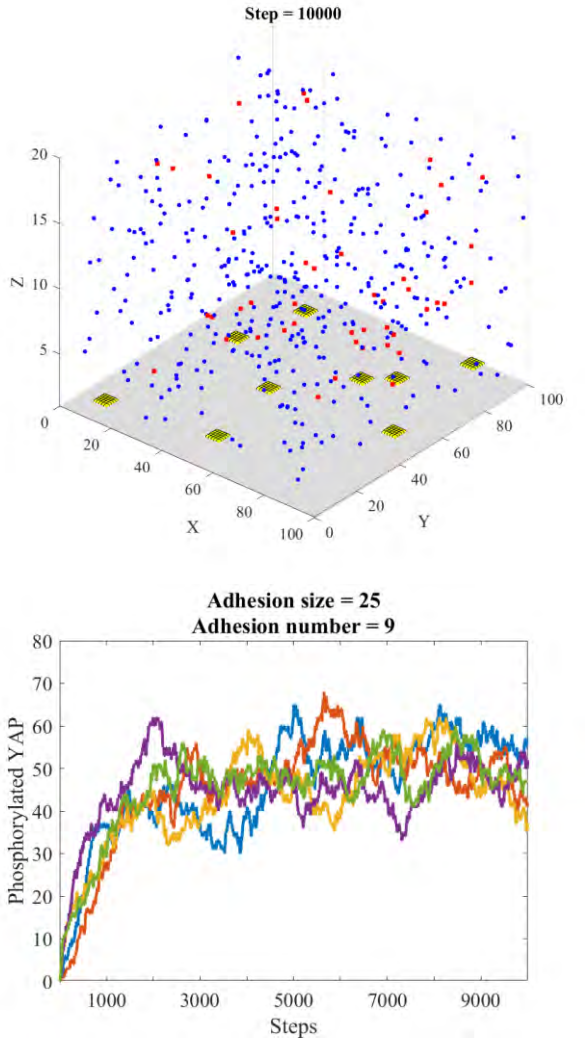

Figure 1. (TOP) 3D spatial model for adhesion-mediated YAP phosphorylation. Phosphorylated and dephosphorylated YAP molecules are shown in red and blue. Integrin adhesions, depicted in yellow, are fixed at random positions on the membrane. (Bottom) the number of phosphorylated YAP molecules for five different initial positions of integrin adhesions and YAP molecules.

Affiliations

-Lidan Shi, Rappaport Faculty of Medicine, Technion—Israel Institute of Technology, Haifa, Israel.
-Haguy Wolfenson, Rappaport Faculty of Medicine, Technion—Israel Institute of Technology, Haifa, Israel.
-Aurélie Carlier, MERLN Institute for Technology-Inspired Regenerative Medicine, Department of Cell Biology-Inspired Tissue

*email: hamidreza.jafarinia@maastrichtuniversity.nl

A developmental tissue engineering approach to study breast cancer metastasis to the bone

A. Lolli[1], E. Ji[1], J. Witte-Bouma[1], B. Tutterow[1], M. Saini[2], N. Aceto[2], E. Farrell[1]

[1]*Department of Oral and Maxillofacial Surgery, Erasmus MC University Medical Centre Rotterdam, Rotterdam*
[3]*Department of Biology, Institute for Molecular Health Sciences, ETH Zurich, Switzerland*

Introduction: Breast cancer metastasis affect most frequently the bone tissue (70%), leading to severe symptoms and high mortality rate. Unfortunately, little is known about the mechanisms and the vulnerabilities of bone metastasis, and the patients are considered incurable. Importantly, experimental models able to recapitulate the bone metastatic environment could lead to a better understanding of the process and aid the development of targeted drugs. Here we took inspiration from endochondral ossification (EO), the developmental process through which long bones are formed, to develop a new approach to study bone metastasis. We generated in vivo bone ossicles through EO and *in vitro* mineralized constructs, and investigated their interactions with human breast cancer cells.

Materials and Methods: Bone marrow-derived human mesenchymal stromal cells (hMSCs) were cultured as pellets ($2x10^5$ cells/pellet) in chondrogenic medium for 21 days to induce cartilage production. The pellets were implanted subcutaneously in athymic mice and bone formation was assessed by micro-computed tomography and histology. To establish an *in vitro* differentiation strategy, chondrogenically primed hMSC pellets were switched to osteogenic conditions by adding 10mM β-glycerophosphate. Mineralization was confirmed by calcium uptake and histology. Cancer cell migration and proliferation was assessed by transwell assay and DNA quantification, respectively. Infiltration of hMSC pellets by CFDA-labeled cancer cells was analysed by fluorescence microscopy.

Results: Chondrogenically primed hMSC pellets implanted subcutaneously in mice underwent EO generating vascularized ossicles with bone marrow within 8 weeks. In co-culture experiments, explanted ossicles enhanced the migration of human metastatic breast cancer cells (MDA-MB-231) (12-fold increase), but did not affect the migration of non-metatastic cells (MCF7). *In vitro*, exposure of chondrogenic pellets to osteogenic stimuli induced successful mineralization of the cartilage template. When *in vitro* mineralised pellets were co-cultured with MDA-MB-231, cancer cell migration was strongly enhanced (36-fold increase). Exposure of MDA-MB-231 to conditioned medium from *in vitro* mineralised pellets enhanced cancer cell proliferation and migration, further indicating that factors secreted from the pellets can induce a metastatic behavior in cancer cells. Finally, when MDA-MB-231 and *in vitro* mineralised pellets were directly co-cultured in Matrigel, cancer cell infiltration in the pellets was detected within 72h.

Conclusions: Our data demonstrate the possibility to exploit a tissue engineering approach using EO to mimic specific aspects of the process of cancer metastasis to the bone. *In vivo*- and *in vitro*-generated bone/mineralised constructs were successfully co-cultured with invasive breast cancer cells and were able to induce a metastatic response. Follow-up studies are ongoing to investigate the migration of cancer cells towards the pellets within a bioreactor system with flow. These experimental models may be applied for studying the molecular basis of the bone metastatic process and to develop new targeted drugs.

Acknowledgements: The study was supported by the European Union Horizon 2020 Research and Innovation Program under grant agreement 801159.

Development of Novel Cyclodextrin-based Nanogels

Yanjing (Y.) Ji, dr. Patrick van Rijn
W.J. Kolff Institute for Biomedical Engineering and Materials Science, University of Groningen/ University Medical Center Groningen (UMCG), Ant. Deusinglaan 1, Groningen, The Netherlands

Introduction

Nanohydrogels or hydrogel nanoparticles with nanoscale 3D structure, well-known as nanogels, are made of physically or chemically cross-linked hydrophilic polymers and water [1,2]. Nanogels have attracted much attention as drug carriers with excellent properties, such as high water content, high porosity, excellent hydrophobic and hydrophilic drug binding ability, good biodegradability, and with different biological activities. As a consequence, these excellent properties allow nanogels to exhibit superior performance over other nanocarriers and have promising drug delivery in disease treatment [3]. Here in, we modified the Heptakis-(6-amino-6-deoxy)-β-Cyclodextrin heptahydrochloride (Ha-β--CD) with Acrylic acid N-hydroxysuccinimide ester (AA-NHS) to obtain the functional group of acrylamide. Afterwards, the poly(N-Isopropylmethacrylamide-*co*-Acrylamide cyclodextrin) (p(NIPMAM-*co*-AACD)) nanogels was synthesized.

Methods

Acrylamide functionalization of Ha-β-CD was performed according to the previous report [4]. Precipitation polymerization was used for the synthesis of p(NIPMAM-*co*-AACD)) nanogels. we characterized the modification of AACD with Fourier-transform infrared spectroscopy (FTIR), proton nuclear magnetic resonance spectroscopy (^{1}H NMR), and High-performance liquid chromatography (HPLC). The physical and chemical properties of p(NIPMAM--*co*-AACD) nanogels were studied with dynamic light scattering (DLS), transmission electron microscopy (TEM), and ^{1}H NMR.

Results and Discussion

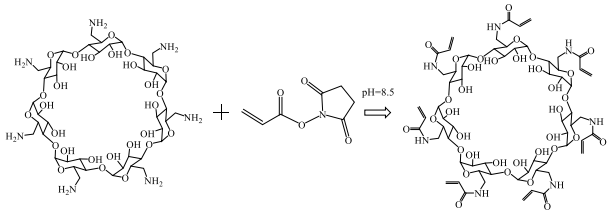

Figure 1. The synthesis scheme of acryloyl groups functionalized cyclodextrin (AACD).

As illustrated in **Figure 1**, the introduction of polymerizable acryloyl groups on Ha-β-CD molecule using AA-NHS in pH 8.5 50 mM sodium carbonate buffer, which reacts with the free amino groups present in Ha-β-CD. Conjugation of acryloyl groups to Ha-β-CD showed changes in the FT-IR spectra. The peak of 3369 cm^{-1}, 1609 cm^{-1}, and 700-1000 cm^{-1} contributed to the N-H stretching of primary amine, N-H bending of primary amine, and the glucopyranose ring, respectively. The new peak at 1246cm^{-1}, 1623cm^{-1}, and 1663cm^{-1} correspond to C-N stretching, C=C stretching, and C=O stretching, which indicate crosslinking of acryloyl groups with Ha-β-CD through AA-NHS.

After that, the polymer was formed by radical polymerization using three different monomers: NIPMAM, AACD, and N, N'-methylene(bisacrylamide)

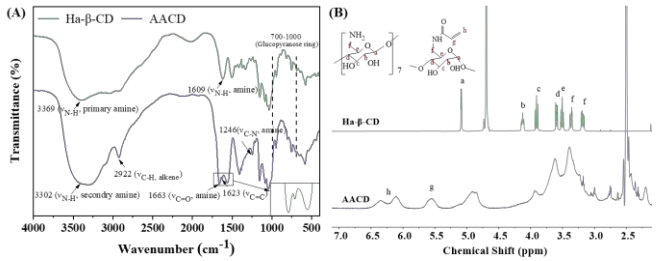

Figure 2 FTIR (A) and ^{1}H NMR (B) of Ha-β-CD and AACD.

(BIS) as cross-linker, in molar ratio 93.5:1:5.5, respectively. The polymerization was initiated by adding a solution of ammonium persulfate (APS), yielding the p(NIPMAM-*co*-AACD) nanogels after 4 h at 70°C under N_2. We also synthesized p(NIPMAM) nanogels without AACD according to the above composition ratio.

To prove the copolymerization of AACD with NIPMAM, the Zeta potentials of AACD, p(NIPMAM) nanogels, and p(NIPMAM-*co*-AACD) nanogels were measured. The Zeta potential of AACD and p(NIPMAM) nanogels is around +17 and -11 mV. After AACD copolymerization, the Zeta potential of p(NIPMAM--*co*-AACD) nanogels increased to -6 mV compared with p(NIPMAM) nanogels, which indicated the presence of positively charged AACD, and successful copolymerization.

Conclusions

In this study, we introduced polymerizable acryloyl groups on Ha-β-CD molecule using AA-NHS and successfully copolymerized AACD with NIPMAM. Further study needs to focus on the degrees of acryloyl group modification, the morphology and temperature--dependent measurements of nanogel.

References

[1] A. V Kabanov, S. V Vinogradov, *Angew. Chemie Int. Ed.* **2009**, *48*, 5418.

[2] H. Wang, L. Gao, T. Fan, C. Zhang, B. Zhang, O. A. Al-Hartomy, A. Al-Ghamdi, S. Wageh, M. Qiu, H. Zhang, *ACS Appl. Mater. Interfaces* **2021**, *13*, 54621.

[3] D. Huang, H. Qian, H. Qiao, W. Chen, J. Feijen, Z. Zhong, *Expert Opin. Drug Deliv.* **2018**, *15*, 703.

[4] M. Yan, J. Du, Z. Gu, M. Liang, Y. Hu, W. Zhang, S. Priceman, L. Wu, Z. H. Zhou, Z. Liu, T. Segura, Y. Tang, Y. Lu, *Nat. Nanotechnol.* **2010**, *5*, 48.

Uniaxial and equibiaxial strain differently affect the phenotypic switching of vascular smooth muscle cells

C. Karakaya[1,2], E.A.N. van den Hurk[1], C.M. Sahlgren[1,2,3], C.V.C. Bouten[1,2], S. Loerakker[1,2]

[1]Department of Biomedical Engineering, Eindhoven University of Technology, The Netherlands
[2]Institute for Complex Molecular Systems, Eindhoven University of Technology, The Netherlands
[3]Faculty of Science and Engineering, Åbo Akademi University, Finland

Introduction:
Vascular diseases are among the major causes of morbidity and mortality worldwide. Diseased vessels often need to be replaced with autologous tissues or synthetic grafts via surgical interventions. However, autologous grafts have limited availability, and synthetic grafts are often associated with complications affecting the long-term patency, especially for small-diameter vessels. *In situ* vascular tissue engineering, aiming to transform biodegradable materials into living vascular tissues inside the body, is promising to overcome these limitations. To develop *in situ* engineered vascular replacements that are superior to current options and to control their regeneration which can accelerate the clinical translation, a mechanistic understanding of vascular growth and remodeling processes is needed.
Vascular smooth muscle cells (VSMCs) are important regulators of vascular growth and remodeling, with their ability to express different phenotypes. VSMCs demonstrate a contractile quiescent phenotype in mature and homeostatic vessels, and switch towards a more proliferative and migratory synthetic phenotype upon changes in hemodynamic conditions to induce growth and remodeling. VSMCs are exposed to cyclic strain in the vessel wall due to the pulsatile blood flow, and this mechanical strain is known to affect the VSMC phenotype. However, cyclic strain has been reported to both up- and downregulate the expression of contractile phenotype markers compared to the static controls. The differences in results could be explained by the application of different strain levels, exposure time as well as the application of strain in different directions. Recently, we have shown that applying equibiaxial strain causes loss of contractile features of contractile VSMCs (Karakaya *et al.* 2022, *Front. in Cell and Dev Biol.*). The current study aims to explore and compare the effect of equibiaxial strain, mimicking the radial strain in the vessel wall, and uniaxial strain, similar to the circumferential strain on the vessel wall, on the phenotypic changes of VSMCs.

Materials and Methods:
Human coronary artery smooth muscle cells (Lonza) were cultured at least 7 days in either smooth muscle cell growth medium (Cell Applications Inc.) to obtain synthetic VSMCs, or smooth muscle differentiation medium (Cell Applications Inc.) to obtain contractile VSMCs. Bioflex culture plates (Flexcell) were coated with collagen I from rat tail (Gibco) in the center of the wells. One day after cell seeding on the Bioflex plates, cells were stretched either equibiaxially or uniaxially with the Flexcell Tension System at 7% and 0.5 Hz for 48 hours. The membranes of each well were marked and tracked with a camera. The displacement was analyzed, and the corresponding strain was calculated via digital image correlation. Immunofluorescence staining and quantitative polymerase chain reaction were conducted to characterize the changes in cell phenotype upon stretch.

Results and Discussion:
Synthetic and contractile VSMCs showed their phenotypic characteristics in static conditions, with contractile VSMCs expressing more and fibrous alpha smooth muscle actin compared to synthetic VSMCs, and synthetic VSMCs being more proliferative. The application of equibiaxial strain at 0.5 Hz resulted in a transition in contractile VSMCs towards the synthetic phenotype, similar to our previous observations with the application of equibiaxial strain at 1 Hz [1]. On the other hand, contractile VSMCs preserved their contractile features upon the application of uniaxial strain.

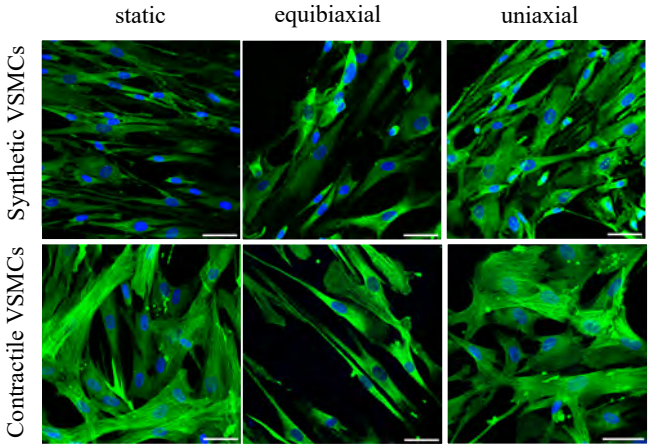

Figure 1: The representative immunofluorescence images of contractility marker alpha-smooth muscle actin in green and DAPI in blue for static, uniaxially stretched and equibiaxially stretched synthetic and contractile VSMCs (scale bar: 100 um).

Conclusion: Our results suggest that uniaxial strain is perceived by VSMCs as more physiological compared to equibiaxial strain in which the phenotypic switching has been detected. This observation could help us to control the VSMC fate via changing the direction of strain and improve the scaffold designs for *in situ* vascular tissue engineering. Further efforts will be focused on understanding the differences in the underlying mechanisms.

Acknowledgements: This project has received funding from the European Research Council (ERC) under the European Union's Horizon 2020 research and innovation programme (Grant agreement No. [802967]).

Osteogenic and osteoimmunogenic performance of Cu-doped bioactive glass nanoparticles loaded with flavonoid

A. Khodaei[a,b], Q. Nawaz[a], S. AminYavari[b], H. Weinans[b], A.R. Boccaccini[a]

[a] Department of Materials Science and Engineering, Institute of Biomaterials, University of Erlangen-Nuremberg, 91058 Erlangen, Germany

[b] Department of Orthopedics, University Medical Center Utrecht, Utrecht, The Netherlands

Introduction

Considering orthopaedic applications, variety of biomaterials have been developed incorporating bioactive glass nanoparticles (BGNPs) to release bioactive elements. Among all the elements, Copper (Cu) as osteogenic, angiogenic, and antibacterial element is favourable in bone regeneration and repair [1]. Regarding the very early interaction, it is believed that Cu ions are the main reason of inflammation due to the increase of serum copper levels in rheumatoid arthritis patients [2]. Moreover, it is well known that immune reactions play a key role in bone regeneration. During the first phase (inflammation phase) of bone healing, innate and adaptive cells including macrophages migrate to the bone defect site and develop an inflammatory environment. The released inflammatory cytokines such as TNF-α, IL-6, IL-8, and IL-17 recruit and differentiate MSCs to the osteoblasts. In the second phase (repair phase), IL-10 and IL-4 rich anti-inflammatory environment inhibits osteoclastogenesis and leads to higher bone density. Icariin (Ic) as the bioactive flavonoid compound extracted from the chines herb epimedium is an ancient drug known for modulating MSCs osteogenesis, angiogenesis and anti-inflammatory properties [3]. However, the osteogenic properties of different concentrations of this drug have been studied through MSCs-based in vitro models which are not translatable to in vivo models [4].

Materials and methods

In this study, mesoporous Cu-doped BGNPs (containing 3 and 5% copper) were synthesized using microemulsion modified sol-gel method. In the following, the mesopores were loaded with icariin to provide a local delivery platform. To see the indirect effect of Cu and icariin on osteoimmunogenic performance, an in-vitro model including THP-1 derived macrophage cell line and hMSCs was used. Cytotoxicity and alkaline phosphatase (ALP) activity of loaded and non-loaded nanoparticles in different concentrations was studied to explain the immunomodulatory effect of this novel biomaterial. Cu-free bioactive glass, Cu ions, Cu complex with icariin and hydroxyapatite (HA) nanoparticles were also studied as the controls. For the whole in-vitro study, the released supernatant of the nanoparticles in osteogenic media (complete mem-alpha containing 1 mg/ml dexamethasone) was collected and used.

Results and Discussion

Transmission electron microscopy (TEM) showed the particle size of 102±6 nm for BG sample. The loading efficiency of 32% was estimated using UV-Vis spectroscopy. After indirect incubation of THP-1 derived macrophages, 0.1 mg/ml of loaded and non-loaded nanoparticles was determined as the non-toxic concentration of the nanoparticles. The released icariin also showed a slight improvement in the metabolic activity determined by Alamar blue assay. To compare the osteogenic and osteoimmunogenic properties of the released ions and drug, hMSCs were incubated without and with immune stimulation. Bare nanoparticles could increase the osteoimmunogenesis (ALP activity) due to the released ions such as Ca and Cu (**Figure 1a).** Adding icariin as the drug, the osteogenic properties of the biomaterial increased. However, the osteoimmunogenesis decreased (**Figure 1b)**. This effect can be explained based on the role of inflammation in bone formation. Metal ions can develop the beginning inflammation phase as it was mentioned before [2]. Nevertheless, Icariin as an anti-inflammatory drug inhibits the inflammation phase which can damp the ALP activity.

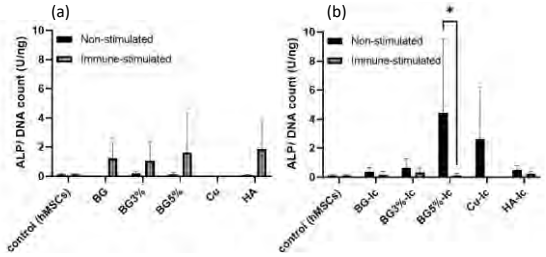

Figure 1- ALP activity after 7 days incubation in non-stimulated and immune-stimulated setups for non-loaded (f) and icariin-loaded (g) nanoparticles (BG: bioactive glass, BGn%: BG doped with n%Cu, BGn%-Ic: BG doped with n%Cu loaded with icariin, Cu-Ic: Cu ions chelated with icariin).

Conclusions

Macrophage containing model used in this study showed that in-vitro models based on MSCs are not able to predict the bioactivity of biomaterials used for bone formation. Although icariin is known as an osteogenic drug, the anti-inflammatory properties of this chemical could interrupt osteogenesis.

References

[1] F. Westhauser, S. Decker, Q. Nawaz, F. Rehder, S. Wilkesmann, A. Moghaddam, E. Kunisch, A. R. Boccaccini, *Materials (Basel).* **2021**, *14*, 1864.

[2] A. J. Lewis, *Agents Actions* **1984**, *15*, 513.

[3] Z. Wang, D. Wang, D. Yang, W. Zhen, J. Zhang, S. Peng, *Osteoporos. Int.* **2018**, *29*, 535.

[4] P. Khokhani, N. R. Rahmani, A. Kok, F. C. Öner, J. Alblas, H. Weinans, M. C. Kruyt, M. Croes, *Materials (Basel).* **2021**, *14*, 1119.

OviChip : 3D in vitro human oviduct model

J. Kim, E. Escarda Castro, K. van Kampen, R. Hoogenboom, L. Moroni, P. Wieringa
Department of Complex Tissue Regeneration, MERLN Institute for Technology-Inspired Regenerative Medicine, Maastricht University, Universiteitssingel 40, 6229 ER Maastricht, The Netherlands

Introduction: The oviduct, also called the fallopian tube in humans, is a conduit shaped tissue connecting ovaries and the upper part of the uterus, providing a passage for sperms and oocytes released from ovaries. The oviduct consists of three parts: isthmus, ampulla and infundibulum. The luminal epithelium of oviduct is composed of ciliated and secretory cells providing a microenvironment, which facilitates the locomotion of oocytes, sperms and embryos [1-2]. Oviduct has been shown its importance on hosting a period of early embryo's epigenetic reprogramming, a process that is susceptible to changes in environmental conditions. Thus, investigations on the fine regulation of oviduct microenvironment have been of great interest as a prerequisite for fertilization, early embryo development and ultimately, successful pregnancy [3-5]. Here, one of major factors disrupting the oviduct microenvironment is infections caused by sexually transmitted Chlamydia trachomatis (CT). This bacterial pathogen triggers fibrotic inflammatory immune responses, recruiting stromal fibroblasts that causes permanent scarring at multiple sites of oviduct. This is a leading cause of tubal factor infertility (TFI), and in turn, high rates of in vitro fertilization (IVF) [4-6].

Despite this crucial role, tubal functions and the impact of tubal inflammation have not been fully elucidated due to ethical limitations in studying the human reproductive system. As a result, in vitro modeling has emerged as alternatives to respond to the demand on the oviduct research [7]. Current oviduct models, however, do not reflect neither the geometry nor essential biology of the native tissue. Most commonly used models are established on 2D monolayer culture with low capability of producing ciliated or secretory cells, or oviduct models based on organoid cultures or air-liquid interface via adopting porous trans-wells, which enhanced the formation of functional epithelial monolayers [8-10]. Nonetheless, these 2D and 2.5D models do not fully imitate the tubular structure of the original organ and in turn, its functions brought by unique geometry of oviduct. Hence, we propose the fabrication of a reproducible and standardized 3D in vitro oviduct model with structural complexity that enables us to recapitulate fibrotic responses observed during tubal inflammation. This abstract presents the first steps towards the development of the channel device.

Materials and methods: A mesoscale fluidic platform reflecting the isthmus structure of oviduct was fabricated by following steps. After bonding a coverslip on the bottom of polydimethylsiloxane (PDMS) device, ø 1mm polyoxazoline filament was fixed within the open middle-chamber of it. Then, hydrogel of interest was added in the chamber embedding the filament and when cross-linked, the device was placed to be cooled below lower critical solution temperature (LCST) triggering filament dissolution and formation of a channel. To check the channel formation and sterilize the inner lumen for further cell culture, 70% ethanol was inject through the channel. Afterwards, cells were seeded by gentle pipetting in the channel and let inner surface covered.

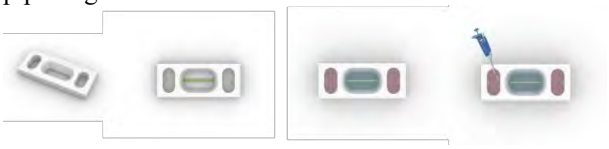

Figure 1. Schematics of channel device fabrication.

Results & Discussions: Our preliminary result showed successful fabrication of a simple channel device with polyoxazoline filament in combination with collagen I or polyacrylamide. Subsequently, we showed the potential of the channel device as a 3D in vitro model with tubular geometry by culturing Caco-2 epithelial cells covering the inner surface of the channel.

Conclusion & Perspective: Here, we have shown the first step towards the development of a channel device to be used for 3D in vitro human oviduct model. Further steps include characterization of oviduct tissues, and formation of organoid to create a concrete cellularized oviduct channel device. In addition, we aim to include hormone gradient to mimic native cell behaviors upon the existence of female steroid hormones. Subsequently, stromal layer components such as fibroblast will be introduced in the hydrogel to address the fibrotic response in stromal environment and its effect on oviduct epithelium observed during induced tubal infection and inflammation.

References:

[1] C. Chumduri & M. Y. Turco, 2021, Journal of molecular medicine, 99(4), 531-553.
[2] H. Ashraf et al., 2018, Mathematical biosciences, 300, 64-75.
[3] S. Pérez-Cerezales et al., 2018, Biology of reproduction, 98(3), 262-276.
[4] P. Ventura-Juncá et al., 2015, Biological research, 48, 68.
[5] U. Besenfelder et al., 2012, Reproduction in domestic animals = Zuchthygiene, 47 Suppl 4, 156-163.
[6] R. M. Johnson, 2004, Infection and immunity, 72(7), 3951-3960.
[7] L. Moroni et al., 2018. Nature reviews. Materials, 3(5), 21-37.
[8] M. Ferraz et al., 2018, Nature communications, 9(1), 4934.
[9] B.E. McQueen et al., 2020, Infection and immunity, 88(9), e00105-20.
[10] M. Ferraz et al., 2017, Annals of Biomedical Engineering, 45, 1731–1744.

Discovery of the Relationship between Biomaterials Properties and Cell Physiology in Implant Related Encapsulation.

Nikita Konshin[1], Jasper Aarts[1], Victor Veenbrink[1], Patricia Dankers[1], Shantanu Singh[2], Jan de Boer[1]

[1] Institute for Complex Molecular Systems & Department of Biomedical Engineering, Eindhoven University of Technology, Eindhoven, The Netherlands
[2] Imaging Platform , Broad Institute, Boston, USA

Introduction

Biomaterials are encapsulated inside a body, where immune cells such as macrophages play crucial role in this process. While it is known material properties affect cells, we don't know Mechanisms of Actions (MoA) that regulate those processes. In order to reveal MoA we aim to use Cell Paint. An approach that correlates the morphological shape of cell body and its organelles to a specific genetic state experienced by a cell. The method is high throughout, originally designed for a robot-laboratory to perform from thousands up to millions of screens via staining up to eight cellular organelles with six dyes cocktail applied simultaneously. Obtained data is aligned into a so-called "perturbation database", containing morphological cellular fingerprints for each of the drug affecting a cell line. The idea of this PhD project is to downscale Cell Paint staining protocol from an automated high throughput core, down to a manual laboratory usage. This would gather an entrance key into the hands of one who desires to use vast amounts of perturbation libraries available at the moment. Novel perspective materials, e.g. ureido-pyrimidinone (UpY) moieties crosslinked with various peptides, will form collaborations for this project.

Experimental design

1. A549 cells are cultured until 80% confluency;
2. Seeded in 96-well plate;
3. Perturbed with small molecules/polymers;
4. Fixed and stained with 6 dyes after 24/48 hours;
5. Imaged with Nikon Ti2 high throughput microscope;
6. Cellular compartments are segmented via Cell Profiler;
7. Data is normalized to a positive/negative control;
8. Database is ready to be aligned against analogous morphological screens with known MoA;
9. *MoA of the investigated substance finally can be revealed and ranked.*

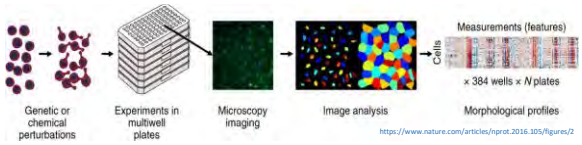

Figure 1. Schematics of the experimental method.

Results

Cell Paint protocol has been modified to be used manually in the laboratory. To illustrate its efficiency, calibration experiment has been carried out with 8 small molecules used to alter regular homeostasis of the cell. Perturbates enforce cells into various states, e.g. slowed proliferation, DYRK1A/B inhibitor, TGF-beta receptor type I/II (TbetaRI/II) dual inhibitor.
Activation/deactivation of various genetical ques resulted in distinct morphologies of affected cells.
Ladder Euclidian distance clustering has showed clear separation between samples.

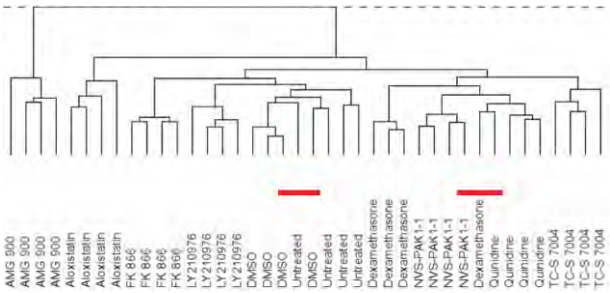

Figure 2. Euclidian distance clustering of the calibration small molecules. (Imperfections highlighted with red lines)

Discussion

The platform is close to be optimized for the discovery purposes. As it can be seen on the ladder cluster, most of the perturbations are distinct from others and cluster away. However, there are some imperfections present. Their cause is most like to be unideal image acquisition, that is responsible for a signal bleedthrough. Considering high precision of the method even at the case when one dye is completely removed, SYTO 14 will be excluded from the master mix. Moreover, it has been shown SYTO 14 causes bleedthrough on 3 channels of our set up. By removing it, we hope to increase precision further and get rid of cluster imperfections.

N. Konshin (n.konshin@tue.nl)

In vitro optimization of extracellular matrix production by primary human mesenchymal cells from fetal and adult dermal skin and eschar tissue

M. Gomes[1,2,3], B. Boekema[2,3], E. Middelkoop [2,3], P. Krijnen[1,2], H. Niessen[1,2]
[1]Amsterdam UMC location AMC / Department of Pathology, Meibergdreef 9 1105AZ Amsterdam, The Netherlands
[2]Amsterdam UMC location VUmc / Department of Plastic, Reconstructive and Hand Surgery, De Boelelaan 1117 1081HVAmsterdam, The Netherlands
[3]Association of Dutch Burn Centers, Zeestraat 27-29 1941AJ Beverwijk, The Netherlands

In contrast to full-thickness wounds in adults, fetal skin wounds in the early developmental stages heal via tissue regeneration and do not result in scar formation. We hypothesize that the microenvironment created by mesenchymal cells (MCs) during wound healing – including newly produced extracellular matrix (ECM) – directs the outcome. Therefore, the comparison of ECM secreted by fetal *vs* adult skin MCs, as well as healthy *vs* wounded skin MCs may identify key aspects shaping wound healing. This study intended to optimize ECM production by three primary human skin MC populations: fetal, adult dermal, and eschar; and provide an initial insight on their ECM differences. CnT-PR-ECM medium and media supplemented with various concentrations of vitamin C (from 0 to 180 µg/ml) were tested. MCs were cultured for 2-3 weeks after cells reached confluency. Initially, expression of ECM-related genes was analyzed by PCR and presence of ECM was monitored macroscopically. CnT-prime-medium did not induce ECM formation by dermal MCs contrary to vitamin C supplemented media. No differences between vitamin C conditions were observed macroscopically and at the RNA-level, revealing no correlation between protein and RNA-level expression. Therefore, ECM production over time was further analyzed at the protein level: macroscopic observation with eosin staining, ECM contraction recording, and soluble/insoluble collagen content measurement using SIRCOL collagen kits. No macroscopic differences were found in ECM amount for 10 and 65 µg/ml of vitamin C, but 180 µg/ml showed enhanced contraction and lower collagen amount produced by fetal MCs. Furthermore, both soluble and insoluble collagens increased over time for fetal and eschar MCs, with an earlier appearance of soluble collagen. Fetal MCs showed the highest collagen secretion, whereas dermal MCs produced the lowest. Since 10 µg/ml of vitamin C better resembles the *in vivo* situation (5 – 15 µg/ml), results support to use this concentration for optimal ECM production by MCs and minimal ECM contraction *in vitro*. Finally, results suggest a higher ECM production by fetal MCs, followed by eschar and, finally, dermal ECMs.

Self-synthesizing materials for tissue culture applications

K. Mikhailov[1,2*], I. Marić[1], L. Yang[2], R. Bron[2], P. van Rijn[2] and S. Otto[1]

[1]Stratingh Institute for Chemistry, University of Groningen, Nijenborgh 4, 9747 AG Groningen, the Netherlands
[2]University Medical Center Groningen, Department of Biomedical Engineering and W. J. Kolff Institute, University of Groningen, Antonius Deusinglaan 1, 9713 AV, Groningen, the Netherlands
*k.mikhailov@rug.nl

Key words: hydrogel, supramolecular chemistry, tissue engineering

Introduction

Peptide-based hydrogels are important materials in cell culture research due to their close resemblance to the extracellular matrices, which allows their utilization as scaffolds for tissue engineering, wound healing and drug delivery[1,2]. In recent years, hydrogels were successfully applied in a wide variety of materials[1,2]. In this work, we report on the creation of cell-compatible self-synthesizing peptide-based hydrogel scaffolds that can be used in tissue culture applications. Cells as a living material would potentially benefit from a material that also displays life-like character in terms of spontaneous emergence of a highly ordered self-assembled supramolecular structure from a complex mixture of simple molecules. Hence, here we combine a new conceptual hydrogel approach as a cell culture platform.

Experimental methods

Oxidation of a peptide building block modified with a thiol-containing moiety at the C-terminus and with a hydrazide moiety at the N-terminus (**1**) results in a dynamic equilibrium of various sized macrocycles upon stirring (Fig. 1).

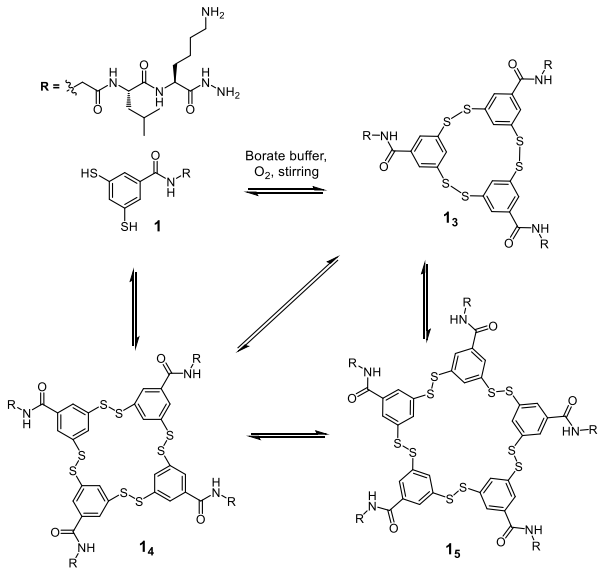

Figure 1. Formation of dynamic combinatorial library

Out of the mixture, only pentamers $\mathbf{1_5}$ stack on each other and form fibers that have hydrazide groups on their surfaces. When the dynamic combinatorial library is dominated by $\mathbf{1_5}$, this network of fibers is cross-linked with a dialdehyde to form a hydrogel. The $\mathbf{1_5}$ fibers can also be modified with aldehyde-containing molecules via the same hydrazone linkage, which opens vast possibilities of hydrogel modifications with bioactive peptides and other moieties.

Results and discussion

These novel, innovative hydrogels were used for cell culture experiments to determine their biocompatibility and cell proliferation. Three types of samples were investigated: unmodified hydrogel ($\mathbf{1_5}$) and hydrogels modified with 10 mol % glyoxylyl-functionalized RGD (**1_5-RGD**) and LDV (**1_5-LDV**) peptides. All hydrogels showed cell viability and good spreading in live/dead staining experiments after 24 hours of culturing (Fig. 2a, b)[3].

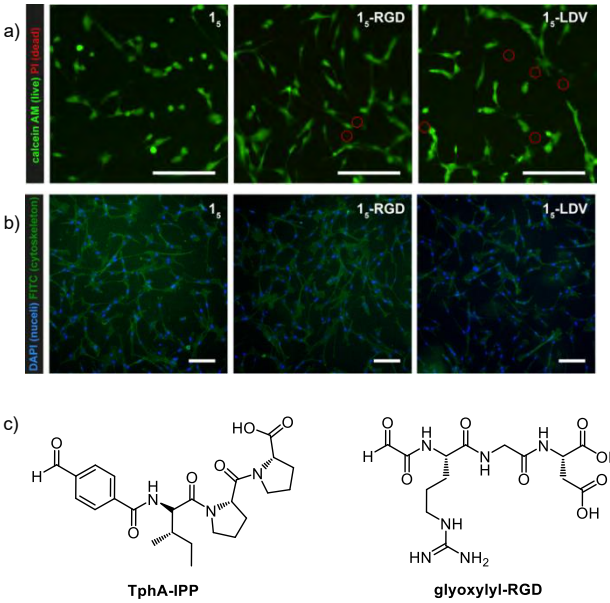

*Figure 2. (a) Live/dead staining with calcein-AM (alive cells, green) and propidium iodide (dead cells, red) of hBM-MSCs of the hydrogel samples after 24 h. (b). DAPI (nuclei, blue) and FITC-phalloidin (cytoskeleton, green) staining, after 24 h. Scale bars equal 150 µm. (c) Chemical structures of **TphA-IPP** and **glyoxylyl-RGD**.*

To evaluate the properties of the modified hydrogel as a biological scaffold, we are currently investigating the process of osteogenic differentiation of Saos-2 osteoblast-like cells and hBM-MSCs. For this purpose, we have synthesized terephthalaldehydic modified IPP peptide (**TphA-IPP**, Figure 2c), which has a positive influence on osteoblast function[4].

Conclusion

Here we show the development of biocompatible and self-synthesizing hydrogel, which can be applied as a tissue engineering scaffold. The osteogenic differentiation studies utilizing these hydrogels as scaffolds are currently in progress.

References

1. X. Ding *et al.*, *Adv. Drug Deliver. Rev.*, **2020**, *160*, 78–104
2. J. Li *et al.*, *Soft Matter*, **2019**, *15*, 1704-1715
3. I. Maric, Unpublished results.
4. M.M. Huttunen *et al.*, *J. Nutr. Biochem.*, **2008**, *19*, 708–715

Cell-instructive and Bactericidal Nanopatterned Meta-biomaterials

K. Modaresifar, L. E. Fratila-Apachitei, A. A. Zadpoor
Department of Biomechanical Engineering, Faculty of Mechanical, Maritime, and Materials Engineering, Delft University of Technology, Mekelweg 2, 2628CD, Delft, The Netherlands

Introduction

High aspect ratio nanostructured surfaces offer a combination of rare properties and functionalities which frame them as meta-biomaterials [1]. Here, reactive ion etching (RIE) was used to fabricate specific types of high aspect ratio nanostructures on Ti surfaces (a relevant choice of material for the fabrication of orthopedic implants) in an attempt to generate surfaces with optimized dual biofunctionality, namely bactericidal and osteogenic properties. The effects of these surfaces (also known as black Ti) on bacterial and mammalian cells and the underlying mechanisms governing the cell response were studied.

EXPERIMENTAL METHODS

A previously described ICP RIE protocol [2] was used to create high aspect ratio nanopillars on titanium surfaces. Ti specimens were etched for 10 min with Cl_2 and Ar gases (flow rates of 30 and 2.5 sccm, respectively) under varying chamber pressures and temperatures. The interactions of S. aureus bacteria, MC3T3-E1 preosteoblasts, and human mesenchymal stem cells with these surfaces were investigated by a variety of biological assays including immunostaining of the focal adhesions, live/dead staining of the bacteria, and measuring metabolic activity of the cells.

To study the role of focal adhesion kinase (FAK), Rho-associated protein kinase (ROCK), and YAP in the regulation of Runx2 as an osteogenic marker in hMSCs when exposed to high aspect ratio nanopillars, each of those factors was inhibited in separate dedicated experiments. 10 µM PF-573228, 10 µM Y-27632, and 10 µM Verteporfin were added to the culture medium upon cell seeding and medium refreshing to inhibit FAK, ROCK, and YAP, respectively. In each condition, Runx2 was stained after 9 days of culture, and quantifications were done similar to the previous part. The statistical analysis was performed using GraphPad Prism v.9.2.0 and a *p*-value below 0.05 was considered to be statistically significant.

RESULTS AND DISCUSSION

The high aspect ratio nanopillars with balanced bactericidal and osteogenic properties had a height between 700 nm and 1 µm with an average aspect ratio of 12.1. These nanopillars could kill the bacteria by penetrating their cell wall. While the high aspect ratio nanopillars did not impair the attachment, survival, and metabolic activity of the cells, they gave rise to a cell morphology that was different from the one observed on the polished flat surfaces. The altered cell morphology was also associated with differences in the organization of the cytoskeleton and the formation of FAs. Our findings showed that the cell nucleus is more elongated and less rounded on the bTi surfaces as compared to the flat Ti which might be linked to the different distribution of FAs. Moreover, the intensities of nuclear YAP and Runx2 were significantly higher in cells residing on bTi surfaces (Figure 1).

The inhibition of both FAK and ROCK significantly altered the morphological characteristics of hMSCs residing on bTi surfaces. These inhibitions were also correlated with a significantly decreased Runx2 signal intensity. These results indicate that the regulation of adhesion and contractility of hMSCs on nanopillars and their subsequent osteogenic marker expression are highly dependent on the activity of FAK and ROCK (Figure 2). The effect of YAP inhibition on cell morphology was not as evident as that of FAK and ROCK but it also resulted in a decrease in Runx2 intensity on bTi surfaces.

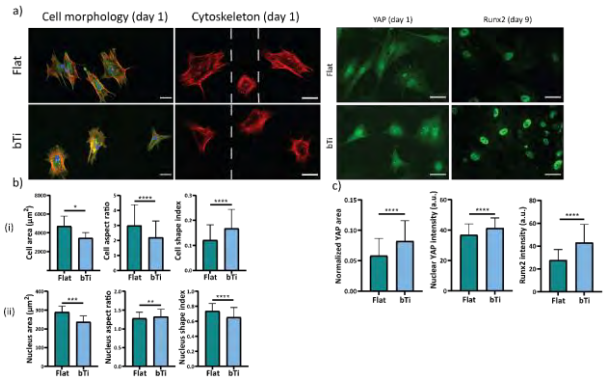

Figure 1

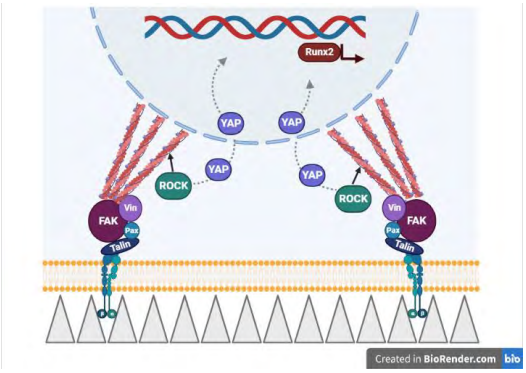

Figure 2

CONCLUSION

High aspect ratio bactericidal bTi nanopillars enhance Runx2 expression in hMSCs by manipulating cell adhesion as regulated by FAK, cell contractility as regulated by ROCK, and the nuclear translocation of transcriptional factors such as YAP.

ACKNOWLEDGMENTS

This research has received funding from European Research Council (Grant no: 677575).

REFERENCES

[1] Higgins S.G. *et al.*, Adv. Mater., 2020
[2] Ganjian M. *et al.*, Sci. Rep., 2019

Functional materials for high resolution 3D bioprinting in kidney engineering

M. Neumann[1], G. Di Marco[1], D. Iudin[1], J. Hak[1], T. Vermonden[1]

[1]Department of Pharmaceutics, Faculty of Science, Utrecht Institute for Pharmaceutical Sciences (UIPS), Utrecht University, 3584 CG, Utrecht, the Netherlands

This project aims at developing new functional biomaterials suitable for high resolution 3D bioprinting. The main focus lies on the reproduction of kidney structures suitable for regenerative medicine purposes but also for disease modeling and drug toxicity studies.
It has been stipulated that the kidney function is highly dependent on the size and shape of the different structures. To enhance the printing resolution and reach physiologically relevant sizes, hydrogel-based bioinks can be printed and subsequently shrunk by means of an external trigger. The shrinking process relies on an increase in the hydrophobicity of the crosslinked polymers inducing a partial water expulsion and thus size reduction.

We developed thermosensitive poly-(N-isopropylacrylamide) PNIPAM-based hydrogels with a reversible shrinking and swelling behavior. Furthermore, we study shrinkable hydrogels based on complexation reactions between a hydrophilic polyionic polymer network (e.g. HAMA) and a solution of polyions of the opposite net charge (e.g. chitosan).
In addition to the shrinking capacity, the printability and hence the mechanical properties are crucial in 3D bioprinting applications. The hydrogels need to combine good mechanical stability and adapted visco-elasticity which is crucial for their cytocompatibility. In order to find the right balance, the use of dynamic covalent bonds as crosslinkers is currently investigated in this project.

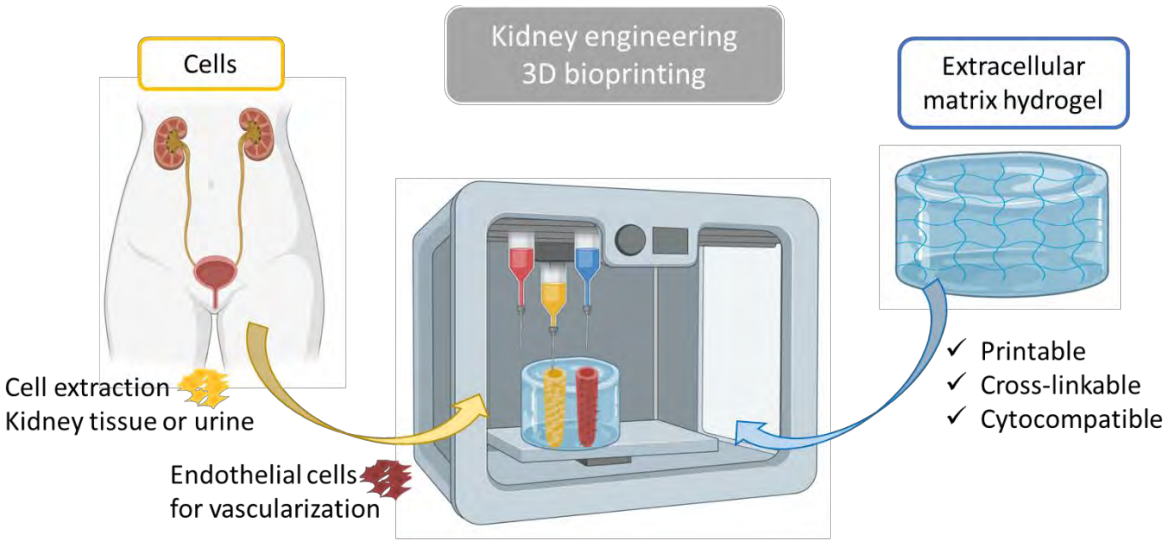

References

[1] Levato, R. et al. Advanced Materials 32, 1906423 (2020).
[2] Najafi, M. et al., In Temperature-Responsive Polymers: Chemistry, Properties, and Applications, Khutoryanskiy, V. V.; Georgiou, K. T., Eds. John Wiley & Sons, pp 1-34 (2018).
[3] Gong, J. et al. Nature Communications 2020 11:1 11, 1–14 (2020).

AI-Based 3D-Printed Multi-Material Mechanical Metamaterials

H. Pahlavani[a*], M. Amani[a], M. Cruz Saldívar[a], J. Zhou[a], M. J. Mirzaali[a], A. A. Zadpoor[a]

[a] Department of Biomechanical Engineering, Faculty of Mechanical, Maritime, and Materials Engineering, Delft University of Technology (TU Delft), Mekelweg 2, 2628 CD, Delft, The Netherlands
* H.pahlavani@tudelft.nl

Nowadays, the emergence of advanced multi-material 3D printing techniques made multi-material mechanical metamaterials of interest to researchers. The spatial distribution of material properties within a lattice structure leads to independent tailoring of elastic properties in different directions (i.e., anisotropic behaviour) and, therefore, is desirable for diverse , especially in the design of medical devices and orthopaedic implants. The initial step to achieving multi-material lattices with desired anisotropic mechanical properties and even rare-event properties (i.e., combining the double-auxeticity with high stiffness values) is to find the specific micro-architectures with the potential to reach the desired properties. Soft and hard phases of material properties are then randomly distributed within the selected structures, and computational models can be used to study the mechanical response of these structures. However, due to the curse of dimensionality, the number of structures that need to be evaluated is so large ($\approx 7.7 \times 10^{43}$) that high-speed models are required to calculate their mechanical properties.

We, therefore, used computational models and artificial intelligence (AI) for ultra-fast prediction of the mechanical properties of multi-material metamaterials, thereby (i) reducing the computational time required for evaluating each design to $\approx 2.4\times10^{-6}$ s and (ii) making the process of evaluating the different designs highly parallelizable. Moreover, we used additive manufacturing techniques for creating these (bio)materials with tailor-made properties. Towards this aim, we selected ten designs to be fabricated using the polyjet multi-material 3D printing technique and mechanically tested them. We used digital image correlation to characterize their behavior under a displacement-controlled tension test. The experimental results showed a good agreement with our simulations and proved that our deep learning-based models are able to accurately predict the mechanical behaviour of the multi-material metamaterials. The presented approach enables the evaluation of $\approx 10^{12}$ designs per month with a mid-range workstation, paving the way for the discovery of multi-material mechanical metamaterials with very rare combinations of anisotropic elastic properties.

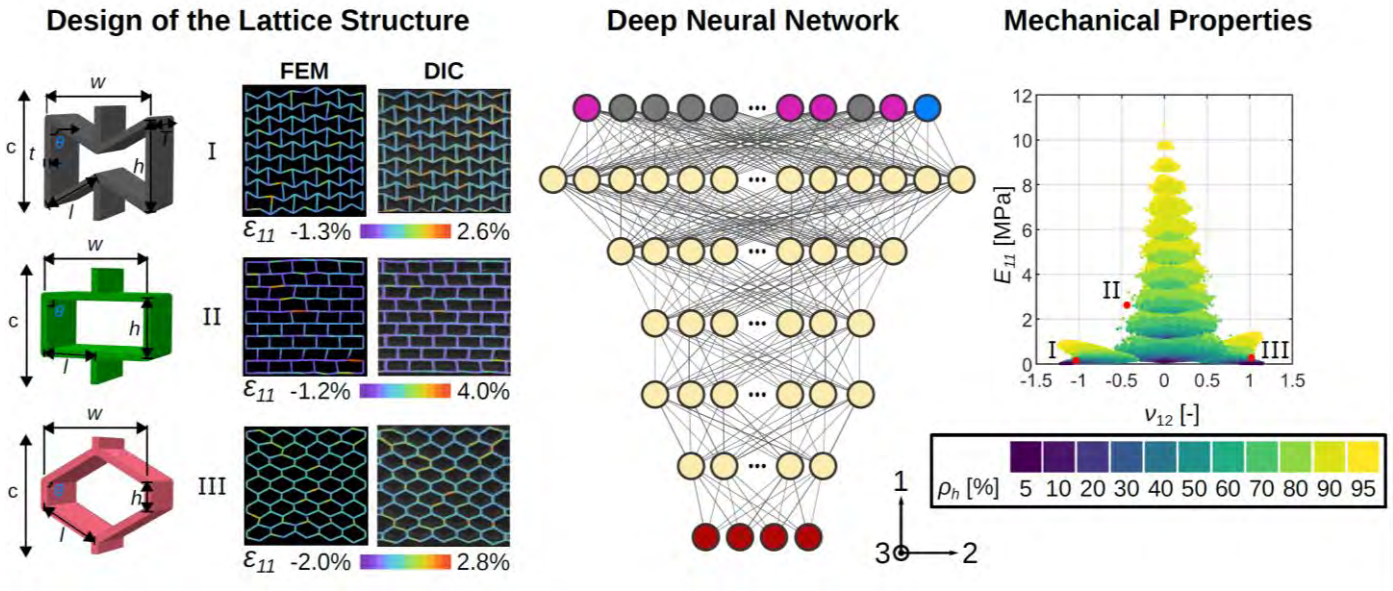

MiRNAs as Potential Regulators of Enthesis Healing in a Rodent Injury Model

C.J. Peniche Silva[1], R.E. De la Vega[1,2], V. Joris[1], C.H. Evans[2], E.R. Balmayor[2,3], M. van Griensven[1,2]
[1]cBITE, MERLN Institute for Technology-Inspired Regenerative Medicine, Maastricht University; Universiteitssingel 40, 6229 ER Maastricht, the Netherlands.
[2]Musculoskeletal Gene Therapy Laboratory, Rehabilitation Medicine Research Center, Mayo Clinic; 221 4th Ave SW, 55905, Rochester, MN, USA.
[3]Experimental Orthopaedics and Trauma Surgery, Department of Orthopaedic, Trauma and Reconstructive Surgery, RWTH Aachen University Hospital; Pauwelsstraße 30, 52074 Aachen, Germany.

Introduction: MicroRNA (miRNAs) are short non-coding RNA sequences with the ability to inhibit the expression of target mRNAs at the post-transcriptional level. Here, we aimed to characterize a rodent enthesis injury model in terms of miRNA expression upon injury. The tendon-to-bone enthesis is a challenging site of injury, and the identification of miRNAs that might play a relevant role in the healing response of the enthesis would increase the understanding of the healing mechanisms of such complex tissue. Additionally, this would unveil a new source of powerful molecular tools to better tune and direct the regenerative process in injured entheses.

Materials and Methods: A longitudinal defect was created in a rat patellar enthesis (n=20) and explants were collected at time points 1 and 10 days after injury (n=10 respectively). MiRNA expression was investigated by a miScript qPCR array specific for fibrosis. Later, mRNA target prediction for the aberrantly expressed miRNAs was performed by Ingenuity Pathway Analysis (IPA) and the expression of those mRNA targets relevant for enthesis healing was assessed by qPCRs. The protein levels of collagens type I, II, III, and X were investigated by western blots and immunostaining at both time points of observation. Safranin O and Alcian blue staining were performed to assess the healing process of the patellar enthesis at both time points. Additionally, *in situ* hybridization experiments (ISH) were performed to specifically localize the tissue-specific distribution of the most strongly deregulated miRNAs.

Results and Discussion: The miScript qPCR array allowed for the identification of miRNAs that were deregulated after the injury. Of those, IPA identified 13 miRNAs (figure 1) with potential mRNA targets relevant for tendon, cartilage, or enthesis healing.

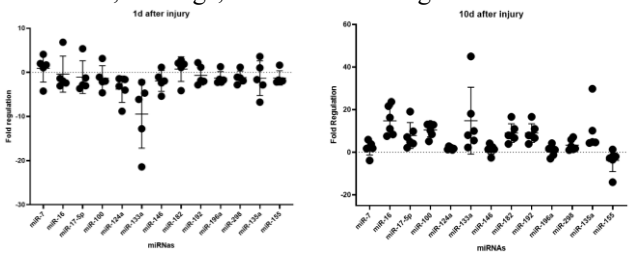

Figure 1: Fold regulation of the expression of the deregulated miRNAs in the injured samples with respect to the native tissue.

Moreover, the qPCRs performed for the mRNA targets revealed that the expression patterns of Egfr1, Col2a1, Runx2, Smad2, and Smad3 (figure 2) were in line with the up- or down-regulation of their respective targeting miRNA, which included miR-16, -17, -100, -124, -133a, -155 and -182.

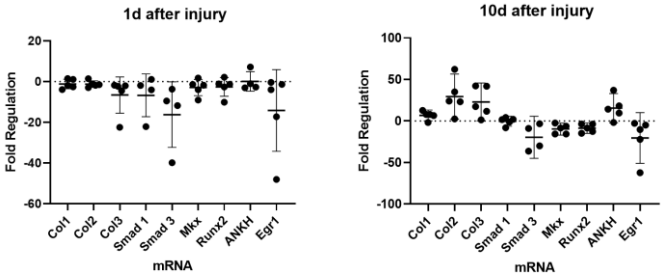

Figure 2: Fold regulation of the expression of the targets mRNAs in the injured samples.

The protein expression of collagen type I and II decreased immediately after the injury and increased back to normal levels after 10 days while the expression of collagen type III and X showed the opposite pattern.

The histological assessment of the injured samples revealed the occurrence of ectopic bone depositions in the tendon portion of the enthesis, and a large area of poorly organized collagen fibers that was absent in the healthy tissue. The ISH demonstrated a strong staining for miRNA-16-5p and miRNA-133a-3p in the fibrotic portion of the injured tendon and the surroundings of the ectopic bone deposition (figure 3), which associates the occurrence of improper healing to the overexpression of such miRNAs.

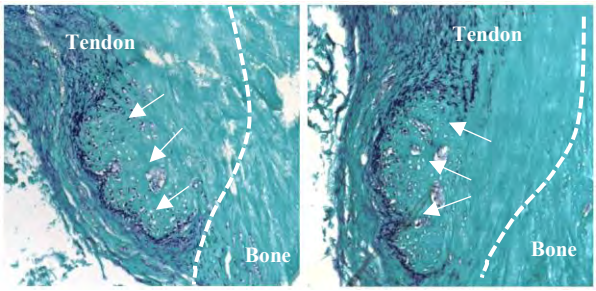

Figure 3: ISH staining for miR-16-5p (left) and miR-133a-3p (right) in the injured patellar enthesis (10 days). Blue=miRNA, Green =counter staining. The arrows indicate the ectopic bone deposition in the tendon area of the enthesis.

Summary: Here we used an *in vivo* injury model to investigate the possible roles of miRNAs in the early healing response of the patellar enthesis. We have identified at least 13 miRNAs that are deregulated at time points 1 day and 10 days after injury. Future studies could explore the therapeutic potential of such miRNAs to tune the expression of their mRNA targets and improve the regeneration of injured entheses.

Acknowledgment: This work was supported by the Province of Limburg, Limburg Invests in its Knowledge Economy (LINK) and the ON Kick Starter Grant (p.n 20-105). Prof. Evans' research is partly funded by the John and Posy Krehbiel Professorship in Orthopedics.

In vitro and *in silico* Analysis of *Staphylococcus epidermidis* Extracellular Polymeric Tethers: Viscoelastic Failure and Adaptability to Increasing Shear Stress During Adhesion

BW Peterson[1], F da Silva[1,3], J Sjollema[1], CL Hall[2], H Kaper[1], ED de Jong[1], HC van der Mei[1], HJ Busscher[1]
[1]University of Groningen and University Medical Center Groningen, Department of Biomedical Engineering (FB-40), P.O. Box 196, 9700 AD Groningen, the Netherlands
[2]Department of Biomedical Engineering, The College of New Jersey, Armstrong Hall, Room 181, P.O. Box 7718, The College of New Jersey, Ewing, NJ, 08628, USA.
3 Department of Bioengineering, University of Porto, Rua Dr. Roberto Frias, s/n, 4200-465 Porto, Portugal
Email: b.w.peterson@umcg.nl

Introduction: Biomaterials have a common enemy: bacterial adhesion. Bacterial adhesion has been extensively described in phyisco-chemical terms with interactions between a variety of surfaces. However, most of these interactions are described from the variation of surfaces, without regards to the ability of bacteria to produce extracellular polymers or adapt to their environments. In this study, the second partner of bacterial adhesion interface, namely the bacteria, is modified, and the adhesion properties are measured and modelled to better understand how bacteria adapt to their physical environments.

Materials and Methods: *Staphylococcus epidermidis* ATCC 35983, a producer of extracellular polymeric material (called "tethers" when utilized for adhesion) was cultured from a frozen stock and harvested concentrated phosphate buffer. The bacterial suspension was treated with DNaseI, N-acetyl-L-cysteine (NAC) or their combination to cut or dissolve the extracellular polymers surrounding the bacterial cell.

Bacteria were allowed to adhere to a glass slide in a parallel plate flow chamber in dilute phosphate buffer (static to 50 s^{-1} wall shear stress) until adhesion reached 4 x 10^6 cm^{-2}. Wall shear stress was arrested for 15 min, and the bacterial centre of mass was captured for 40 s (2000 frames at 50 fps) using a phase contrast microscope and home-made mapping software (MATLAB).

Bacterial movement was analysed to obtain the mean squared displacement (MSD), spring constant, and diffusion coefficient. The experimentally determined spring constant and tether length for static adhesion were used as inputs for the *in silico* tether modelling system (Labview). Tether rupture distance and number of starting tethers were changed to obtain, *in silico*, the experimental MSD and diffusion coefficient.

Results and Discussion: Bacterial movement on the surface was greatly reduced when exposure to increased wall shear stress during adhesion (Fig. 1).

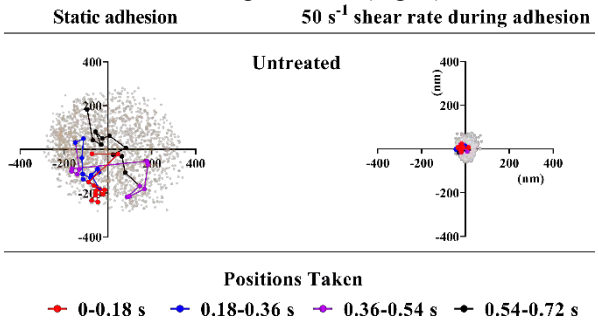

Fig. 1 Examples of time-resolved position-map of *S. epidermidis* ATCC 35983.

However, the reduction was not gradual, but occurred in a narrow range of shear stress, indicative of a viscoelastic failure event. This was found comparing the spring constants against wall shear stress for all four treatments but occurred at a higher shear stress (29 and 36 s^{-1}) when DNaseI was present than when it was absent (13 and 15 s^{-1}). For the diffusion coefficient, only bacteria treated with NAC were able to have their transitions be successfully modelled (7 and 15 s^{-1}). The untreated staphylococci had the smallest change in diffusion coefficient and spring constant across the entire tested shear stress spectrum (Fig. 2).

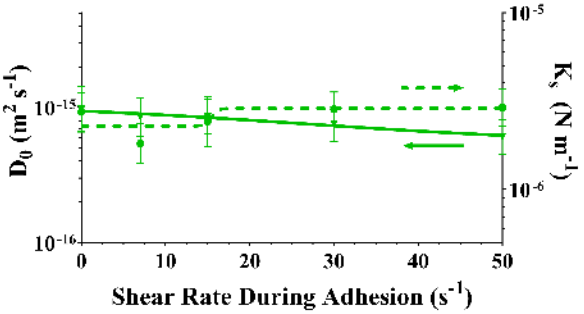

Fig. 2 Diffusion coefficients (solid, left axis) and spring constants (dashed, right axis) as a function of shear rate during adhesion of untreated *S. epidermidis* ATCC 35983. Regression curves were created by an EC50 analysis.

The spring constant and tether length were used as inputs into the *in silico* model, and the output of the model diffusion coefficient and MSD were matched to the experimental model. The rupture distance was negatively correlated with the spring constant, while NAC treated bacteria (including combination) had the most remaining attached tethers, having 28 attached tethers.

Differences in spring constants, diffusion coefficients, tether rupture distance, number of tethers, and MSD (both *in vitro* and *in silico*) were used to determine how the extracellular polymers of *S. epidermidis* ATCC 35983 provide a means to adapt to their physical environment for survival.

Conclusions: The extracellular polymeric tethers of *S. epidermidis* ATCC 35983 have an integrated effect on the adaptability to the surrounding physical environment during adhesion. The relatively small differences in physical properties makes it easier for the bacteria to naturally adapt to the environment by making small changes in its exterior tethers, thus promoting survival.

A Co-Culture Model For Innervation In Bone Regeneration Using NGF cmRNA

C. Polain[1], M. Haartmans[2], R. Mohren[2], F. Poulhes[3], E. Bonvin[3], C. Plank[4], B. Cillero Pastor[1], M. van Griensven[1,5], E. R. Balmayor[5,6]

[1]cBITE Department, MERLN Institute, Maastricht University, Maastricht, the Netherlands,[2]M4I, Maastricht University, Maastricht, the Netherlands,[3]OZ Biosciences SAS, Marseille, France,[4]Ethris GmbH, Planegg, Germany,[5] Musculoskeletal Gene Therapy Laboratory, Rehabilitation Medicine Research Center, Mayo Clinic, Rochester, MN, USA,[6] Experimental Orthopaedics and Trauma Surgery, Department of Orthopaedic, Trauma, and Reconstructive Surgery, RWTH Aachen University Hospital, Aachen, Germany

Introduction

Bone tissue engineering efforts have progressed vastly in regenerative medicine in the past few decades. Besides bone tissue, blood vessels and nerve fibers are distributed throughout the skeletal tissue. They are crucial for bone development and repair as they supply oxygen, nutrients, and cells. While vascularization has been considered in many investigations, efforts regarding innervation for bone regeneration have been poor. The exact role of innervation in bone regeneration and healing remains unclear. In a mature skeleton, innervation is responsible for sensing of pain and other sensory stimuli, however, the nervous system also plays an important role in bone by regulating bone homeostasis, bone formation, and bone resorption. To stimulate innervation *in vitro*, nerve growth factor (NGF) is often used. This molecule is known to induce axonal outgrowth of neuronal cells. However, NGF like other growth factors is known to have several disadvantages, such as the overstimulation of pathways due to the use of supraphysiological amounts. Gene and transcript therapies have been proposed as alternatives. Transcript therapy is based on the administration of a protein-coding mRNA to induce *in situ* protein production by the cells. As native mRNA is unstable and immunogenic, chemical modifications to mRNA (cmRNA) increase its stability and biocompatibility.

In this research we propose a model for inducing innervation during bone regeneration using a co-culture of NGF cmRNA-transfected hMSCs and PC-12 (Adrenal pheochromocytoma-derived) cells. The aim is to induce differentiation of PC-12 cells to the neuronal phenotype.

Materials and Methods

Transfection of PC-12 cells

PC-12 cells were cultured on 12 mm coverslips using 5 x 10^4 cells. The coverslips were previously coated with 2 ng/mL laminin and 10 ng/mL poly-D-lysine (PDL), and thereafter placed in 24-wells plates. Adherent PC-12 cells were transfected with either 15 or 20 pg NGF cmRNA/cell using two different lipid vectors: Lipofectamine Messenger Max (Invitrogen, cmRNA:lipid ratio of 1:1) and NL37 (OZBioscience, cmRNA:lipid ratio of 1:4). As a positive control, cells were stimulated with 50 ng/mL rhNGF (Sigma Aldrich). Untransfected cells were used as a negative control. Upon stimulation with NGF, PC-12 cells are expected to differentiate to a neuronal phenotype and develop neurites. PC-12 were fixed with 4% paraformaldehyde (PFA) 1, 2, 3, 5, and 7 days after transfection and stained with Phalloidin and anti-β-3-Tubulin and imaged. Neurite length was measured. Supernatant was collected for NGF determinations by ELISA.

Co-culture of transfected hMSCs and PC-12 cells

1. Functional assessment

For co-culture, 2.5 x 10^5 PC-12 cells were seeded, at the bottom of 24-wells plates on a laminin and PDL coated coverslip. hMSCs were transfected in suspension using several cmRNA concentrations, namely 15.6 pg/cell, 31.25 pg/cell, 62.5 pg/cell, and 1 pg/cell. Subsequently, transfected hMSCs were plated into the transwell (Corning) at a density of 2.4 x 10^4 cells/cm^2. After observation times of 1, 2, 3, 5, and 7 days were reached, PC-12 cells were fixed with 4% PFA and stained with Phalloidin and anti-β-3-Tubulin and imaged. Neurite length was measured. Supernatant was collected for NGF determination by ELISA.

2. Secretome analysis

A transwell system was used as described before, but upscaled to a 6-wells plate. For this, 2.1 x 10^5 PC-12 cells were seeded on a 32 mm coverslip. hMSCs were transfected in suspension using 31.2 pg/cell NGF cmRNA and Lipofectamine Messenger Max as a transfection agent, and thereafter plated using 2.4 x 10^4 cells/cm^2 in CellQArt transwell. Supernatants were collected at 3 and 7 days after co-culture. Liquid Chromagraphy Mass Spectrometry (LC-MS) was performed to analyse the secretome of the co-culture. Single cultures were used as control.

Results and Discussion

Transfection of PC-12 cells with NGF cmRNA was most optimal when using 15 pg cmRNA/cell complexed with Lipofectamine Messenger Max as confirmed by ELISA. When using this concentration, the PC-12 cells were able to differentiate and form neurites, which proves the functionality of the produced NGF. The obtained results were comparable to the use of recombinant NGF protein. In co-culture using transwells, hMSCs transfected with NGF cmRNA successfully produced NGF. The optimal concentration and lipid vector was 31.25 pg cmRNA/cell and Lipofectamine Messenger Max in a 1:1 cmRNA:lipid ratio. The secreted NGF was able to differentiate PC-12 cells into a neuronal phenotype. LC-MS analysis revealed that the secretome consisted of around 1500 proteins, including several neuronal markers. Future investigations include proteomics on cell lysates and pathway analysis

Conclusions / Summary

We can conclude that NGF cmRNA was successful in inducing functional NGF protein production in PC-12 and hMSCs. Produced NGF upon transfection was able to induce differentiation of PC-12 cells into the neuronal phenotype and the presence of sprouting neurites was detected. LC-MS analysis indicated the involvement of neurogenic pathways through neuronal markers, yet this needs to be investigated further.

Acknowledgments

This work has been performed under the scope of the cmRNAbone project and has received funding from the European Union's Horizon 2020 research and innovation programme under the Grant Agreement No 874790.

Novel antimicrobial release coating using SAAP-148 to combat biomaterial-associated infection

Deeksha Rajkumar, Payal P.S. Balraadjsing, Martijn Riool, Sebastian A.J. Zaat

Department of Medical Microbiology & Infection Prevention, Amsterdam Institute for Infection and Immunity, Amsterdam UMC, University of Amsterdam, Meibergdreef 9, 1105 AZ Amsterdam, The Netherlands.

d.rajkumar@amsterdamumc.nl

The use of biomaterials carries a significant risk of medical device (biomaterial)-associated infections (BAIs). Staphylococci are mostly responsible for these infections. Generally, these infections are difficult to treat due to tolerance or resistance to antibiotics. Biofilm formation on the implant surface contributes to phenotypic tolerance, and possibly to antimicrobial resistance (AMR) and persistent infection. The bacteria can also survive intracellularly in peri-implant tissue, increasing their resistance to antibiotic treatment. As many antibiotics are incapable of eliminating bacteria in biofilms on the implant surface and in peri-implant tissue, it is imperative to develop and validate alternative antimicrobial technologies. These technologies should additionally enhance the efficacy of current antibiotics allowing combination therapy. In this study, we will develop a novel non-antibiotic antimicrobial release coating using Synthetic Antimicrobial and Antibiofilm Peptide 148 (SAAP-148). By combining SAAP-148 with a polymer coating on titanium bone implants, we intent to prevent infections on implant surface as well as peri-implant tissue. We will assess the potency of this novel antimicrobial coating by testing the release kinetics profile, antimicrobial efficacy and cytotoxicity *in vitro*. Ultimately, this novel antimicrobial coating might contribute to safer medical devices and lower the risks of antibiotic resistance.

Development of nanogels for crossing of the blood-brain barrier and penetration into glioblastoma spheroids

[1]L. Ribovski, [1]P. Schaafsma, [1]I.S. Zuhorn
[1.] Department of Biomedical Engineering, University of Groningen, University Medical Center Groningen, A. Deusinglaan 1, 9713 AV, Groningen, the Netherlands
e-mail:l.ribovski@umcg.nl

Introduction

Cancer resistance to treatment is not only caused by genetic factors and cellular mechanisms but also the ability of the therapeutic to penetrate the tumor. Nanotherapeutics may improve tumor penetration, and at the same time protect the loaded drugs from degradation, thereby improving treatment efficacy. Nanoparticle (NP) physicochemical properties determine if NPs penetrate to the core of the tumor tissue, and modulating these properties can maximize infiltration.[1]
Here, we investigate the ability of a library of polymeric nanogels (NGs) of different stiffnesses and sizes to penetrate into glioblastoma neurospheroids. The NGs are hydrogel-like soft NPs in which hydrophilic polymers are chemically crosslinked, while the cross-linker density provides control over NG stiffness. A parallel investigation on the NGs efficiency to cross the blood-brain barrier allows to select for the most suitable properties to face each biological barrier, i.e., BBB and tumor microenvironment, and further tune NPs properties accordingly.

Materials and Methods

Poly(N-isopropylmethacrylamide) (pNIPMAM) nanogels are prepared by precipitation polymerization in the presence of surfactant.[2] Both reaction time and surfactant concentration are used to control NG size and dispersity. NG stiffness is varied using different amounts of cross-linker during the polymerization reaction, with higher cross-linker density leading to stiffer NGs.
Neurospheroids are prepared using GSC23 glioblastoma stem cells (GSCs). GSC spheroids are formed in microwells of 1 mm in diameter for 72 hours, which gives control over size and shape of the spheroids. To assess NG penetration into GSC spheroids we employ confocal imaging to observe the tumor accumulation of fluorescently-labelled NGs. We analyze how far into the center of the spheroids the NGs are distributed.

Results and Discussion

Preliminary results indicate that both stiffness and size play an important role in tumor penetration, where higher stiffness and smaller size improve penetration depth, but larger size favors accumulation. For now, the results are restricted to NGs in the range of 200 to 450 nm in diameter, but we are expanding the library to allow for a better correlation.

Conclusions

Nanogel penetration into GSC spheroids is dependent on its physicochemical properties. These properties may be optimized in order to reach improved tumor accumulation and distribution, and ultimately better treatment efficacy.

Acknowledgements

This work is part of the project Shape-Shifting Nanoparticles for Drug Delivery to the Brain: an Integrative Approach to Targeted Drug Delivery (18683) of the research programme Innovational Research Incentives Scheme (Vici) which is (partly) financed by the Dutch Research Council (NWO). We thank M.A Reina Mahecha for the support on the microwells preparation.

References

1. Tchoryk, A. *et al.* Penetration and Uptake of Nanoparticles in 3D Tumor Spheroids. *Bioconjug. Chem.* **30**, 1371–1384 (2019).

2. Ribovski, L. *et al.* Low nanogel stiffness favors nanogel transcytosis across an in vitro blood–brain barrier. *Nanomedicine Nanotechnology, Biol. Med.* **34**, 102377 (2021).

Synthetic supramolecular hydrogels to steer the polarity of kidney epithelial cells and intestinal organoids in 3D

L Rijns[1], M.J. Hagelaars[1], J.A.P.M. Wijnakker[2], W. de Lau[2], J.W. Peeters[4], H.M. Janssen[4], S. Loerakker[1], H. Clevers[2,3], C.V.C. Bouten[1], P.Y.W. Dankers[1]

[1] Department of Biomedical Engineering, Laboratory for Cell and Tissue Engineering, Eindhoven University of Technology, the Netherlands [2] Hubrecht Institute, University Medical Center (UMC) Utrecht, the Netherlands, [3] Roche, Switzerland, [4] SyMO-Chem B.V., Eindhoven University of Technology, the Netherlands

Introduction: An abundant and important receptor that regulates numerous ECM-cell interactions is the integrin receptor. To illustrate, integrins influence the cells' polarity by controlling the apical-basal orientation. Kidney epithelial cells and intestinal organoids cultured in suspension and thus in the absence of matrix, invert their polarization, with an apical membrane pointing outwards. To better understand the mechanisms underlying cellular polarity, we investigate if the matrix' stiffness and degree of bioactivity could influence the orientation of polarization, thereby steering epithelial morphogenesis and controlling organoid behavior.

To do so, we use synthetic, supramolecular hydrogels based on the ureido-pyrimidinone (UPy) motif, which uses directional, non-covalent interactions. These assemblies are eminently suitable to study cell-material interactions, as herein we have full and independent control over several different properties, like stiffness and ligand concentration, allowing that the effects of such microenvironment components can be assessed individually. The UPy hydrogels consist of 3 molecules: monofunctional (**M**), bifunctional (**B**) and bioactive (**cRGD**) UPys (Figure 1). Herein, the **M-UPys** can form one-dimensional fibers, while the **B-UPys** could act as a crosslinker between the **M-UPys** to create a network with adjustable mechanical properties, by changing the M/B UPy ratio or by varying the hydrogel's concentration. And finally, **UPy-cRGDs** are mixed in as integrin-binding ligands.

In this work, we investigate the influence of stiffness and degree of bioactivity on the polarity of renal epithelial cells and intestinal organoids in 3D using UPy supramolecular hydrogels.

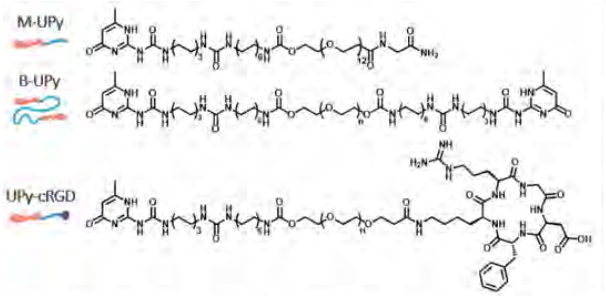

Figure 1: Molecular design of UPy supramolecular hydrogel, consisting of **M-UPy, B-UPy** and **UPy-cRGD** molecules. Throughout all conditions, a fixed molecular ratio of 80/1 = M/B (mol) is used. For B type molecules, a PEG chain with 10 kDa (n~227) is used.

Materials and Methods: UPy supramolecular hydrogels were prepared in a fixed molecular ratio of 80 **M** to 1 **B** molecules at the desired concentration (w/v%). For cell studies in 3D, **UPy-cRGD** molecules are incorporated into the hydrogels as part of the M-type molecules. Rheological experiments were measured at 1 rad/s and 1% strain.

Results and Discussion: Madin Darby Canine Kidney (MDCKs) were cultured inside UPy hydrogels with different hydrogel concentrations, i.e. 0.6, 1.25 and 2.5 w/v%, corresponding with a bulk stiffness (i.e. G') of ~ 0.1, 1 and 2 kPa, respectively, and different ligand concentrations, i.e. 0, 0.5 and 2 mM **UPy-cRGD**. After 10 days of culture, different 3D epithelial structures were formed and classified in to three regimes: cell aggregates with inverted polarity (no lumen), polarized structures with multiple lumens (multi lumen) and well-polarized cysts with a central lumen (single lumen). In general, we observe an increased number of polarized structures for increased gel concentrations (i.e. stiffness) as well as for increasing ligand concentrations. Zooming in, for the 0.6 w/v% gels with the lowest bulk stiffness, we find the highest prevalence of cell aggregates with inverted polarization, dominated by cell-cell interactions. Increasing the ligand concentration can slightly shift this to more polarized structures with either a multi lumen or central lumen. In contrast, for the stiffer, 2.5 w/v% gels, well-polarized cysts are predominantly formed, dominated by cell-matrix interactions. Varying the ligand concentration here substantiates the relevance of adhesive ligands, as only cell aggregates are observed in the 2.5 w/v% hydrogels with 0 mM **UPy-cRGD**.

Conclusions: In general, we observe an increased number of polarized structures for increased gel concentrations (i.e. stiffness) as well as for increasing ligand concentrations. In more detail, cells cultured in gels with the lowest bulk stiffness result in a high frequency of cell aggregates with inverted polarization, dominated by cell-cell interactions. However, cells cultured in the stiffer gels result in the formation of well-polarized cysts, now dominated by cell-matrix interactions. Changing the ligand concentration here substantiates the relevance of adhesive ligands, as only cellular aggregates are observed in absence of ligands. In summary, our results indicate that stiffness and ligand concentration dictate epithelial polarization synergistically. Currently, we are investigating the influence of stiffness (i.e. different w/v% UPy gels) and bioactivity (i.e. UPy conjugated to small peptides and larger proteins) on the growth and polarity of intestinal organoids, in close collaboration with Joost Wijnakker, Wim de Lau and Hans Clevers.

Assessment of cytotoxicity of antimicrobial peptides LL-37 and SAAP-148 for orthopaedic applications

M. Salandova, M. Klimopoulou, L.E. Fratila-Apachitei, I. Apachitei, A. Zadpoor
Delft University of Technology, Department of Biomechanical Engineering, Mekelweg 2 2628 CD Delft, The Netherlands

Introduction:

Implant-associated infection (IAI) is still one of the leading causes of implant failure, affecting approximately 2% of patients undergoing primary total hip arthroplasty (Karachalios *et al.*, 2018). Once developed, mature bacterial biofilms present a major treatment challenge to clinicians, often requiring surgical debridement and revision surgery alongside systemic administration of antibiotics. Due to the use of antibiotics in the treatment of IAI and the speed with which bacterial strains acquire resistance towards antibiotics, we may be on the road towards a relatively grim future, unless we prepare and equip ourselves with new antimicrobial solutions.

Antimicrobial peptides (AMPs) are a recognized alternative to antibiotics due to their selectivity for bacterial membrane driven by their cationic character (Omardien *et al.,* 2018). They represent the first line of defence in humans and manifest lower propensity towards development of antimicrobial resistance (AMR) in comparison to traditional antibiotics. Therefore, the incorporation of AMPs into the surface of orthopaedic implants and the control of their release kinetics represent a novel approach to address the IAIs while overcoming the AMR.

To this end, the aim of this study was to compare the natural peptide LL-37 and its synthetic analogue SAAP-148 regarding their cytotoxicity for bone-like and immune cells.

Materials and Methods:

Mouse macrophages (J774.A1) and preosteoblasts (MC3T3-E1) were cultured with different concentrations of peptides LL-37 and SAAP-148 over a period of 1-7 days. The cell response was evaluated by Presto Blue assay and live/dead staining.

Results and Discussion:

Cytotoxicity of LL-37 and SAAP towards preosteoblasts was detected at concentrations > 4.0 µM (Fig. 1A). Macrophages tolerated the LL-37 peptide up to 10 µM while SAAP-148 was tolerated only up to 4.0 µM (Fig. 1B). The findings are in line with the available literature (Bankell *et al.*, 2021), although our study indicated that SAAP-148 is more cytotoxic than LL-37.

The non-cytotoxic levels of both peptides were well above the reported minimal bactericidal concentration (MBC), which is between 1-2 µM (*in vitro*) (De Breij *et al*., 2018).

Summary:

In this study, we have compared the LL-37 and SAAP-148 antimicrobial peptides regarding their cytotoxicity to mouse macrophages and preosteoblasts. Both type of cells showed very good viabilities at levels exceeding the MBC concentrations of the two peptides. Therefore, these peptides represent good candidates for new antimicrobial solutions in orthopaedic applications.

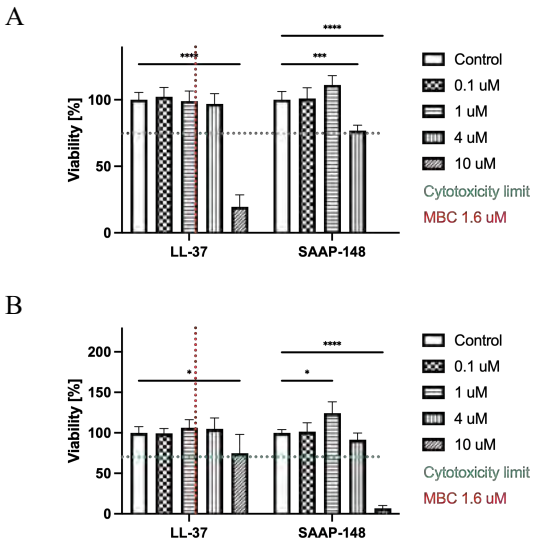

Figure 1. *Viability of (A) preosteoblasts (MC3T3-E1) and (B) macrophages (J774.A1) cultured with LL-37 and SAAP-148 peptides for 3 days.*

Acknowledgement:

This publication is part of the project DARTBAC (with project number NWA.1292.19.354 of the research programme NWA-ORC which is (partly) financed by the Dutch Research Council (NWO).

References:

Bankell et al. (2021). LL-37-induced caspase-independent apoptosis is associated with plasma membrane permeabilization in human osteoblast-like cells. *Peptides*, *135*(June 2020), 15–19. https://doi.org/10.1016/j.peptides.2020.170432

De Breij et al. (2018). The antimicrobial peptide SAAP-148 combats drug-resistant bacteria and biofilms. *Science Translational Medicine*, *10*(423). https://doi.org/10.1126/scitranslmed.aan4044

Karachalios et al. (2018). Total hip arthroplasty: Survival and modes of failure. *EFORT Open Reviews*, *3*(5), 232–239. https://doi.org/10.1302/2058-5241.3.170068

Omardien et al. (2018). Synthetic antimicrobial peptides delocalize membrane bound proteins thereby inducing a cell envelope stress response. *Biochimica et Biophysica Acta - Biomembranes*, *1860*(11), 2416–2427. https://doi.org/10.1016/j.bbamem.2018.06.005

Bioengineering a Modular, Immunoprotective, and Microporous Mini-Pancreas for Type 1 Diabetes

M.R. Schot[1], N. Araújo-Gomes[1], P. Blokzijl[1], B. Zoetebier-Liszka[1], J. Leijten[1]
[1]*Leijten Lab, Department of Developmental BioEngineering, TechMed Centre, University of Twente, The Netherlands*

Introduction: Type 1 diabetes is an autoimmune disease in which the insulin producing pancreatic β-cells are destroyed by the body, which leads to unregulated blood glucose levels. Typical temporary, symptomatic, and invasive treatments exist in the form of regular insulin injections. More permanent solutions such as pancreas transplantation are unable to meet clinical demand as type 1 diabetes affects over 9 million patients, and its prevalence is expected to progressively increase in the future.[1,2] More recently, transplantation of the pancreas' insulin producing cells named β-cells has emerged as a promising treatment. However, the success of this emerging treatment is still hindered by immunological transplant rejection.[3] To prevent islet transplant rejection, we aim to engineer immunoprotected mini-pancreases composed of β-cells that were microfluidically encapsulated in immunoprotective micrometer-sized hydrogels named microgels. Moreover, enzymatic annealing of the microgels allowed for the engineering of macro-sized living matter with an open, highly dense, and interconnected internal pore network resembling the native tissues capillary network, which could be achieved in a highly scalable manner. Advantageously, this yielded an immunoprotective, easily handleable, and safely retrievable miniature pancreas with vastly improved diffusion limitations as compared to classical bulk hydrogel implants (figure 1).

Methods: To generate immunoprotective microgels, a microfluidic droplet generator was used in flow focus mode in which tyramine conjugated polyethyleneglycol (PEG-TA) containing cells was flown as the dispersed phase and 3% span80 in n-hexadecane as a continuous phase. After emulsification, PEG-TA was crosslinked downstream in an outside-in manner using cytocompatible levels of hydrogen peroxide and horseradish peroxidase. This robustly and reproducibly generated core-shell microgels (figure 2A) in high throughput (524 Hz). Microgels were demonstrated to possess immunoprotective properties as shown by the inability of fluorescently labelled IgG antibodies to penetrate into the microgels. Importantly, molecules such as glucose and insulin are substantially smaller than antibodies, and were proven able to readily diffuse through the microgels (figure 2B). Microgels can be annealed into microporous annealed particle networks (MAPs) by densely packing microgels into a mold followed by crosslinking of the residual tyramine groups using ruthenium, sodium persulfate, and visible light, resulting in a highly permeable microporous construct (figure 2C).

Results: Functional microtissues were produced by encapsulating the cells of the insulin producing β-cell line MIN6 within the hollow core of the microgel at a high level of viability (figure 2C). Microencapsulated cells were able to rapidly aggregate and form glucose responsive cellular spheroids within the hollow microgels, which remained functional for at least 30 days (figure 2D). Spheroid functionality was showcased by immunofluorescent staining of glucagon and insulin (figure 2E). Finally, these immunoprotected microtissues can be crosslinked into a MAP using the aforementioned visible light crosslinking system while maintaining high viability (figure 2C).

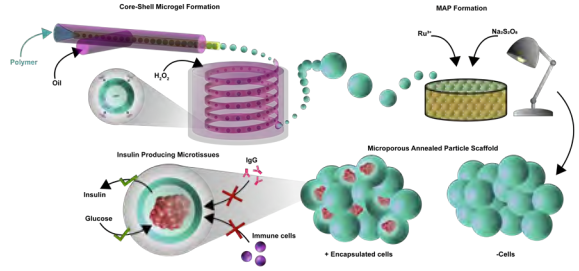

Figure 1. Schematic representation of the experimental workflow. Microgels are produced using a flow focusing microfluidic droplet generator combined with an inside-out crosslinking method to enable the microfabrication of core-shell microgels. Microgels can be annealed together using a visible-light based crosslinker to obtain microporous annealed particle scaffolds (MAPs). The generated cell-laden microgels or MAPs are semi-permeable, resulting in an immunoprotective microenvironment for encapsulated cells.

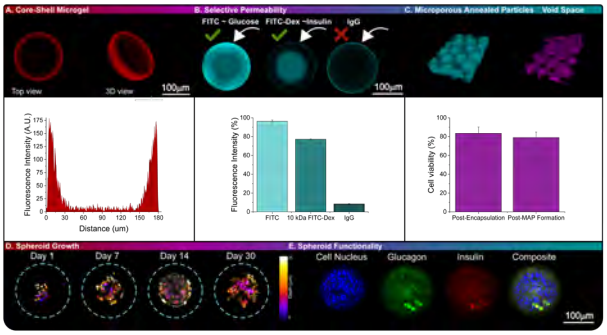

Figure 2. A. Top-down and 3D view of core-shell microgel. Core/shell size is quantified in the graph below. **B.** Selectivity of the microgels is tested using various compounds. FITC and FITC-DEX 10kDa (chosen as approximate size equivalent substitutes for glucose and insulin, respectively) readily diffuse through the microgel shell, while IgG is blocked. **C.** Microgels were annealed into microporous annealed particle scaffolds. The graph below shows the cell viability post-encapsulation and post MAP formation. **D.** Spheroid growth over time (DAPI signal translated into a depth-chart). **E.** Spheroids remained functional after a 30 day culture period as indicated by positive immunofluorescence signals for glucagon and insulin.

Conclusion

Here we present a bottom-up bioengineered, modular mini pancreas through the covalent bonding of encapsulated, immunoprotected microtissues. Currently, we are testing the in vitro and in vivo functionality of the mini pancreas as a treatment for type 1 diabetes.

Acknowledgements:

Financial support was received from the European Research Council (ERC, Starting Grant, #759425).

Bibliography:

1 Green, A. *et al. Diabetologia,* 64.12, 2741-2750 (2021)
2 Subramanian, S. *et al. Endotext,* (2021)
3 Rickels, M. R. *et al. Endocrine Reviews,* 40.2, 631-668 (2019)

Contact

M.R. Schot; +31-534-898-152; m.r.schot@utwente.nl

Extended storage of soft callus mimetics permits endochondral bone regeneration

F. Staubli[1,2], L. de Silva[1,2], A. J. W. P. Rosenberg[1], D. Gawlitta[1,2]
[1]Dept. of Oral and Maxillofacial Surgery & Special Dental Care, [2]Regenerative Medicine Center Utrecht, University Medical Center Utrecht, Utrecht, the Netherlands.

In endochondral bone regeneration (EBR), the natural development of long bones during embryogenesis and fracture repair is mimicked by the implantation of a cartilaginous template, a soft callus mimetic, into a defect, which is eventually remodeled into bone. Autologous, multipotent mesenchymal stromal cells (MSCs) are commonly used to generate such soft callus mimetics. However, the use of patient-own cells is associated with donor-to-donor variability in chondrogenic differentiation potential, relatively high costs and no off-the-shelf treatments. A promising alternative is the use of non-autologous MSCs, where it is possible to pre-select chondrogenically potent donors, generate large pooled MSC batches and cells can be stored.
Devitalization of soft callus mimetics, generated from allogeneic MSCs, previously led to full defect bridging of a critical size rat femur defect without hindrance of an immune reaction.[1] Furthermore, devitalization could potentially allow to store such callus mimetics over a prolonged period without the loss of bioactivity to induce bone regeneration *in vivo*. If this is confirmed, the proposed approach can offer a real off-the-shelf solution for bone regeneration. This study therefore aimed at evaluating the shelf-life of devitalized soft callus mimetics, generated from allogeneic MSCs.

To achieve this, MSCs were harvested from Dark Agouti rats and differentiated towards the chondrogenic lineage *in vitro* for 28 days, using rat tail collagen I as a biomaterial carrier ($1x10^6$ MSCs/spheroid). The generated soft callus spheroids were harvested and devitalized by a mild procedure[2] and then stored at -80°C for either 7 or 9 months before subcutaneous implantation in Brown Norway rats for 8 or 12 weeks (n = 16). The samples were retrieved, and the formation of new bone tissue was assessed by measuring the mineralization volume by micro-CT analysis. The results were compared to results from a previous experiment in which soft callus spheroids from the same batch as the 9 months group were stored for a maximum of up to 1 month at -80° C (short storage group) and implanted subcutaneously in Brown Norway rats (n = 7) for 12 weeks followed by micro-CT analysis.

Overall, several samples of all groups could not be retrieved, most likely due to resorption, which is common for unloaded bone tissue at ectopic implant locations. Eight weeks post-implantation, 2.0 ± 1.5 mm^3 and 2.5 ± 1.7 mm^3 of mineralized tissue per implant was found for the 7 and 9 months storage groups, respectively. Twelve weeks post-implantation, 2.6 ± 1.6 mm^3 of mineralized tissue was found for the short storage group, while 0.6 ± 0.3 mm^3 and 2.2 ± 1.5 mm^3 of mineralized tissue was found for the 7 and 9 months storage groups, respectively (Figure 1).

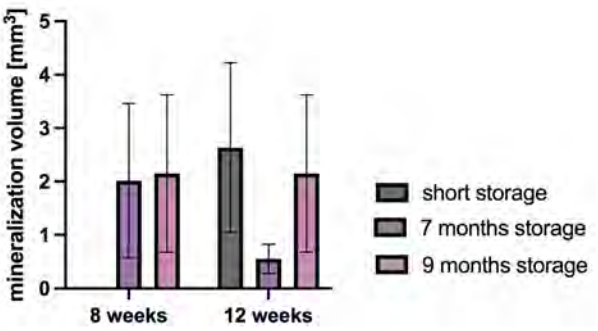

Figure 1: Quantification of the mineralization volume of stored soft callus mimetics after different implantation periods.

Eight weeks post-implantation, comparable amounts of mineralized tissue were detected for the 7 and 9 months storage groups. 12 weeks post-implantation, comparable amounts were detected for the short storage and the 9 months storage groups, whereas decreased amounts were detected for the 7 months storage group.
This decrease might have been caused by batch-to-batch variation of the implanted samples, or by the previously mentioned resorption of bone samples at subcutaneous locations. Further studies need to be conducted to understand how spheroid composition and structure vary between batches and how this affects bone regeneration potential, spheroid resorption and bioactivity.

Comparable amounts of mineralized tissue volume in short and 9 months storage groups indicate that storage for up to 9 months at -80° C does not affect bioactivity and potential to induce bone regeneration of devitalized soft callus mimetics. This is promising in the light of clinical translation to an off-the-shelf osteoinductive product.

References:

[1] Longoni et al. Endochondral Bone Regeneration by Non-autologous Mesenchymal Stem Cells. Front Bioeng Biotechnol. 2020 Jul 9;8:651.
[2] Longoni et al., Acceleration of Bone Regeneration Induced by a Soft-Callus Mimetic Material. Adv Sci (Weinh). 2022 Feb;9(6):e2103284.

High throughput screening of topographies to mitigate fibrosis in glaucoma filtration surgery devices

Phanikrishna Sudarsanam[1], Tim J.M. Kuijpers[1], Ralph J.S. van Mechelen[2], Theo G.M.F. Gorgels[2], Leonard Pinchuk[3], Henny J.M. Beckers[2] and Jan de Boer[1]

[1] Eindhoven University of Technology, Department of Biomedical Engineering and Institute for Complex Molecular Systems Eindhoven, the Netherlands

[2] University Eye Clinic Maastricht, School for Mental Health and Neuroscience, Maastricht, the Netherlands

[3]InnFocus Inc., Miami, Florida, USA

Contact: p.k.sudarsanam@tue.nl, Ph. no: +31 (0) 617623600

Introduction

Glaucoma is one of the leading causes of irreversible blindness. It is caused by high intraocular pressure due to increased flow of aqueous humor, which is a clear liquid in the anterior chamber of eye. Severe glaucoma is treated by use of glaucoma filtration surgery devices, which drain the liquid from the eye into a bleb, a spongy tissue made of loosely packed collagen formed between the Tenon's capsule and sclera. A frequently occurring problem with this treatment is the formation of a dense fibrous tissue at the outlet that blocks the outflow of aqueous humor and thus causes implant failure. However, the role of bleb thickening mediated by aqueous humor leading to failure of implant is often ignored. We hypothesise that the crosstalk between macrophages and fibroblasts at the interface and in the bleb plays a huge role in implant-related fibrosis. Both these cell types respond to the physical and chemical cues of biomaterials, so we set out to identify surface topographies that attenuate the fibrotic process.

Methods

A poly (styrene-block-isobutylene-block- styrene) (SIBS) Topochip containing 2176 distinct topographies was fabricated using hot embossing. Three screens were performed, one with primary tenon fibroblasts where we quantified expression of the trans-differentiation marker alpha-smooth muscle actin (α-SMA) and a second where proliferation was quantified through EdU staining by automated image analysis. A third screen was done using primary macrophages for differential attachment. Surfaces were ranked and hits from the screen were chosen and validated for the same readouts and for multiplex ELISA for the macrophage's secretion profile of pro- and anti-inflammatory cytokines.

Results and discussion

Screening results showed varied response between the topographies on all read outs and have shown a strong effect on tenon fibroblast morphology and stress fiber formation relative to flat control. We ranked top and bottom hits based on the imaging data and noticed that α-SMA and EdU show a 4-fold differences between top and bottom hits. We opted to go for a dynamic three- pronged approach in selection of the hits for validation work that will be used *in vivo* model, one for tissue integration, another for pro-encapsulation and lastly for anti-fouling. The chosen hits were fabricated using SIBS polymer in enlarged surfaces and validated using the same readouts.

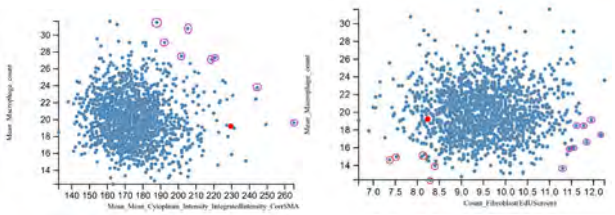

Fig: Scatter plots showing the screening results from which hits chosen were rounded. Left plot shows hits for pro encapsulation with α-SMA expression on X-axis and macrophage attachment on Y-axis. Right plotted with macrophage and fibroblast attachment on X-axis and Y-axis respectively shows hits chosen for antifouling (red) and tissue integration fibroblasts (purple).

Among the hits, three topographies were chosen for each approach. Topography 1153 was chosen for pro-encapsulation, topography 79 for tissue integration and topography 509 for anti-fouling.

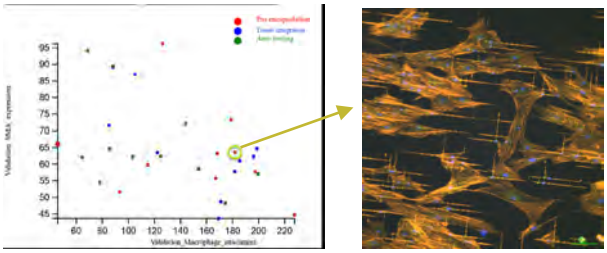

Fig: Scatter plot showing validation results from the selected hits for each condition (on left), Topo 1153 shown rounded in the plot which has highest expression of α-SMA expression (on right) along with high macrophage attachment from both the screening and validation work.

Chosen hits were correlated with cytokine analysis where we found topography 1153 with high expression of pro-inflammatory cytokine IL-6, IL-1β, TNF-α compared to other hits whereas topography 79 showed higher expression of arginase, IL- 1RA with low levels of IL-6, IL-1β and TNF-α.

Future Work

Based on the screening and validation results, we chose three topographies which will be used to fabricate a device for the animal trials to test which can induce a better bleb survival in an *in vivo* rabbit model.

Acknowledgements

This research was conducted under the framework of the Chemelot Institute for Science & Technology (InSciTe).

Rationally Designed Antimicrobial Peptides Show Antimicrobial Activity Against Gram-Negative Bacteria in a 3D Human Skin Equivalent Model.

Nikitha Vavilthota[1], Gizem Babuccu[1], Muhanad Ali[2], Peter H. Nibbering[2] Jan Wouter Drijfhout[3], Robert A. Cordfunke[3] Colin Bournez[4], Gerard J.P. van Westen[4], Martijn Riool[1], Sebastian A.J. Zaat[1]

1. Department of Medical Microbiology & Infection Prevention, Amsterdam institute for Infection and Immunity, Amsterdam UMC, University of Amsterdam, Meibergdreef 9, 1105 AZ Amsterdam, The Netherlands
2. Department of Infectious Diseases, Leiden University Medical Center, 2300 RC Leiden, The Netherlands
3. Department Immunology, Leiden University Medical Center, 2300 RC Leiden, The Netherlands
4. Division of Medicinal Chemistry, Drug Discovery and Safety, Leiden Academic Centre for Drug Research, Leiden University, P.O. Box 9502, 2300 RA, Leiden, The Netherlands

n.vavilthota@amsterdamumc.nl

Recent decades have witnessed an significant surge in antibiotic resistance in bacteria. With the current emergence of multidrug-resistant strains there is an imminent treat towards the "post antibiotics era". Ever since the discovery of antimicrobial peptides (AMPs) of the innate defense system have been hailed as potent alternative antimicrobials. Wound site infections, particularly in skin, apart from having numerous challenges to treat due to biofilm formation and multidrug resistance, can have debilitating effects on patients' health.

Low resistance development, broad spectrum activity, biofilm treatment, wound healing and immunomodulatory properties of the AMPs, make them ideal candidates to tackle wound infections and heal them. Finding potent AMPs through classical wet lab approaches is time consuming, laborious and an expensive process. Using a machine learning approach, peptides with antimicrobial activity were identified[1]. The current project under the European Marie Skłodowska training network STIMULUS[2] "Stimuli Responsive Materials for the Rapid Detection and Treatment of Healthcare Associated Infections" aims at creating medical devices that signal when an infection is present and thereby reduces the unnecessary prescription of antibiotics and hence the spread of antibiotic resistance.

One of the objectives of this project is the development and testing of the diagnostic and antimicrobial capacity of the device in advanced *in vitro* and *in vivo* systems.

On this line, a 3D human skin equivalent (HSE) system was used to test the antimicrobial activity of novel AMPs against *Acinetobacter baumannii* and *Staphylococcus aureus. In vitro* skin models pose many similar properties as normal human skin, making them a relevant system for skin infections. Skin equivalents were prepared using the immortal human keratinocyte cell line hTert/KER-CT. After initial *in vitro* screening for antimicrobial activity of peptides obtained from the machine learning approach, four top hit peptides were selected: AMP-038, AMP-045 and their retro-inverso variants (RI). The equivalents were infected with inoculum suspensions of *A. baumannii* RUH875 or *S. aureus* JAR060131 for 90 minutes followed by peptide treatment for four hours. At 30 µM concentrations of AMP-038 and AMP-045, neither planktonic nor adherent cells of *S. aureus* and *A. baumannii,* survived on treated skin equivalents. At 10 µM concentrations of AMP-038, AMP-045 and their retro-inverso variants, the planktonic *S. aureus* cells show no survival. Moreover, AMP-045 was able to kill all planktonic cells of *S. aureus* at 3 µM. In conclusion, novel AMPs, identified using a new machine learning method, show broad-spectrum antimicrobial activity at low concentrations.

Next, for assessing the *in vivo* activity of peptides, an infection model is established by disruption of the skin barrier by partial removal of the epidermal layer of mouse by tape stripping. This will be followed by subsequent application of bacteria and peptide treatment.

1. Dutch Scientific Council (NWO) LIFT program (729.001.024).
2. This project has been supported by European Union's Horizon 2020 research and innovation program under the Marie Skłodowska-Curie grant agreement No. 955664.

Screening Peptide-Functionalized Supramolecular Assemblies Using Cell Morphological Profiles

V.A. Veenbrink, N. Konshin, J. de Boer and P.Y.W Dankers
Institute for Complex Molecular Systems, Laboratory for Cell and Tissue Engineering and Chemical Biology, Department of Biomedical Engineering, Eindhoven University of Technology, The Netherlands

Introduction

One of the holy grails of tissue engineering is the development of a synthetic extra cellular matrix (ECM) mimicking material. To this end supramolecular hydrogels were developed which allow for the tuning of mechanical, dynamic and biological signals. The modular nature of supramolecular materials makes it possible to rapidly generate libraries of various combinations of cell adhesive peptide-functionalized supramolecular assemblies. The resulting libraries can be screened for their ability to mimic natural ECM derived materials. In this study peptides functionalized with a ureidopyrimidinone (UPy) moiety were used. UPy moieties are capable of forming supramolecular assemblies through a combination of dimerization by quadruple hydrogen bonding and the stacking of UPy dimers through π-π interactions, hydrogen bonding and hydrophobic interactions. The resulting UPy assemblies can be made bioactive through peptide-functionalized UPys with sequences derived from cell-adhesive proteins such as Laminin-111 and Fibronectin.[1] In order to screen the effect of peptide-functionalized UPy assemblies on cell morphology the Cell Painting protocol developed by the Broad Institute was used.[2] This protocol generates a morphological fingerprint at the single cell level. The protocol was adapted to use peptide-functionalized UPy assemblies as perturbants. As a proof of concept a library was generated using all eight possible combinations of UPy-cRGDfK, UPy-PHSRN and UPy-IKVAV (Figure 1). The assemblies consisted of a backbone of 84 mol% UPy-G functionalized with 16 mol% UPy-peptide or combinations of multiple peptides. A549 cells were incubated with these assemblies in solution at a total UPy concentration of 100 µM for 48 hours before their morphological fingerprints were measured.

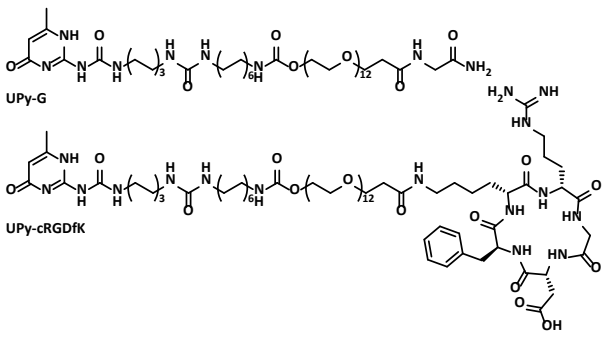

Figure 1: Examples of the molecular structures of peptide-functionalized UPys.

Results and Discussion

It was possible to adapt the Cell Painting protocol to be used for screening libraries of peptide-functionalized UPy assemblies (Figure 2). The resulting morphological profiles were aggregated at the well level and compared using a Pearson correlation matrix. This correctly identified replicate wells and could be used to accurately distinguish between controls, cells incubated with each of the peptide-functionalized UPys and combinations of multiple peptide-functionalized UPys.

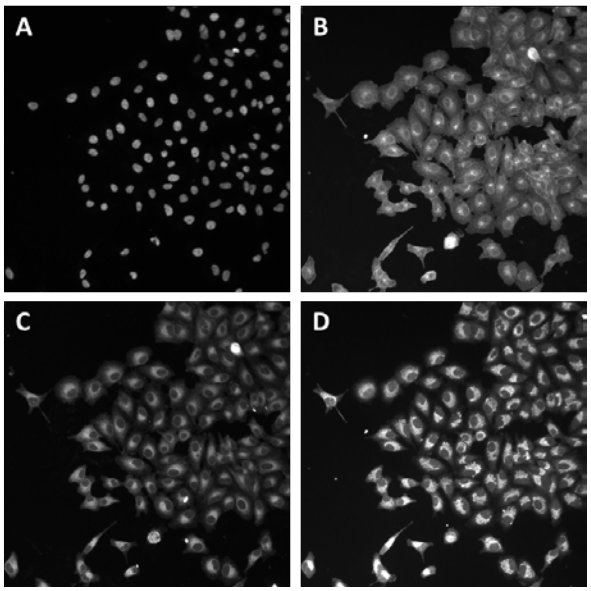

Figure 2: A549 cells incubated with UPy-cRGDfK assemblies stained with Hoechst 33342 (DNA)(A), phalloidin 568 and wheat germ agglutin 555 (Actin, Golgi, Plasma membrane)(B), Concavalin A (Endoplasmic reticulum)(C) and MitoTracker deep red (Mitochondria)(D).

Conclusions and Outlook

It was demonstrated that it is possible to distinguish between treatment with different peptide-functionalized UPy assemblies through morphological profiles generated with the Cell Painting protocol. In future the scope of the study will be expanded by increasing the number of peptide functionalized UPys, and thereby the number of possible combinations. Furthermore, it will be investigated if the profiles can be used to identify a combination of peptide-functionalized UPys which mimics the effect of natural ECM proteins using a machine learning guided approach.

References

1. Diba, M. *et al.* Engineering the Dynamics of Cell Adhesion Cues in Supramolecular Hydrogels for Facile Control over Cell Encapsulation and Behavior. *Advanced Materials* **33**, 2008111 (2021).
2. Bray, M. A. *et al.* Cell Painting, a high-content image-based assay for morphological profiling using multiplexed fluorescent dyes. *Nature Protocols 2016 11:9* **11**, 1757–1774 (2016).

On the Interplay between Cell Metabolism and Biomaterial Properties

J. Verbakel[1], R. S. Polishchuk[2], A. Khodjakov[3], and J. de Boer[1]

[1], Eindhoven University of Technology, Department of Biomedical Engineering and Institute for Complex Molecular Systems, Eindhoven, The Netherlands
[2] Telethon Institute of Genetics and Medicine, Pozzuoli, Italy
[3] Wadsworth Center, New York State Department of Health, New York, USA
Contact: j.verbakel@tue.nl

Background. Surface topographical cues provide cells with signals to maintain or change their physiology and play therefore an essential role in controlling cell phenotype. Mechanosensitive signaling pathways influenced by these surface structures control expression of genes involved in differentiation, proliferation and metabolism. Cells cultured on topographically enhanced substrates show a reduced size, lower number of organelles, and a decreased proliferation rate. Downregulation of mitotic spindle related genes along with differential gene expression of genes in cytoskeleton and microtubule cytoskeleton organization in cells cultured on topographies raises questions whether and how these micro-topographies influence the architecture of the cell's microtubule network, as well as additional processes regulated by microtubule network organization. Interestingly, disruption of this network results in dramatic effects on the normal centrosomal localization and morphology of the Golgi complex, as hundreds of functional Golgi islands disperse throughout the cytoplasm. In consideration of these observation, topography-induced rearrangement of the microtubule network is expected to result in reorganization of the Golgi complex.

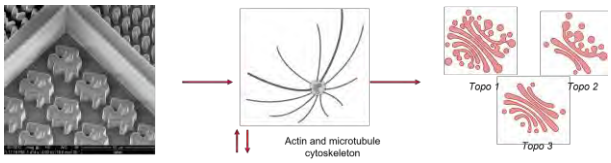

Experimental design. First indications of the effects of surface micro-topographies on microtubule network organization and consecutive dynamic reorganization of the Golgi complex structure in human dermal fibroblasts were confirmed via immunofluorescent techniques.

Results. Whereas fibroblasts cultured on flat polystyrene surfaces show a well-defined microtubule network with spread tubule fibers from the nucleic site over the whole cell body and filamentous subsurface structures are visible, rearrangement of this network can be observed in cells cultured on micro-topographies. An overall increased homogenous distribution of tubulin fluorescence, indicating uniform distribution of tubulin dimers over the cell body, is accompanied by local regions of increased microtubule density.

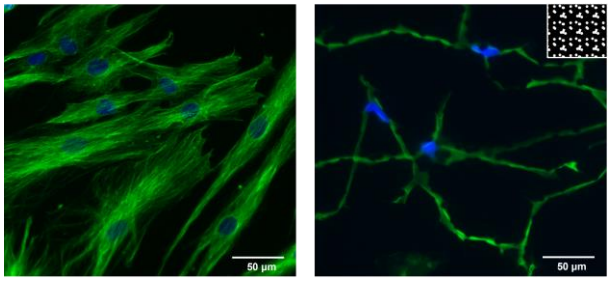

Fibroblasts cultured on flat (left) versus topography 1008 enhanced (right) substrates are stained for α-tubulin (green) and DAPI (blue).

In addition, contrary to the well-organized Golgi ribbon structure in fibroblasts cultured on flat surfaces, a more compact Golgi morphology and decreased surface area can be observed in cells on micro-topographies. These fibroblasts exhibit a disorganized cisternal stack structure in which the limits of the membrane and lumen are difficult to distinguish. Moreover, the characteristic perinuclear position seems to be less maintained, as well as the typical loose interconnected network of vesicles and tubules.

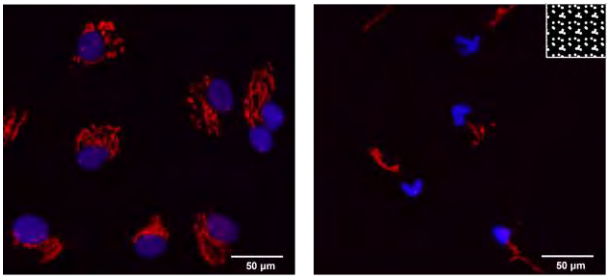

Fibroblasts cultured on flat (left) versus topography 1008 enhanced (right) substrates are stained for Golgi-resident protein GM130 (red) and DAPI (blue). Topography-induced changes in Golgi structure are characterized by increased compactness and less defined ribbon structure.

Future perspectives. In order to confirm the association between microtubule network organization and Golgi architecture, it will be attempted to rescue the topography-induced phenotype by the addition of small molecules that either stabilize or disrupt this microtubule network. In order to determine whether structural changes are associated with specific features defining the topography, these effects will be analyzed for cells cultured on Phenome28 (i.e. 28 groups of topographically-patterned surfaces) using image analysis pipelines. In addition to proceeding the analysis of topography-induced changes on microtubule network organization and Golgi architecture, future steps include the examination of topography-induced effects on functional capacity of the Golgi complex. Moreover, time-lapse imaging is expected to shed more light on the dynamic reorganization of the Golgi complex over time. Eventually, it is aimed to sort out the possible underlying (molecular) mechanism responsible for topography-induced changes is intended to be performed, i.e. elucidate the relation between mechanotransduction and Golgi morphology and functioning.

J. Verbakel (J.verbakel@tue.nl)
R. S. Polishchuk (polish@tigem.it)
A. Khodjakov (alexey.khodjakov@health.ny.gov)
J. De Boer (j.d.boer@tue.nl)

Thermosensitive Shrinking Behavior of Biopolymer-based Hydrogels for High Resolution Printing

Martina Viola[1,2], Marta Garcia Valverde[3], Jaap van Trijp[1], Paulina Nuñez Bernal[2], Carl.C.L. Schuurmans[1], Cornelus F. van Nostrum[1], Riccardo Levato[4,2] and Tina Vermonden[1]

1. Department of Pharmaceutical Sciences (UIPS), Faculty of Science, Utrecht University, Utrecht, The Netherlands.
2. Department of Orthopaedics, University Medical Center Utrecht, Utrecht, The Netherlands.
3. Department of Pharmacology, Utrecht University, Utrecht, the Netherlands.
4. Department of Clinical Sciences, Faculty of Veterinary Medicine, Utrecht University, Utrecht, The Netherland.

m.viola@uu.nl

INTRODUCTION

Printing high resolution constructs with complex geometries and sizes below 100 μm of soft hydrogel materials is not only a challenge, but also of high interest in biofabrication for the regeneration of renal tubules and blood vessels. Hydrogel shrinking techniques (complexation or pH-dependent) have recently been proposed to print high resolution 3D scaffolds which are subsequently shrunken to go beyond the maximum resolution guaranteed by the printer. Since both complexation and pH-dependent techniques impose a non-cell-friendly environment, in this work we propose a thermosensitive hydrogel that reduces its dimension when exposed to a temperature increase to 37°C.

This thermosensitive shrinking method is based on the lower critical solution temperature (LCST) of poly N-isopropyl acrylamide (pNIPAM).

EXPERIMENTAL METHODS

Hydrogels based on biopolymers (gelatin and silk fibroin) were functionalized with methacryloyl moieties, crosslinked with NIPAM through UV exposure and the shrinking behavior was evaluated upon heating above the LCST (Fig.1). The hydrogels were applied to volumetric 3D printing, the printability, the ability to maintain geometry and proportions following shrinking were evaluated.

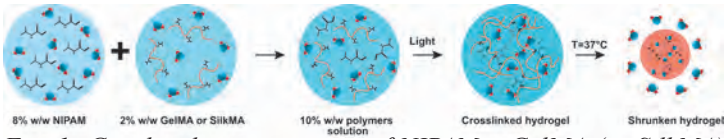

Fig. 1; Graphical representation of NIPAM – GelMA (or SilkMA) hydrogel formation and shrinking behavior when exposed to 37°C.

RESULTS AND DISCUSSION

Both GelMA/NIPAM and SilkMA/NIPAM hydrogels reduce their size in volume by a factor 2 when heated to 37 °C. This shrinking effect was found to be fully reversible when samples were cooled back below the LCST. After the shrinking both hydrogels showed an increase in the gel strength and an increase in the Young's modulus (Fig. 2).

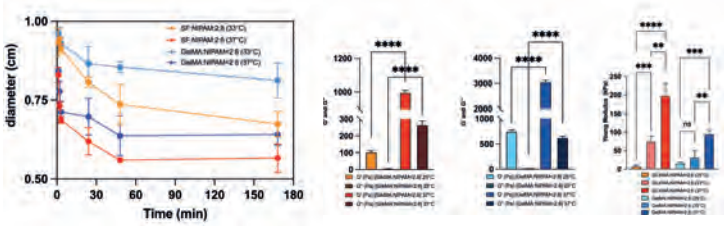

Fig. 2; Kinetics of shrinking for GelMA:NIPAM and SilkMA:NIPAM hydrogels at 25°C and 37°C; Storage and Loss modulus calculated for angular frequency 1 rad/s during a frequency sweep, for GelMA:NIPAM and SilkMA:NIPAM at 25°C, 33°C and 37°C.

Both volume reductions and cell viability of conditionally immortalized proximal tubule cells were observed to be correlated with increased ratios of NIPAM to methacroylated-polymer concentrations while keeping total polymer concentrations at optimal 10% (w/w).

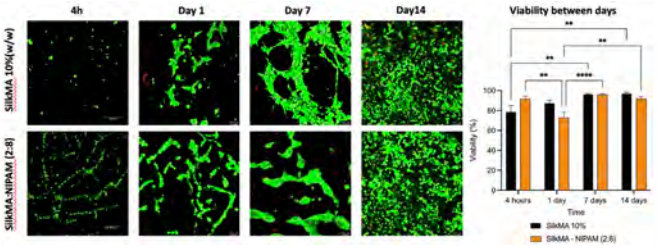

Fig. 3; Human conditionally immortalized proximal tubular epithelial cells seaded on SilkMA:NIPAM hydrogels and SilkMA alone as control for 14 days.

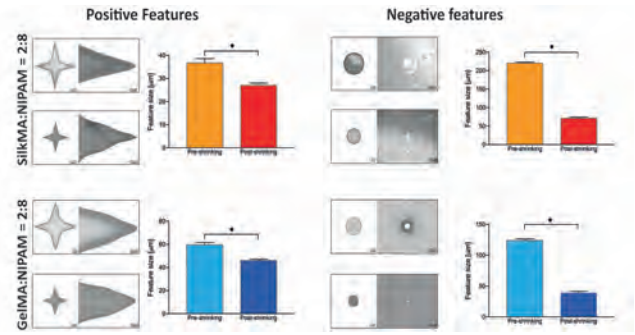

Fig. 4; GelMA:NIPAM and SilkMA:NIPAM positive and negative features printed with volumetric printing.

Positive figures were printed with the volumetric printer with a resolution of 600 μm at room temperature that was enhanced to 30 μm upon shrinking (Fig. 2). For the negative figures a resolution enhancement from 200 to 50 μm was reached.

CONCLUSION

This work shows a versatility of materials applicable to volumetric printing with the ability to reach resolutions above the technical capacity of the machine, also demonstrating an inclination of cells to grow on the stiffened hydrogel following shrinking.

REFERENCES

1. Gong, J.; Schuurmans, C. C.L. et al. Complexation-induced resolution enhancement of 3D-printed hydrogel constructs. Nature Communications 2020, 11 (1), 1-14.

2. Hirano, T.; Nakamura, K. et al. Hydrogen-bond-assisted syndiotactic-specific radical polymerizations of N-alkylacrylamides: The effect of the N-substituents on the stereospecificities and unusual large hysteresis in the phase-transition behavior of aqueous solution of syndiotactic poly (N-n-propylacrylamide). Journal of Polymer Science Part A: Polymer Chemistry 2008, 46 (13), 4575-4583.

ACKNOWLEDGMENTS

This study is supported by the NWO/VICI project (no. 18673) the Gravitation Program "Materials Driven Regeneration" (024.003.013) and the Reprint project (OCENW.XS5.161) by the Netherlands Organiza-tion for Scientific Research, and the Marie Skłodowska-Curie Actions (RES-CUE #801540).

A dialysis medium refreshment cell culture set-up for an osteoblast-osteoclast coculture

M.A.M. Vis, B.W.M. de Wildt, K. Ito, S. Hofmann
Orthopaedic Biomechanics, Department of Biomedical Engineering and Institute for Complex Molecular Systems, Eindhoven University of Technology, P.O. Box 513, 5600 MB Eindhoven, the Netherlands

Introduction: Culture medium exchange leads to loss of valuable auto- and paracrine factors produced by the cells. However, frequent renewal of culture medium is necessary for nutrient supply and to prevent waste product accumulation Thus it remains the gold standard in cell culture applications. The use of dialysis as a medium refreshment method could provide a solution as low molecular weight molecules such as nutrients and waste products could easily be exchanged, while high molecular weight components such as growth factors, used in cell interactions, could be maintained in the cell culture compartment. This study investigates a dialysis culture approach for an *in vitro* bone remodeling model.

Materials and Methods: In this model, both the differentiation of human mesenchymal stromal cells (MSCs) into osteoblasts and monocytes (MCs) into osteoclasts was studied. A custom-made simple dialysis culture system with a commercially available cellulose dialysis insert was developed. A monoculture of MSCs and a coculture of MSCs and MCs was performed for 28 days. Osteogenic differentiation was investigated by alkaline phosphatase (ALP) activity assays and immunohistochemical staining for the expression of the osteopontin. Extracellular matrix production was visualized using collagen type 1 and calcium (Alizarin Red) stainings. Osteoclastic differentiation was investigated by tartrate-resistant acid phosphatase (TRAP) activity assays and visualization of the cells by scanning electron microscopy (SEM).

Results: The data reported here revealed increased osteoblastic and osteoclastic activity in the dialysis groups compared to the standard non-dialysis groups, mainly shown by significantly higher ALP and TRAP activity, respectively.

Conclusion: This simple culture system creates a microenvironment that preserves growth factor effects and therefore allows for more efficient cell interactions via secreted factors, both in mono- and cocultures. It has the potential to be applied for other tissues where cell interactions via secreted factors are of interest.

Acknowledgements: This work is part of the research program TTW with project number TTW 016.Vidi.188.021, which is (partly) financed by the Netherlands Organisation for Scientific Research (NWO).

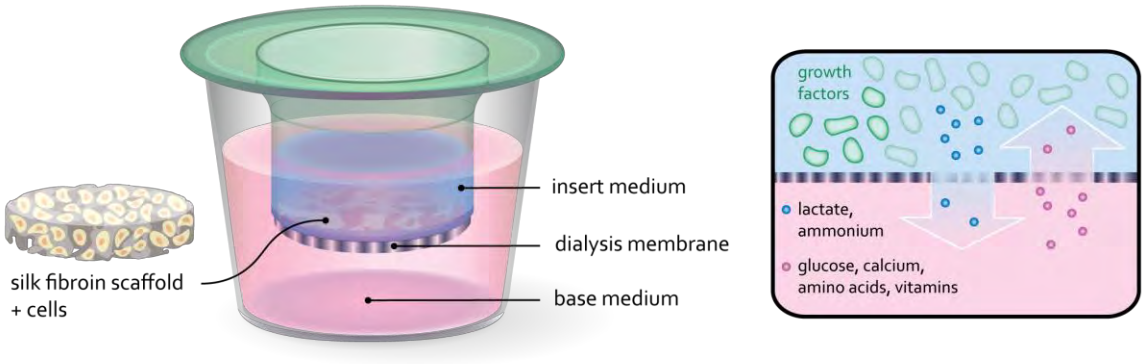

Figure 1 Experimental set-up: A silk fibroin scaffold is seeded with cells and cultured in a custom-made dialysis culture dish. The dialysis membrane ensures retaining of high molecular weight growth- and communication factors in the cell culture insert. Nutrients and waste products of low molecular weight can pass the dialysis membrane and will be supplied and removed by diffusion across the membrane.

Bifunctional Bone Substitute Granules Loaded with Cisplatin Aiming to Minimize Malignant Bone Tumor Recurrence via Local Treatment

Z Wang[1], M Kregel[2], J Meijers[2], J Serracanta[3], ICM Van Der Geest[4], SCG Leeuwenburgh[1], JJJP van den Beucken[1]
[1]Dentistry - Regenerative Biomaterials, Radboudumc, Philips van Leydenlaan 25, Nijmegen, The Netherlands
[2]Department of Dentistry, Radboudumc, Philips van Leydenlaan 25, Nijmegen, The Netherlands
[3] Department of Plastic Surgery and Major Burn, Vall d'Hebron University Hospital, 08193 Bellaterra, Barcelona, Spain
[4]Department of Orthopedics, Radboudumc, Geert Grooteplein Zuid 10, Nijmegen, the Netherlands

Introduction: Residual tumor cells left in the bone defect after malignant bone tumor resection can result in local tumor recurrence and high mortality. Therefore, ideal bone filling materials should not only aid bone regeneration, but also exert local chemotherapeutic efficacy. However, common bone substitutes used in clinics are barely studied for local delivery of chemotherapeutic drugs. Here, we aimed to use facile manufacturing methods to render xenogeneic granules (Bio-Oss®) and synthetic calcium phosphate (CaP) granules (MBCP®) suitable for local delivery of cisplatin to limit bone tumor recurrence.

Materials and Methods: The chemotherapeutic drug cisplatin was loaded on two types of granular bone substitutes via adsorption. Then, the morphology and physicochemical properties of those granules were characterized by using scanning electron microscopy (SEM) and X-ray diffraction (XRD). Cisplatin release kinetics were analyzed using ICP-MS for the element platinum. The anticancer efficacy of immobilized and released cisplatin against metastatic breast cancer cells (MDA-MB-231) and metastatic prostate cancer cells (PC3) was evaluated by the Cell Counting Kit-8 (CCK-8) assay. The MUSE® Count & viability kit was used to assess the cytostatic effects of released cisplatin on cell proliferation of MDA-MB-231, PC3, giant cell tumor cells (GCTs) and human bone marrow stem cells (hBMSCs). Cell cycle and caspase 3/7 assays were carried out to investigate the anticancer mechanism. Additionally, a rat critical-sized femoral condyle defect model was developed to assess the *in vivo* biosafety and regenerative capacities of the two different cisplatin-loaded granules.

Results and Discussion: Through scanning electron microscopy and X-ray diffraction analysis, MBCP® granules were found to have higher porosity and crystallinity compared to Bio-Oss® granules (Fig. 1).

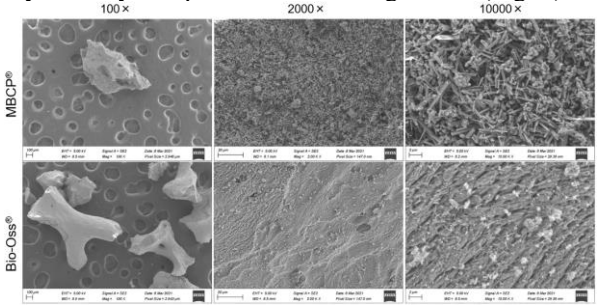

Figure 1 Surface morphologies of MBCP® and Bio-Oss® granules with the magnification of 100x, 2000x and 10000x.

Drug release profiles showed that about 30% of cisplatin was released from Bio-Oss® granules, while less than 2% cisplatin was released from MBCP® granules over 28 days (Fig. 2). The immobilized and released cisplatin retained its anti-cancer efficacy and showed dose-dependent cytostatic effects on different metastatic bone tumor cells (Fig. 3). Furthermore, cell cycle and caspase 3/7 analyses revealed that cisplatin induced cell cycle arrest and apoptosis via caspase 3/7 activation for tumor cells, while hBMSCs were less sensitive to cisplatin.

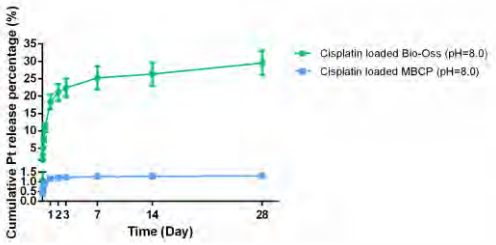

Figure 2 Release profile of cisplatin from cisplatin-loaded MBCP® and Bio-Oss® granules assessed by ICP-MS.

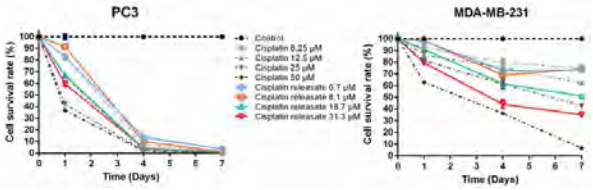

Figure 3 Cytotoxic effects of Pt release from cisplatin-loaded Bio-Oss® granules against MDA-MB-231 and PC3. Media containing different concentrations of free cisplatin were used as control groups.

Application of cisplatin-loaded bone substitutes in rat bone defects showed negligible cisplatin accumulation in kidneys and livers at 30 days after implantation. Importantly, no adverse effects on bone regeneration were observed compared to cisplatin-free controls (Fig. 4).

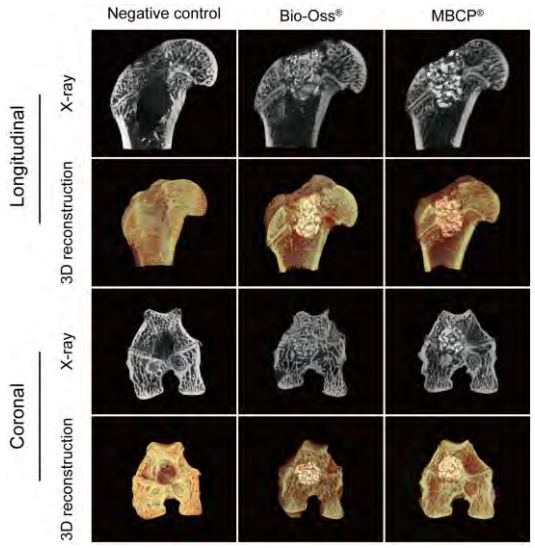

Figure 4 Representative micro-CT images and 3D reconstructions of femoral condyle defects in rats 30 days after implantation.

Conclusions: Granular bone substitute can be rendered therapeutically active for anticancer efficacy by facile loading with cisplatin, without affecting bone regenerative efficacy. As such, our data suggest that bifunctional cisplatin-loaded granular bone substitutes represent a viable adjunct treatment option to lower recurrence of bone tumors after surgical resection.

Steering Stem Cell Fate within 3D Living Composite Tissues using Stimuli-responsive Cell-adhesive Micromaterials

N.G.A. Willemen*, T. Kamperman*, C.L. Kelder, M. Koerselman, M. Becker, L. Lins, M. Karperien, and J. Leijten
Department of Developmental BioEngineering, Faculty of Science and Technology, Technical Medical Centre, University Twente, Drienerlolaan 5, 7522NB Enschede, The Netherlands. Contact: n.g.a.willemen@utwente.nl

Introduction:

Engineered living microtissues such as cellular spheroids and organoids have enormous potential for the study and regeneration of tissues and organs.[1] These models are typically formed via self-assembly of cells via cellular adhesion.[2] Consequently, these microtissues are material-free, and thus offer little to no mechanical or biochemical control over their local microenvironment,[3] which has severely limited control over their behavior, functional performance, and on-demand adaptivity. Here, we report on the development of stimuli-responsive cell-adhesive micromaterials (SCMs) that can self-assemble with cells into 3D living composite microtissues via integrin binding, even under serum-free conditions. We demonstrate that SCMs homogeneously distribute within engineered microtissues and possess on-demand *in situ* tunable biophysical and biochemical properties, which enables cell programming via cell-material interactions by controllably designing the microtissue microenvironment. Specifically, cell behavior can be controlled based on the size, stiffness, number ratio, and biofunctionalization of SCMs in a temporal manner via orthogonal secondary crosslinking strategies.

Materials and Methods:

Microbuilding block production and functionalization: Hydrogel precursor droplets composed of 5% (w/v) Dextran-Tyramine-Biotin (DexTAB; ~1 mM biotin) and 22 U/mL horseradish peroxidase in phosphate buffered saline (PBS) were emulsified in 2% (w/w) Pico-Surf 1 containing Novec 7500 Engineered Fluid using a microfluidic droplet generator with subsequent crosslinking on a separate controlled hydrogen peroxide (H_2O_2) supplementation.[4, 5]

Modular tissue engineering: RGD-functionalized SCMs were homogeneously co-seeded with cells into non-adherent 3% (w/v) agarose microwell chips at a density of ~50 units per microwell.

In situ biochemical tuning: SCM-laden constructs were sequentially endowed with 1 µM neutravidin, washed, incubated with 1 µM biotinylated or desthiobiotinylated molecule-of-interest, and washed again.[6]

In situ stiffening: SCMs within modular tissues were *in situ* stiffened by incubating them with 2.5 mM of sodium persulfate and 1 mM of Ruthenium. Free radical crosslinking was induced using 60 seconds of visible light irradiation. Lineage commitment was visualized using histochemical staining, and imaged using confocal (fluorescence) microscopy, and analyzed using image analysis software.

Results:

Microgel precursor droplets were formed in a microfluidic droplet generator and crosslinked by controlled supplementation with H_2O_2 (Figure 1A,B). This resulted in formation of monodisperse DexTAB SCMs. The building block's stiffness predictably correlated with H_2O_2 supplementation (Figure 1C).

Next, the biotins in the SCM shell were functionalized with c(RGDfK), which enabled the self-assembly of SCMs within microaggregates owing to cell-microgel interactions (Figure 1D).

In situ biochemical control was shown by sequentially endowing SCMs with (desthio)biotinylated molecules (i.e. fluorophores or antibodies; Figure 1E).

Cell-microgel and cell-cell interactions within the microaggregate were optimized by controlling the amount, stiffness and/or size (Figure 1F) of the SCMs within the construct. Our data showed that all can be leveraged to control the osteogenic or adipogenic lineage commitment of 3D stem cell spheroids.

Moreover, photo-induced crosslinking allowed for on-demand control SCM stiffness. Stem cell fate toward osteogenic and adipogenic lineages was temporally steered by *in situ* tuning the SCM stiffness within modular tissues (Figure 1G).

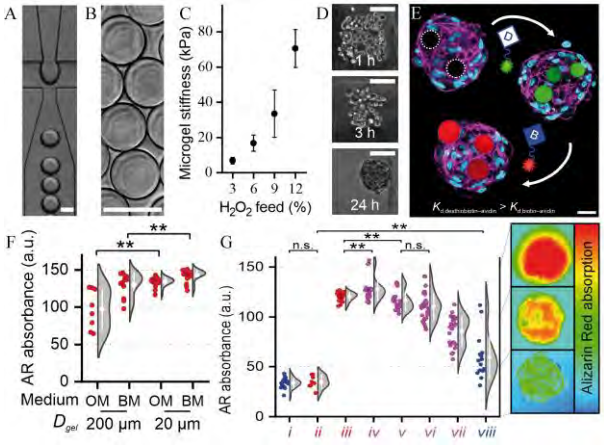

Figure 1: *A) Generation of aqueous droplets in droplet generator. B) DexTAB microgels post-crosslinking. C) Microgel stiffness was controlled by H_2O_2 supplementation. D) RGD-functionalized SCMs self-assemble with cells into microaggregates. E) In situ control over biochemical moieties using (desthio)biotin complex. F) Cell-sized SCMs induce higher osteogenic lineage commitment compared to larger SCMs. G) Osteogenic differentiation was temporally steered by in situ stiffening of soft SCMs.*

Conclusion:

In conclusion, we developed the first biochemically, biophysically, and spatiotemporally controlled smart building blocks for modular tissue engineering. This allowed for the creation of highly tunable and defined cellular microenvironments, which more accurately resembled the dynamic microenvironment of cells in native tissues.

References:

[1] S. M. Oliveira *et al*, *Biotechnology Advances*, 33 (6), 2015.
[2] M. C. Decarli *et al, Biofabrication*, 13, 2021
[3] A. J. Engler *et al*, *Cell*, 126, 2006.
[4] T. Kamperman *et al.*, *Adv. Mat.*, 33, 2021.
[5] T. Kamperman *et al, Small*, 13 (22), 2017
[6] T. Kamperman *et al, Nat. Commun*, 10, 4347, 2019

Fabrication of visibly degradation-monitored PCL/FNDs (Fluorescent nanodiamonds) bioscaffolds using MEW method

XX. Wu[1], T. Vedelaar[1], RR. Li[1], R. Schirhagl[1], Marleen kamperman[2], Malgorzata Wlodarczyk-Biegun[2,3]
1. Department of Biomedical Engineering, University Medical Center Groningen and University of Groningen, Ant. Deusinglaan 1, 9713 AV Groningen, The Netherlands. Email:sissi.wu@rug.nl
2. Department of Polymer Chemistry, Zernike Institute for Advanced Materials, University of Groningen, Nijenborgh 4, 9747 AG, The Netherlands

Silesian University of Technology, Krzywoustego 8, 44-100 Gliwice, Poland

Introduction: MEW is expected as an effective method to design and manufacture thermoplastic scaffold benefited by the easy-operated and environmental-friendly features. To modify the bio-inert nature and properties like low mechanical strength and high hydrophobicity of these polymerized materials, fillers including graphene, protein and calcium phosphate, nanodiamonds were added inside.
Nanodiamond, which is a novel biocompatible material, has been gradually investigated for its distinct chemical, physical, magnetometry and quantum properties. During the exploration, multifunctional nanodiamonds have been proved that they can enhance polymeric properties as well as cell behaviour when introduced into biopolymers and also they show great potential to design sensors when properly doped.. Based on these features, beside the reinforced effect to substrates, it may broaden our horizons not only on sensoring but also non-invasive detecting and treating on biomedical fields, which will provide a promising platform to fabricate localizable and visibly degradation-monitored implants in vivo and discover something new in biology using treatment method that is different from the past.
Herein we fabricated polycaprolactone (PCL)/FNDs fibres at micrometre scale using melt electrowriting (MEW) method. Under the investigation of a large number of relevant literature, we find the peculiar properties of FNDs could make it practical to precisely explore how FNDs will influence the degradation process and the following bifunctionality of the composite scaffolds using our printed meshes. At the mean time, revealing of the potential of FNDs acted as a detector determinating the deterioration degree using traceable fluorescence and T1 relaxation measurements was achieved.

Material and methods: 70 nm FNDs were imbedded into PCL composite, PCL-FNDs square meshes with 230 μm pore size were printed using MEW machine under adjusted parameters. Mechanical properties of printed scaffolds with variable FND concentration (0, 0.001, 0.005, 0.01, 0.1 wt%) were measured. Scaffolds printed using PCL with 0.001 wt% of FNDs was used for biocompatibility testing. The assessment of impact of FNDs on scaffold thermal stability, degradation profile and cell behavior was carried out. Potential tracking using fluorescence from FNDs and quantification capability using T1 test for FNDs encapsulated in these filaments, which can explore the degraded stage of the polyster.

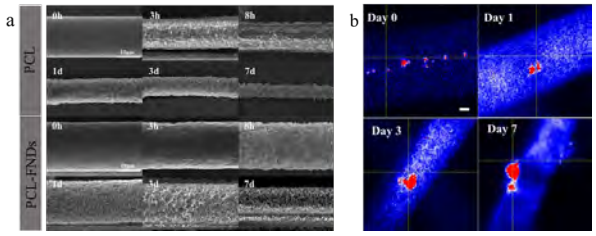

Figure 1. Degradation study. a, SEM images showing the fibres incubated in enzyme solution after 0 hour, 3 hours, 8 hours, 1 day, 3 days, 7 days; b, Use of nanodiamonds to track degradation process. Fluorescent images of nanodiamonds (0.001 wt%) in PCL fibres after 0-hour, 1-day, 3-day and 7-day enzymatic degradation. Scale bar: 3 μm.

Results and Discussion: Rising concentration of FNDs in PCL does not compromise the modulus in comparison with averages from PCL films. Based on the mechanical property and confocal results, concentration at 0.001 wt% showed optimal modulus (7.5 MPa) and were selected to make PCL-FNDs blends for further degradation and cell behavior research. With the acceleration scheme of degradation enzyme, experimental data including SEM images which showed roughness and mass loss of PCL-FNDs mesh increased slower as the degradation time went by, water contact angles and fibre diameters mildly decreased. That indicated when there were FNDs in substrates, a retard effect of fibre degradation could be perceived. High cell viability and proliferation rate gave robust confirmation of the biosafety and promotion on cell growth. Meanwhile, quantified comparison on PCL degradation level which was determinated by T1 relaxation constants showed that there was a decrease on T1 values when degradation went further. The movement of polymer chains caused by degradation weaken the connection of chains with FNDs and thus the T1 relaxation time was shortened.

Conclusion: PCL meshes with the addition of FNDS were successfully prepared using MEW method. The results demonstrated that mixture of FNDs enhanced PCL scaffold modulus, thermal and chemical stability at a low concentration of 0.001 wt%. The fluorescent images showed that FNDs added were homogenously distributed. PCL/FNDs composite scaffolds releaved good biocompatibility and good cell proliferation. Diamond magnetometry and T1 relaxation time values of FNDs in fibres under various degradation times proved its applicability of this approach to study degradation of printed meshes.

Osteoinductive Biomimetic Calcium Phosphate in Repair of Cancer-related Bone Defect

C. Xu[1], M. Wang[1], L. Wei[1, 2, 3] Y. Sun[1, 2], Y. Liu[1]

1. **Academic Centre for Dentistry Amsterdam (ACTA), Vrije University Amsterdam and University of Amsterdam, Amsterdam, the Netherlands**
2. **Shanghai Ninth People's Hospital, Shanghai Jiao Tong University, Shanghai, China**
3. **Yantai Stomatological Hospital, Yantai, China**

Introduction

Osteosarcoma (OS) usually causes critical-size bone defect due to erosion of cancer cells and extended surgical margins. Although various bone substitutes have been developed for rehabilitation of bone defect, it is still challenging to use these substances to repair cancer-related bone defects because of the potential recurrence of cancer and no anti-cancer properties of these biomaterials. Calcium phosphate materials have been widely used for the repair of bone defect. However, calcium phosphate-based materials lack osteoinduction, which makes it inferior to autografts. To address this issue, we developed an osteoinductive biomimetic calcium phosphate material via additional μg-BMP-2 (100 μg in 1 g biomimetic CaP material), and this calcium phosphate material presented increased capacity of bone regeneration in clinical trials. However, it is still unclear whether it is safe for the application of our osteoinductive biomimetic CaP material to repair OS-related bone defect. Hence, this project aims to probe the potential anti-OS effect and application of this novel CaP material for bone reconstruction in cancer cases.

Material and method

BMP-2 with gradient concentrations (0, 25, 50, 100, 200 ng/ml) was used to treat OS cells (MG-63) for 24 and 72 h. At these two time points, the viability of MG-63 cells was detected using prestoblue solution respectively. After synthesis of the osteoinductive biomimetic CaP material in our lab following our previous work, this material was used to treat MG-63 cells and human bone marrow mesenchymal stem cells for the assays of anticancer efficiency and biocompatibility respectively, and β-TCP was employed as control groups.

Results

200 μg BMP-2 alone inhibited viability of MG-63 cells after 72 h. Our novel CaP presented ideal biocompatibility and stabilizing suppression effect on MG-63 cells. However, the anti-OS effect of β-TCP was attenuated with the increased concentration.

Conclusion

Osteoinductive biomimetic CaP material has anti-cancer effect, which might be safe for bone-defect repair in bone tumor cases.

Acknowledgement

We appreciate funding support from Dutch NWO grant (No. 729001041).

Melt Electrowriting of Scaffolds for Soft-to-Hard Tissue Engineering

Piotr Zielinski[1], Zhaohang Zhang[2], Marcus Koch[3], Anastasiia Krushynska[2], Marleen Kamperman[1], Malgorzata Wlodarczyk-Biegun[1,4]

[1]Polymer Science - Zernike Institute for Advanced Materials, University of Groningen, Nijenborgh 4, 9747 AG Groningen, The Netherlands

[2]Engineering and Technology Institute Groningen, University of Groningen, Nijenborgh 4, 9747 AG Groningen, The Netherlands

[3]Leibniz Institute for New Materials, Campus D2 2, 66123 Saarbrücken, Germany

[4]Biofabrication and Bio-Instructive Materials- Biotechnology Center, Silesian University of Technology, B. Krzywoustego 8, 44-100 Gliwice, Poland

Contact: p.s.zielinski@rug.nl

Introduction:

High-stress and strain localizations and gradient structure of soft-hard tissue interfaces make these interfaces extremely prone to damage [1,2]. The injuries make the connections between soft and hard tissue a major contributor to disability worldwide [3]. Due to the complex mechanical and biological properties of the enthesis, it is a challenge to treat these injuries effectively.

Therefore, the aim of these projects is the development of scaffolds for soft-hard interfaces that will mimic the hierarchical architecture of native tissues, and deliver drugs to help expedite the regeneration process. In addition, modeling will be introduced to accelerate the production process.

Materials and methods:

Polycaprolactone (PCL) scaffolds were printed using Melt Electrowriting (MEW). This method allowed the printing of scaffolds with easily adjustable architecture. Mechanical properties (stiffness, force at break) were investigated using a universal testing device. COMSOL Multiphysics was used to predict mechanical properties in the elastic region of printed scaffolds. Poly(D, L-lactide-co-glycolide) nanoparticles (PLGA NPs) with encapsulated Rhodamine have been produced using a double emulsion technique with solvent evaporation. NPs were characterized in terms of an average size and polydispersity index (PDI) by dynamic light scattering (DLS). Rhodamine-loaded PLGA NPs were mixed with PCL powder, melted, and the composite material was printed with MEW

Results:

Scaffolds with different architecture (square, rhombus, triangular, wavy, and gradient) as well as varying number of layers, and fiber thickness were printed with good accuracy (Fig. 1). The tensile test has shown that the mechanical properties of the scaffold are dependent on the scaffold's architecture. Gradient scaffolds revealed a gradual response to the applied force. Mechanical properties of homogenous scaffolds were well-predicted using computer simulations.

The average size and PDI of PLGA NPs were found to be 253 nm, and 0.074, respectively. After the encapsulation of Rhodamine, the PLGA NPs were fluorescent. After melting, the NPs remained fluorescent and were found across the whole PCL fiber (Fig.2). Scaffolds were successfully printed using PCL with NPs.

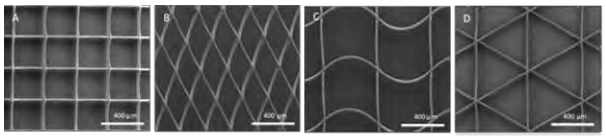

Fig.1 SEM images of pure PCL printed scaffolds using MEW.

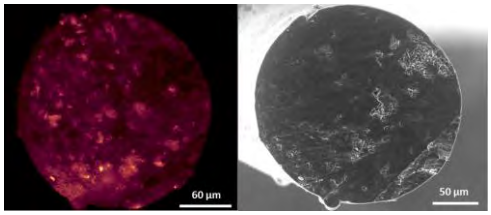

Fig. 2 Fluorescent (left) and SEM (right) images of PCL fiber cross-section matrix with Rhodamine-loaded PLGA NPs.

Summary and conclusions:

Scaffolds with varying architecture were printed with good precision using MEW. The mechanical properties of the scaffolds could be tuned by changing the size and shape of the pores. Gradient scaffolds showed a similar stress-strain response to the one observed at the interface tissue during movement. Computer simulations will be extended with other designs, including gradient ones to predict scaffold's mechanical properties. The gradient scaffolds will be improved to even more closely mimic the mechanical and structural properties of soft-to-hard tissue interfaces.

Encapsulation of Rhodamine allowed visualization of PLGA NPs within the PCL matrix. In the future, further printability of drug-loaded NPs in the PCL matrix will be checked as potential drug delivery systems.

References:

1. Mirzaalim M.J., et al., *Fracture Behavior of Bio-Inspired Functionally Graded Soft–Hard Composites Made by Multi-Material 3D Printing: The Case of Colinear Cracks*. Materials 2019, 12, 2735.

2. Patel S, et al., *Integrating soft and hard tissues via interface tissue engineering*. J Orthop Res. 2018 Apr;36(4):1069-1077.

3. Blyth, F.M., et al., *The Global Burden of Musculoskeletal Pain-Where to From Here?* American journal of public health, 2019. 109(1): p. 35-40.